The role of GRAS-domain proteins in arbuscular mycorrhizal symbiosis

LEONIE HELENE LUGINBUEHL

November 2016

Thesis submitted to the University of East Anglia for the degree of Doctor of Philosophy

ABSTRACT

A major limitation to plant growth is the restricted access to nutrients in the soil. To improve nutrient acquisition, the majority of land plants enter a beneficial symbiosis with arbuscular mycorrhizal (AM) fungi. The accommodation of fungal hyphae in roots requires the extensive transcriptional reprogramming of host cells. Several GRAS-domain proteins, including NSP1 (NODULATION SIGNALLING PATHWAY 1), NSP2, and RAM1 (REQUIRED FOR ARBUSCULAR MYCORRHIZATION 1), have emerged as important transcriptional regulators during mycorrhization. Interaction studies suggest that these proteins form multicomponent complexes, raising the question whether they regulate similar or different mycorrhizal processes. Here, the functions of *NSP1*, *NSP2* and *RAM1* during AM development were investigated by detailed phenotypic and transcriptional analyses of the corresponding loss-of-function mutants.

Global gene expression profiling of *nsp1-1* revealed that *NSP1* is required for the expression of a large number of genes involved in strigolactone and gibberellin biosynthesis at the pre-contact stage of AM development. Strigolactones are known to attract the fungus to the root. In line with this, the quantification of mycorrhizal structures showed a delay in mycorrhization in *nsp1-1*. Transcriptional profiling confirmed that the expression of the majority of mycorrhizal-induced genes was delayed, but not abolished in *nsp1-1*, suggesting that *NSP1* only has a minor role in the transcriptional regulation once the contact between the fungus and the roots has been established. Unlike *NSP1*, *RAM1* plays a critical role in the transcriptional regulation at later stages of AM symbiosis. Mycorrhization was strongly impaired in *ram1-1*, and transcriptional profiling revealed that *RAM1* is essential for the expression of several genes involved in arbuscule development and the nutrient exchange between the symbionts. Meanwhile, the exact function of *NSP2* remains unclear, as no effect on mycorrhization was observed in *nsp2-2* under the conditions tested here. These findings suggest that *NSP1*, *NSP2* and *RAM1* play largely different roles in the transcriptional regulation during AM development.

LIST OF CONTENTS

LIST OF ABBREVIATIONS

BNM	buffered nodulation medium
bp	base pair
CCaMK	calcium- and calmodulin-dependent protein kinase
cDNA	complementary DNA
ChIP	chromatin immunoprecipitation
Ct	threshold cycle
Da	Dalton
DIP	DELLA interacting protein
DMI	does not make infections
DNA	deoxyribonucleic acid
dNTP	deoxynucleotide triphosphates
dpi	days post inoculation
dsRed	*Discosoma sp.* red fluorescent protein
DWA	distilled water agar
EMSA	electrophoretic mobility shift assay
fwd	forward
g	gram
GA	gibberellins
GFP	green fluorescent protein
GRAS	GAI, RGA and SCR
GUS	β-glucuronidase
h	hour
HA	human influenza hemagglutinin antigen
IPD3	interacting protein of DMI3
L	lysogeny broth - Lennox
LB	lysogeny broth
LCO	lipochitooligosaccharides
LRR-RLK	Leucine-rich repeat receptor-like kinase

LUC	luciferase
M	mili
µ	micro
M	molar
MIG	mycorrhiza-induced GRAS
modFP	modified Fahraeus medium
MtGEA	*Medicago truncatula* gene expression atlas
MUG	4-methylumbelliferyl- β-D-glucuronide
n	nano
NS-LCOs	non-sulphated lipochitooligosaccharides
NSP	nodulation signalling pathway
OD	optical density / absorbance
PCR	polymerase chain reaction
qRT-PCR	quantitative reverse transcription PCR
RAD	required for arbuscule development
RAM	required for arbuscular mycorrhization
rev	reverse
RNA	ribonucleic acid
RNAi	RNA interference
RNA-seq	RNA sequencing
s	second
SEM	standard error of the mean
S-LCOs	sulphated lipochitooligosaccharides
SOC	super orbital broth with catabolite repression
T1	offspring of transformed plants
T2	offspring of T1 generation
TY	rhizobium complete medium
WGA	wheat germ agglutinin
wpi	weeks post inoculation
wt	wild type

PUBLICATIONS

During the course of this project, the following manuscript has been published:

Luginbuehl L, Oldroyd GED (2016). Calcium signaling and transcriptional regulation in arbuscular mycorrhizal symbiosis. Chapter 8, in *Molecular Mycorrhizal Symbiosis* (ed F. Martin), John Wiley & Sons, Inc., Hoboken, NJ, USA.

Chapter 1 of this thesis includes material from this publication.

ACKNOWLEDGEMENTS

There are so many people who have supported me in the last four years and without whom I would not have been able to finish my PhD thesis. First of all, I would like to thank Giles Oldroyd for all his support, encouragement, and invaluable input throughout my PhD. I am very grateful to have had the opportunity to work on a topic that has kept me excited until the very end of my project.

I would also like to thank Lars Ostergaard and Robert Sablowski for their feedback and guidance. Discussing my ideas and results with scientists outside of the symbiosis field has been very helpful to gain new perspectives and advance my scientific thinking. I am also thankful to Peter Eastmond and Jeremy Murray for taking the time to discuss my results and helping me to put them into context.

I have been lucky to be surrounded by excellent scientists who have taught me many experimental techniques and have helped me with my experimental designs. I would like to thank Katharina Schiessl for teaching me how to perform RNA extractions and ChIP assays and how not to despair of confocal microscopy, Jodi Lilley for showing me how to set up qRT-PCRs in a sensible way, Ben Miller for teaching me how to perform large numbers of hairy root transformations in a short amount of time, Sarah Shailes for showing me the meditative quality of crossing *Medicago* plants early in the morning, Nuno Leitao for refreshing my knowledge on how to handle *Arabidopsis*, and Myriam Charpentier for showing me how to get mycorrhizal fungi to colonize plants. I would also like to thank Guru Radhakrishnan for all his help with bioinformatics and phylogenetic analyses, Eleni Soumpourou for her help with the DNA synthesis and transferring hundreds of *Medicago* seedlings to soil, and my summer student Heather Bland for her help with the cloning of constructs and with transactivation assays.

I am thankful to all the members of the media kitchen and the horticultural services who have provided large volumes of growth media and have taken such great care of my plants in the growth rooms and glasshouses. I would also like to thank the BioImaging team at JIC for their help with microscopy.

Being part of the Rotation PhD programme has been a wonderful experience and I am very grateful to Nick Brewin and Steph Bornemann for making this such a great programme. I would also like to thank Caroline Dean and Sarah O'Connor for supervising

me during my first two rotations and allowing me to get insights into their exciting research areas.

I especially want to thank all the people at the John Innes Centre who have made my time in the lab and outside of the lab so enjoyable and who have supported me through the more difficult times. Thomas, Jan, Zane, Scott, Nuno, Guru, Jodi, Jo, Matt, Aisling, Sarah and Katharina, thank you for your friendship.

I am truly grateful to my friends outside of JIC for reminding me that there is a life outside of science. Laura, Cristina, Fatima and Amitesh, I cannot thank you enough for always being there for me.

Finally, I would like to thank my family for their support and love throughout all these years. You have always encouraged me to pursue my own goals and dreams I am very thankful for that. Tristan, I wish you were here. We would have celebrated by eating excessive amounts of delicious food, would have prepared beforehand by stretching our stomachs with lots of water, and would have had to recover for days afterwards.

CHAPTER 1

General introduction

1.1 Symbioses between plants and microbes

1.1.1 The arbuscular mycorrhizal symbiosis

Plants have developed many sophisticated strategies to ensure access to nutrients in their environment. One successful approach to efficiently acquire essential macro- and micronutrients is by entering mutually beneficial symbioses with soil microbes. The oldest and most commonly established symbiosis in plants is the arbuscular mycorrhizal (AM) symbiosis, which is formed by 80-90% of all land plant species with fungi of the phylum *Glomeromycota* (Smith and Read, 2008). In the AM symbiosis, the obligate biotrophic fungus receives fixed carbon from the plant and in return delivers water and mineral nutrients from the soil to the roots (Smith and Smith, 2011). Mycorrhization greatly improves the nutrient status of the plant, and there is evidence for substantial amounts of phosphate, nitrogen, and sulphur being transported to mycorrhized roots (Tanaka and Yano, 2005; Leigh et al., 2009; Allen and Shachar-Hill 2009; Casieri et al., 2012). Phosphate in particular is required in large quantities by the plant and, together

with nitrogen, is often a limiting nutrient for plant growth (Agren et al., 2012). Similarly, large amounts of fixed carbon are transported from the plant to the fungus. It has been estimated that up to 20% of the plant photosynthesis products are consumed by mycorrhizal fungi (Bago et al., 2000). Thus, the AM symbiosis plays a key role in plant nutrition and the global carbon cycle (Harrison, 2005).

During AM development, fungal hyphae colonize plant roots and form an intimate association with host cells by penetrating the cell lumen and developing highly branched, tree-like structures called arbuscules. Each hyphal branch is surrounded by a plant-derived membrane, which excludes the fungal hyphae from the plant cytoplasm. Arbuscules are thought to be the site of nutrient transfer between the plant and the fungus and therefore play a critical role in AM symbiosis (Harrison, 2012). Fossil evidence from the Rhynie chert in Scotland shows that arbuscules were already present in some of the earliest land plants, and it has been proposed that the symbiosis with mycorrhizal fungi was instrumental in enabling plants to colonize land 450 million years ago (Remy et al., 1994; Parniske, 2008; Humphreys et al., 2010). In line with this, several key components of the signalling pathway required for the establishment of AM symbiosis were found to be conserved in charophytes, the closest living relatives to the algal ancestors of land plants, suggesting that land plant ancestors were pre-adapted for AM symbiosis (Delaux et al., 2015). Thus, the ability to enter a symbiosis with arbuscular mycorrhizal fungi is likely to have emerged once very early during the evolution of land plants and has since been retained in most land plant lineages (Parniske, 2008). Some exceptions exist, including the model plant *Arabidopsis thaliana* and most other members of the *Brassicales*, which have lost the ability to establish a symbiosis with mycorrhizal fungi, and this correlates with the loss of AM-specific genes in these non-host species (Delaux et al., 2014).

1.1.2 The root-nodule symbiosis

A more recently evolved symbiosis that has been studied extensively in the past decades is the association of plants of the orders *Fabales*, *Fagales*, *Cucurbitales*, and *Rosales* with nitrogen-fixing bacteria of the family *Rhizobiacea* or the genus *Frankia*. This symbiosis is commonly known as the root-nodule symbiosis, and a key feature of this association is the *de novo* formation of unique root organs called nodules, which accommodate the bacterial symbiont and provide a low-oxygen environment for efficient nitrogen fixation

(Oldroyd and Downie, 2004). In this process, the bacterial enzyme nitrogenase converts atmospheric nitrogen into ammonium, which can be used by the plant as a nitrogen source. In return, the plant delivers fixed carbon, mostly in the form of malate and succinate, to the nitrogen-fixing bacteria (Prell and Poole, 2006).

In most legumes, including the two model species *Medicago truncatula* and *Lotus japonicus*, the infection of root cells by rhizobia is initiated by the attachment of bacteria to growing root hairs. The bacterial cells are entrapped within an infection pocket by root hair curling, and an infection thread is formed that guides the dividing bacteria to the base of the root hair cell and into the cortical layers of the root. Simultaneous to the formation of infection threads in root hairs, cortical cells start to divide to initiate the formation of nodules, which are infected and inhabited by the bacteria. Similar to the fungal hyphae in the AM symbiosis, the bacterial cells are always surrounded by a plant-derived membrane, excluding them from the cytoplasm of the plant cell (Oldroyd and Downie, 2004).

Based on fossil evidence, the evolution of the root-nodule symbiosis has been dated back to 65 million years ago, and it is thought that nodulation evolved several times independently in members of the *Fabales*, *Fagales*, *Cucurbitales*, and *Rosales* (Kistner and Parniske, 2002). There are several striking commonalities between the AM symbiosis and the root-nodule symbiosis. Although the end results of the infection of plant roots by the two symbionts are very different, the infection process itself requires many of the same developmental and signalling processes (Kistner and Parniske, 2002; Parniske, 2008). Based on these observations, it has been proposed that the root-nodule symbiosis evolved by recruiting the symbiotic programme required for AM symbiosis (Parniske, 2008; Oldroyd, 2013).

1.2 The establishment of AM symbiosis in plant roots

AM development is initiated by the reciprocal exchange of signalling molecules between the plant and mycorrhizal fungi in the soil, and is followed by the growth of fungal hyphae towards the root, where they attach to the root epidermis by forming specialised attachment structures called hyphopodia. After the entry of fungal hyphae through epidermal cells into the underlying root cell layers, there are two different types of fungal colonization strategies, although intermediate forms of these strategies often

occur (Dickson, 2004). The *Arum*-type colonization involves the spreading of hyphae between cortical cells before they penetrate an inner cortical cell to form a terminally differentiated arbuscule. In the *Paris*-type colonization, hyphae spread through intracellular passage of cortical cells, where hyphal coils or arbuscules are formed. The colonization of roots by *Glomus* species is also accompanied by the appearance of lipid-rich vesicles in the apoplast of plant roots, which have been proposed to serve as energy storage units for the fungus (Dickson, 2004).

The colonization of plant roots by fungal hyphae is a complex and tightly controlled process. Until recently, no genetic tools for AM fungi were available, and thus very little is known about the fungal molecular mechanisms that orchestrate the development of mycorrhizal infection structures inside plant roots. On the host plant side, however, research in recent years has unveiled many of the signalling and cellular processes involved in the accommodation of the fungus (Parniske, 2004; Oldroyd et al., 2009; Harrison, 2012; Gutjahr and Parniske, 2013). These findings support the idea that the plant cells actively guide fungal colonization of the root (Parniske, 2004; Oldroyd et al., 2009).

1.2.1 Exchange of diffusible signals at the pre-symbiotic stage of AM symbiosis

The first stage of AM development involves the exchange of diffusible signalling molecules between the two symbiotic partners prior to their physical contact, a process that enables the mutual recognition of the plant and the fungus (Gutjahr and Parniske, 2013; Nadal and Paszkowski, 2013; Bonfante and Genre, 2015). Plant-derived signals induce fungal spore germination and hyphal branching, thereby attracting fungal hyphae to the roots. In return, mycorrhizal fungi release signalling molecules that induce a symbiotic response in plant roots. This reciprocal signal exchange plays an important role at the pre-contact stage of the symbiosis, but is likely to also take place during the intraradical colonization by mycorrhizal fungi.

1.2.1.1 Plant-derived signals

Under nutrient-starved conditions, in particular when phosphorus levels in the soil are limiting, plant roots synthesise and release strigolactones into the rhizosphere (Yoneyama et al., 2007; López-Ráez and Bouwmeester 2008; Liu et al., 2011; Foo et al.,

2013). These plant hormones were originally discovered due to their ability to induce seed germination of parasitic plants of the genus *Striga* (Cook et al., 1966). It was only much later that strigolactones were also found to induce spore germination and hyphal branching of AM fungi (Akiyama et al., 2005; Besserer et al., 2006). Strigolactones trigger multiple responses in mycorrhizal fungi, including the activation of the oxidative metabolism, the division of mitochondria, and the release of fungal-derived symbiotic signalling molecules (Besserer et al., 2006, 2008; Genre et al., 2013; Tsuzuki et al., 2016). Strigolactones are rapidly hydrolysed once released into the rhizosphere (Akiyama and Hayashi, 2006), and it is thought that the resulting steep concentration gradient provides a positional cue for AM fungi (Nadal and Paszkowski, 2013; Ruyter-Spira et al., 2013). It is currently unclear how strigolactones are perceived by AM fungi, however, live-cell imaging showed that strigolactones induce rapid and transient changes in intracellular calcium levels in fungal hyphae, suggesting that calcium signalling plays a role in the perception of strigolactones by mycorrhizal fungi (Moscatiello et al., 2014). In addition to their role in inducing hyphal growth of various fungi, strigolactones also play important roles as endogenous plant hormones in the regulation of plant development, including root and shoot architecture (Al-Babili and Bouwmeester, 2015).

Strigolactones are derived from carotenoid precursors, and several genes involved in strigolactone biosynthesis have been identified (Al-Babili and Bowmeester, 2015). For example, an iron-binding protein encoded by *D27* (*DWARF27)* and the two carotenoid cleavage dioxygenases *CCD7* and *CCD8* have been found to be required for the late steps of strigolactone biosynthesis (Schwartz et al., 2004; Alder et al., 2012). In accordance with a role of strigolactones in AM symbiosis, silencing of *CCD7* in tomato results in a reduction of mycorrhizal colonization (Koltai et al., 2010). Similarly, the strigolactone-deficient *ccd8* mutant of *Pisum sativum* is impaired in AM symbiosis (Gomez-Roldan et al., 2008). To act on AM fungi in the rhizosphere, strigolactones have to be exuded after their biosynthesis in root tissues. The ABC (ATP-binding cassette) transporter *PDR1* in *Petunia hybrida* was shown to be required for the export of strigolactones from root cells (Kretzschmar et al., 2012). In *pdr1* loss-of-function mutants, the strigolactone orobanchol is not released from roots and colonization levels by mycorrhizal fungi are reduced, confirming that the exudation of strigolactones plays an important role in the establishment of AM symbiosis.

In addition to strigolactones, two hydroxy fatty acids from carrot root exudates are able to induce hyphal branching of the AM fungus *Gigaspora gigantea* (Nagahashi and Douds,

2011). Furthermore, flavonoids have been proposed to stimulate hyphal growth of mycorrhizal fungi (Bécard et al., 1992). However, these secondary metabolites do not appear to be essential for the successful establishment of the symbiosis, as maize plants deficient in flavonoid production do not show a reduction in fungal colonization (Bécard et al., 1995).

Besides the hyphal growth-inducing compounds described above, cutin monomers have been proposed to act as plant-derived signalling molecules to the fungus to promote the formation of hyphopodia (Wang et al., 2012). *RAM2* (*REQUIRED FOR ARBUSCULAR MYCORRHIZATION 2*), a glycerol-3-phosphate acyltransferase involved in cutin biosynthesis, was found to be required for hyphopodium formation. In line with this, the external application of cutin monomers restores the formation of hyphopodia in *ram2* roots (Wang et al., 2012). It is currently unclear whether these cutin monomers solely have a signalling function, similar to strigolactones and shorter chain hydroxy fatty acids exuded by carrot roots, or whether they also play a structural or nutritional role for the fungus.

1.2.1.2 Fungal-derived signals

Following the perception of plant-derived strigolactones, AM fungi release signalling molecules that are recognised by the plant as symbiotic cues. Exudates from germinated spores of AM fungi have been found to induce a number of different responses in plant roots, including the induction of extensive gene expression changes, the promotion of root branching, the accumulation of starch, and the activation of rapid, nuclear-associated calcium oscillations in root cells (Kosuta et al., 2003, 2008; Oláh et al., 2005; Navazio et al., 2007; Kuhn et al., 2010; Chabaud et al., 2011; Maillet et al., 2011; Bonfante and Genre, 2015). These cellular, metabolic, and developmental changes in response to diffusible fungal signals are thought to prime plant cells for their colonization by AM fungi. For a long time, the identity of these so-called Myc-factors was unknown. In an effort to purify the fungal-derived symbiotic signalling molecules, a mixture of sulphated and non-sulphated lipochitooligosaccharides (S-LCOs and NS-LCOs) were identified that are able to induce the expression of the symbiotic gene *ENOD11* and stimulate root branching (Maillet et al., 2011). These signalling molecules are surprisingly similar in their structure to Nod factors, signalling molecules that are produced and released by rhizobial bacteria. Both S-LCOs and NS-LCOs were recently shown to activate symbiotic calcium oscillations in *M. truncatula* and *L. japonicus* root epidermal cells (Sun et al.,

2015). In addition to LCOs, AM fungi produce short-chain chitooligosaccharides (COs) that were proposed to also be potential signalling molecules (Genre et al., 2013). Accordingly, it was found that short-chain COs induce sustained nuclear calcium oscillations in root epidermal cells of several plant species (Genre et al., 2013; Sun et al., 2015). Notably, short-chain COs and Myc-LCOs seem to trigger a calcium response only in *L. japonicus* and rice atrichoblasts, but not in trichoblasts, even though fungal hyphae do induce calcium spiking in trichoblasts. Only when COs and Myc-LCOs were mixed, calcium spiking was observed in rice trichoblasts (Sun et al., 2015). Thus, the individual fungal-derived signalling molecules seem to differ in their ability to elicit a symbiotic response, depending on their concentration, the host plant species, the root cell type, and their combination with other fungal signals (Sun et al., 2015).

1.2.2 Fungal infection of epidermal root cells

The exchange of signalling molecules at the pre-contact stage of AM symbiosis is followed by the attachment of fungal hyphae to the epidermal cells of plant roots, where the hyphal tips differentiate to form hyphopodia, before the hyphae enter the root. The penetration of a plant cell by fungal hyphae involves a drastic rearrangement of host cytoskeletal structures and the remodelling of organelles. These cellular changes were described in detail by Genre and colleagues, who studied the dynamics of the ER, microfilaments, and microtubules during hyphal entry of epidermal cells using live cell microscopy (Genre et al., 2005). Upon fungal attachment to an epidermal cell, the cell nucleus rapidly moves to the site of hyphal contact before migrating across the cell to the opposite side. Simultaneous to the nuclear movement away from the fungal attachment site, a highly specialised tunnel-like cellular structure called the pre-penetration apparatus (PPA) is formed (Genre et al., 2005). PPA formation is achieved by accumulation of a dense network of ER cisternae, actin filaments, and microtubules. After the PPA has finished assembling and spans the whole width of the cell, the fungal hypha enters the cell lumen through this pre-formed cytoplasmic bridge, which guides hyphal growth across the cell on a pre-defined path (Genre et al., 2005). Thus, plant cells actively prepare for their penetration by the fungus and guide the growth of fungal hyphae through the cell lumen.

1.2.3 Arbuscule development in inner cortical cells

After the successful entry of fungal hyphae through the epidermal cell layer, they spread inside the plant roots until they reach the inner cortex, where arbuscules are formed. Although the fungus penetrates the cell wall to enter cortical cells, the host plasma membrane does not rupture. Instead, it expands to envelop the hyphal branches and forms the so called periarbuscular membrane (PAM), which separates the fungal hyphae from the host cytoplasm (Figure 1.1, Remy et al., 1994; Harrison, 2005). Live cell imaging of the arbuscule and the surrounding membrane has led to the identification of two different PAM domains, which are defined based on their location and their protein composition (Pumplin and Harrison, 2009). The trunk domain of the PAM surrounds the broad arbuscule trunk and contains proteins that are also present in the plasma membrane, whereas the branch domain of the PAM envelops the fine hyphal branches of the arbuscule and harbours a specialized set of proteins that mediate the nutrient exchange between the plant and the fungus (Pumplin and Harrison, 2009). The area between the PAM and the fungal hyphae has been named the periarbuscular space (PAS) and contains amorphously structured plant cell-wall material, which is in direct contact with the fungal cell walls surrounding the hyphae (Balestrini and Bonfante, 2014). The process of extensive branching of the fungal hyphae during arbuscule development and the simultaneous expansion of the host membrane significantly increases the contact surface area between the plant and the fungus. This places arbuscules in an ideal position to mediate the efficient exchange of nutrients between the symbiotic partners (Parniske, 2008; Harrison, 2012; Balestrini and Bonfante, 2014).

Similar to the hyphal colonization of the epidermis, arbuscule development in inner cortical cells also involves the fungal penetration of the cell lumen. It is therefore not surprising that analogous cellular rearrangements, including nuclear migration and PPA formation, are observed during the early steps of arbuscule formation (Genre et al., 2008). In the *Arum*-type colonization, however, the fungal hyphae do not cross the inner cortical cells entirely as they do in epidermal and outer cortical cells, but grow towards the centre of the cell to terminally differentiate into arbuscules by extensive dichotomous branching. To achieve this, the nucleus positions itself at the centre of the inner cortical cell, where the PPA connects it with the site of hyphal contact to allow hyphal growth and the formation of the broad arbuscule trunk. ER-rich cytoplasm aggregates at spatially restricted sites along the initial arbuscule trunk, and it has been

proposed that these sites of aggregation determine where lateral branches emerge to form the branch domain of the arbuscule (Genre et al., 2008). After completion of arbuscule development, the cytoskeleton reorganizes to connect the fine arbuscule branches (Genre and Bonfante, 1998; Genre et al., 2008). In addition, components of the secretion pathway, including golgi stacks, trans-golgi networks and multivesicular bodies, accumulate around arbuscular hyphae (Genre et al., 2008; Pumplin and Harrison, 2009).

The extensive branching of hyphae during arbuscule development is accompanied by the formation of the plant-derived PAM, a process that has been proposed to involve the *de novo* synthesis of membranes (Toth and Miller, 1984; Pumplin and Harrison, 2009). In addition, PAM-localised proteins, such as the phosphate transporters, have to be secreted and incorporated into the new membrane to achieve the specialised membrane composition required for nutrient exchange with the fungus (Alexander et al., 1989; Gianinazzi-Pearson, 1996; Harrison et al., 2002). The accumulation of the ER, golgi stacks and the trans-golgi network around the arbuscule branches during arbuscule formation suggests that the exocytotic pathway plays a significant role in arbuscule development (Genre et al., 2012). Several studies have provided further evidence for the importance of exocytosis during the formation of the PAM. Using an RNA silencing approach, Ivanov and colleagues have demonstrated that two members of the exocytotic vesicle-associated membrane proteins (VAMPs), the two v-SNARE proteins VAMP721d and VAMP721e, localize to the PAM and are indispensable for the proper formation of arbuscules (Ivanov et al., 2012). Consistent with this, the t-SNARE protein SYP132A has recently been shown to be important for PAM development (Pan et al., 2016). Moreover, the exocyst complex, which is an important component of vesicle trafficking, has been proposed to be involved in arbuscule development based on its localization around developing arbuscule branches (Genre 2012). In accordance with this, a recent study by Zhang and colleagues has found that the EXO70I subunit of the exocyst is required for mycorrhization. Plants carrying a mutation in *EXO70I* are not able to form the finely branched hyphae in the branch domain of arbuscules, resulting in an early arrest of arbuscule development and in their premature degeneration (Zhang et al., 2015). In addition, EXO70I was shown to be required for the efficient incorporation of two ABCG transporters, STR and STR2, into the PAM (Zangh et al., 2010; Gutjahr et al., 2012; Zhang et al., 2015). It is conceivable that EXO70I also functions in the incorporation of other PAM-localized proteins and/or the deposition and expansion of the PAM around the

branch domain; however, this remains to be investigated. Interestingly, several other EXO70s are transcriptionally induced in cells harbouring arbuscules, and it has been hypothesised that arbuscule formation might depend on the concerted action of multiple EXO70 subunits potentially active at different stages during arbuscule development (Zhang et al., 2015).

EXO70I was found to partially co-localize and physically interact with a plant-specific protein called VAPYRIN (Zhang et al., 2015). In *M. truncatula* and *P. hybrida* plants, *VAPYRIN* is required for the epidermal penetration by the fungus. Although hyphopodia are formed in *vapyrin* mutant and knockdown plants, the fungus only rarely is able to enter the root. When it does, the hyphae manage to spread within the root and reach inner cortical cells, but arbuscule formation is abolished at very early stages, revealing a fundamental role of *VAPYRIN* for the intracellular accommodation of AM fungi (Reddy et al., 2007; Feddermann et al., 2010; Pumplin et al., 2010; Murray et al., 2011). The VAPYRIN protein contains two different domains, an amino-terminal major sperm protein (MSP) domain that is also present in VAMP-associated proteins (VAPs) and a carboxy-terminal ankyrin domain. Both domains have been predicted to mediate protein-protein interactions (Feddermann et al., 2010; Pumplin et al., 2010). The VAPYRIN protein is present in the cytoplasm as small puncta, and it has been proposed that this punctuate pattern stems from the association of VAPYRIN with vesicles, potentially originating from the vacuole (Feddermann et al., 2010; Pumplin et al., 2010). The localization and the domain structure of VAPYRIN suggest that it might have a structural role in the rearrangement of cell cytoplasm and/or the formation of the PAM during hyphal colonization (Feddermann et al., 2010; Pumplin et al., 2010); however, until recently no exact function could be attributed to this important protein. The finding that VAPYRIN physically interacts with EXO70I to potentially recruit EXO70I to the PAM substantiates the hypothesis that VAPYRIN acts as a scaffold protein during arbuscule development.

In recent years, evidence has accumulated that supports a fundamental role of exocytosis for PAM formation and the deposition of proteins around arbuscule branches. In an elegant study, Pumplin and co-workers have found an additional mechanism that orchestrates protein deposition into the PAM. By expressing plasma-membrane or PAM-localized proteins under promoters that are induced at different stages of arbuscule development, it was shown that the temporal expression of these genes determines whether they are incorporated into the plasma membrane, the membrane around the

arbuscule trunk, or the membrane around the fine branches (Pumplin et al, 2012). These findings imply that the proper deposition of proteins into the different arbuscule domains requires not only the secretion pathway, but also the precise temporal regulation of gene expression and is mediated by a redirection of exocytosis to the PAM during different stages of arbuscule development (Pumplin et al., 2012).

1.2.4 Senescence and collapse of arbuscules

After having reached the mature state, arbuscules typically only have a very short life span of about 2 to 8 days before they rapidly collapse (Toth and Miller 1984; Alexander et al., 1989, Kobae and Hata 2010). In a functional symbiosis, the degeneration of arbuscules is accompanied by recolonization of the root and formation of new arbuscules, resulting in simultaneous cycles of arbuscule formation and degradation. Signs of degenerating arbuscules include the rapid shrinkage of the highly branched fungal hyphae, followed by the degeneration of the PAM and PAM-localized proteins (Kobae et al., 2010). Several host cellular changes have been found to accompany arbuscule collapse. Most Golgi vesicles were shown to redistribute to the periphery of the cell, while the accumulation of the ER around the arbuscule branches that is observed during arbuscule formation is also maintained in cells with degenerating arbuscules (Pumplin and Harrison, 2009). Peroxisomes accumulate around collapsing arbuscules and stay closely associated with arbuscule branches (Pumplin and Harrison, 2009), possibly assisting in the active breakdown of lipids. Alternatively, it has been hypothesised that peroxisomes might be important to protect the host plant cell from potential damage by sequestering reactive oxygen species (Pumplin and Harrison, 2009). Together, these observations propose that arbuscule degeneration is a regulated, active process ensuring that the host cells remain alive during and after arbuscule collapse to be recolonized later on.

It is currently unclear why arbuscules are recycled so quickly in mycorrhized roots, as the degradation and formation of new arbuscules is a very costly process for both symbiotic partners. Interestingly, plants that carry a mutation in the transporters that mediate phosphate uptake across the PAM show a premature degeneration of arbuscules (Javot et al., 2007; Yang et al., 2012). Based on these findings, it has been proposed that phosphate not only serves as a nutrient, but also acts as a signal to plant cells to maintain AM symbiosis (Yang and Paszkowski, 2011). Thus, the rapid recycling

of arbuscules might provide a means of control that is exerted by the plant over the fungus, resulting in the degeneration of arbuscules that do not provide enough nutrients (Parniske, 2008).

1.3 Nutrient exchange between plants and mycorrhizal fungi

The main function of the AM symbiosis is the exchange of nutrients between the symbiotic partners, where the plant delivers photosynthetically fixed carbon to the fungus, while receiving water and mineral nutrients taken up by fungal hyphae from the soil. In addition to enhancing nutrient uptake, the AM symbiosis has also been described to increase the resistance of plants against some pathogens, although it is unclear whether this induced resistance is due to the improved nutrient status and thus overall improved plant fitness, or due to the activation of specific defence responses (Cordier et al., 1998; Liu et al., 2007; Campos-Soriano et al., 2012). The availability of nutrients in the soil strongly affects the extent of fungal colonization in plant roots (Carbonnel and Gutjahr, 2014). Split root experiments have shown that high levels of phosphate suppress AM development, even when only half of the root system is treated with phosphate, indicating that systemic signals are involved in the phosphate-mediated inhibition of mycorrhization (Breuillin et al., 2010; Balzergue et al., 2011). The suppression of fungal colonization under high nutrient conditions might be a mechanism by which the plant minimizes the amount of fixed carbon that is transported to the fungus to ensure that the costs of AM symbiosis do not outweigh the benefits (Gutjahr and Parniske, 2013). However, the exact molecular processes that underlie the regulation of AM development by nutrients are not well understood (Carbonnel and Gutjahr, 2014).

1.3.1 Nutrient transfer from the fungus to the plant

In mycorrhized roots, the fungi benefit the host plant by facilitating the uptake of water and several essential mineral nutrients, including phosphate, ammonium, and sulphate, from the soil. The thin extraradical fungal mycelium is able to reach and mineralize soil nutrients much more efficiently than plant roots, and mycorrhization significantly improves the nutrient status of the plant (Smith and Smith, 2011). High affinity

phosphate and ammonium transporters have been identified that are expressed in the extraradical fungal hyphae and are likely to be involved in nutrient uptake from the soil to the fungus (Ames et al., 1983; Harrison and van Buuren, 1995; Pao et al., 1998; Maldonado-Mendoza et al., 2001; Benedetto et al., 2005; Govindarajulu et al., 2005; Lopez-Pedrosa et al., 2006; Fiorilli et al., 2013). After uptake into the fungal mycelium, phosphate and nitrogen are transported in the form of polyphosphates and arginine to the arbuscules, where they are released into the PAS as phosphate and ammonium, respectively (Ezawa et al., 2002; Govindarajulu et al., 2005; Tanaka and Yano, 2005; Cruz et al., 2007; Hijikata et al., 2010). It is currently unclear whether the release of nutrients from the fungus into the PAS is a passive process or is actively mediated by as yet unidentified fungal transporters.

The plant phosphate transporters that mediate the uptake of phosphate across the PAM have been studied extensively and are well characterized in several plant species, including *M. truncatula*, potato, and rice (Rausch et al., 2001, Harrison et al., 2002; Paszkowski et al., 2002; Nagy et al., 2005; Maeda et al., 2006; Javot et al., 2007; Yang and Paszkowski, 2011; Tamura et al., 2012; Yang et al., 2012; Xie et al., 2013; Breuillin-Sessoms et al., 2015). They belong to the family of phosphate transporter 1 (Pht1) proton symporters and many of them were shown to complement yeast phosphate transport mutants, confirming that they are indeed able to transport phosphate (Rausch et al., 2001; Harrison et al., 2002; Paszkowski et al., 2002; Tamura et al., 2012; Xie et al., 2013). The *M. truncatula* PT4 transporter and its homologs in rice and soybean localize specifically to the branch domain of the PAM (Harrison et al., 2002; Pumplin and Harrison, 2009; Kobae and Hata, 2010; Tamura et al., 2012). Furthermore, it was shown that *MtPT4* is essential for phosphate transfer from the fungus to the plant as well as for the maintenance of a functional AM symbiosis, as arbuscules in mutant plants degenerate prematurely and the symbiosis is aborted (Javot et al., 2007). Interestingly, the mycorrhizal phenotype of *Mtpt4* mutants can be suppressed by low nitrogen conditions (Javot et al., 2011). Based on these findings, it has been hypothesised that not only phosphate, but also nitrogen transfer to the plant acts as a signal to support arbuscule survival and maintain the symbiosis with AM fungi (Javot et al., 2011).

Although phosphate is thought to be the most important mineral nutrient transported in AM symbiosis, there is also evidence for substantial amounts of nitrogen being transferred to mycorrhized roots (Tanaka and Yano, 2005; Leigh et al., 2009). Labelling studies suggest that nitrogen is transported to the plant in the form of ammonium

(Govindarajulu et al., 2005; Cruz et al., 2007). Consistent with this, plant ammonium transporters have been identified that are transcriptionally induced in mycorrhized roots of several plant species (Gomez et al., 2009; Guether et al., 2009; Kobae et al., 2010; Koegel et al., 2013; Breuillin-Sessoms et al., 2015). Similar to the phosphate transporters, ammonium transporters localize to the periarbuscular membrane, further supporting the concept of the arbuscule being the main site of nutrient transfer to the plant (Kobae et al., 2010; Koegel et al., 2013; Breuillin-Sessoms et al., 2015).

In a recent study, the *M. truncatula* ammonium transporter 2 family protein AMT2-3 was found to be required for the suppression of premature arbuscule degeneration in nitrogen-deprived *Mtpt4* mutant roots (Breuillin-Sessoms et al., 2015). Remarkably, AMT2-3 is not able to complement a yeast ammonium transport mutant and is therefore unlikely to transport ammonium across the PAM. Instead, AMT2-3 has been speculated to have a signalling function to inform the plant about the nutrient status and accordingly regulate arbuscule maintenance. Similarly, the mycorrhizal-induced rice phosphate transporter *PT13* was suggested to function in sensing phosphate levels, as *PT13* does not seem to be able to transport phosphate, but is still required for proper arbuscule development (Yang et al., 2012). Together, these findings indicate that the arbuscule not only is the site of nutrient transfer, but might also provide a platform for symbiotic signalling to maintain AM symbiosis in the root (Javot et al., 2007; Oldroyd et al., 2009; Yang and Paszkowski, 2011; Yang et al., 2012; Breuillin-Sessoms et al., 2015).

The active transport of nutrients across a plant membrane requires energy, which is usually provided by an electrochemical gradient generated via proton transfer. In tobacco and *M. truncatula* roots, a proton ATPase has been identified that is expressed specifically in arbuscule-containing cells (Gianinazzi-Pearson et al., 2000; Krajinski et al., 2002). Two recent studies provide further details on the function of these symbiosis-induced proton pumps (Krajinksi et al., 2014; Wang et al., 2014). *M. truncatula* and rice plants mutated in the proton ATPase *HA1* display underdeveloped arbuscules and are impaired in the symbiotic transfer of phosphate to the plant. Furthermore, overexpression of *HA1* confirmed that it functions as a proton pump and is able to increase the negative potential of membranes (Wang et al., 2014). These results imply that proton ATPases are required to energize the PAM by forming an electrochemical potential, which in turn drives symbiotic nutrient exchange across the PAM (Krajinksi et al., 2014; Wang et al., 2014).

1.3.2 Nutrient transfer from the plant to the fungus

In exchange for obtaining water and mineral nutrients, plants transfer photosynthetically fixed carbon to AM fungi, which are obligate biotrophs and therefore depend entirely on the plant for a carbon source (Ho and Trappe, 1973; Shachar-Hill et al., 1995; Parniske, 2008). It is thought that up to 20% of plant photosynthates are allocated to the fungus (Bago et al., 2000). The carbon sink strength of roots is greatly increased upon mycorrhization, resulting in the redirection of photoassimilates towards mycorrhized roots and a significant accumulation of sugars and lipids (Wright et al., 1998). Consistent with this, sucrose cleaving enzymes such as sucrose synthase and invertases are transcriptionally upregulated during AM symbiosis, and knockdown or loss of these enzymes leads to impaired fungal colonization and arbuscule development in clover, tobacco, *M. truncatula* and tomato (Blee and Anderson, 1998; Wright et al., 1998; Hohnjec et al., 2003; Schaarschmidt et al., 2006; Baier et al., 2010). Furthermore, the mycorrhizal-induced sugar transporter *Mtst1* was found to be expressed in *M. truncatula* root tissues colonized by AM fungi. It has been proposed that this transporter functions in supplying the increased demand of mycorrhized root cells for sugars and/or in providing the fungus directly with hexoses (Harrison, 1996).

Several radiolabelling studies have investigated in which form fixed carbon is transferred to and taken up by the fungus. These studies suggest that hexoses, and in particular glucose, can be taken up by intraradical hyphae, but not by fungal spores or extraradical hyphae (Shachar-Hill et al, 1995; Solaiman and Saito, 1997; Pfeffer et al., 1999; Bago et al., 2000; Douds et al., 2000). The preferential use of glucose over sucrose by the fungus emphasizes the importance of apoplastic invertases and sucrose synthase in mycorrhized roots and proposes cleaved sucrose as a possible source of carbohydrates delivered to the fungus (Helber et al., 2011). The identification and characterization of the mycorrhizal-induced high-affinity monosaccharide transporter *MST2* from the AM fungus *Rhizophagus irregularis* has further advanced our understanding of carbon transfer in AM symbiosis (Helber et al., 2011). Complementation of a yeast transport mutant confirmed that MST2 is able to transport monosaccharides such as glucose, mannose, and fructose. Interestingly, MST2 was also found to efficiently transport plant cell wall monosaccharides, suggesting that sugars from the host cell wall, possibly originating from the PAS, might serve as an additional source of carbohydrates for the fungus (Helber et al., 2011). The expression pattern of

MST2 indicates that sugar uptake takes place in arbuscules and possibly also in intraradical hyphae, as transcripts were shown to be present in both fungal structures (Helber et al., 2011).

After sugars are taken up into the intraradical mycelium, they are incorporated into glycogen and the disaccharide trehalose, and these compounds are exported to the extraradical mycelium (Shachar-Hill et al., 1995; Pfeffer et al., 1996). The main carbon storage form of AM fungi, however, are triacylglycerols (TAGs), which constitute up to 70% of the dry weight of some fungal species (Beilby and Kidby, 1980). Large amounts of lipid droplets are present in all fungal structures, including arbuscules, hyphae, vesicles, and spores, where lipids are essential in providing energy for germination and hyphal growth (Bago et al., 2002). Considering the importance of lipids for AM fungi, it is surprising that extraradical hyphae and fungal spores do not seem to be capable of *de novo* fatty acid synthesis, as has been suggested based on radiolabelling studies (Pfeffer et al., 1999; Trépanier et al., 2005). It has been proposed that *de novo* fungal fatty acid synthesis takes place exclusively in intraradical hyphae in the root compartment, where the expression of fungal fatty acid synthase genes might be induced (Trépanier et al., 2005). However, a recent study investigating lipid biosynthesis and metabolism in *R. irregularis* did not find a gene encoding for a *de novo* fatty acid synthase in the genome of this fungus, implying that the fungus might lack the ability of *de novo* fatty acid synthesis entirely, even when associated with roots (Tisserant et al, 2013; Wewer et al., 2014). Based on these findings, it has been hypothesised that the plant provides reduced carbon not only in the form of sugars, but also in the form of lipids (Wewer et al., 2014).

1.4 The common symbiosis signalling pathway

The successful establishment of AM symbiosis in roots has long been known to require the activation of a chain of signalling events resulting in the extensive transcriptional reprogramming of host cells and the promotion of mycorrhizal colonization. The core to this signalling process is required for both the symbiosis with AM fungi and the root-nodule symbiosis, and has therefore become known as the common symbiosis signalling pathway (CSSP or common Sym pathway; Kistner and Parniske, 2002). A central component of the common Sym pathway is the induction of perinuclear calcium oscillations in the host cell in response to the recognition of symbiotic signals, such as

Myc factors from AM fungi and Nod factors released by rhizobial bacteria. This characteristic calcium response is believed to activate the calcium- and calmodulin-dependent serine/threonine protein kinase CCaMK and this in turn triggers the transcriptional changes downstream of the Sym pathway (Oldroyd, 2013). Plants carrying mutations in components of the common Sym pathway are typically unable to enter a successful symbiosis with AM fungi or rhizobial bacteria (Catoira et al., 2000; Kistner et al., 2005), highlighting the crucial role of this signalling pathway for the establishment of these symbioses.

High-frequency calcium oscillations are induced by diffusible fungal signals in root cells prior to the direct contact between fungal hyphae and the root (described in Section 1.2.1.2), indicating that the common SYM pathway is involved in the regulation of AM establishment already at pre-symbiotic stages of the symbiosis. Furthermore, several components of the common SYM pathway were shown to be required for PPA formation in epidermal cells (Genre et al., 2005). Interestingly, calcium spiking profiles were also found to change with the progressive colonization of the root by mycorrhizal fungi. Low-frequency calcium oscillations occur in outer cortical cells prior to infection, whereas the cell entry by fungal hyphae is associated with a transient switch to high-frequency calcium spiking (Sieberer et al., 2012). In addition, several members of the SYM pathway were suggested to play a role in arbuscule development based on their arbuscular phenotype (Kistner et al., 2005). Thus, the common Sym pathway appears to be crucial for the regulation of AM establishment not only before, but also during the infection by AM fungi.

1.4.1 Recognition of symbiotic signals at the plasma membrane of host cells

The receptors that recognize rhizobial-derived Nod factors at the plasma membrane of root cells are relatively well characterized. Two LysM (lysin motif) receptor-like kinases called NFR5 (Nod factor receptor 5) and NFR1 in *L. japonicus* and NFP (Nod factor perception) and LYK3 (LysM domain-containing receptor-like kinase 3) in *M. truncatula* were found to be required for Nod factor induced calcium spiking and are able to physically interact with Nod factors, providing evidence that these proteins act as the direct receptors of Nod factors (Wais et al., 2000; Ben Amor et al., 2003; Smit et al., 2007; Broghammer et al., 2012).

In *M. truncatula*, NFP was shown to also be involved in the Myc-LCO induced formation of lateral roots (Maillet et al., 2011), suggesting a role for this receptor in mycorrhizal signalling. While *nfp* mutants in *M. truncatula* and other legumes do not appear to be impaired in mycorrhization (Radutoiu et al., 2003; Arrighi et al., 2006; Indrasumunar et al., 2010; Zhang et al., 2015), RNA silencing of *NFP* in the non-legume plants *Parasponia andersonii* and *Solanum lycopersicum* leads to a reduction in fungal colonization and a defect in arbuscule formation (Op den Camp et al., 2011; Buendia et al., 2016). In legumes, the gene encoding for NFP has been duplicated, and the resulting paralog might act redundantly during AM symbiosis, perhaps explaining the lack of a mycorrhizal phenotype in legume *nfp* mutants (Op den Camp et al., 2011). In addition to NFR5/NFP in non-leguminous species, NFR1 in *L. japonicus* and its homologs LYK3 in *M. truncatula* and CERK1 in rice were found to also play a role in AM development, as the corresponding loss-of-function mutants display reduced levels of mycorrhizal colonization (Miyata et al., 2014; Zhang et al., 2015). OsCERK1 has previously been shown to be involved in the immune response to chitin (Shimizu et al., 2010). Based on these findings, it has been proposed that CERK1 acts as a common receptor for symbiotic and immune signalling (Miyata et al., 2014; Zhang et al., 2015). It is currently unclear how the LysM receptor-like kinases work together to recognize the range of different signalling molecules released by mycorrhizal fungi, and how this recognition differs from Nod factor recognition and immune signalling.

In addition to the LysM receptor-like kinases, another plasma-membrane localised protein called SYMRK (SYMBIOSIS RECEPTOR KINASE) in *L. japonicus* and DMI2 (DOESN'T MAKE INFECTIONS 2) in *M. truncatula* was found to be required for both mycorrhization and nodulation (Endre et al., 2002; Stracke et al., 2002; Wais et al., 2000). *SYMRK/DMI2* encodes an LRR (leucine-rich repeat) receptor-like kinase and has been proposed to act as a co-receptor of the Nod- and Myc-factor receptors during symbiosis signalling (Oldroyd, 2013). However, the exact function of this protein remains elusive.

1.4.2 Generation of symbiotic calcium oscillations in the nucleus

Calcium spiking in response to the recognition of fungal and rhizobial signals at the plasma membrane is predominantly associated with the perinuclear region of the cell. The incoming signal therefore has to be transduced to the nucleus to activate the nuclear calcium spiking machinery. Several candidates that could be involved in the production

of secondary messengers or activation of signalling cascades have been proposed, including a mevalonate synthase (HMGR1; Kevei et al., 2007), and a plant mitogen-activated protein kinase kinase (MAPKK; Chen et al., 2012). Both proteins were found to interact with SYMRK/DMI2 and to promote rhizobial associations (Kevei et al., 2007; Chen et al., 2012). In a recent study, HMGR1 has further been shown to be required for the induction of calcium spiking in response to rhizobial and mycorrhizal signals and to act downstream of NFP, but upstream of the nuclear calcium spiking machinery (Venkateshwaran et al., 2015). Interestingly, mevalonate, the product of HMGR1, appears to be sufficient to activate calcium oscillations in root epidermal cells of several species, further supporting a role of this secondary messenger in the common SYM pathway (Venkateshwaran et al., 2015).

For a long time, the identity of the channel that is responsible for the release of calcium during calcium spiking in response to symbiotic signals has been elusive. However, a recent study by Charpentier and colleagues has shown that three members of the cyclic nucleotide-gated channels (CNGCs), *CNGC15a*, *b*, and *c*, are required for the generation of symbiotic calcium oscillations in the nucleus (Charpentier et al., 2016). Plants carrying mutations in these channels display a reduced number of nodules and are impaired in AM symbiosis. Yeast complementation studies and the expression of the symbiotic CNGCs in *Xenopus laevis* oocytes further showed that these channels are permeable to calcium. Consistent with their role in nuclear calcium spiking, CNGC15a, b, and c localize to the nuclear envelope. Interestingly, the three CNGC15s were found to form a complex with the ion channel DMI1 in *M. truncatula* (Charpentier et al., 2016). Like the symbiotic calcium channel, DMI1 and its homologs POLLUX and CASTOR in *L. japonicus* are localized to the nuclear membrane and are indispensable for the induction of calcium spiking (Ané et al., 2004; Peiter et al., 2007; Charpentier et al., 2008; Capoen et al., 2011). These ion channels were found to be preferentially permeable to potassium, making them unlikely to be directly involved in the release of calcium during calcium spiking (Charpentier et al., 2008). Instead, mathematical modelling and yeast expression analyses suggest that DMI1/POLLUX and CASTOR might modulate the activity of the calcium channel (Peiter et al., 2007; Granqvist et al., 2012; Charpentier et al., 2016). Furthermore, potassium movement through DMI1/POLLUX and CASTOR could serve to counter-balance the calcium ions released from the lumen of the nuclear envelope and the ER, the proposed symbiotic calcium stores (Peiter et al., 2007; Capoen et al., 2011; Oldroyd, 2013).

In addition to the calcium and potassium channels, a calcium ATPase, MCA8, was shown to be part of the nuclear machinery required for calcium spiking (Capoen et al., 2011). This calcium pump localizes to the nuclear envelope and has been proposed to function in the re-uptake of released nuclear calcium ions (Capoen et al., 2011). Furthermore, three members of the nuclear pore complex in *L. japonicus*, NUCLEOPORIN85, NUCLEOPORIN133, and the scaffold nucleoporin NENA, are necessary for symbiotic calcium oscillations (Kanamori et al., 2006; Saito et al., 2007; Groth et al., 2010). While the exact role of the nuclear pore complex in the generation of calcium spiking remains unclear, it has been hypothesised that the complex might be involved in the transport of proteins required for calcium spiking to the nuclear envelope or in providing permeability for putative secondary messengers (Groth et al., 2010).

1.4.3 Perception and decoding of symbiotic calcium oscillations

M. truncatula DMI3 has been identified as a candidate protein for decoding symbiotic calcium spiking. Plants mutated in this gene are unable to form a symbiosis with either mycorrhizal fungi or rhizobial bacteria, yet the induction of calcium spiking is not affected (Catoira et al., 2000; Wais et al., 2000). This has placed DMI3 immediately downstream of calcium spiking. The *DMI3* gene encodes a protein belonging to the plant-specific class of CCaMKs (Lévy et al., 2004; Mitra et al., 2004). This class of proteins has a unique structure that allows them to bind calcium in two different ways. In addition to having a calmodulin-binding (CaM) domain next to an amino-terminal serine/threonine kinase domain, plant CCaMKs also possess three calcium-binding EF hands at their carboxyl terminus. These features enable CCaMK to be regulated by both calcium bound to calmodulin and free calcium. It has been proposed that during symbiosis signalling, the nuclear-localized CCaMK is able to decode calcium oscillations by undergoing a calcium dependent two step activation (Lévy et al., 2004). The generation of truncated versions of CCaMK and the introduction of point mutations has provided detailed information on the regulatory functions of the different domains and suggests that the regulation of this kinase is very complex, requiring both positive and negative regulatory mechanisms to allow a fully functional infection by the symbiont (Gleason et al., 2006; Tirichine et al., 2006; Hayashi et al., 2010; Liao et al., 2012; Shimoda et al., 2012; Miller et al., 2013; Routray et al., 2013). The threonine residue 271 located in the kinase domain of *M. truncatula* CCaMK (corresponding to threonine residue 265 in *L. japonicus*) was

found to be autophosphorylated upon calcium binding via the EF hands and to play a crucial role in the regulation of the protein, as mutating this residue leads to the autoactivation of CCaMK (Gleason et al., 2006; Tirichine et al., 2006; Miller et al., 2013). Consistent with these findings, it was shown that deletion or mutation of the EF hands results in an autoactive form of CCaMK (Miller et al., 2013). Based on these observations, it has been suggested that calcium-induced autophosphorylation of Thr-271 negatively regulates the kinase activity by stabilizing an inactive conformation of CCaMK (Miller et al., 2013). By contrast, binding of a CaM/calcium complex to the CaM binding domain blocks Thr-271 phosphorylation and induces a conformational change, thereby activating CCaMK (Takezawa et al., 1996; Miller et al., 2013). Interestingly, autophosphorylation of Thr-271 not only inactivates the kinase, but also primes CCaMK for activation by increasing its affinity for CaM (Sathyanarayanan et al., 2001). This is particularly intriguing with regard to a study showing that basal intracellular calcium levels are sufficient for the binding of calcium to the EF hands, whereas higher calcium concentrations are required for the binding of a CaM/calcium complex to the CaM binding domain (Swainsbury et al., 2012). Together, these findings provide a model for activation of CCaMK during calcium spiking, where basal levels of calcium inhibit CCaMK activity by calcium-induced autophosphorylation of Thr-271/265, while elevated calcium concentrations activate CCaMK for target phosphorylation by binding of CaM to the CaM binding domain (Miller et al., 2013). Two recent studies have provided evidence for additional negative regulation of CCaMK through two phosphorylation sites in the CaM binding domain (Liao et al., 2012; Routray et al., 2013). The inhibitory role of autophosphorylated residues in the CaM binding domain reveals a possible mechanism for the shutdown of CCaMK after the kinase has been activated by calcium spiking (Liao et al., 2012; Routray et al., 2013).

Autoactive CCaMK is able to trigger spontaneous nodule formation in *M. truncatula* and *L. japonicus* roots even in the absence of rhizobia or external rhizobial signals (Gleason et al., 2006; Tirichine et al., 2006). Intriguingly, a more recent study found that gain-of-function CCaMK not only induces the rhizobial signalling pathway, but also triggers the formation of host pre-infection structures required for the establishment of AM associations (Takeda et al., 2012). In addition, gain-of-function CCaMK was found to activate the expression of genes that are induced early during nodulation and mycorrhization (Gleason et al., 2006; Takeda et al., 2012). Mutant analyses showed that autoactive CCaMK is able to fully restore the symbiosis phenotype of loss-of-function

mutations in common Sym pathway genes upstream of CCaMK (Hayashi et al., 2012). These results highlight the central role of calcium spiking and its decoder CCaMK and imply that the primary role of symbiotic calcium oscillations is the activation of CCaMK (Hayashi et al., 2010; Madsen et al., 2010).

1.4.4 Transcriptional regulators downstream of CCaMK

The main output of the common Sym pathway is the transcriptional reprogramming of host cells. The establishment of root symbioses requires extensive changes in gene expression to ensure the proper accommodation of the symbiotic partners, and during both mycorrhization and nodulation, hundreds of genes have been found to be differentially expressed (Journet et al., 2001; Liu et al., 2003; Wulf et al., 2003; Manthey et al., 2004; Mitra et al., 2004; Weidmann et al., 2004; Hohnjec et al., 2005; Krajinski and Frenzel, 2007; Küster et al., 2007, Benedito et al., 2008; Gutjahr et al., 2008; Gomez et al., 2009; Hogekamp et al., 2011; Czaja et al., 2012; Breakspear et al., 2014; Roux et al., 2014; Camps et al., 2015; Handa et al., 2015; Hohnjec et al., 2015).

Although the same signalling pathway is activated upon recognition of mycorrhizal fungi and rhizobia, specificity in symbiosis signalling is maintained, resulting in either the promotion of fungal colonization or the formation of nodules. The developmental similarities and differences of both symbioses are reflected in the transcription patterns of host cells, with mycorrhization and nodulation inducing both common as well as specific sets of genes (Manthey and Krajinski 2004; Hohnjec et al., 2005; Küster et al., 2007). A study investigating the gene expression patterns of *M. truncatula* roots in response to individual Nod factors and Myc factors found that all individual LCOs tested (Nod factors, S-LCOs, NS-LCOs, and a mix of S-LCOs and NS-LCOs) are able to trigger specific transcriptional changes in addition to activating a common set of genes, suggesting that the plant is capable of discriminating between these individual signalling molecules, even though the structures of some of these signals are extremely similar, and many of the same receptors appear to be involved in their recognition (Wais et al., 2000; Ben Amor et al., 2003; Smit et al., 2007; Broghammer et al., 2012; Czaja et al., 2012; Op den Camp et al., 2011; Miyata et al., 2014; Zhang et al., 2015).

The majority of transcriptional changes require signalling through the common Sym pathway, as gene induction upon mycorrhization and nodulation is dramatically reduced

by loss-of-function mutations in Sym pathway components (Kistner et al., 2005; Takeda et al., 2011; Czaja et al., 2012). The importance of the common Sym pathway in symbiosis-induced gene expression is further highlighted by the observation that autoactive CCaMK is able to trigger the induction of a number of symbiotic genes (Gleason et al., 2006; Takeda et al., 2012). Meanwhile, several studies have provided evidence for Sym pathway-independent gene induction, indicating that parallel signalling pathways must act during symbiosis (Kosuta et al., 2003; Siciliano et al., 2007; Gutjahr et al., 2008; Kuhn et al., 2010). It is likely that these parallel signalling pathways contribute to the observed specificity in the transcriptional response to mycorrhizal fungi and rhizobia. A recent study has identified some components of a putative parallel signalling pathway required for the establishment of AM symbiosis. This pathway involves the rice receptor DWARF14LIKE (D14L), which has been shown to be essential for the recognition of mycorrhizal fungi at the pre-symbiotic stage of the symbiosis (Gutjahr et al., 2015). Fungal colonization and the transcriptional changes in response to germinated spore exudates of AM fungi are almost completely abolished in a *d14l* deletion mutant. D14L is known to act together with the F-box protein MAX2/DWARF3 (D3; Nelson et al., 2011), and consistent with this, the rice *d3* mutant was found to be strongly impaired in mycorrhization (Gutjahr et al., 2015). The ligand that is bound by D14L in the context of AM symbiosis is currently unknown, and it remains to be investigated whether there is a crosstalk between this D14L pathway and components of the common Sym pathway.

A large number of transcriptional regulators have been identified that are involved in the transcriptional reprogramming during AM development and act downstream of calcium spiking and decoding by CCaMK. A key transcription factor is a nuclear coiled-coil protein called IPD3 (INTERACTING PROTEIN OF DMI3) in *M. truncatula* (CYCLOPS in *L. japonicus*), which is required for the successful establishment of both the mycorrhizal and the root-nodule symbiosis (Messinese et al., 2007; Yano et al., 2008). In addition, the family of the GRAS-domain proteins have emerged as important transcriptional regulators, particularly during the establishment of AM symbiosis, although some of these proteins are also involved in regulating gene expression during nodulation.

1.4.4.1 IPD3/CYCLOPS

Genetic screens and interaction studies have identified IPD3/CYCLOPS as an interaction partner and phosphorylation substrate of CCaMK (Messinese et al., 2007; Yano et al., 2008). IPD3/CYCLOPS is essential for the development of both the AM and the root-nodule symbiosis, but similar to CCaMK, it is not required for the induction of symbiotic calcium oscillations (Kistner et al., 2005; Miwa et al., 2006). In *L. japonicus*, mutations in this gene result in an impaired intracellular infection by AM fungi, with fungal hyphae showing abnormal swelling in the epidermis and cortex and a failure to develop arbuscules in the cortex (Yano et al., 2008). In addition, *CYCLOPS* was found to be important for infection thread formation during root nodule symbiosis. While *M. truncatula* IPD3 also plays a role in infection thread progression during nodulation, the phenotype of *ipd3* mutants is much weaker for nodule organogenesis and AM development than *L. japonicus cyclops* mutants, perhaps implying a degree of redundancy for this gene function in *M. truncatula* (Horváth et al., 2011; Ovchinnikova et al., 2011). An orthologue of *IPD3* has also been identified in rice, where it was found to be required for mycorrhization (Chen et al., 2008; Gutjahr et al., 2008).

For a long time, the exact role of CYCLOPS during symbiosis signalling was not known; however, a recent study by Singh and colleagues has shed light on the function of this protein. It has been shown that CYCLOPS is able to directly bind DNA and acts as a transcription factor to induce the expression of *NIN* (*NODULE INCEPTION*), a gene playing a key role in nodulation (Schauser et al., 1999; Singh et al., 2014). CCaMK was found to phosphorylate two serine residues of CYCLOPS, resulting in the activation of CYCLOPS (Singh et al., 2014). Intriguingly, phosphomimetic replacement of the two serine residues results in a gain-of-function version of CYCLOPS (CYCLOPS-DD) that is able to trigger not only *NIN* expression, but also spontaneous nodule formation in the absence of rhizobia similar to autoactive CCaMK (Singh et al., 2014). In addition to regulating *NIN*, CYCLOPS has recently been found to also induce the expression of a GRAS-domain protein called *RAM1 (REQUIRED FOR ARBUSCULAR MYCORRHIZATION 1)*, which itself acts as a transcriptional regulator and is specifically involved in AM symbiosis (Gobbato et al., 2012; Pimprikar et al., 2016). The overexpression of *RAM1* in *cyclops* mutants restores the arbuscular defect, further confirming that RAM1 acts downstream of CYCLOPS (Pimprikar et al., 2016). These results provide a direct link between the activation of CCaMK by symbiotic calcium oscillations and the downstream induction of gene expression by CCaMK-regulated transcription factors.

1.4.4.2 GRAS-domain proteins

GRAS-domain proteins belong to a large family of plant-specific proteins that are characterized by the presence of a conserved GRAS domain at their C-terminus (Bolle, 2004). The GRAS domain consists of several motifs, namely two leucine-rich repeat motifs (LHRI and LHRII), a VHIID motif, a PFYRE motif, and a SAW motif (all termed after the most conserved amino acid residues present in these motifs). In contrast to the relatively well conserved C-terminus, the N-terminus of GRAS-domain proteins is highly variable. GRAS-domain proteins were named after the first three members identified (GAI, RGA and SCR) and function in a range of different plant processes, including gibberellic acid signalling, root and shoot development, abiotic stress, and light signalling (Bolle, 2004).

Two members of the GRAS-domain protein family in legumes, NSP1 (NODULATION SIGNALLING PATHWAY 1) and NSP2, play an essential role in symbiosis signalling (Catoira et al., 2000; Wais et al., 2000; Oldroyd and Long 2003; Kaló et al., 2005; Smit et al., 2005). Both the *nsp1* and the *nsp2* mutant are unable to form infection threads and nodules and have a dramatically reduced capability to induce symbiotic gene expression (Catoira et al., 2000), however, they are not affected in the induction of calcium spiking (Wais et al., 2000; Oldroyd and Long 2003). NSP1 and NSP2 were shown to act as transcription factors through the formation of a heteromeric complex that induces the expression of early nodulation genes such as *ENOD11*, *ERN1* and *NIN* (Hirsch et al., 2009; Cerri et al., 2012). *In vitro* DNA binding studies demonstrated that the two LHR motifs in NSP1 are involved in the direct binding of this protein to the promoter sequences of symbiotic genes (Hirsch et al., 2009). Importantly, NSP1 was found to require NSP2 to be able to bind to these target promoters *in vivo* (Hirsch et al., 2009), and only the complex of NSP1 and NSP2, but not NSP1 by itself, was reported to induce gene expression in a transient reporter system in *Nicotiana benthamiana* (Cerri et al., 2012). In line with this, introducing a point mutation in NSP2 that reduces the interaction with NSP1 also leads to a reduction in nodule number, further highlighting the importance of the NSP1-NSP2 complex formation for the root-nodule symbiosis (Hirsch et al., 2009). Notably, NSP1 and NSP2 seem to be functionally conserved in non-legumes, because the rice homologs OsNSP1 and OsNSP2 are able to fully complement the nodulation phenotype of the corresponding *L. japonicus* mutants (Yokota et al., 2010). More recently, it has been discovered that NSP1 and NSP2 also play a role in mycorrhization; *nsp1* and *nsp2* single mutants as well as *nsp1nsp2* double mutants show decreased levels

of mycorrhizal colonization when inoculated with a weak mycorrhizal inoculum, although arbuscule development appears normal (Liu et al., 2011; Maillet et al., 2011; Delaux et al., 2013). In *M. truncatula* and rice, both *NSP* genes were found to be required for the expression of *D27*, a gene involved in strigolactone biosynthesis (Liu et al., 2011). As mutations in strigolactone biosynthesis genes in tomato and pea similarly reduce the level of root mycorrhization (Gomez-Roldan et al., 2008; Koltai et al., 2010), it has been proposed that NSP1 and NSP2 regulate AM development at least partly through their direct control of strigolactone levels (Liu et al., 2011). Interestingly, the regulation of strigolactone biosynthesis by NSP1 and NSP2 seems to be independent of the common Sym pathway, indicating that NSP1 and NSP2 might be activated by an alternative signalling pathway (Liu et al., 2011). Recent studies have also provided evidence for more direct roles of NSP1 and NSP2 in Myc factor signalling, with *NSP2* being involved in NS-LCO induced lateral root growth (Maillet et al., 2011), and *NSP1* being required for the induction of three mycorrhizal genes in response to NS-LCOs (Delaux et al., 2013).

The first transcription factor that was found to function specifically in mycorrhizal signalling was RAM1 (Gobbato et al., 2012). RAM1 is a member of the GRAS-domain protein family and shows a strong transcriptional induction in mycorrhized roots (Gobbato et al., 2012, 2013). Plants mutated in *RAM1* display severely reduced levels of fungal colonization with a decreased number of hyphopodia at the root surface and small, undeveloped arbuscules in the cortex (Gobbato et al., 2012; Gobbato et al., 2013). Similar to *NSP2, RAM1* was found to be essential for Myc-LCO induced root branching (Maillet et al., 2011; Gobbato et al., 2012). However, *RAM1* is not required for Nod factor induced gene expression and lateral root growth, suggesting that RAM1 acts specifically in mycorrhizal signalling. The only confirmed direct target gene of RAM1 to date is the glycerol-3-phosphate acyltransferase *RAM2*, which has been proposed to be involved in the biosynthesis of cutin monomers that act as signalling molecules to the fungus and promote the formation of hyphopodia at the root surface (Wang et al., 2012; described in Section 1.2.1.1). Two recent studies have suggested that RAM1 is also involved in the regulation of several genes important for arbuscule development, including *STR* and *EXO70I*, but it is not yet clear whether these genes are directly or indirectly regulated by RAM1 (Rich et al., 2015; Park et al., 2015). Using bimolecular fluorescence complementation assays, RAM1 was shown to be able to form a complex with NSP2. Based on these findings, it was proposed that analogous to the NSP1-NSP2 complex in

nodulation, RAM1 and NSP2 act together to regulate the expression of mycorrhizal genes (Gobbato et al., 2012).

Recent results from a study in *L. japonicus* indicate that another GRAS-domain protein called RAD1 (REQUIRED FOR ARBUSCULE DEVELOPMENT 1) is important for fungal colonization and arbuscule development (Xue et al., 2015). Due to the high occurrence of degenerated arbuscules in *rad1* mutants, it has been suggested that RAD1 is required for maintaining the mycorrhizal symbiosis (Park et al., 2015; Xue et al., 2015). Interestingly, RAD1 is able to form a complex with RAM1 and NSP2 *in vivo* and has therefore been proposed to contribute to the regulation of mycorrhizal genes such as *RAM2* (Xue et al., 2015).

A number of additional GRAS-domain proteins were found to be involved in mycorrhization. Amongst them are the DELLA proteins, originally discovered for their function as repressors in gibberellic acid signalling. Studies in *A. thaliana* and rice have shown that DELLAs interact with and inhibit a range of different transcription factors (Gao et al., 2011). Upon perception of gibberellic acid, DELLA proteins are targeted for degradation, which relieves the repression on their interaction partners and allows for the induction of changes in gene expression. In *M. truncatula* and rice, DELLA proteins were found to be required for arbuscule formation during AM symbiosis, but do not appear to be involved in the formation of hyphopodia (Floss et al., 2013; Yu et al., 2014). In accordance with the antagonizing function of DELLAs and gibberellic acid, it was shown that while DELLA proteins play a positive regulatory role in AM development, exogenously applied gibberellic acid represses fungal colonization and arbuscule formation. In addition, mutants deficient in gibberellic acid display increased levels of mycorrhization in pea, *M. truncatula* and rice (Floss et al., 2013; Foo et al., 2013; Yu et al., 2014). Meanwhile, it has also been reported that gibberellic acid accumulates in roots during mycorrhization, suggesting that gibberellic acid has both negative and positive effects on the colonization of host roots by AM fungi (Takeda et al., 2015). DELLA proteins have recently been proposed to act upstream of *RAM1*, as the ectopic overexpression of *RAM1* is sufficient to restore arbuscule formation in roots treated with gibberellic acids (Pimprikar et al., 2016). In line with this observation, it was found that DELLA proteins are able to form a complex with CCaMK and CYCLOPS to enhance the transcriptional induction of *RAM1* (Pimprikar et al., 2016). Furthermore, the overexpression of a constitutively active DELLA protein leads to the transcriptional induction of *RAM1* in the absence of mycorrhizal fungi (Park et al., 2015). These findings

suggest that the expression of *RAM1* is regulated by both symbiotic signalling through CCaMK and CYCLOPS and gibberellic acid signalling through the DELLA proteins.

A study in rice identified DIP1 (DELLA INTERACTING PROTEIN 1) as an interaction partner of the single rice DELLA protein SLR1 (Yu et al., 2014). DIP1 is also a member of the GRAS-domain protein family and RNAi knockdown of this gene results in a decrease in mycorrhizal colonization (Yu et al., 2014). Interestingly, DIP1 was found to form a complex with rice and *M. truncatula* RAM1, while RAM1 itself does not directly interact with DELLA proteins (Yu et al., 2014). These observations reveal a possible physical link between the NSP2/RAD1/RAM1 complexes and the DELLA proteins.

A GRAS-domain protein called MIG1 (MYCORRHIZA-INDUCED GRAS 1) has recently been found to regulate radial cell expansion in the cortex to enable proper arbuscule formation in *M. truncatula* roots (Heck et al., 2016). Consequently, arbuscule development is impaired when *MIG1* is transcriptionally silenced. Intriguingly, MIG1 appears to be able to interact with DELLA1, and it has been proposed that a MIG1-DELLA1 complex regulates root development to accommodate the fungal infection structures during AM symbiosis (Heck et al., 2016). MIG1 belongs to a novel clade of GRAS-domain proteins that is absent in the non-host *A. thaliana*, and several members of this clade are transcriptionally upregulated during mycorrhizal colonization, suggesting that additional GRAS-domain proteins could play a role in AM development (Heck et al., 2016).

The characterisation of plants carrying mutations in the DELLAs show that these proteins not only act during the establishment of AM symbiosis, but are also required for infection thread formation and nodule development in the symbiosis with rhizobial bacteria (Jin et al., 2016; Fonouni-Farde et al., 2016). Interestingly, DELLA proteins were shown to interact with NSP2 and enhance the induction of *ERN1* by the NSP1-NSP2 complex in a transactivation assay in *A. thaliana* protoplasts (Jin et al., 2015; Fonouni-Farde et al., 2016). Thus, DELLAs appear to be involved in several transcription factor complexes that regulate gene expression during the establishment of both mycorrhization and nodulation.

Together, these findings show that a large number of GRAS-domain proteins are required for the establishment of the AM association, and all of them form multicomponent complexes with other members of the GRAS-domain protein family. In the root-nodule symbiosis, the complex formation of NSP1 and NSP2 has been shown to

be essential for the upregulation of rhizobial-responsive genes such as *ERN1* and *ENOD11* (Hirsch et al., 2009; Cerri et al., 2012). It is likely that in a similar way, complex formation is a pre-requisite for the function of GRAS-domain proteins during mycorrhization, and that different complexes function during different stages of mycorrhization to achieve the required stage and cell type-specific transcriptional reprogramming of host cells (Figure 1.2). However, all of the protein-protein interactions described above were tested in heterologous systems, and not in *M. truncatula* roots. Thus, more research is required to investigate the relevance of complex formation for the activity of different GRAS-domain proteins under symbiotic conditions and in different tissues and cell types.

1.4.4.3 Other transcription factors involved in mycorrhization

Gene expression analyses of mycorrhized plants and roots treated with Myc factors have led to the identification of a large number of putative transcription factors that are induced upon colonization by AM fungi and might play a role in the regulation of mycorrhizal genes. Amongst these are proteins belonging to a range of different transcription factor classes, including CCAAT-binding, MYB, AP2/ERF, WRKY, and ARF domain transcription factors (Gomez et al., 2009; Hogekamp et al., 2011; Gaude et al., 2012; Schaarschmidt et al., 2013; Xue et al., 2015). These findings suggest that numerous transcriptional regulators are involved in the reprogramming of host cells during mycorrhization. However, how and at which stages these putative transcription factors function in symbiosis signalling and whether they are specific to mycorrhization or are also involved in nodulation remains elusive.

1.5 Research objectives

Research in recent years has uncovered a critical role for members of the GRAS-domain protein family in the transcriptional reprogramming of roots during the establishment of the symbiosis between plants and AM fungi. Many of these transcription factors were found to form multicomponent protein complexes. For example, NSP1 and NSP2 have previously been shown to physically interact, and this complex formation appears to be crucial for the establishment of the root-nodule symbiosis with rhizobia. NSP2 was also found to interact with RAM1, a transcription factor that is specifically involved in AM symbiosis. These findings raise the question whether these three GRAS-domain proteins regulate the same or different sets of genes during AM development.

The aim of this project was to characterise the functions of *NSP1*, *NSP2* and *RAM1* in the transcriptional regulation of roots during mycorrhization to gain insights into the mycorrhizal processes that are regulated by these transcription factors. In order to get a better understanding of the developmental stages during which *NSP1*, *NSP2*, and *RAM1* are active, the mycorrhizal phenotypes of the corresponding loss-of-function mutants were assessed in detail in a time course experiment (Chapter 2). The roles of these transcription factors in the regulation of global gene expression were examined by transcriptional profiling of wild-type plants and loss-of-function mutants at several time points during mycorrhization. In addition, the functions of *NSP1*, *NSP2*, and *RAM1* in the regulation of gene expression in the absence of mycorrhizal fungi were investigated (Chapter 3). This approach led to the identification of a large number of novel candidates for genes that might be under the direct or indirect control of the GRAS-domain proteins. An in-depth functional analysis of these potential target genes was performed to gain further insights into the mycorrhizal processes that are regulated by *NSP1*, *NSP2*, and *RAM1*. In addition, several tools were developed to investigate whether these putative target genes are directly or indirectly regulated by the GRAS-domain proteins (Chapter 4 and 5).

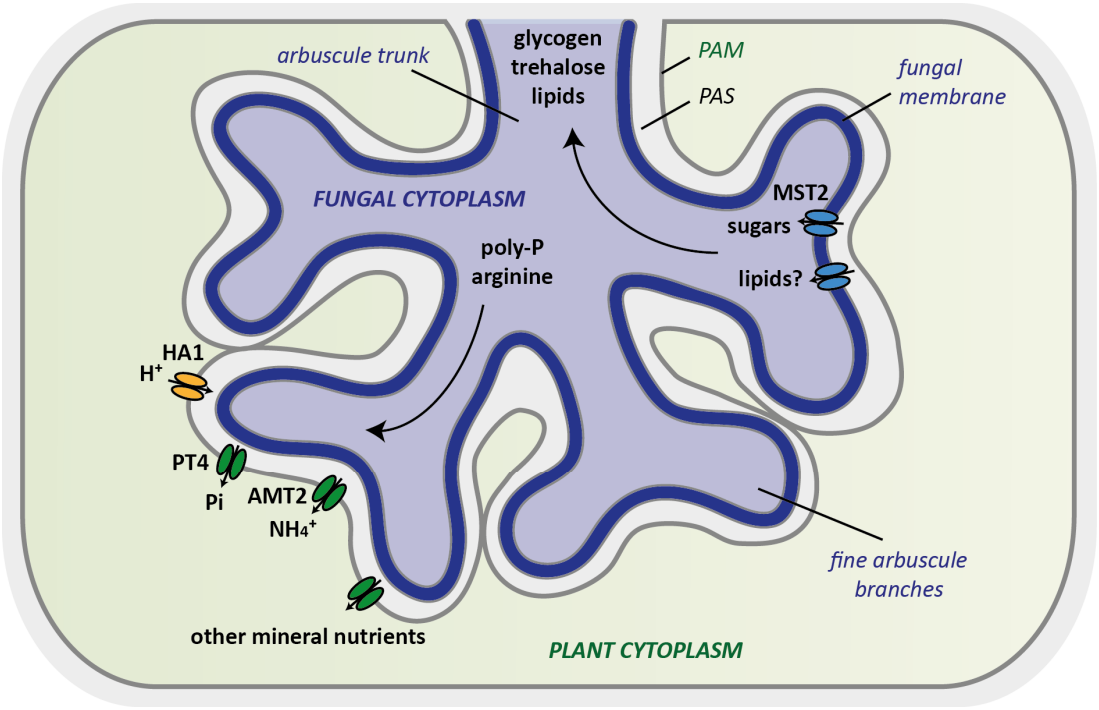

Figure 1.1: Arbuscules are the site of nutrient exchange between the plant and the fungus during AM symbiosis. Fungal hyphae form extensively branched structures called arbuscules in inner cortical cells of plant roots. Arbuscules consist of a broad arbuscule trunk and fine arbuscule branches. The fungal hyphae are surrounded by a plant membrane called the periarbuscular membrane (PAM). The area between the PAM and the fungal hyphae has been named the periarbuscular space (PAS) and contains amorphously structured plant cell-wall material. The fungus delivers mineral nutrients such as phosphate, ammonium, and sulphate to the plant. Within fungal hyphae, phosphate and ammonium are transported in the form of poly-phosphates (poly-P) and arginine, respectively. In *M. truncatula*, the PAM-localised protein PT4 is required for phosphate (Pi) transport to the plant. Ammonium transporters of the AMT2 family are likely to be involved in the transport of ammonium (NH_4^+) across the PAM. The proton (H^+)-ATPase HA1 is thought to be involved in producing a proton gradient across the PAM to provide energy for the uptake of nutrients. In return for receiving mineral nutrients, plants provide the fungus with fixed carbon in the form of sugars. The fungal sugar transporter MST2 is expressed in arbuscule containing cells and is likely to be involved in the uptake of sugars from the PAS. In addition to sugars, lipids have been proposed to be delivered to fungal hyphae, however, the transporters involved in this process have not been identified yet.

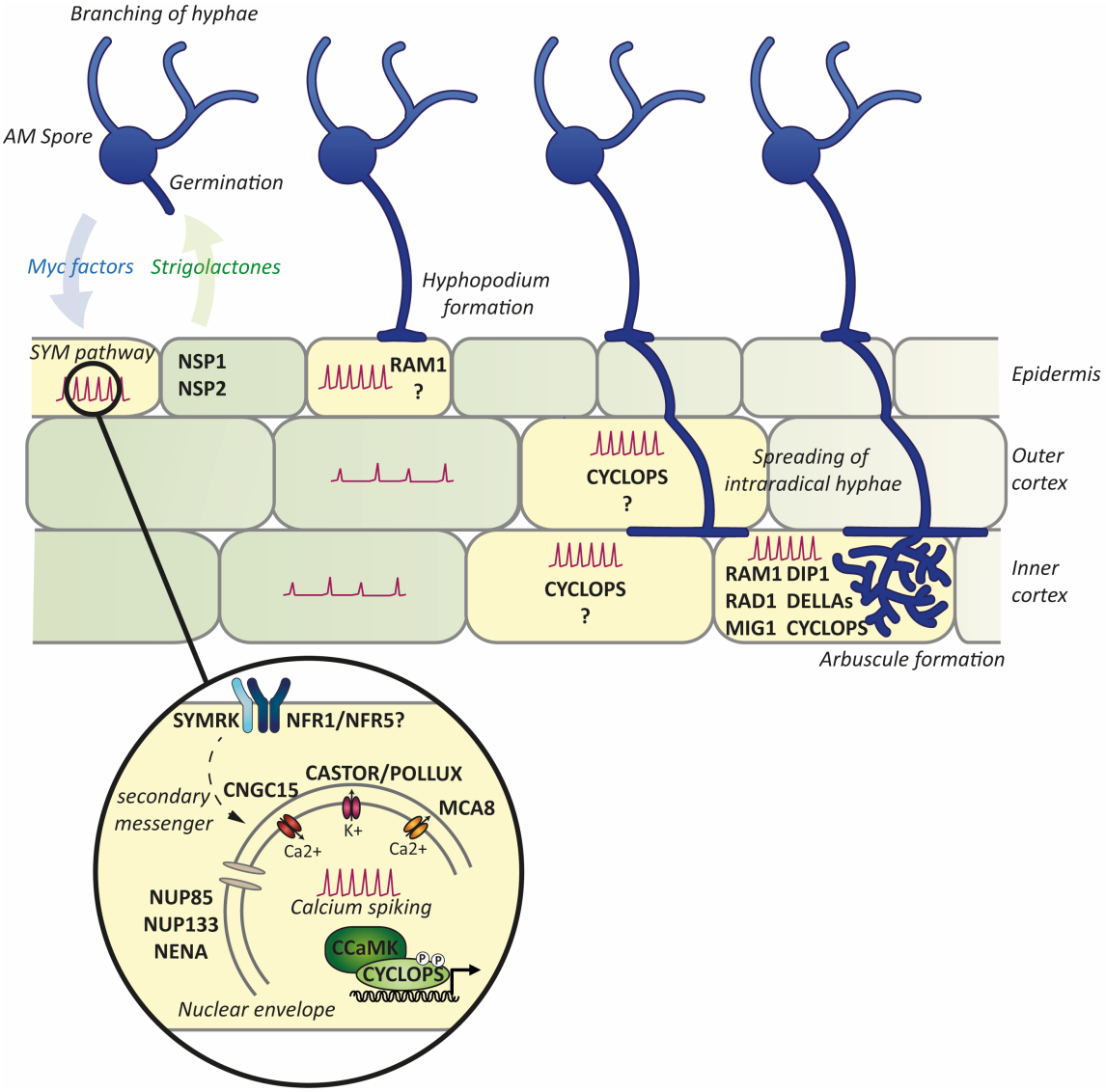

Figure 1.2: The common Sym pathway and downstream transcription factors mediate the transcriptional reprogramming of roots during different stages of AM development. Plant roots release strigolactones, which induce arbuscular mycorrhizal (AM) spore germination and branching. The transcription factors NSP1 and NSP2 are required for strigolactone production. In turn, AM fungi release signalling molecules called Myc factors. These are recognized at the plasma membrane by NFR1 and potentially NFR5, both of which interact with SYMRK. Three members of the cyclic nucleotide-gated channels CNGC15s, the potassium channels CASTOR and POLLUX, the calcium ATPase MCA8, NUP85, NUP133, and the nucleoporin NENA are involved in the generation of calcium spiking. The calcium response is decoded by CCaMK, which phosphorylates and thereby activates the transcription factor CYCLOPS. RAM1 is required at the stage of hyphopodium formation at the root epidermis. CYCLOPS is important during the spreading of intraradical hyphae in the cortex. RAM1, RAD1, DIP1, MIG1, DELLAs and CYCLOPS are required for arbuscule development in the inner cortex of the root (adapted from Luginbuehl and Oldroyd, 2016).

CHAPTER 2

Comparative analysis of mycorrhizal colonization in the GRAS protein mutants *ram1-1*, *nsp1-1,* and *nsp2-2*

2.1 Introduction

AM development is initiated by plant roots releasing strigolactones, which induce fungal spore germination and branching of hyphae, thus directing fungal growth towards the roots (Akiyama et al., 2005; Besserer et al., 2006). Upon contact of the hyphae with the root epidermis, the fungus forms attachment structures called hyphopodia. In a highly regulated process, the hyphae enter epidermal cells and spread within the root to eventually form arbuscules in the inner cortex, where nutrients are exchanged between the two symbionts (Harrison, 2012). The colonization of roots by *Glomus* species is accompanied by the appearance of lipid-rich vesicles, which serve as energy storage units for the fungus (Dickson, 2004). With the development of extraradical mycelia and the formation of new spores, the fungal life cycle is completed.

In recent years, forward and reverse genetic approaches have identified many plant genes involved in the development and regulation of mycorrhization. Mutations in these

genes lead to an impaired or altered colonization by the fungus, and the nature of the resulting phenotype is typically indicative of the function of the gene carrying the mutation. For example, mycorrhization is generally blocked at very early stages in common SYM pathway mutants such as *dmi3* (Catoira et al., 2000). By contrast, the loss of function of the symbiotic phosphate transporter *PT4* in *M. truncatula* does not affect the initiation and early stages of the symbiosis, but leads to the premature senescence of arbuscules (Javot et al., 2007).

RAM1 was first discovered to be involved in mycorrhization based on the phenotype of a deletion mutant in *M. truncatula* (Gobbato et al., 2012). Fungal colonization in the *ram1* mutant is almost entirely absent and the number of hyphopodia strongly reduced compared to the wild type. In addition, a weaker mutant allele of *RAM1* displays small, undeveloped arbuscules in instances where colonization of the inner cortex is successful, suggesting that *RAM1* plays a role in arbuscule formation (Gobatto et al., 2013). Importantly, all of these observations were made at late time points during mycorrhization, when the symbiosis was already fully established in wild-type plants. It is therefore unclear whether *ram1* also shows defects in mycorrhization at earlier time points, when fungal colonization is initiated.

NSP1 and *NSP2* were initially thought to specifically function in Nod factor signalling and nodulation, as the respective mutants did not show a defect in fungal colonization (Catoira et al., 2000; Wais et al., 2000; Oldroyd and Long, 2003; Kaló et al., 2005; Smit et al., 2005, Murakami et al., 2006; Heckmann et al., 2006). It was only later that these two proteins were found to play a role in mycorrhization, when weak mycorrhizal inocula were used to assess the phenotypes of the respective mutants. Both *nsp1* and *nsp2* show a reduction in total fungal colonization at late time points (Maillet et al., 2011; Lauressergues et al., 2012; Delaux et al., 2013). However, early time points have not been analysed in these mutants, and no detailed analyses of the individual infection structures have been reported.

The aim of the research presented in this chapter was to investigate the mycorrhizal phenotypes of the GRAS protein mutants *ram1-1*, *nsp1-1* and *nsp2-2* in detail to gain a better understanding of the developmental stages and processes that might be regulated by these transcription factors. In order to be able to compare the observed phenotypes, the different mutants were tested in parallel using the same fungal inoculum and growth conditions, as these factors strongly influence the efficiency and dynamics of fungal colonization. Taking into account that the phenotype of a mutant often depends on the

time point at which mycorrhization is assessed, the characterisation of the phenotypes was extended to include not only late, but also early and intermediate time points.

2.2 Results

2.2.1 *ram1-1* is transiently colonized by AM fungi and unable to form fully developed arbuscules at any time point during AM establishment

To assess the phenotypes of the GRAS protein mutants, fungal infection structures (hyphopodia, intraradical hyphae, arbuscules, and vesicles) were quantified in wild-type and mutant plants in a mycorrhizal time course experiment at 8 days post inoculation (dpi), 13 dpi and 27 dpi (Figure 2.1). At the earliest time point, the first signs of colonization were visible in wild-type roots, with hyphopodia being the predominant infection structure, and relatively few arbuscules or vesicles being present. At 13 dpi, fungal colonization in wild-type roots was only slightly more advanced, while at 27 dpi, arbuscules were present in the majority of the root segments tested and the symbiosis with the fungus was fully established.

Compared to the wild type, *ram1-1* showed a slight, but not statistically significant reduction of hyphopodia at 8 dpi (Figure 2.1). The quantification of fungal infection structures in *ram1-1* was repeated multiple times for very early time points, and a slight reduction in the number of hyphopodia was always visible, although the statistical significance was variable, suggesting that hyphopodia formation is only weakly affected in *ram1-1* at early time points (Figure 2.2). The reduction in the number of hyphopodia was more pronounced and significant at 13 dpi and 27 dpi (Figure 2.1). Interestingly, the percentage of hyphopodia decreased between 13 dpi and 27 dpi in *ram1-1*, while it increased in the wild type. The same trend was also visible for the number of vesicles, suggesting that fungal colonization in *ram1-1* is gradually lost at later time points. Strikingly, *ram1-1* roots did not seem to form arbuscules at any of the tested time points. To investigate this further, roots of all three time points were stained with Alexa Fluor 488 wheat germ agglutinin (WGA), and the appearance of fungal infection structures was observed under the fluorescence microscope (Figure 2.3, 2.4, and 2.5). This analysis revealed that *ram1-1* was not able to form fully developed arbuscules as they occur in wild-type plants. Instead, small, undeveloped arbuscules were present in cortical cells. These tiny arbuscules resembled thick, intraradical hyphae when roots were stained

with ink and were therefore quantified as such, resulting in the significant increase in abundance of intraradical hyphae in *ram1-1* compared to the wild type at 13 dpi (Figure 2.1). Taken together, the presence of hyphopodia, intraradical hyphae and vesicles in *ram1-1*, particularly at earlier time points, suggests that the mutant is transiently colonized by mycorrhizal fungi. However, the observed decrease in mycorrhization at 27 dpi indicates that the symbiosis is not maintained, leading to a loss of fungal colonization at later time points.

Next, I investigated whether the *ram1-1* mutant phenotype, specifically arbuscule development and low colonization levels at late time points, could be complemented by inoculation with a strong nurse plant inoculum. At 32 dpi, the wild type exhibited a fungal colonization level of around 85 %, while *ram1-1* was only slightly less colonized (70%), indicating that the presence of nurse plants allows the symbiosis in *ram1-1* roots to be maintained even at late time points (Figure 2.6). However, arbuscule formation was still impaired in the mutant and could not be complemented by nurse plants, suggesting that RAM1 plays a direct role in the regulation of arbuscule development.

2.2.2 Fungal colonization in *nsp1-1* is reduced at both early and late time points during mycorrhization

The abundance of most fungal infection structures, including hyphopodia, arbuscules, and vesicles, was reduced in *nsp1-1* by approximately 50% at 8 dpi compared to the wild type (Figure 2.1). This trend continued at 13 dpi, although the reduction was slightly less pronounced, and persisted at 27 dpi. Interestingly, even though the extent of colonization was reduced in *nsp1-1* roots, the fungal infection structures, including arbuscules, appeared normal at all three time points when assessed under the microscope, suggesting that the development of mycorrhizal structures is not impaired in *nsp1-1* (Figure 2.3, 2.4, and 2.5). Consistent with this, the abundance of all fungal infection structures increased over time in *nsp1-1* at a similar rate as in the wild type. These results indicate that *NSP1* is not required for the normal development of the symbiosis within the root. Instead, the colonization pattern suggests that the onset of fungal colonization in *nsp1-1* might be delayed, while colonization proceeds normally once the fungus is inside the root.

2.2.3 Mycorrhization in *nsp2-2* is not impaired at any of the time points tested but might be affected at later time points

Unlike *ram1-1* and *nsp1-1*, *nsp2-2* did not show any quantitative or qualitative differences in mycorrhization compared to the wild type under the conditions tested here. No significant reduction in the abundance of mycorrhizal structures was observed in *nsp2-2* roots at any of the assessed time points (Figure 2.1), and the fungal infection structures appeared normal under the fluorescence microscope (Figure 2.3, 2.4, and 2.5). Interestingly, the number of arbuscules and vesicles did show a slight trend towards a reduction compared to the wild type at 27 dpi (Figure 2.1). While this difference was not statistically significant, it seems possible that *NSP2* might play a role at later time points during mycorrhization, and it would be interesting to test whether fungal colonization is reduced in *nsp2-2* at time points later than 27 dpi.

2.3 Discussion

In this chapter, the functions of *RAM1*, *NSP1* and *NSP2* in AM development were investigated by assessing the mycorrhizal phenotypes of the respective mutants in detail in a time course experiment. While both *ram1-1* and *nsp1-1* displayed a significant reduction in mycorrhizal colonization, the analysis also revealed key differences between the mutant phenotypes.

The findings of a previous study showed that the deletion of the gene encoding for RAM1 in *M. truncatula* causes very low levels of mycorrhization and a drastically reduced number of hyphopodia at 6 weeks after inoculation with fungal spores (Gobbato et al., 2012). The results presented here indicate that at earlier time points, the fungus is able to transiently colonize *ram1-1*, with the number of hyphopodia and vesicles being only slightly reduced in the mutant compared to the wild type. At late time points, the level of mycorrhization was strongly impaired in *ram1-1*. Recent studies assessing the phenotype of *ram1* mutants in *P. hybrida*, *L. japonicus* and *M. truncatula* confirm these findings (Park et al., 2015; Rich et al., 2015; Xue et al., 2015; Pimprikar et al., 2016). The loss of fungal colonization at later time points is likely caused by the inability of *ram1-1* to form fully developed arbuscules, a defect that was also observed in weaker *ram1* mutant alleles in *M. truncatula* and in *P. hybrida* and *L. japonicus ram1* mutants (Gobbato et al., 2013; Park et al., 2015; Rich et al., 2015; Xue et al., 2015; Pimprikar et al., 2016).

Inoculation of *ram1-1* with a nurse plant inoculum showed that although the reduction of fungal colonization at late time points was almost fully complemented by the presence of nurse plants, arbuscule development was not rescued. Together, the results presented in this chapter and the recently published work in other species imply that *RAM1* is essential for arbuscule development in inner cortical cells, but is not absolutely required for initial entry and spreading of fungal hyphae within the roots.

The *nsp1-1* mutant showed a very different mycorrhizal phenotype compared to *ram1-1*. While a reduction in mycorrhizal infection structures was observed in *nsp1-1* at all three time points tested, the development of fungal structures was not affected and colonization inside the roots proceeded normally. These findings indicate that *NSP1* plays a role at very early stages of AM symbiosis, but is not required for the spreading and normal development of mycorrhizae within the root. NSP1 has previously been shown to regulate the expression of the strigolactone biosynthesis gene *D27* under low phosphate conditions in *M. truncatula* and rice, resulting in the complete lack of strigolactones in *nsp1* root exudates (Liu et al., 2011). Considering the role of strigolactones in the induction of AM fungal spore germination and hyphal branching (Akiyama et al., 2005; Besserer et al., 2006), it seems likely that the delayed onset of mycorrhization in *nsp1-1* observed here is, at least partly, caused by the lack of strigolactones released into the rhizosphere. *L. japonicus nsp1* mutants similarly show a decreased level of mycorrhization at early time points, and this correlates with a reduction in *D27* expression (Takeda et al., 2013). Interestingly, Takeda and colleagues found that while the external treatment of *L. japonicus nsp1* roots with strigolactones increases the level of mycorrhization, it does not fully complement the mycorrhizal phenotype, suggesting that *NSP1* must also regulate other plant processes important for the establishment of the symbiosis (Takeda et al., 2013).

Surprisingly, no significant difference in mycorrhization was observed in *nsp2-2* under the conditions tested here. This is in contrast with two earlier studies, which found a significant reduction of fungal colonization in the *nsp2* mutant compared to the wild type (Maillet et al., 2011; Lauressergues et al., 2012). It is possible that the fungal inoculum used in this study was too strong to observe a phenotype, and that a weaker inoculum is required to see a mycorrhizal defect in the *nsp2* mutant. The severity of the mycorrhizal phenotype of *nsp1* has previously been shown to depend on the amount of spores used to inoculate the plants. A decrease in mycorrhization was only visible when plants were inoculated with a low number of spores (Delaux et al., 2013). The same might also apply

to the *nsp2* mutant. Alternatively, a reduction in fungal colonization in *nsp2* might only be visible at very late time points during the symbiosis. Although not statistically significant, a small reduction in the number of arbuscules and vesicles was visible in *nsp2-2* at 27 dpi. This reduction might become more pronounced at even later time points, however, this hypothesis has not been tested here.

NSP1 and NSP2 are known to form a protein complex, and this interaction is required for the activation of target genes and the establishment of the root nodule symbiosis with rhizobial bacteria (Hirsch et al., 2006; Cerri et al., 2012). Based on these findings and the observation that the phenotypes of the *nsp1* and *nsp2* mutants in nodulation are very similar, it has been proposed that NSP1 and NSP2 act together to regulate the same processes in nodulation (Kaló et al., 2005; Smit et al., 2005; Hirsch et al., 2009). However, it is unclear whether these two transcription factors also carry out the same functions in mycorrhization. Here, I found that *nsp1-1* is impaired in fungal colonization, while *nsp2-2* does not have a mycorrhizal phenotype under the conditions and at the time points tested. Considering that the identical fungal inoculum and growth conditions were used to assess the phenotypes, this observation implies that *NSP1* and *NSP2* have different roles in mycorrhization. The regulation of strigolactone biosynthesis provides one example of a pathway that has been found to be differentially regulated by *NSP1* and *NSP2* (Liu et al., 2013). Although the expression of the strigolactone biosynthesis gene *D27* is reduced in both *nsp1* and *nsp2*, this reduction is weaker and not sufficient to prevent the production of strigolactones in *nsp2* (Liu et al., 2013). Instead, exudates of *nsp2* mutant roots contain higher levels of the strigolactone orobanchol, while the mutant seems to be blocked in the conversion of this substrate into other forms of strigolactones (Liu et al., 2013). This difference in strigolactone biosynthesis in *nsp1* and *nsp2* could be one possible reason for the difference between the mycorrhizal phenotypes observed here.

In summary, the comparative analysis of mycorrhizal phenotypes presented here provides evidence that *RAM1*, *NSP1* and *NSP2* are involved in the regulation of different mycorrhizal processes. While *RAM1* appears to be important at early and late time points during mycorrhization, and in particular for arbuscule formation and the maintenance of fungal colonization, *NSP1* seems to play a role in the initiation of AM development. Meanwhile, no effect on mycorrhization was observed in *nsp2-2* under the conditions tested here, and the role of *NSP2* in mycorrhization remains unclear.

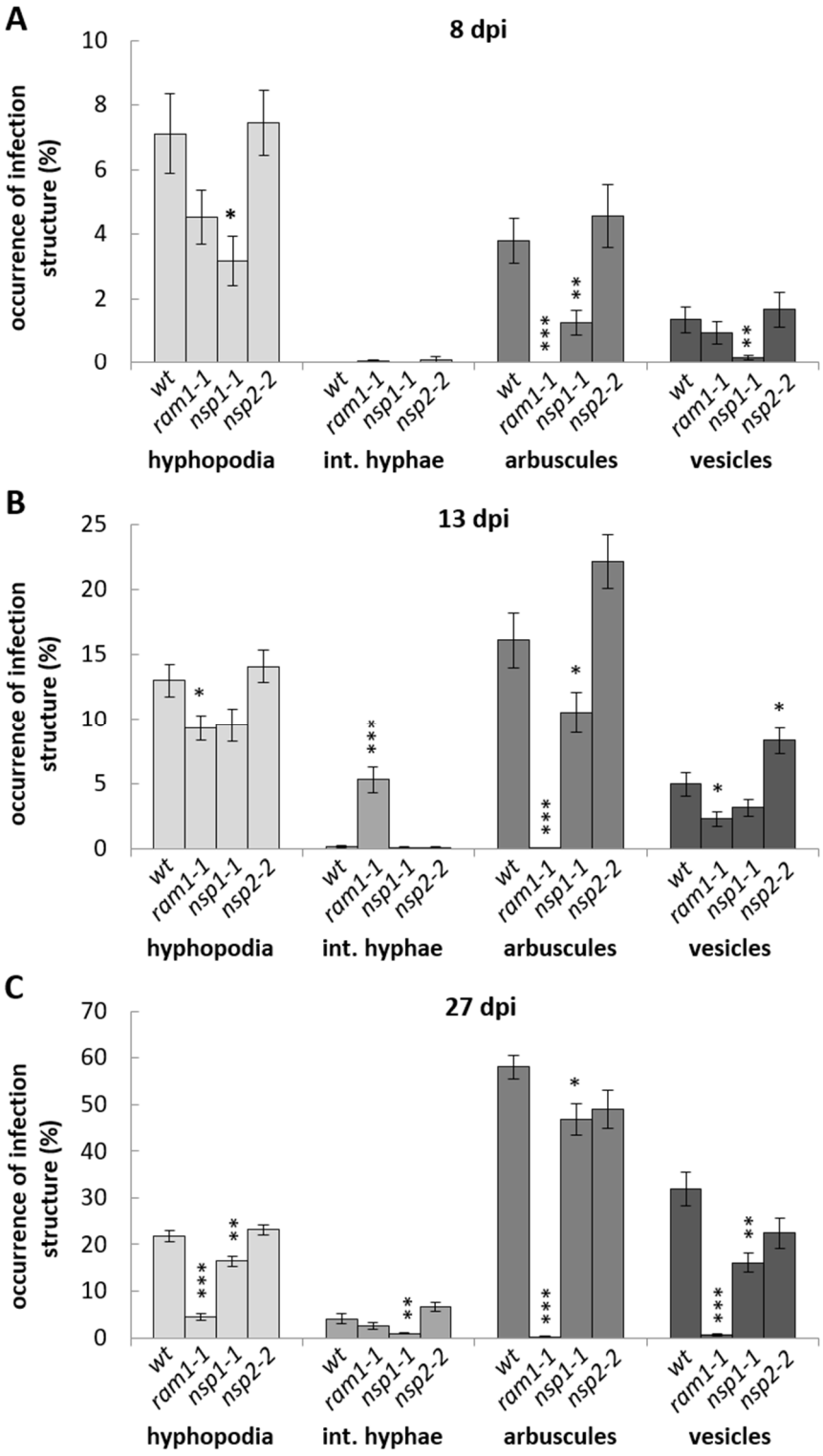

Figure 2.1: Quantification of fungal infection structures in wild-type (wt), *ram1-1*, *nsp1-1* and *nsp2-2* roots**.** The occurrence of hyphopodia, intraradical hyphae (int. hyphae), arbuscules, and vesicles in ink-stained root pieces is shown as percentage of the total number of root pieces assessed. Fungal infection structures were quantified at 8 dpi **(A)**, 13 dpi **(B)**, and 27 dpi **(C)**. Bars represent the average of at least 12 biological replicates ± SEM. Asterisks indicate significant differences between the wild type and the mutant lines in each group of infection type (Student's t-test; *, $P < 0.05$; **, $P < 0.01$; ***, $P < 0.001$).

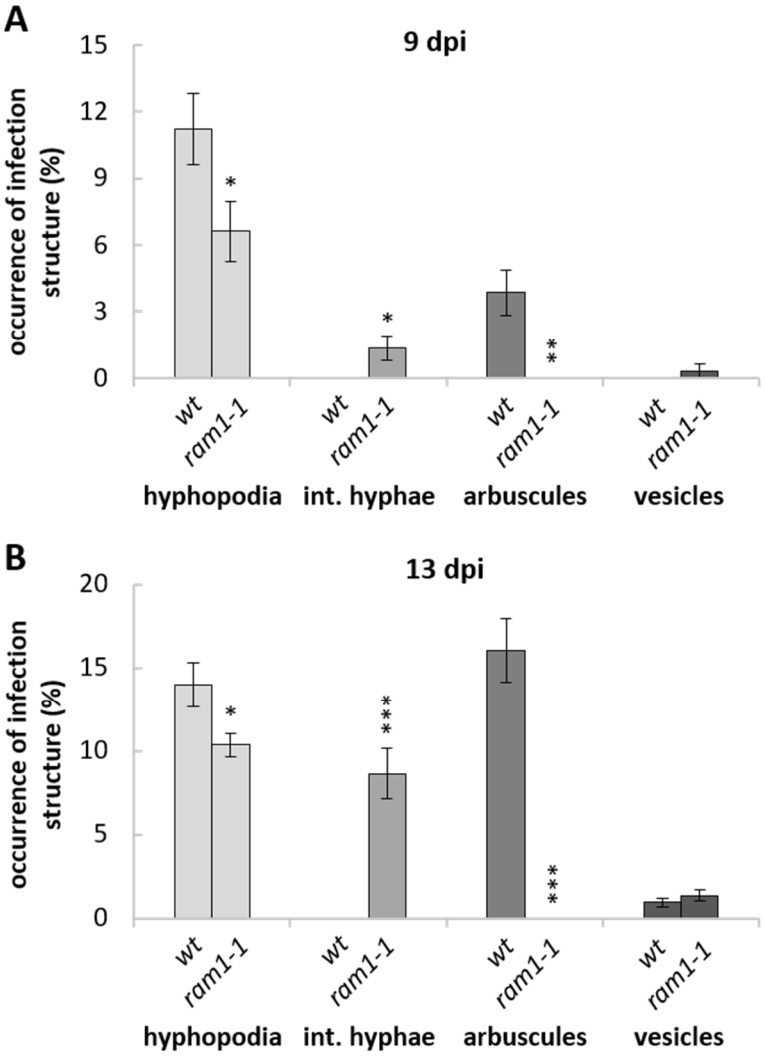

Figure 2.2: Quantification of fungal infection structures in wild-type (wt) and *ram1-1* roots**.** The occurrence of hyphopodia, intraradical hyphae (int. hyphae), arbuscules, and vesicles in ink-stained root pieces is shown as percentage of the total number of root pieces assessed. Fungal infection structures were quantified at 9 dpi **(A)** and at 13 dpi **(B)**. Bars represent the average of 12 biological replicates ± SEM. Asterisks indicate significant differences between the wild type and *ram1-1* in each group of infection type (Student's t-test; *, $P < 0.05$; **, $P < 0.01$; ***, $P < 0.001$).

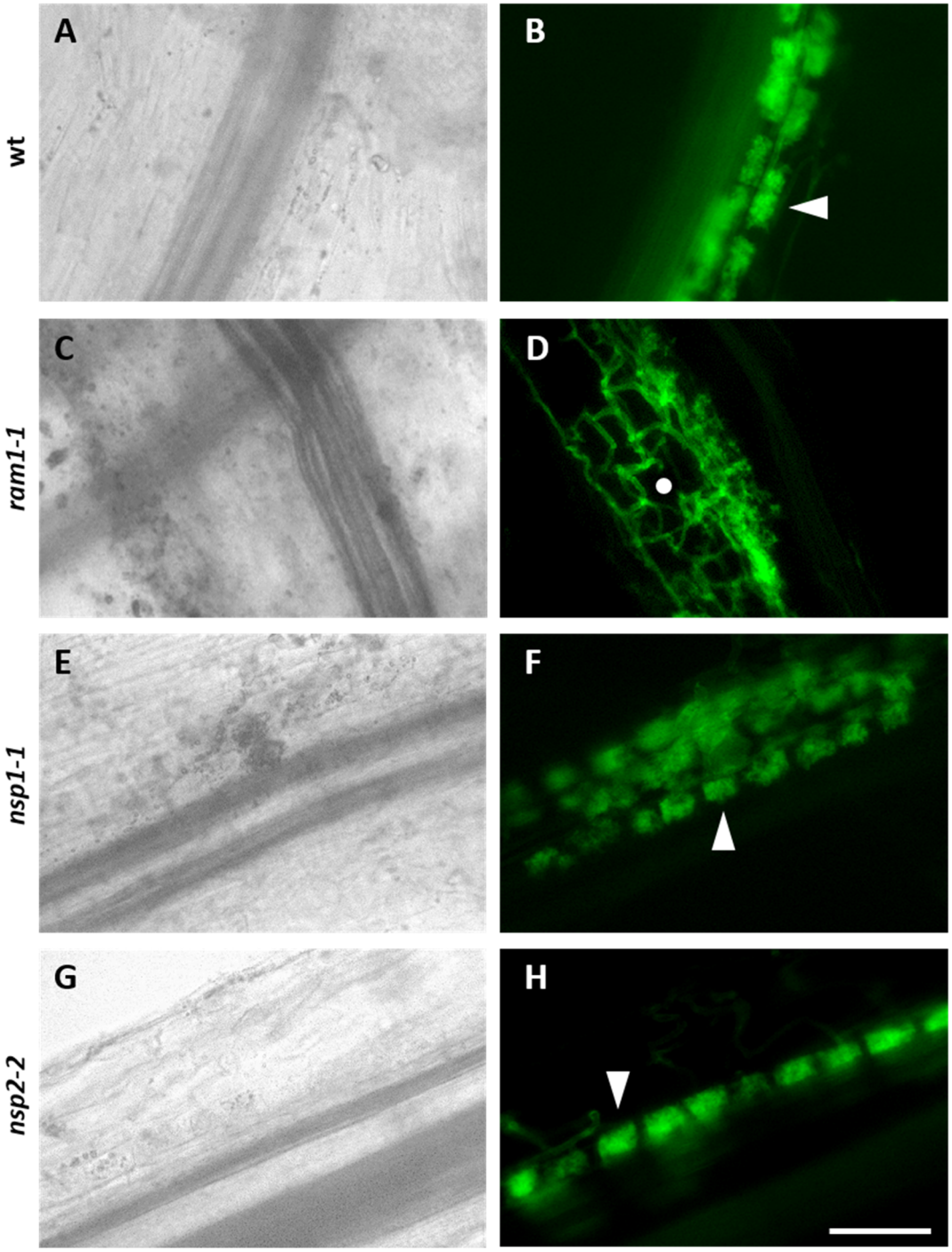

Figure 2.3: Appearance of fungal infection structures in wild-type (wt), *ram1-1*, *nsp1-1* and *nsp2-2* roots at **8 dpi**. Colonized wild-type (**A**, **B**), *ram1-1* (**C**, **D**), *nsp1-1* (**E**, **F**) and *nsp2-2* (**G**, **H**) roots were stained with Alexa Fluor 488 WGA. Bright field (**A**, **C**, **E**, **G**) and respective green fluorescence (**B**, **D**, **F**, **H**) images are shown. Arrowheads indicate fully developed arbuscules. Circles indicate intraradical hyphae. Scale bar = 100 µm.

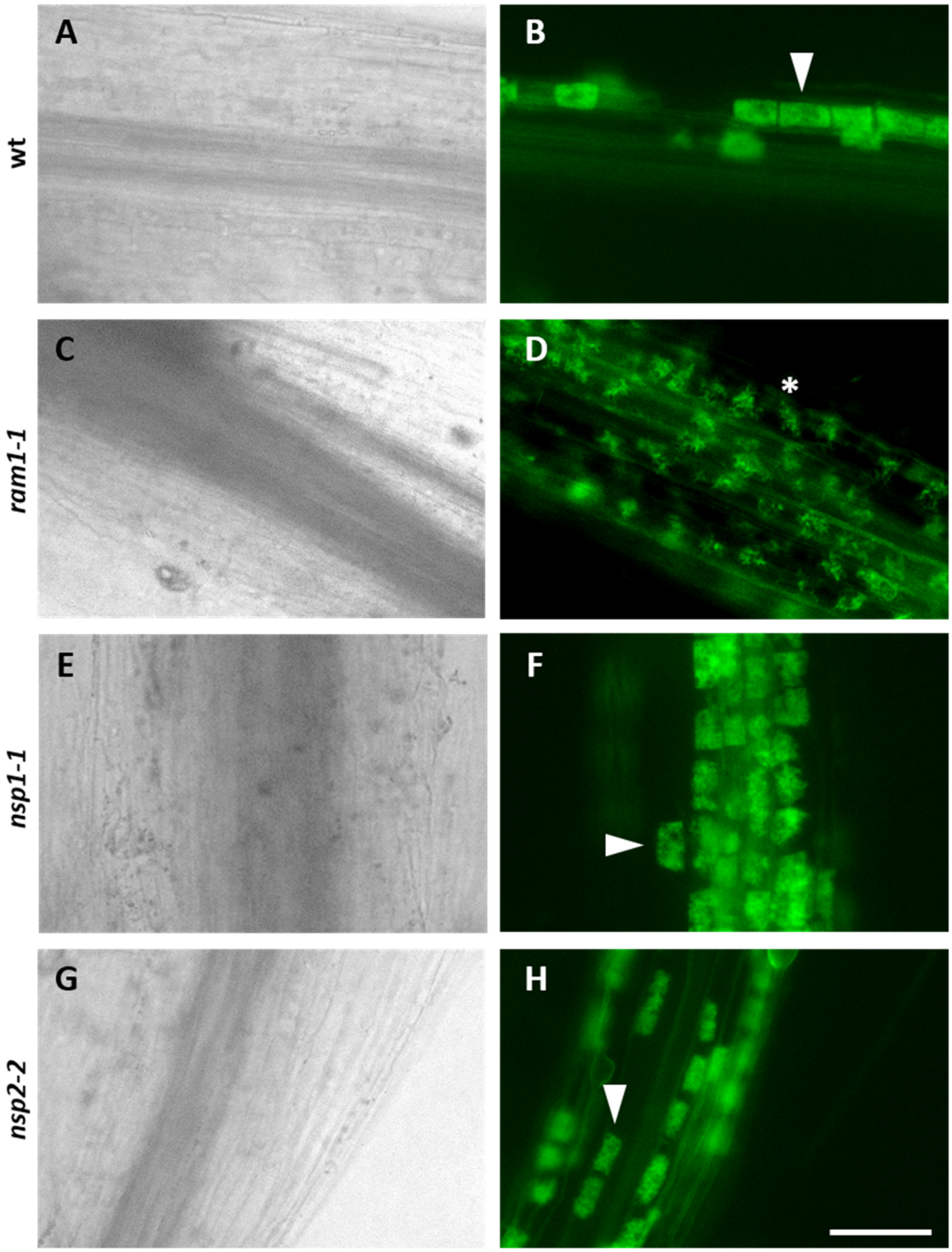

Figure 2.4: Appearance of fungal infection structures in wild-type (wt), *ram1-1*, *nsp1-1* and *nsp2-2* roots at **13 dpi**. Colonized wild-type (**A**, **B**), *ram1-1* (**C**, **D**), *nsp1-1* (**E**, **F**) and *nsp2-2* (**G**, **H**) roots were stained with Alexa Fluor 488 WGA. Bright field (**A**, **C**, **E**, **G**) and respective green fluorescence (**B**, **D**, **F**, **H**) images are shown. Arrowheads indicate fully developed arbuscules. Asterisks indicate underdeveloped arbuscules. Scale bar = 100 µm.

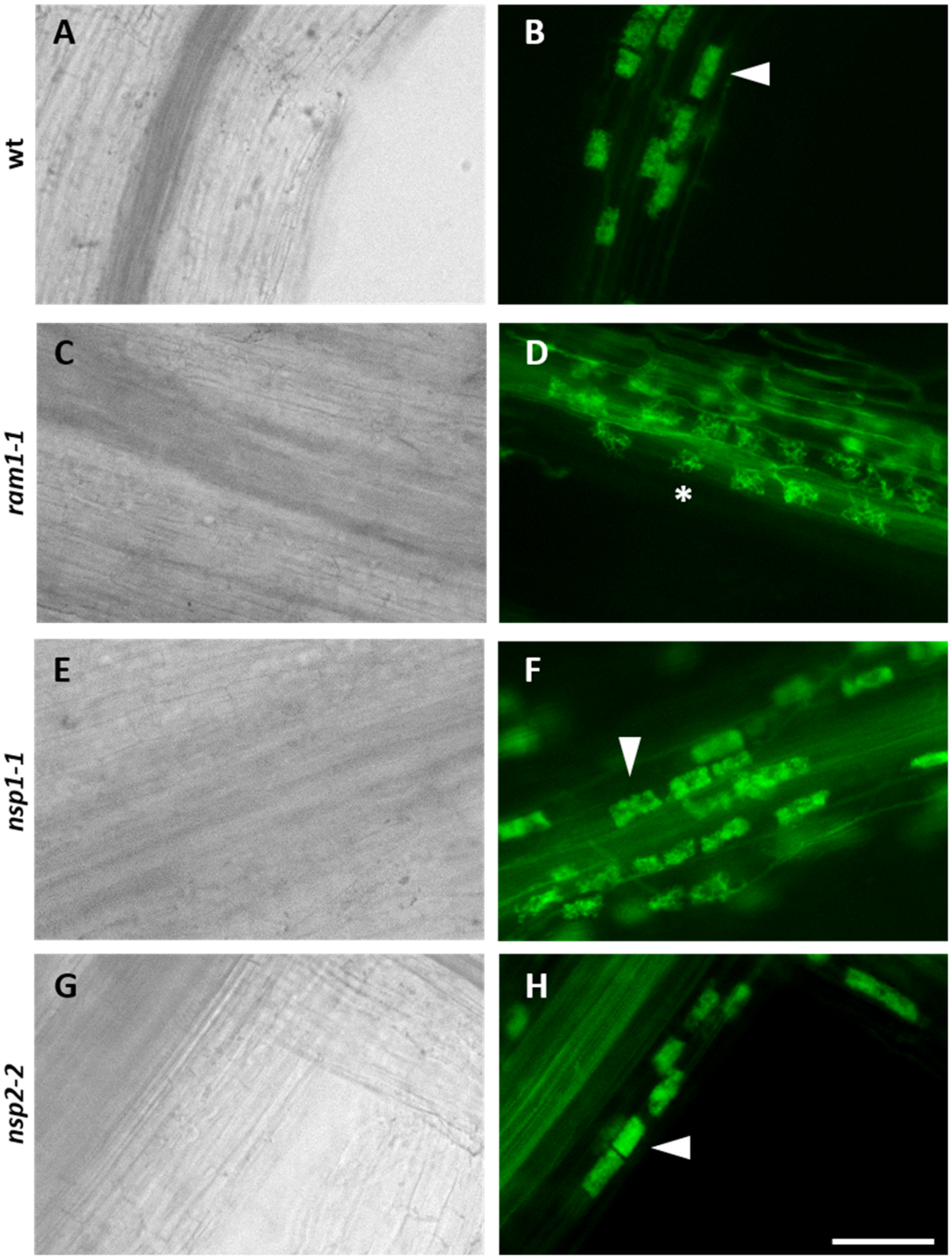

Figure 2.5: Appearance of fungal infection structures in wild-type (wt), *ram1-1*, *nsp1-1* and *nsp2-2* roots at **27 dpi**. Colonized wild-type (**A**, **B**), *ram1-1* (**C**, **D**), *nsp1-1* (**E**, **F**) and *nsp2-2* (**G**, **H**) roots were stained with Alexa Fluor 488 WGA. Bright field (**A**, **C**, **E**, **G**) and respective green fluorescence (**B**, **D**, **F**, **H**) images are shown. Arrowheads indicate fully developed arbuscules. Asterisks indicate underdeveloped arbuscules. Scale bar = 100 µm.

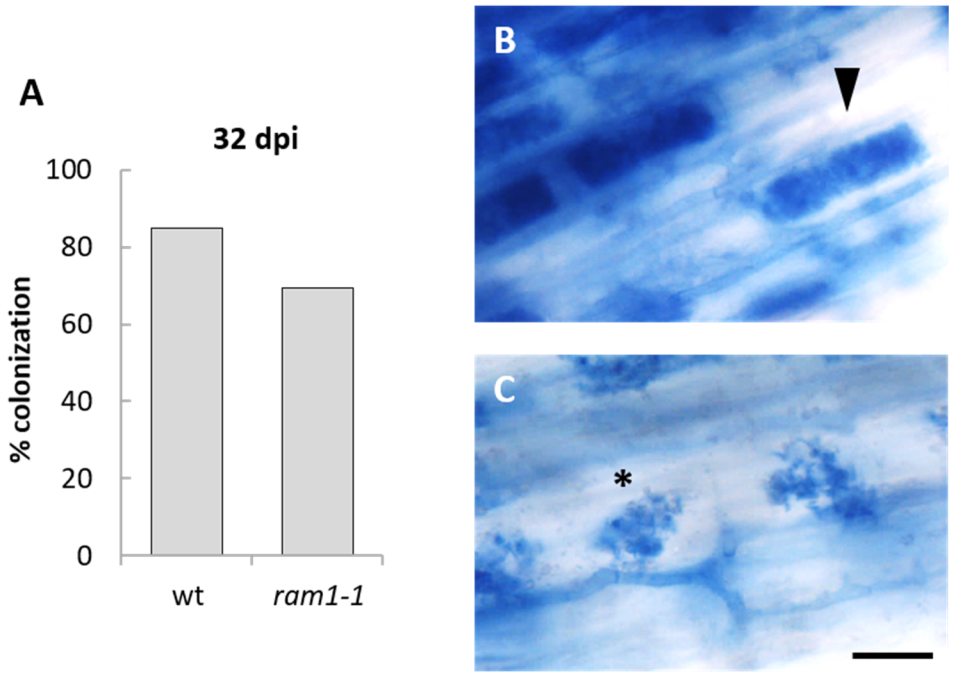

Figure 2.6: Total colonization levels and appearance of arbuscules in wild-type (wt) and *ram1-1* roots grown with nurse plant inoculum. (**A**) The occurrence of fungal infection structures (% colonization) in ink-stained root pieces is shown as percentage of the total number of root pieces assessed at 32 dpi. Bars represent the average of two biological replicates. Bright field images of ink-stained wild-type roots (**B**) and *ram1-1* roots (**C**) are shown. Arrowheads indicate fully developed arbuscules. Asterisks indicate underdeveloped arbuscules. Scale bar = 25 µm.

CHAPTER 3

Ascertaining the role of *NSP1*, *NSP2*, and *RAM1* in the regulation of global gene expression during AM development

3.1 Introduction

Extensive gene expression analyses have been carried out in the past few years to investigate the transcriptional reprogramming of plant roots during AM development. To date, hundreds of mycorrhization-induced genes have been identified, reflecting the complex developmental changes that occur in the root during the colonization by AM fungi (Liu et al., 2003; Wulf et al., 2003; Manthey et al., 2004; Weidmann et al., 2004; Hohnjec et al., 2005; Krajinski and Frenzel, 2007; Küster et al., 2007, Gutjahr et al., 2008; Gomez et al., 2009; Hogekamp et al., 2011; Czaja et al., 2012, Handa et al., 2015). These studies have uncovered transcriptional changes in genes involved in a number of different cellular processes, including defence responses, primary and secondary metabolism, nutrient transfer across membranes, cell wall and cell membrane modifications, and signal transduction (Krajinski et al., 2002; Liu et al., 2003; Brechenmacher et al., 2004; Manthey et al., 2004; Güimil et al., 2005; Hohnjec et al., 2005;

Küster et al., 2007). For example, some of the most highly induced genes during mycorrhization are plant lectins, phosphate and ammonium transporters, proteases, and transcription factors (Kistner et al., 2005, Frenzel et al., 2006; Takeda et al., 2009; Hogekamp et al., 2011). In addition to the analysis of whole mycorrhized roots, gene expression changes have also been studied in specific cell types, such as arbuscule-containing cells, using laser capture microdissection (Hogekamp et al., 2011; Gaude et al., 2012; Hogekamp and Küster, 2013). Moreover, the transcriptional response to diffusible fungal signals was profiled to investigate the induction of mycorrhizal genes at the pre-contact stage of the symbiosis (Kosuta et al., 2003; Weidmann et al., 2004, Siciliano et al., 2007; Kuhn et al., 2010; Czaja et al., 2012; Camps et al., 2015; Hohnjec et al., 2015). These studies have provided detailed information on the transcriptional changes that take place during different developmental stages of AM symbiosis. By contrast, relatively little is known about the transcriptional regulators that mediate these specific changes in gene expression during mycorrhization. Studies investigating the functions of GRAS-domain proteins and other transcription factors such as IPD3/CYCLOPS have been limited to the analysis of only a few potential target genes at late time points during AM development (Liu et al., 2011; Gobbato et al., 2012; Delaux et al., 2013; Park et al., 2015; Pimprikar et al., 2016). These analyses have resulted in the identification of only a handful of confirmed direct target genes regulated by these transcription factors during fungal colonization. Thus, specific knowledge about the role of mycorrhizal transcription factors in the regulation of global gene expression during different stages of AM development is currently lacking.

The aim of the work presented in this chapter was to analyse the global gene expression changes during mycorrhizal colonization and investigate the functions of *RAM1*, *NSP1*, and *NSP2* in this process. To gain insights into how gene expression in mycorrhized roots changes over the time course of infection and to investigate potential differences in the roles of the GRAS-domain proteins at different stages of fungal colonization, global gene expression profiling was performed at early, intermediate and late time points during mycorrhization. In addition, the roles of *RAM1*, *NSP1* and *NSP2* at pre-symbiotic stages were investigated by comparing global gene expression in roots grown without mycorrhizal fungi. These transcriptional analyses were further used to infer commonalities and differences in the functions of *RAM1, NSP1*, and *NSP2* before and during mycorrhization.

3.2 Results

3.2.1 Experimental design

To identify genes that are differentially expressed during AM symbiosis and under non-symbiotic conditions, wild-type, *ram1-1*, *nsp1-1* and *nsp2-2* plants were grown under low phosphate conditions and in the presence or absence of AM fungal inoculum. In addition, plants were supplied with high levels of nitrate to suppress the formation of nodules, as the presence of rhizobia in the fungal inoculum could not be excluded. The total RNA of 4 biological replicates (each containing the pooled roots of five individual plants) for each treatment and genotype was obtained at 8 dpi, 13 dpi and 27 dpi. For each time point, the colonization levels in three wild-type plants were assessed by staining roots with ink before proceeding with the harvesting of the roots for RNA extraction. At 8 dpi, up to 10 infection events per root system were visible. At 13 dpi, total levels of fungal colonization in stained roots were between 12% and 17%, and at 27 dpi, these levels increased to 70%. Thus, fungal colonization levels at the tested time points were comparable to the levels observed in wild-type roots at the same time points in Chapter 2. In addition, roots were examined for the presence of nodules. Only very few individual roots were found that occasionally showed small, white nodules, and these roots were removed before harvesting the remaining roots.

To validate the experimental set up, the expression levels of *PT4* were quantified in each RNA sample by performing qRT-PCR (Figure 3.1). This gene encodes a phosphate transporter that localizes to the periarbuscular membrane and is commonly used as a marker for the extent of fungal colonization in roots (Harrison et al., 2002; Pumplin and Harrison, 2009). *PT4* was highly expressed in mycorrhized root samples of wild-type, *nsp1-1* and *nsp2-2* plants. Furthermore, expression levels increased in mycorrhized roots over the time course of fungal colonization. By contrast, only very low relative expression levels were detected in non-mycorrhized root samples of all genotypes and in mycorrhized root samples of *ram1-1*. The low expression levels of *PT4* in mycorrhized *ram1-1* roots are consistent with the inability of these plants to form fully developed arbuscules at any time point during colonization (Chapter 2).

To quantify global gene expression, RNA sequencing (RNA-seq) was performed by IMGM laboratories (Martinsried, Germany). The reads obtained by sequencing were mapped against the most recent version of the *M. truncatula* genome (Mtv4.0). Differentially

expressed genes (DEGs) were identified by pair-wise comparisons of expression levels (total exon reads) between mycorrhized and non-mycorrhized roots of the same genotype or between non-mycorrhized roots of different genotypes at the corresponding time points (Figure 3.2). For further analyses, only DEGs with a fold change larger than 1.5 and a false discovery rate (FDR)-corrected p-value smaller than 0.05 were considered.

3.2.2 Genes differentially expressed in mycorrhized versus non-mycorrhized wild-type roots include many known mycorrhizal genes

To test whether known mycorrhizal genes were identified using RNA-seq with the experimental set up used here, I first analysed the genes that were found to be differentially expressed during mycorrhization in wild-type roots. Comparing the levels of gene expression in mycorrhized versus non-mycorrhized wild-type roots resulted in the identification of 421, 1056, and 1475 genes that were significantly upregulated by more than 1.5 fold at 8 dpi, 13 dpi, and 27 dpi, respectively (Figure 3.3 A). This increase in the number of mycorrhizal-induced genes over time is consistent with the observed increase in fungal colonization. The majority (346/421) of the genes that were induced in mycorrhized roots at 8 dpi also showed an increased expression at 13 dpi and 27 dpi (Figure 3.3 B). Similarly, most (854/1056) of the genes whose expression was induced at 13 dpi were also upregulated at 27 dpi. Consequently, only a small proportion of the mycorrhizal-induced genes showed an increased expression at only 8 dpi or 13 dpi and were not induced at any other time point.

Compared to the mycorrhizal-induced genes, a considerably smaller number of genes, namely 40, 100, and 118 genes at 8 dpi, 13 dpi and 27 dpi, respectively, were significantly downregulated in wild-type roots upon mycorrhization (Figure 3.3 A). Furthermore, these downregulated genes showed very little overlap between the tested time points, with only 2 genes being common to all three time points (Figure 3.3 B).

The differentially expressed genes identified in wild-type roots during fungal colonization included many genes that had previously been described to play a role in mycorrhization (Table 3.1). Consistent with the qRT-PCR results (Figure 3.1), the phosphate transporter *PT4* was one of the most highly upregulated genes in mycorrhized roots. In addition, several other genes previously described to be involved in arbuscule development and function were found to be induced during the mycorrhizal

time course, including the ammonium transporters *AMT2-3*, *AMT2-4* and *AMT2-5* (Breuillin-Sessoms et al., 2015), the two ABCG transporters *STR* and *STR2* (Zangh et al., 2010; Gutjahr et al., 2012), the exocyst subunit *EXO70I* (Zangh et al., 2015), the proton ATPase *HA1* (Krajinski et al., 2014; Wang et al., 2014), the GRAS-domain protein *RAD1* (Xue et al., 2015), and the glycerol-3-phosphate acyltransferase *RAM2* (Wang et al., 2012). These genes generally showed an increase in induction over time, consistent with the expected increase in the number of arbuscules at later time points. By contrast, the ankyrin-repeat protein *VAPYRIN* displayed a consistent induction of 6 to 7 fold at all three time points (Table 3.1). In accordance with this, *VAPYRIN* has previously been demonstrated to be required for the successful penetration of cells by fungal hyphae, a process that takes place at early as well as later time points during the symbiosis (Feddermann et al., 2010; Pumplin et al., 2010; Murray et al., 2011). Interestingly, some genes were found whose induction was high at early time points but decreased at later time points. This group of genes included the CCAAT-box transcription factors *Cbf1*, *Cbf2*, and *Cbf3*. *Cbf1* and *Cbf2* have previously been shown to be expressed in epidermal and cortical cells during mycorrhization, while *Cbf3* has been proposed to be predominantly active in epidermal cells at stages prior to the direct contact with fungal hyphae (Hogekamp et al., 2011; Hogekamp and Küster, 2013).

Changes in gene expression during mycorrhization were also observed for *RAM1*, *NSP1*, and *NSP2* (Table 3.1). *RAM1* showed a very strong and significant induction in gene expression in wild-type roots, with the highest fold change (>2000) being found at 13 dpi. By contrast, only a weak upregulation of approximately 2 fold was observed for *NSP1* at all three time points. Meanwhile, *NSP2* showed a weak transcriptional induction at 13 dpi and 27 dpi, but was not significantly induced at 8 dpi.

Due to the potential presence of rhizobial bacteria in the mycorrhizal inoculum used, the expression levels of genes that are known to be highly upregulated during nodulation were assessed to exclude the possibility that the observed gene expression changes were caused by rhizobia rather than mycorrhizal fungi. No significant difference in gene expression was observed for the nodulation markers *NIN* (Schauser et al., 1999) and *NPL* (*NODULE PECTATE LYASE;* Xie et al., 2012), two strongly induced genes during the root nodule symbiosis. These findings confirm that potential changes in gene expression caused by rhizobial bacteria were too diluted to be detectable.

Table 3.1: Fold changes of previously described mycorrhizal genes in mycorrhized versus non-mycorrhized wild-type roots. 'N.s.' depicts a statistically non-significant fold change. FDR-corrected p-value < 0.05 for all fold changes shown.

		Fold change		
Mtv4.0 ID	**Annotation**	**8 dpi**	**13 dpi**	**27 dpi**
Medtr6g027840	Ankyrin-repeat protein Vapyrin	6	7	6
Medtr2g081600	CCAAT box transcription factor Cbf1	46	17	n.s.
Medtr2g081630	CCAAT box transcription factor Cbf2	36	17	n.s.
Medtr8g091720	CCAAT box transcription factor Cbf3	9	8	n.s.
Medtr1g017910	Exocyst subunit EXO70I	2	13	18
Medtr8g107450	ABCG transporter STR	3	33	70
Medtr5g030910	ABCG transporter STR2	7	205	364
Medtr5g011320	Subtilisin-like serine protease SbtM1	11	60	136
Medtr8g006790	Proton ATPase HA1	78	953	1552
Medtr1g040500	Glycerol-3-phosphate acyltransferase RAM2	4	39	72
Medtr8g074750	Ammonium transporter AMT2-3	n.s.	72	55
Medtr7g115050	Ammonium transporter AMT2-4	15	365	1043
Medtr1g036410	Ammonium transporter AMT2-5	242	7735	3979
Medtr1g028600	Phosphate transporter PT4	1298	22666	12472
Medtr4g104020	GRAS-domain protein RAD1	40	238	697
Medtr7g027190	GRAS-domain protein RAM1	161	2412	1508
Medtr8g020840	GRAS-domain protein NSP1	1.7	2	1.6
Medtr3g072710	GRAS-domain protein NSP2	n.s.	1.8	1.6

3.2.3 *RAM1* is required for mycorrhizal gene induction at both early and late time points during mycorrhization

To investigate the role of *RAM1* in the regulation of global gene expression at different time points during mycorrhization, the transcriptional changes during fungal colonization identified in wild-type roots were compared to the changes observed in *ram1-1* roots. Due to the considerably lower number of mycorrhizal-repressed genes

identified in wild-type roots and their limited overlap between the different time points, only genes that were upregulated during mycorrhization were taken into account for further analyses.

In *ram1-1*, 607, 811, and 865 genes showed a significantly increased expression with a fold change higher than 1.5 in mycorrhized versus non-mycorrhized roots at 8 dpi, 13 dpi, and 27 dpi, respectively (Figure 3.3 A). Comparing the mycorrhizal-induced genes identified in the wild type at 8 dpi to the genes induced in *ram1-1* at the same time point revealed 109 genes whose induction was abolished in *ram1-1*. Thus, the induction of 27% (109/421) of all upregulated genes in the wild type at 8 dpi were dependent on *RAM1* (Figure 3.4 A). The same comparisons for the two later time points showed that the proportion of *RAM1*-dependent genes increased to 50% (530/1056) at 13 dpi and reached 59% (874/1475) at 27 dpi, suggesting that the loss of *RAM1* function strongly affects global gene expression, particularly during the late stages of mycorrhization (Figure 3.5).

The comparison of mycorrhizal-induced genes in the wild type and *ram1-1* revealed a number of genes whose induction was dependent on *RAM1* at specific time points. These *RAM1*-dependent genes likely include direct targets of RAM1, but might also include genes that are only indirectly regulated by this transcription factor. To identify genes that are more likely to be directly regulated by RAM1 during mycorrhization, I next looked for genes whose induction was consistently dependent on *RAM1* at all three time points tested. To this end, the *RAM1*-dependent genes from each time point identified above (1092 genes in total) were clustered based on their expression pattern in *ram1-1* roots over the whole mycorrhizal time course (Figure 3.6 A). Out of these 1092 genes, the cluster analysis identified a set of 768 genes (70%) that showed no induction in *ram1-1* at any of the three time points tested. To further investigate at which time point(s) during mycorrhization these 768 *RAM1*-dependent genes were induced in wild-type roots, the extent of overlap in gene induction across the time course was assessed. This analysis revealed that the majority of genes that were consistently dependent on *RAM1* were upregulated in the wild type at all three time points or were induced at both 13 dpi and 27 dpi (Figure 3.6 B). By contrast, fewer *RAM1*-dependent genes were specifically induced at just one time point, i.e. at 8 dpi or 13 dpi, during AM development. These results indicate that *RAM1* is involved in the regulation of a large set of mycorrhizal genes that are induced at both early and late time points in the wild type. The remaining 30% (306/1029) of the genes analysed by clustering displayed an

abolished upregulation at some, but not all three time points in *ram1-1*, suggesting that the transcriptional regulation of these genes during mycorrhization might only be indirectly dependent on *RAM1* (Figure 3.6 A).

3.2.4 *nsp1-1* shows a delay in the induction of gene expression during mycorrhization

In *nsp1-1*, 416, 669 and 1467 genes showed a significant induction of more than 1.5 fold upon fungal colonization at 8 dpi, 13 dpi, and 27 dpi, respectively (Figure 3.3 A). Comparing the mycorrhizal-induced genes in the wild type to the genes induced in *nsp1-1* revealed that the induction of 45% (189/421) of all genes upregulated in the wild type at 8 dpi was dependent on *NSP1* (Figure 3.4 B). The proportion of *NSP1*-dependent genes increased to 48% (510/1056) at 13 dpi, but was reduced to 28% at 27 dpi (411/1475). These findings suggest that *NSP1* is predominantly involved in the regulation of gene expression during the early time points of mycorrhization, but has a less important role at later stages (Figure 3.5).

To identify genes whose induction during mycorrhization was consistently dependent on *NSP1* at all three time points and might therefore be under the direct control of NSP1, the *NSP1*-dependent genes from each time point (938 genes in total) were clustered based on their expression pattern in *nsp1-1* roots over the whole mycorrhizal time course. Surprisingly, only 56% (527/938) of all *NSP1*-dependent genes showed a complete lack of induction at all three time points in *nsp1-1* (Figure 3.7 A). Moreover, comparing the expression pattern of these 527 *NSP1*-dependent genes across the three time points in wild-type roots revealed that the majority (299/527) of the *NSP1*-dependent genes were induced in the wild type only at 27 dpi (Figure 3.7 B). The remaining 44% (411/938) of the genes analysed by clustering were dependent on *NSP1* at only one or two, but not all three time points during fungal colonization. Notably, the majority of the genes whose upregulation was dependent on *NSP1* at 8 dpi (72%) or 13 dpi (58%) were induced at later time points in *nsp1-1* roots. In summary, these results suggest that the majority of the genes upregulated at early time points in the wild type were delayed but not consistently abolished in their induction in *nsp1-1*. Meanwhile, the majority of the genes that were consistently dependent on *NSP1* were only induced at late time points in the wild type.

3.2.5 Global changes in gene expression upon mycorrhization are altered at intermediate and late time points in *nsp2-2*

In *nsp2-2*, 652, 828, and 1166 genes showed a significantly increased expression with a fold change of more than 1.5 in mycorrhized versus non-mycorrhized roots at 8 dpi, 13 dpi, and 27 dpi, respectively (Figure 3.3 A). Comparing the mycorrhizal-induced genes in the wild type to the genes induced in *nsp2-2* revealed that only 9% (39/421) of all genes induced at 8 dpi in the wild type were dependent on *NSP2* (Figure 3.4 C). At 13 dpi, 32% (348/1056) of the mycorrhizal-induced genes lacked induction in *nsp2-2*, and this proportion increased to 34% (510/1475) at 27 dpi (Figure 3.4 C). These findings suggest that *NSP2* might play a role in the regulation of gene expression at later stages during AM development (Figure 3.5).

To identify genes whose induction during mycorrhization was consistently dependent on *NSP2*, the *NSP2*-dependent genes from each time point (792 genes in total) were clustered based on their expression pattern in *nsp2-2* roots over the whole mycorrhizal time course. This analysis identified 517 genes out of 792 (65%) whose induction was dependent on *NSP2* at all three time points (Figure 3.8 A). Only 4 of the genes consistently dependent on *NSP2* displayed an increased expression in the wild type at all three time points, while most genes were upregulated at 13 dpi and/or 27 dpi (Figure 3.8 B).

3.2.6 *RAM1*, *NSP1*, and *NSP2* have partially overlapping functions in the regulation of gene expression during fungal colonization

After identifying genes that might be under the direct control of RAM1, NSP1, and NSP2 during mycorrhization, I next investigated whether these three transcription factors target specific or overlapping sets of genes during fungal colonization. To this end, the degree of overlap between the genes that were consistently dependent on *RAM1*, *NSP1* or *NSP2* at all three time points during mycorrhization was determined (Figure 3.9). This analysis revealed 184 genes whose induction was dependent on all three transcription factors. Meanwhile, a number of transcription factor-specific target genes were identified. The largest number of specific target genes was found for *RAM1*, which was required for the upregulation of 456 genes (out of 768 *RAM1*-dependent genes) that did not appear to be affected in either *nsp1-1* or *nsp2-2*. By contrast, a lower proportion of

specific potential target genes were identified for *NSP1* and *NSP2*, with only 81 genes out of 527 genes being specifically dependent on *NSP1*, and 69 genes out of 517 being specifically dependent on *NSP2*. Furthermore, a considerable overlap (199 genes) was found between the genes that were dependent on *NSP1* and *NSP2*. Together, these data suggest that *RAM1*, *NSP1* and *NSP2* might have partially overlapping functions in the transcriptional regulation during AM development, while also regulating specific sets of target genes.

3.2.7 *RAM1*, *NSP1*, and *NSP2* are involved in the regulation of gene expression under non-symbiotic conditions

The establishment of AM symbiosis involves the exchange of a variety of signalling molecules before the first physical contact takes place between the roots and the fungal hyphae. To investigate whether *RAM1*, *NSP1* and *NSP2* could play a role in the regulation of gene expression at the pre-contact stage of AM symbiosis, global gene expression levels in non-mycorrhized *ram1-1*, *nsp1-1*, and *nsp2-2* roots were compared to the gene expression levels in non-mycorrhized wild-type roots at 8 dpi, 13 dpi and 27 dpi.

This comparison identified 20, 326, and 15 genes that were significantly downregulated and 31, 111, and 14 genes that were significantly induced by more than 1.5 fold in non-colonized *ram1-1* roots at 8 dpi, 13 dpi and 27 dpi, respectively (Figure 3.10 A). From these genes, 11 were differentially expressed at all three time points. (Figure 3.10 B). Comparatively more genes were differentially expressed in *nsp1-1* and *nsp2-2* under non-symbiotic conditions. In *nsp1-1* roots, 115, 237, and 284 genes were significantly downregulated, while 258, 426, and 575 genes were significantly upregulated at 8 dpi, 13 dpi and 27 dpi, respectively (Figure 3.10 A). Comparing these genes between the different time points showed that 194 genes were differentially expressed in *nsp1-1* at all three time points (Figure 3.10 B). Finally, the largest number of differentially expressed genes were identified in non-mycorrhized *nsp2-2* roots, with 142, 321, and 395 genes being significantly repressed and 374, 338, and 917 genes being significantly upregulated by more than 1.5 fold at 8 dpi, 13 dpi and 27 dpi, respectively (Figure 3.10 A). Furthermore, 193 of these genes were differentially expressed at all three time points in *nsp2-2* roots (Figure 3.10 B). These results suggest that NSP1 and NSP2, and to a smaller extent RAM1, directly or indirectly regulate a number of genes under non- or pre-symbiotic conditions.

Comparing the genes that were consistently differentially expressed in *ram1-1*, *nsp1-1*, and *nsp2-2* roots at all three time points in the absence of mycorrhizal fungi further revealed that most of these genes were specifically dependent on either *RAM1*, *NSP1*, or *NSP2*, indicating that there is very little overlap in the functions of these three transcription factors in the transcriptional regulation of roots under non- or pre-symbiotic conditions (Figure 3.11).

3.3 Discussion

In this chapter, the roles of *RAM1*, *NSP1*, and *NSP2* in the regulation of global gene expression before and during mycorrhizal colonization were investigated by profiling and comparing the transcriptomes of the corresponding loss-of-function mutants at different time points during AM development.

A number of studies have previously investigated the transcriptional changes that take place in roots during AM symbiosis and have identified hundreds of genes that are differentially expressed (Liu et al., 2003; Wulf et al., 2003; Manthey et al., 2004; Weidmann et al., 2004; Hohnjec et al., 2005; Krajinski and Frenzel, 2007; Küster et al., 2007, Gutjahr et al., 2008; Gomez et al., 2009; Hogekamp et al., 2011; Czaja et al., 2012, Handa et al., 2015). Many of these genes were also significantly induced in mycorrhized wild-type roots in this study, confirming that the experimental set up used here is suited to identify differentially expressed genes during mycorrhization. Comparing the expression of these mycorrhizal-induced genes in wild-type roots over the whole time course further showed that the majority of the genes that were upregulated at a specific time point were also induced at all later time points. This is not surprising, considering that all fungal infection structures, including hyphopodia, arbuscules and vesicles, were already present in wild-type roots grown under the same conditions at 8 dpi, with the main difference at later time points being the increased quantity of these structures (Chapter 2). In accordance with this, genes involved in arbuscule development and function, such as *EXO70I* and *STR* (Zangh et al., 2010; Gutjahr et al., 2012; Zangh et al., 2015), were generally induced at the earliest time point already, and showed a further increase in their fold change at later time points. Meanwhile, several genes, including the transcription factor *Cbf3* (Hogekamp and Küster, 2013), had a time-point specific induction and might therefore have functions that are required only at certain stages of mycorrhization.

A comparison of the mycorrhizal-induced genes between wild-type and *ram1-1* roots showed that *RAM1* was required for the induction of approximately a third of all genes that were induced in the wild type at 8 dpi. This suggests that RAM1 is involved in the regulation of a number of genes at the early stages of AM symbiosis. In line with this, a recent study has investigated the transcriptional response of wild-type plants and several symbiotic mutants to exogenously applied Myc-LCOs and has found that *RAM1* is required for the regulation of many of the genes that are induced upon recognition of these early signalling molecules (Hohnjec et al., 2015). At later time points, the proportion of *RAM1*-dependent genes increased to almost 60%, consistent with the drastically reduced levels of mycorrhization observed in *ram1-1* roots at late time points (Chapter 2). Considering the pattern of fungal colonization in *ram1-1* roots, it seems likely that the lack of gene induction observed in the mutant at late time points is partly caused by the loss of fungal infection and is not necessarily a direct consequence of the absence of the transcriptional activity of RAM1. Thus, only a subset of the genes that were dependent on *RAM1* at 27 dpi are expected to be directly regulated by RAM1. Indeed, several genes that showed no induction at 27 dpi were upregulated in *ram1-1* at early time points, indicating that these genes are only indirectly regulated by RAM1. Nevertheless, a large number of genes were identified whose induction was consistently dependent on *RAM1* at all three time points, and these genes are good candidates for potential direct targets of RAM1 during AM development. Furthermore, many of these genes were upregulated during two or all three time points in the wild type, suggesting that *RAM1* regulates a core set of mycorrhizal genes that play a role at both early and late stages of AM symbiosis.

Unlike in *ram1-1*, the mycorrhizal phenotype of *nsp1-1* is relatively subtle. Compared to the wild type, *nsp1-1* only showed a small reduction in the quantity of fungal infection structures throughout the mycorrhizal time course, while the development of these infection structures was not impaired (Chapter 2). It was therefore surprising to find that the induction of almost half of all mycorrhizal-induced genes was dependent on *NSP1* at early time points. At 27 dpi, the proportion of *NSP1*-dependent genes decreased considerably, an observation that might suggest that *NSP1* is mainly involved in the regulation of genes during the early time points of AM development. However, the majority of these early *NSP1*-dependent genes were upregulated at later time points during mycorrhization in *nsp1-1* and are therefore likely to be only indirectly regulated by *NSP1*. Furthermore, the genes that were consistently dependent on *NSP1* during fungal colonization were predominantly induced at 27 dpi in wild-type roots, and it is

possible that at least some of these genes might show an upregulation at time points later than 27 dpi in *nsp1-1* roots. These observations suggest that the transcriptional induction of a large proportion of mycorrhizal genes is delayed in *nsp1-1*, but not completely abolished. This delay in gene induction is in accordance with the slight reduction in fungal colonization observed at all three time points in *nsp1-1* roots (Chapter 2). Meanwhile, only a small number of the genes induced at early or intermediate time points in wild-type roots were found to be consistently dependent on *NSP1*, suggesting that *NSP1* only plays a minor role in the transcriptional regulation during fungal colonization.

Consistent with the observation that the colonization levels in *nsp2-2* did not differ significantly from wild-type levels at 8 dpi (Chapter 2), only very few genes were found to be dependent on *NSP2* for their induction upon fungal colonization at the earliest time point. However, the proportion of *NSP2*-dependent genes increased at 13 dpi and 27 dpi, suggesting that *NSP2* might be involved in regulating mycorrhizal gene expression at later time points during AM symbiosis. Although not statistically significant, *nsp2-2* showed a slight reduction in the number of arbuscules and vesicles at 27 dpi (Chapter 2), which might be the result of the lack of induction of the *NSP2*-dependent genes identified here.

In summary, the results of the transcriptomic profiling of mycorrhized roots indicate that the three GRAS-domain proteins play largely different roles in the regulation of global gene expression during AM development. *RAM1*, *NSP1*, and *NSP2* themselves appear to be transcriptionally regulated during mycorrhization, and consistent with the proposed differences in the functions of these transcription factors, differences were also found in the levels of transcriptional induction of these genes during fungal colonization. *RAM1* expression was highly induced throughout the mycorrhizal time course, consistent with the strong upregulation that has previously been described in several other studies (Gobbato et al., 2012; Park et al., 2015; Rich et al., 2015; Xue et al., 2015). By contrast, *NSP1* and *NSP2* only showed a very subtle induction of around 1.5 to 2 fold. Delaux and colleagues have reported a similar 2-fold induction in mycorrhized roots for *NSP1* (Delaux et al., 2013). The slight increase in *NSP2* expression during mycorrhization observed here is in accordance with the weak upregulation of *NSP2* described in the gene expression atlas of *M. truncatula* (http://mtgea.noble.org/v2/). Meanwhile, the expression of *NSP2* has also been described to decrease during fungal colonization through the action of a microRNA that targets *NSP2* transcripts specifically

in the root elongation zone, thereby preventing an over-colonization by AM fungi in this area of the root (Lauressergues et al., 2012).

Comparing the mycorrhizal-induced genes in the wild type to the ones in the GRAS-domain protein mutants not only identified genes with a lack of induction in the mutants, but also revealed a number of genes that were upregulated in the mutants while showing no increase in expression in the wild type. The induction of these genes might be directly or indirectly repressed during mycorrhization by the GRAS-domain proteins in wild-type roots, and the lack of repression of these genes in the mutant backgrounds might contribute to the mycorrhizal phenotypes described in Chapter 2.

The comparison of global gene expression in non-mycorrhized roots revealed that the loss of GRAS-domain proteins also affects the expression of a number of genes under non-symbiotic conditions. Interestingly, a comparable number of both up- and downregulated genes were observed in the mutants, again suggesting that the GRAS-proteins might act as both transcriptional activators and repressors. It is likely that some of the genes regulated by the GRAS-domain proteins under non-symbiotic conditions are involved in the pre-symbiotic stage of the AM symbiosis. One example of such a gene is the strigolactone biosynthesis gene *D27*, which was shown to be upregulated in roots grown under low phosphate or nitrogen conditions in the absence of mycorrhizal fungi, and this induction was found to depend on *NSP1* and, to some extent, on *NSP2* (Liu et al., 2011). Meanwhile, the GRAS-domain proteins might also play a role in the regulation of genes that do not have a direct function in symbiosis. This hypothesis is particularly attractive for *NSP1* and *NSP2*, which are conserved even in plants that are not able to form symbioses with AM fungi or rhizobial bacteria, including members of the *Brassicales* such as *A. thaliana* (Delaux et al., 2013; Delaux et al., 2014).

In conclusion, work presented in this chapter has identified a number of genes that are likely to be directly or indirectly regulated by RAM1, NSP1, and NSP2 before and during AM symbiosis. Investigating gene expression over several time points during mycorrhization has proven particularly useful to further limit the list of potential target genes. This approach has revealed genes whose induction was consistently dependent on *RAM1*, *NSP1*, and/or *NSP2* and are therefore good candidates for direct targets of these transcription factors. Furthermore, the time course has also allowed the identification of genes whose expression is likely to be only indirectly regulated by *RAM1*, *NSP1*, and *NSP2* during mycorrhization, including genes whose expression was delayed but not entirely abolished in *nsp1-1*, and genes that were dependent on *RAM1* at

late, but not at early time points. At the same time, a very stringent fold change cut-off was used to identify genes as potential targets in this study, as only genes whose induction was completely abolished in the GRAS protein mutants were considered to be good candidates. However, many genes also showed a reduced or increased induction during fungal colonization in *ram1-1*, *nsp1-1*, and *nsp2-2* compared to the wild type. It is possible that this group of genes also includes direct targets of the GRAS-domain proteins, but their expression might be regulated by several different transcription factors that could be partially redundant in their function. Thus, the approach described here is unlikely to identify all the genes targeted by RAM1, NSP1, and NSP2 during mycorrhization. Nevertheless, global gene expression profiling has provided a large number of novel potential targets of the GRAS-domain proteins. The in-depth functional analysis of these candidates and their transcriptional regulation before and during mycorrhization is described in the following chapters.

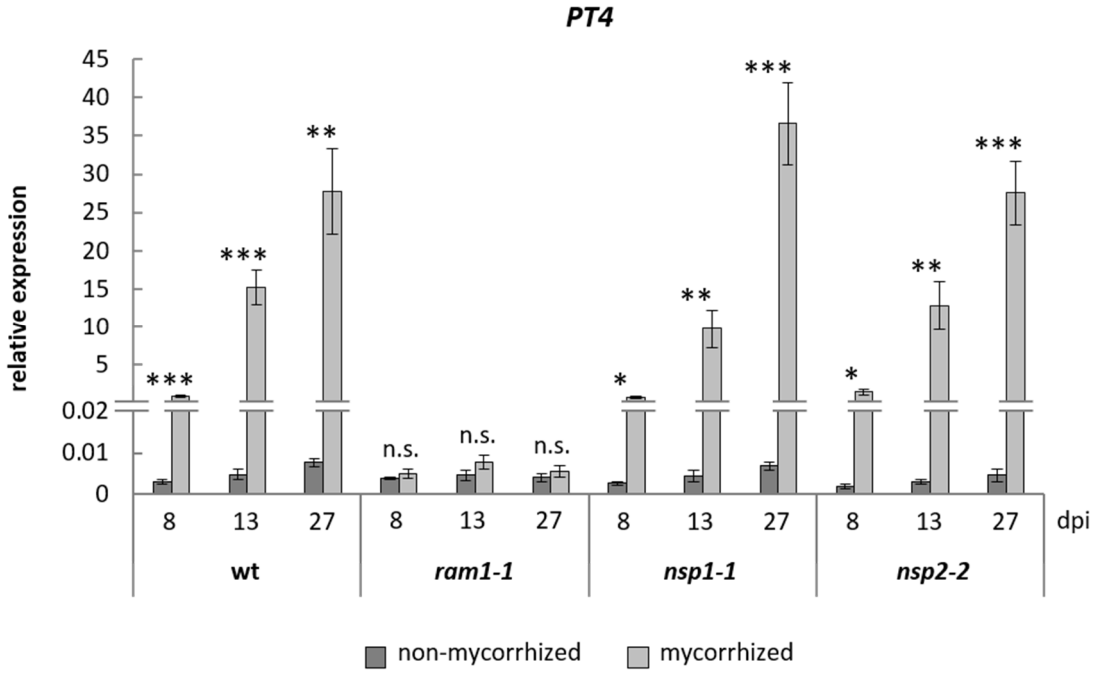

Figure 3.1: Quantification of *PT4* expression measured by qRT-PCR in non-mycorrhized and mycorrhized wild-type (wt), *ram1-1*, *nsp1-1*, and *nsp2-2* roots at 8 dpi, 13 dpi, and 27 dpi. The expression levels were normalized to *Ubiquitin* expression. Bars represent means of 4 biological replicates ± SEM. Asterisks indicate significant differences between expression levels in mycorrhized and non-mycorrhized roots of the same genotype at the corresponding time point (ANOVA, post hoc Tukey, *, $P < 0.05$; **, $P < 0.01$; ***, $P < 0.001$, n.s., $P > 0.05$).

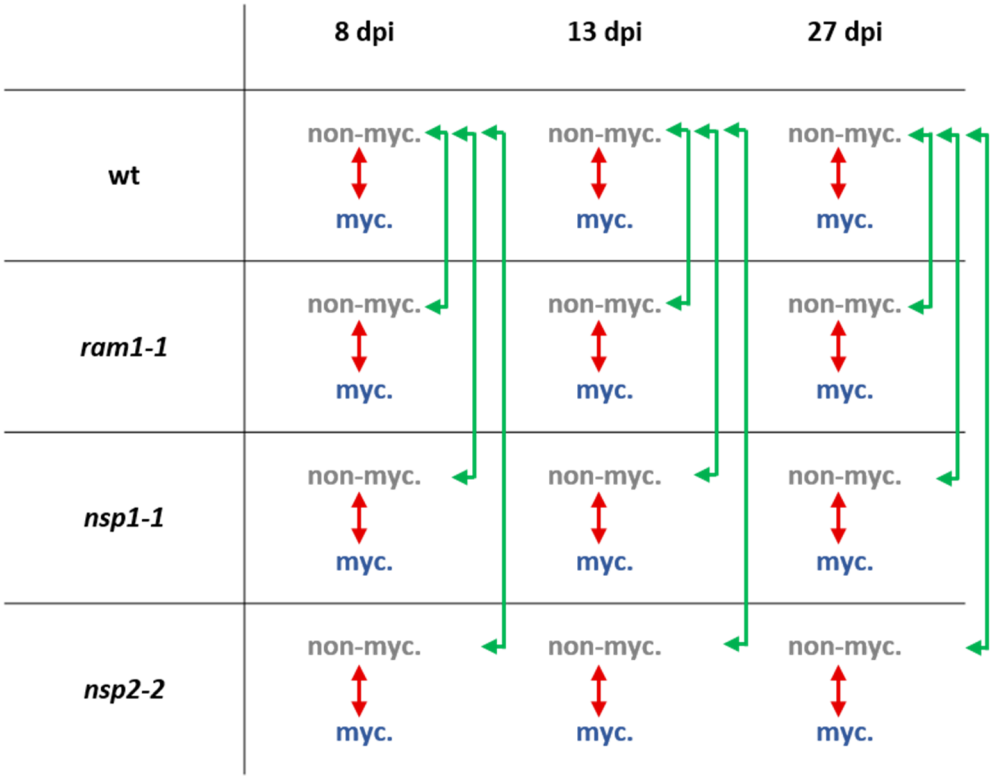

Figure 3.2: Identification of differentially expressed genes (DEGs) by pair-wise comparisons of expression levels. To identify DEGs over the time course of fungal infection, gene expression levels in non-mycorrhized (non-myc.) roots were compared to the gene expression levels in mycorrhized (myc.) roots of the same genotype (wild type (wt), *ram1-1*, *nsp1-1* or *nsp2-2*) and at the same time point (comparisons indicated by red arrows). To identify DEGs under non-symbiotic conditions, the gene expression levels in non-mycorrhized wild-type roots were compared to the gene expression levels in non-mycorrhized mutant roots at the same time point (comparisons indicated by green arrows).

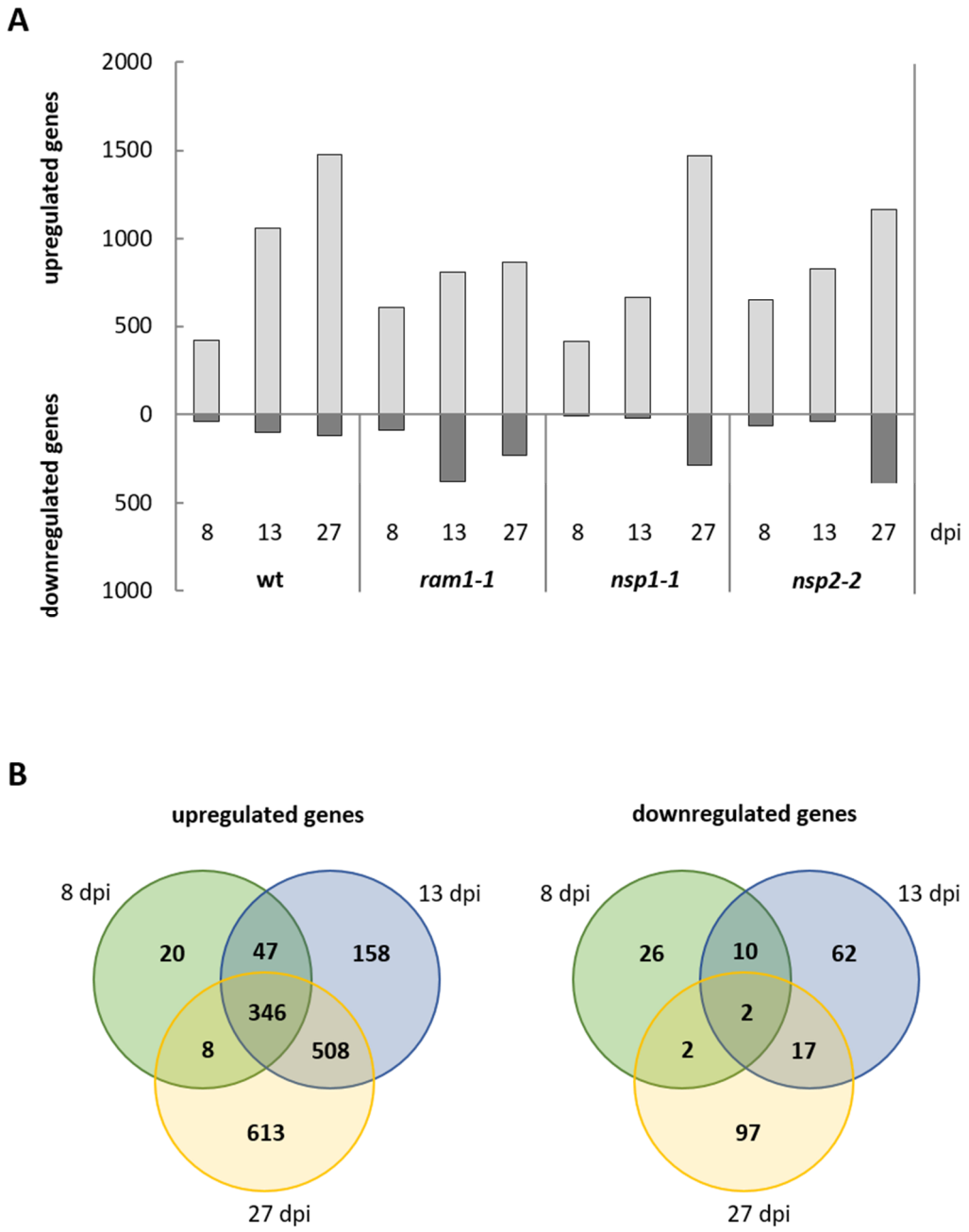

Figure 3.3: Overview of significantly up- and downregulated genes in mycorrhized versus non-mycorrhized roots. **(A)** Number of differentially expressed genes (DEGs) during mycorrhization in wild-type (wt), *ram1-1*, *nsp1-1*, and *nsp2-2* roots at 8 dpi, 13 dpi and 27 dpi. **(B)** Venn diagrams showing the extent of overlap of significantly upregulated genes (left) and downregulated genes (right) at 8 dpi, 13 dpi, and 27 dpi in wild-type roots. Only DEGs with a fold change of more than 1.5 and an FDR-corrected p-value smaller than 0.05 are shown.

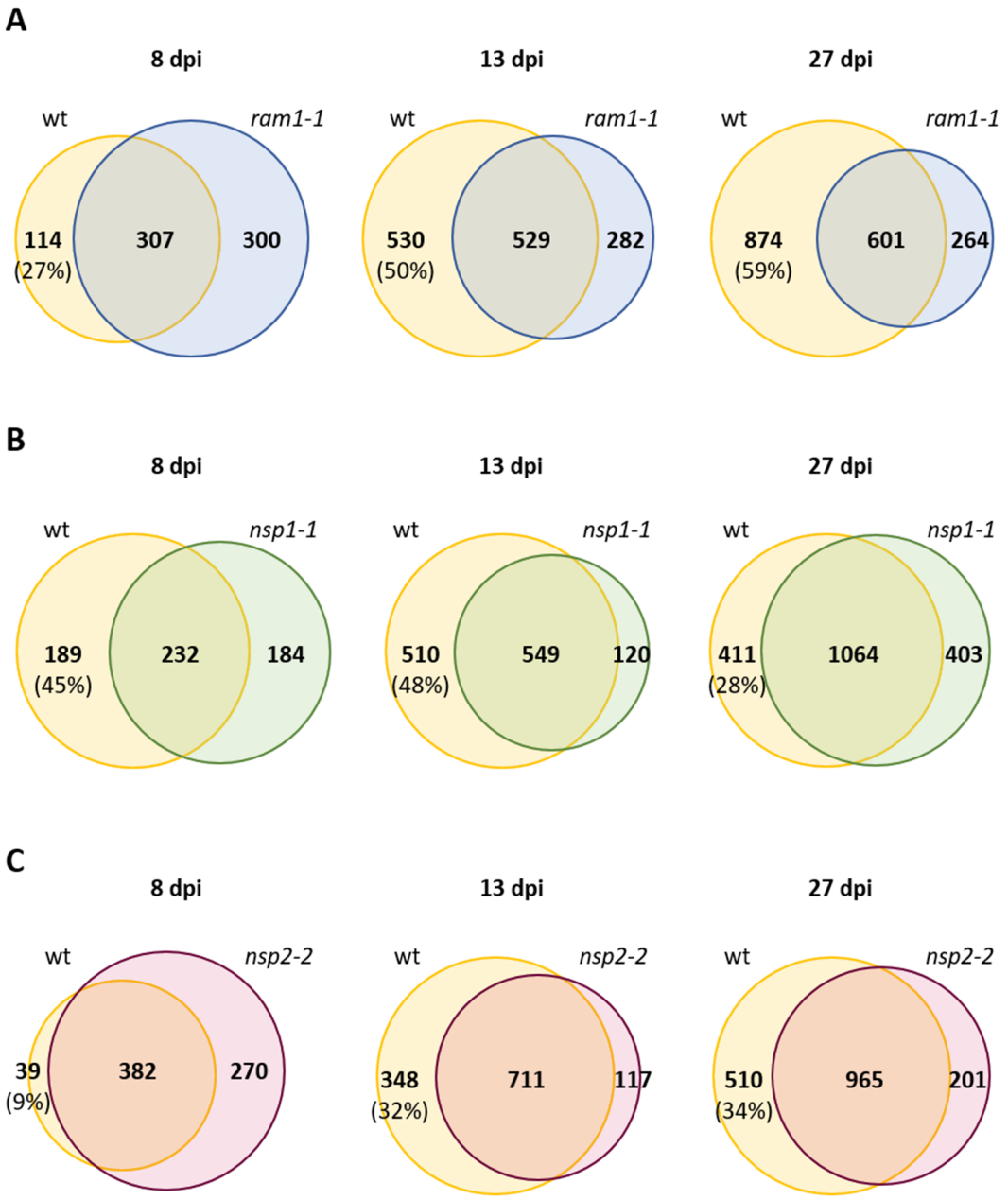

Figure 3.4: Comparison of mycorrhizal-induced genes in wild-type (wt) and *ram1-1*, *nsp1-1*, and *nsp2-2* roots. Proportional Venn diagrams showing the extent of overlap of genes induced in mycorrhized versus non-mycorrhized wild-type and *ram1-1* **(A)**, wild-type and *nsp1-1* **(B)**, and wild-type and *nsp2-2* **(C)** roots at 8 dpi, 13 dpi, and 27 dpi. The numbers in brackets indicate the proportion of genes that were induced in the wild type but not in the respective mutants relative to the total number of genes induced in the wild type at a specific time point. Significantly induced genes with a fold change of more than 1.5 and an FDR-corrected p-value smaller than 0.05 are shown.

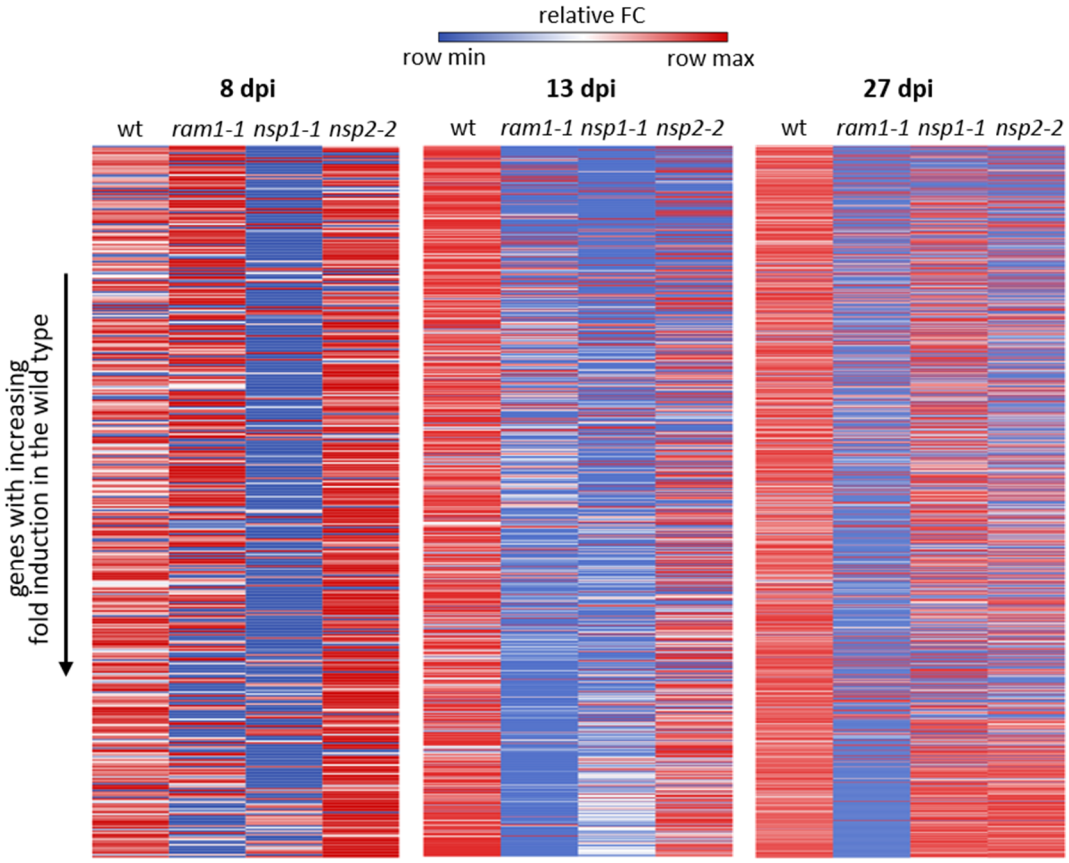

Figure 3.5: Overview of the fold changes of mycorrhizal-induced genes in wild-type (wt), *ram1-1*, *nsp1-1,* and *nsp2-2* roots at 8 dpi, 13 dpi, and 27 dpi. Heat maps showing the relative log2 fold changes of genes that were significantly induced in the wild type. The relative log2 fold changes of the same genes in the different mutant backgrounds are shown in each row. Genes are ordered according to their fold changes (FC) in wild-type roots as indicated by the arrow.

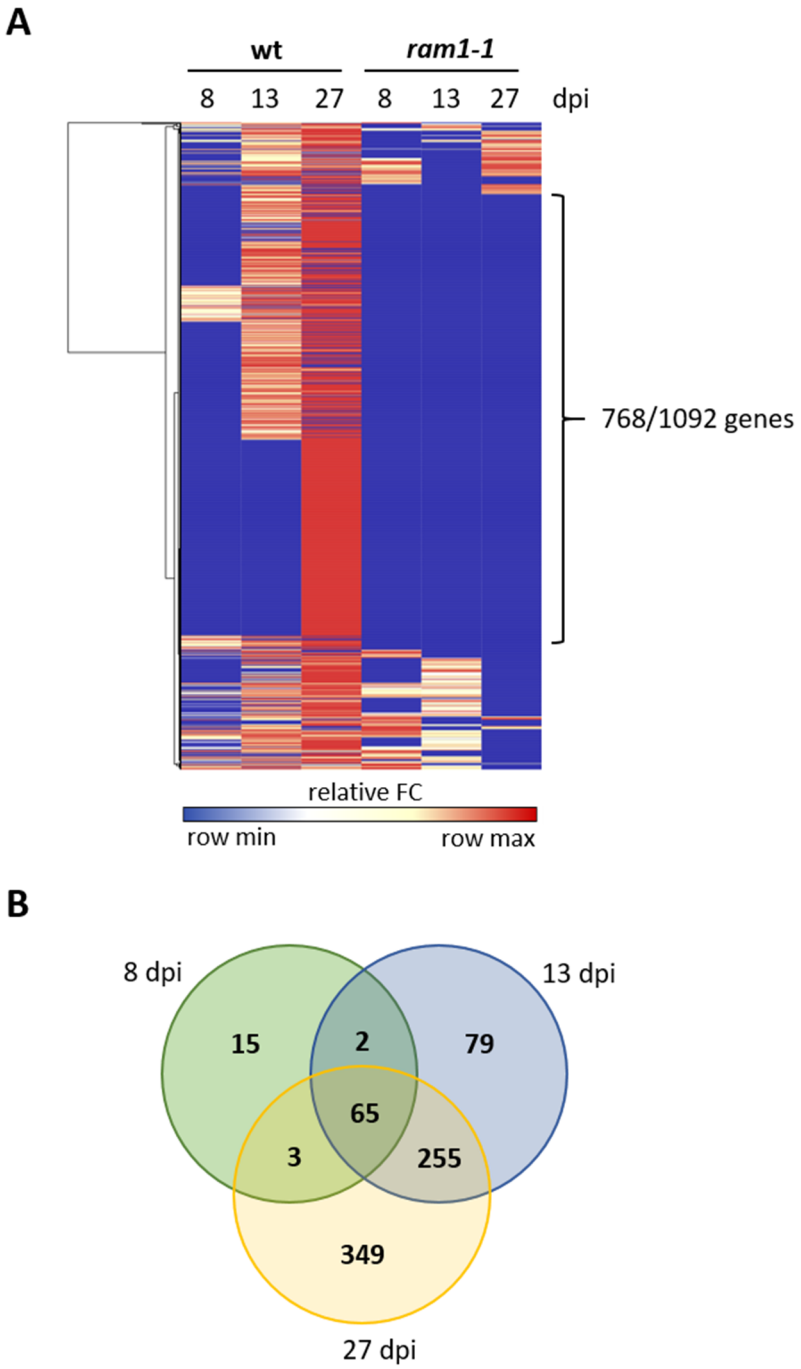

Figure 3.6: Overview of genes whose induction during mycorrhization was dependent on *RAM1*. **(A)** Heat map showing the relative log2 fold changes (FC) of genes that were induced in mycorrhized versus non-mycorrhized wild-type (wt) roots at 8 dpi, 13 dpi, and/or 27 dpi and were dependent on *RAM1* for their induction during at least one of these time points. Cluster analysis performed using the analysis tool GENE-E showed that out of 1092 genes analysed in total, 768 were not induced in *ram1-1* upon mycorrhization at any of the three time points tested. **(B)** Venn diagram showing the extent of overlap of the expression of the 768 *RAM1*-dependent genes identified in (A) at 8 dpi, 13 dpi, and 27 dpi in wild-type roots. Significantly induced genes with a fold change of more than 1.5 and an FDR-corrected p-value smaller than 0.05 are shown.

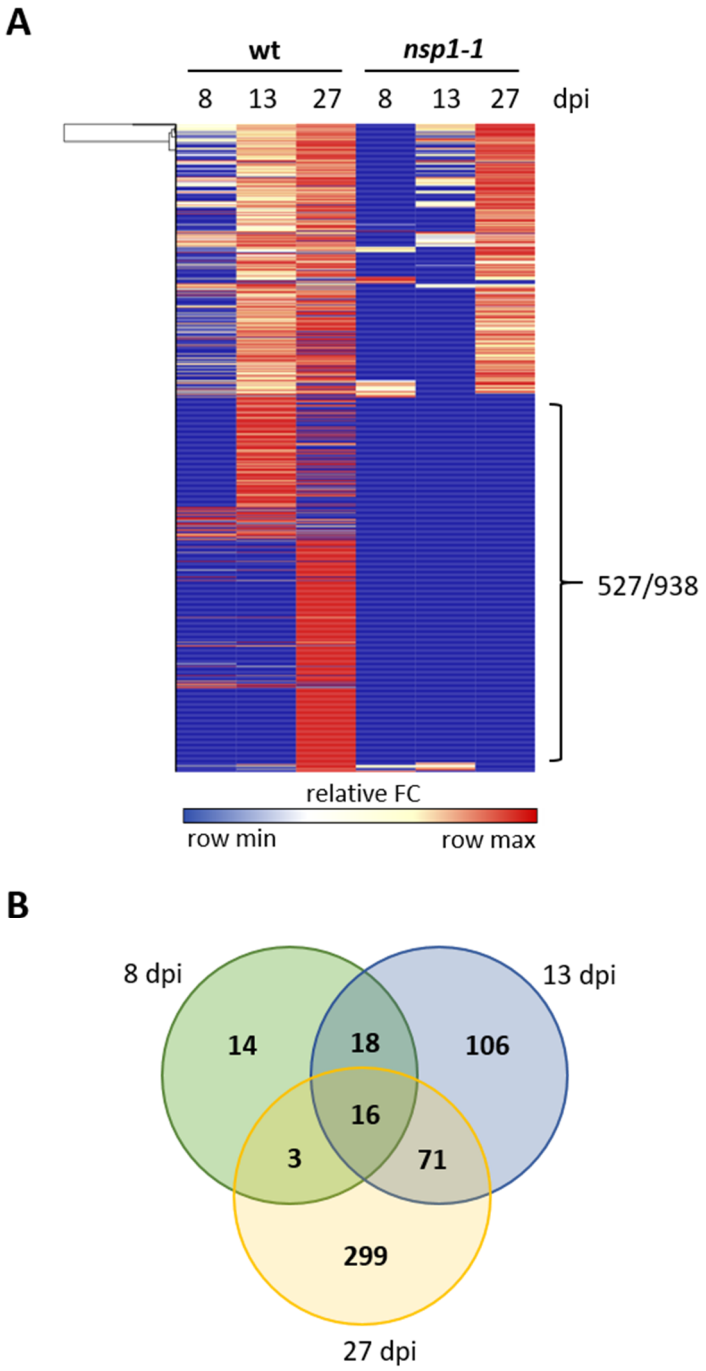

Figure 3.7: Overview of genes whose induction during mycorrhization was dependent on *NSP1*. **(A)** Heat map showing the relative log2 fold changes (FC) of genes that were induced in mycorrhized versus non-mycorrhized wild-type (wt) roots at 8 dpi, 13 dpi, and/or 27 dpi and were dependent on *NSP1* for their induction during at least one of these time points. Cluster analysis performed using the analysis tool GENE-E showed that out of 938 genes analysed in total, 527 were not induced in *nsp1-1* upon mycorrhization at any of the three time points tested. **(B)** Venn diagram showing the overlap of the expression of the 527 *NSP1*-dependent genes identified in (A) at 8 dpi, 13 dpi, and 27 dpi in wild-type roots. Significantly induced genes with a fold change of more than 1.5 and an FDR-corrected p-value smaller than 0.05 are shown.

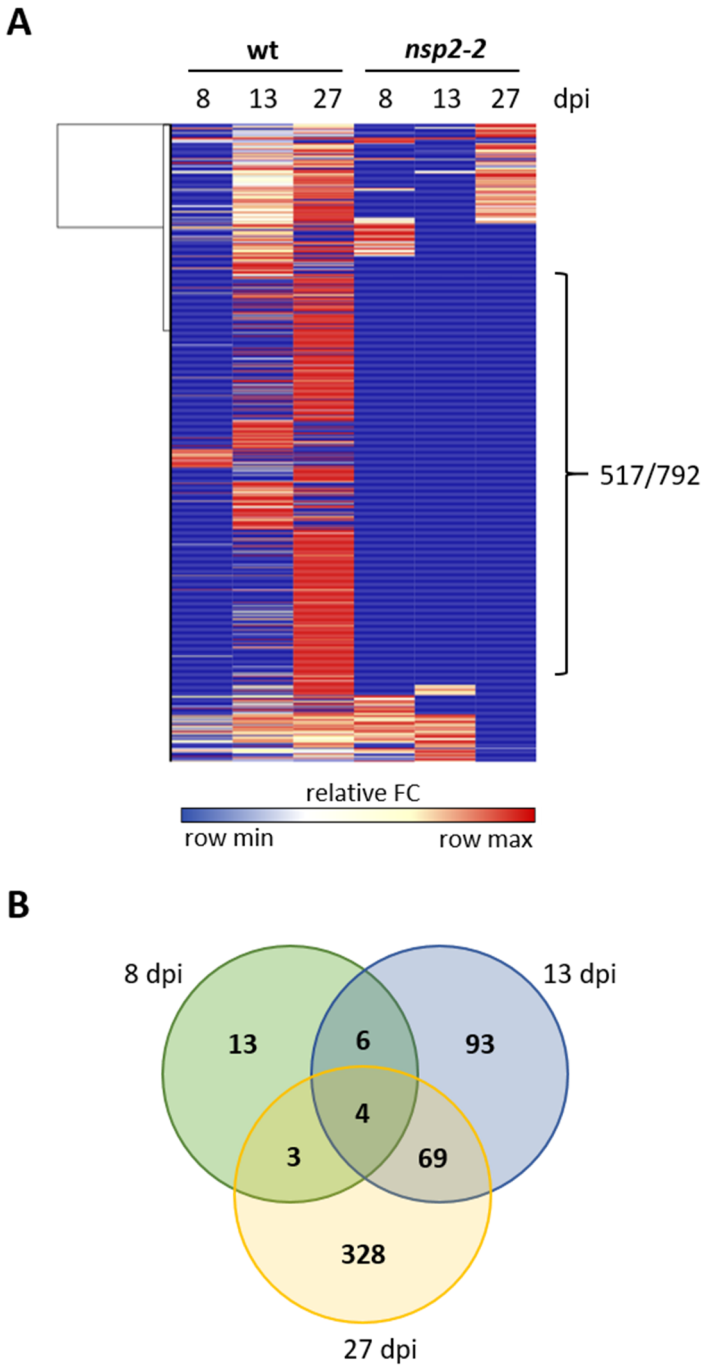

Figure 3.8: Overview of genes whose induction during mycorrhization was dependent on *NSP2*. **(A)** Heat map showing the relative log2 fold changes (FC) of genes that were induced in mycorrhized versus non-mycorrhized wild-type (wt) roots at 8 dpi, 13 dpi, and/or 27 dpi and were dependent on *NSP2* for their induction during at least one of these time points. Cluster analysis performed using the analysis tool GENE-E showed that out of 792 genes analysed in total, 517 were not induced in *nsp2-2* upon mycorrhization at any of the three time points tested. **(B)** Venn diagram showing the overlap of the expression of the 792 *NSP2*-dependent genes identified in (A) at 8 dpi, 13 dpi, and 27 dpi in wild-type roots. Significantly induced genes with a fold change of more than 1.5 and an FDR-corrected p-value smaller than 0.05 are shown.

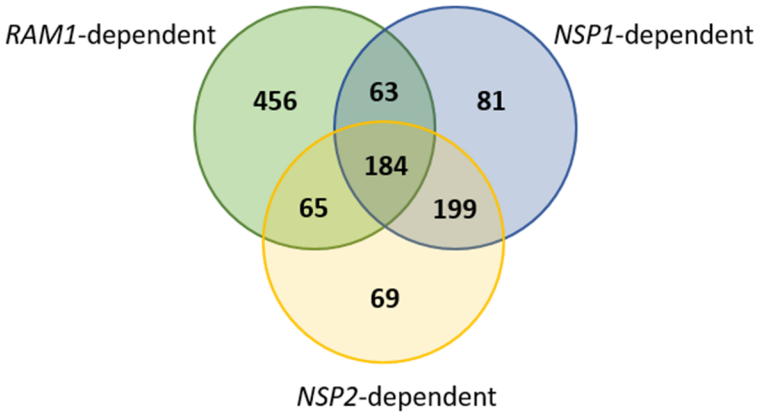

Figure 3.9: Venn diagram showing the extent of overlap of potential target genes of RAM1, NSP1 and NSP2 during AM development. Only genes whose expression was consistently dependent on *RAM1*, *NSP1* or *NSP2* at all three time points during mycorrhization were included in the analysis. Significantly induced genes with a fold change of more than 1.5 and an FDR-corrected p-value smaller than 0.05 are shown.

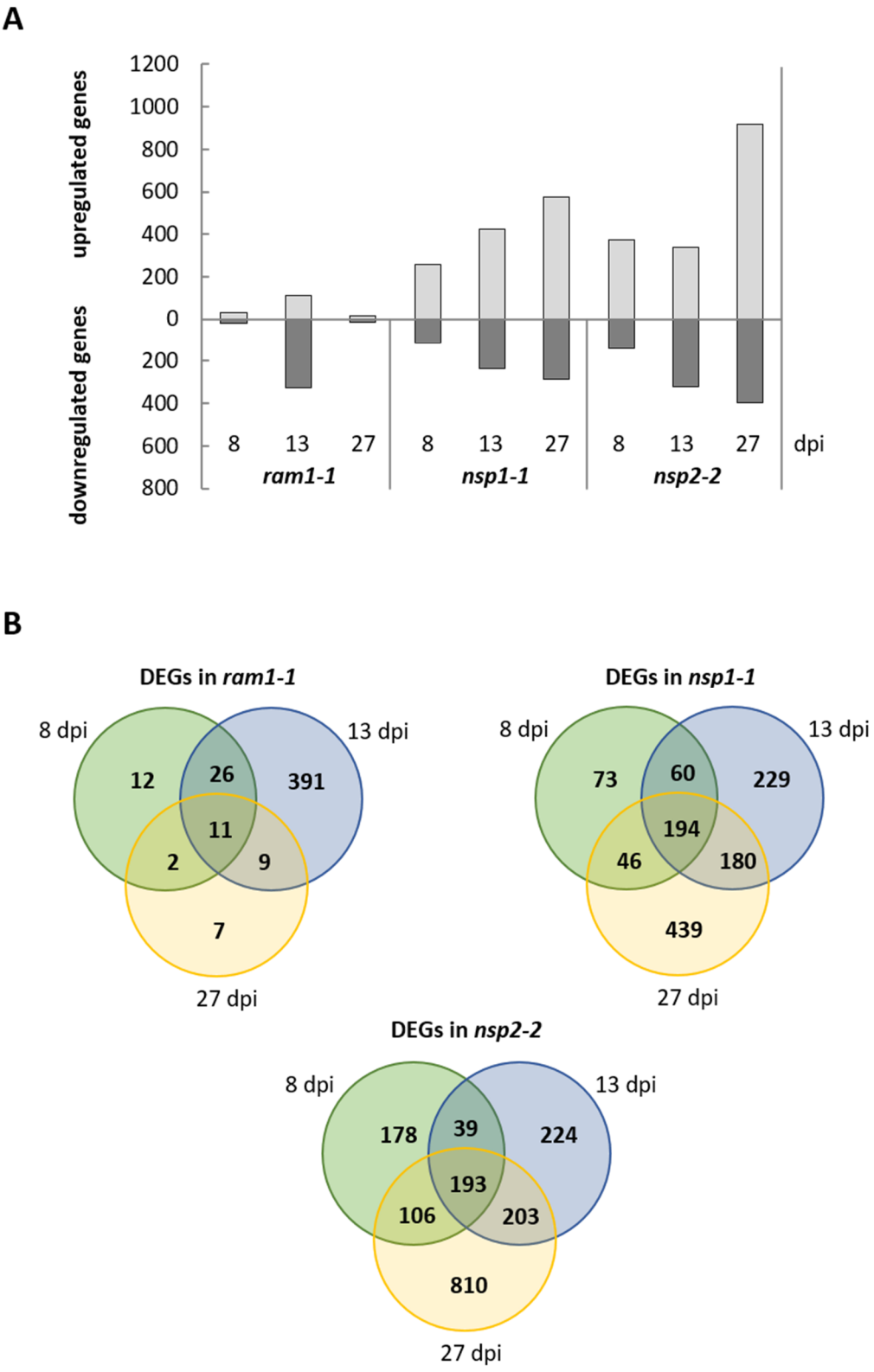

Figure 3.10: Overview of differentially expressed genes (DEGs) in non-mycorrhized *ram1-1*, *nsp1-1*, or *nsp2-2* roots compared to non-mycorrhized wild-type (wt) roots. **(A)** Number of DEGs in mutant versus wild-type roots at 8 dpi, 13 dpi and 27 dpi. **(B)** Venn diagrams showing the extent of overlap of DEGs in mutant versus wild-type roots at 8 dpi, 13 dpi, and 27 dpi. DEGs with a fold change of more than 1.5 and an FDR-corrected p-value smaller than 0.05 are shown.

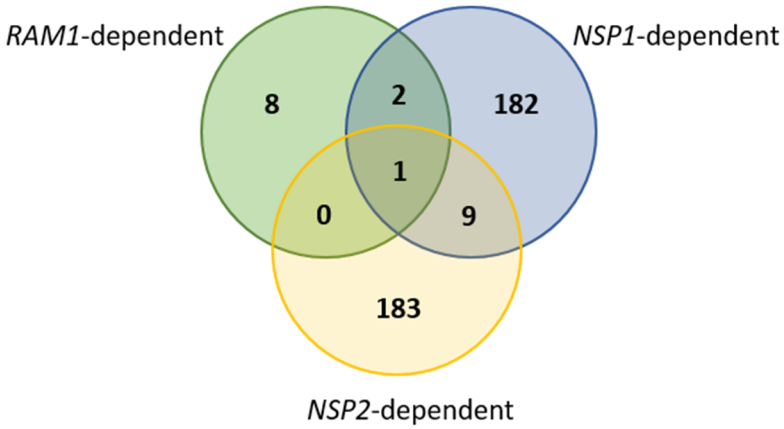

Figure 3.11: Venn diagram showing the extent of overlap of potential target genes of RAM1, NSP1, and NSP2 under non-symbiotic conditions. Only genes whose expression was consistently dependent on *RAM1*, *NSP1* or *NSP2* at all three time points tested were included in the analysis. Significantly induced genes with a fold change of more than 1.5 and an FDR-corrected p-value smaller than 0.05 are shown.

CHAPTER 4

Mycorrhizal processes regulated by *NSP1* and *NSP2*

4.1 Introduction

NSP1 and *NSP2* have only recently been discovered to play a role in AM development, as both mutants were found to show reduced levels of mycorrhizal colonization when inoculated with a weak fungal inoculum (Liu et al., 2011; Maillet et al., 2011; Delaux et al., 2013; Takeda et al., 2013). In accordance with this, a slight reduction in the level of mycorrhization was observed in *nsp1-1* at both early and late time points under the conditions tested here. Meanwhile, fungal colonization within the roots proceeded normally (Chapter 2). These findings suggest that the onset of mycorrhization is delayed in *nsp1-1* compared to the wild type. The transcriptional profile of mycorrhized *nsp1-1* roots further supports this hypothesis, with the induction of the majority of mycorrhizal-induced genes being delayed, but not completely abolished in *nsp1-1*. By contrast, a large number of genes were differentially expressed in *nsp1-1* in the absence of mycorrhizal fungi (Chapter 3).

To date, the only gene that is known to be regulated by NSP1 in the context of AM symbiosis is the strigolactone biosynthesis gene *D27*, whose expression is strongly

reduced in *nsp1* roots under phosphate-starved conditions, resulting in the complete lack of strigolactones in *nsp1* root exudates (Liu et al., 2011). It is currently unclear whether NSP1 only targets *D27*, or whether it also regulates other genes involved in strigolactone biosynthesis. Furthermore, even though the role of strigolactones in attracting fungal hyphae during the pre-contact stage of AM symbiosis is relatively well understood, it is not known whether these plant hormones also affect fungal colonization inside the roots, and if so, whether *NSP1* is required for strigolactone production at later stages of the symbiosis as well as at pre-symbiotic stages.

The role of *NSP2* in mycorrhization is less well understood. Although a reduction in fungal colonization has previously been reported in *nsp2* roots (Maillet et al., 2011; Lauressergues et al., 2012), no effect on mycorrhization was observed in *nsp2-2* under the conditions tested here, indicating that *NSP2* might be required for AM development only under certain conditions (Chapter 2). Nonetheless, a considerable number of genes were found to be dependent on *NSP2* at late time points during AM development. In addition, many genes were differentially expressed in *nsp2-2* roots under non-symbiotic conditions (Chapter 3). Similar to NSP1, NSP2 has been proposed to be involved in the regulation of *D27*, however, *nsp2-2* root exudates contain high levels of some strigolactone variants (Liu et al., 2011). Thus, the exact role of *NSP2* in the regulation of strigolactone biosynthesis remains unclear. It is currently not known whether *NSP2* has additional roles in the transcriptional regulation during the establishment of AM symbiosis, and whether these potential roles differ from the ones of *NSP1*.

The transcriptional profiling described in Chapter 3 has provided a large number of novel candidates for potential target genes of NSP1 and NSP2 before and during fungal colonization. To gain further insights into the mycorrhizal processes that are regulated by these two transcription factors, an in-depth functional analysis of the genes that were dependent on *NSP1* and *NSP2* for their expression before and during AM symbiosis was performed. In addition, this chapter also describes the development of tools that can be used to investigate whether these potential target genes are directly or indirectly regulated by NSP1 and NSP2.

4.2 Results

4.2.1 *NSP1* is required for the expression of many genes involved in the biosynthesis of strigolactones and gibberellins in the absence of AM fungi

As *NSP1* has previously been described to have a role in the pre-contact stage of AM development, I first investigated the functions of the genes that were differentially expressed in *nsp1-1* grown under low phosphate conditions and in the absence of mycorrhizal fungi. Global gene expression profiling has identified a large number of genes that were significantly up- or downregulated in *nsp1-1* compared to the wild type. Comparing the expression pattern of these genes across the whole time course revealed 194 genes that were differentially expressed at all three time points tested, and were therefore considered to be the most promising candidates for genes that might be directly regulated by NSP1 (Chapter 3, Figure 3.10).

To gain further insights into the functions of these genes, a singular enrichment analysis of gene annotation (GO) terms was performed with the whole *M. truncatula* genome as background using the web-based tool Agrigo (http://bioinfo.cau.edu.cn/agriGO/). This analysis identified several enriched GO terms that were associated with isoprenoid and lipid metabolism, suggesting that *NSP1* is involved in the regulation of metabolic pathways (Figure 4.1 A). To investigate the potential functions of the differentially expressed genes in more detail, a BLAST search with the corresponding protein sequences was conducted against the *A. thaliana* proteome, and the function of the best hit in *A. thaliana* for each gene was further analysed. As expected, the strigolactone biosynthesis gene *D27* was strongly downregulated in non-mycorrhized *nsp1-1* roots compared to the wild type, consistent with the findings of Liu and colleagues (Liu et al., 2011; Table 4.1). In addition, transcript levels of several carotenoid cleavage dioxygenases (CCDs) were significantly reduced in *nsp1-1*, including *CCD7* and *CCD8*, two enzymes required for the late steps of strigolactone biosynthesis (Alder et al., 2012). Surprisingly, a large number of genes that have been proposed to be involved in isoprenoid biosynthesis were also significantly reduced in non-mycorrhized *nsp1-1* roots (seven genes in total, including genes encoding 1-deoxy-xylulose-5-phosphate synthase (DXS), 1-deoxy-xylulose-5-phosphate reductoisomerase (DXR), 4-hydroxy-3-methylbut-2-enyl diphosphate reductase (HDR), and geranylgeranyl pyrophosphate synthase (GGPS)). Furthermore, several genes with a function in carotenoid biosynthesis showed a significant downregulation in *nsp1-1* roots (ten genes in total, including genes

encoding phytoene synthase (PSY), phytoene dehydrogenase (PDS), zeta-carotene isomerase (Z-ISO), and zeta-carotene desaturase (ZDS)). In addition, a homolog of the cauliflower *Orange* gene, which is involved in promoting the formation of carotenoid-accumulating chromoplasts (Lu et al., 2006), displayed a reduced expression in *nsp1-1* at all three time points tested. Isoprenoids are the precursors of carotenoids, from which strigolactones are derived (Al-Babili and Bouwmeester, 2015; Figure 4.2). Together, these results suggest that under low phosphate conditions and in the absence of AM fungi, *NSP1* is involved in the regulation of several biosynthetic pathways that participate in the production of strigolactones.

Among the group of differentially expressed genes in *nsp1-1* roots were a number of genes that are involved in the biosynthesis of gibberellins, which are plant hormones that are derived from the isoprenoid intermediate geranyl geranyl pyrophosphate (GGDP; Hedden and Thomas, 2012; Figure 4.2). The transcript levels of several genes involved in the early steps of gibberellin biosynthesis, including genes encoding homologs of copalyl diphosphate synthase (CPS), ent-kaurene oxidase (KO), and ent-karenoic acid oxidase (KAO2), were significantly reduced in *nsp1-1* roots compared to the wild type at all three time points tested (Table 4.1). Meanwhile, two homologs of gibberelin-20-oxidase and one homolog of gibberellin-3-oxidase showed a significant transcriptional induction in *nsp1-1* across the whole time course. In *A. thaliana*, gibberellin-20-oxidases and gibberellin-3-oxidase-1 have been shown to be transcriptionally upregulated as part of a feedback regulation when gibberellin levels in plants are low (Mitchum et al., 2006; Rieu et al., 2008; Hedden and Thomas, 2012). Overall, these findings suggest that *NSP1* is involved in the regulation of gibberellin production in roots under non-symbiotic conditions, possibly through the direct control of early gibberellin biosynthesis genes.

Notably, many of the genes involved in isoprenoid, carotenoid, strigolactone and gibberellin biosynthesis that were found to be differentially expressed in *nsp1-1* roots in the absence of mycorrhizal fungi were significantly upregulated in wild-type roots during fungal colonization (Table 4.1, genes shown in blue). These results indicate that strigolactones and gibberellins might not only play a role under pre-symbiotic conditions, but might also be important at later stages of mycorrhization.

Table 4.1: List of genes that were differentially expressed in *nsp1-1 roots* compared to the wild type at all three time points tested in the absence of mycorrhizal fungi. Fold changes of transcript levels in non-mycorrhized *nsp1-1* roots versus non-mycorrhized wild-type roots are given. FDR-corrected p-value < 0.05 for all fold changes shown. Genes that were significantly induced upon mycorrhization by more than 1.5 fold and during at least one time point in the wild type are indicated in blue.

			Fold change in *nsp1-1*		
Mtv4.0 ID	**Annotation**	**ID and description of best BLAST hit in A. thaliana (TAIR)**	**8 dpi**	**13 dpi**	**27 dpi**
Isoprenoid biosynthesis					
Medtr8g068265	1-deoxy-xylulose-5-phosphate synthase	AT4G15560 (1-deoxyxylulose 5-phosphate synthase)	-3.0	-6.3	-8.7
Medtr8g068300	1-deoxy-xylulose-5-phosphate synthase	AT4G15560 (1-deoxyxylulose 5-phosphate synthase,)	-18.8	-23.9	-33.7
Medtr4g106870	1-deoxy-xylulose 5-phosphate reductoisomerase	AT5G62790 (1-deoxy-xylulose 5-phosphate reductoisomerase)	-1.9	-2.3	-3.0
Medtr3g437340	4-diphosphocytidyl-2-methyl-erythritol kinase	AT2G26930 (4-(cytidine 5'-phospho)-2-methyl-erithritol kinase)	-2.1	-2.5	-3.0
Medtr2g094160	4-hydroxy-3-methylbut-2-enyl diphosphate synthase	AT5G60600 (4-hydroxy-3-methylbut-2-enyl diphosphate synthase)	-1.7	-2.3	-2.4
Medtr4g069030	4-hydroxy-3-methylbut-2-enyl diphosphate reductase	AT4G34350 (4-hydroxy-3-methylbut-2-enyl diphosphate reductase)	-1.7	-2.0	-2.1
Medtr5g019460	geranylgeranyl pyrophosphate synthase	AT4G36810 (geranylgeranyl pyrophosphate synthase)	-127	-201	-193
Carotenoid and strigolactone biosynthesis					
Medtr3g083630	squalene/phytoene synthase	AT5G17230 (phytoene synthase)	-114	-445	-665
Medtr3g084830	phytoene dehydrogenase/chromoplastic protein	AT4G14210 (phytoene desaturase)	-1.8	-2.0	-2.3
Medtr3g084850	phytoene dehydrogenase/chromoplastic protein	AT4G14210 (phytoene desaturase)	-1.9	-1.9	-2.3
Medtr8g097190	15-cis-zeta-carotene isomerase	AT1G10830 (15-cis-zeta-carotene isomerase)	-3.6	-4.5	-5.8
Medtr1g081290	zeta-carotene desaturase	AT3G04870 (zeta-carotene desaturase)	-1.8	-2.4	-2.9
Medtr2g086700	capsanthin/capsorubin synthase	AT3G10230 (lycopene β-cyclase)	n.s.	-1.5	-1.8
Medtr1g054965	carotenoid isomerase	AT1G06820 (carotenoid isomerase)	-5.6	-5.6	-5.2

continued overleaf

Table 4.1: continued.

			Fold change in *nsp1-1*		
Mtv4.0 ID	**Annotation**	**ID and description of best BLAST hit in A. thaliana (TAIR)**	**8 dpi**	**13 dpi**	**27 dpi**
Medtr3g104560	cytochrome P450 family protein	AT2G26170 (member of the CYP711A cytochrome P450 family)	-3.3	-3.6	-3.9
Medtr7g079440	cytochrome P450 family monooxygenase	AT1G31800 (protein with β-ring carotenoid hydroxylase activity)	-4.1	-5.0	-5.9
Medtr1g471050	beta-carotene isomerase D27	AT1G03055 (unknown protein)	-15.4	-23.3	-38.2
Medtr7g045370	carotenoid cleavage dioxygenase CCD7	AT2G44990 (carotenoid cleavage dioxygenase CCD7)	-2.2	-2.5	-2.8
Medtr3g109610	carotenoid cleavage dioxygenase CCD8	AT4G32810 (carotenoid cleavage dioxygenase CCD8)	-2.9	-5.8	-7.4
Medtr7g063800	carotenoid cleavage dioxygenase	AT4G32810 (carotenoid cleavage dioxygenase CCD8)	-6.3	-12.9	-18.4
Medtr8g037315	carotenoid cleavage dioxygenase CCD1	AT3G63520 (9-cis-epoxycarotenoid dioxygenase)	-1.7	-2.1	-2.3
Medtr3g110195	retinal pigment epithelial membrane protein	AT3G63520 (9-cis-epoxycarotenoid dioxygenase)	-2.8	-3.1	-4.6
Medtr4g035650	chaperone dnaJ-like protein	AT5G61670 (encodes a close homolog of the Cauliflower Orange protein)	-2.2	-2.4	-3.2
Gibberellic acid biosynthesis					
Medtr7g011663	copalyldiphosphate synthase	AT4G02780 (copalyl pyrophosphate synthase)	-43.6	-52.9	-59.5
Medtr7g011730	copalyldiphosphate synthase	AT4G02780 (copalyl pyrophosphate synthase)	-15.8	-7.1	-4.7
Medtr7g011770	copalyldiphosphate synthase	AT4G02780 (copalyl pyrophosphate synthase)	-8.5	-7.5	-9.0
Medtr2g105360	ent-kaurenoic acid oxidase	AT5G25900 (ent-kaurene oxidase)	-2.8	-3.6	-4.7
Medtr0045s0080	cytochrome P450 family 90 protein	AT2G32440 (ent-kaurenoic acid hydroxylase)	-18.0	-6.0	-9.7
Medtr0045s0070	cytochrome P450 family 90 protein	AT2G32440 (ent-kaurenoic acid hydroxylase)	-448	-795	-302
Medtr0045s0060	cytochrome P450 family 90 protein	AT2G32440 (ent-kaurenoic acid hydroxylase)	-268	-126	-64.3
Medtr1g102070	gibberellin 20-oxidase	AT5G51810 (gibberellin 20-oxidase)	5.8	4.6	3.8
Medtr6g464620	gibberellin 20-oxidase	AT4G25420 (gibberellin 20-oxidase)	2.1	2.2	3.6
Medtr2g102570	gibberellin 2-beta-dioxygenase	AT1G15550 (gibberellin-3-oxidase-1)	1.8	1.6	1.9

4.2.2 *NSP1* is required for the induction of a subset of genes involved in strigolactone and gibberellin biosynthesis during mycorrhizal colonization

Next, the role of *NSP1* in the transcriptional reprogramming during fungal colonization was investigated. To this end, the functions of the genes that were dependent on *NSP1* for their induction upon mycorrhization were analysed in more detail. To limit the list of potential target genes of NSP1, only genes that showed a dependence on *NSP1* for their upregulation across all three time points were considered to be good candidates for direct targets and were included in the analyses.

A singular GO term enrichment analysis with these *NSP1*-dependent genes using the whole *M. truncatula* genome as background revealed that similar to the proposed target genes of NSP1 under non-symbiotic conditions, the potential target genes of NSP1 during mycorrhization were associated with isoprenoid and lipid metabolism (Figure 4.1 B). Indeed, several of the genes involved in strigolactone and gibberellin biosynthesis described above were found to be among the *NSP1*-dependent genes induced during mycorrhization, including two genes encoding enzymes from the isoprenoid biosynthesis pathway (DXS and 4-hydroxy-3-methylbut-2-enyl diphosphate synthase (HDS)), six genes encoding enzymes involved in carotenoid and strigolactone biosynthesis (Z-ISO, ZDS, a homolog of lycopene β-cyclase, CCD8, the closest homolog of CCD8, and the homolog of the cauliflower *Orange* gene), and three genes required for gibberellic acid biosynthesis (*KO*, *KAO2*, and *GA20ox*; Table 4.2).

Interestingly, many of the remaining genes involved in strigolactone and gibberellin biosynthesis that were identified to be downregulated in *nsp1-1* under non-symbiotic conditions, including *D27*, showed a significant induction in *nsp1-1* roots upon fungal colonization. These findings suggest that other transcription factors must be involved in the transcriptional upregulation of these genes during mycorrhization. Together, these results indicate that *NSP1* is required for the regulation of only a subset of genes required for strigolactone and gibberellin biosynthesis during mycorrhizal colonization of the roots.

Table 4.2: List of mycorrhizal genes whose induction was consistently dependent on *NSP1* across the whole time course of fungal colonization. Fold changes of transcript levels in mycorrhized versus non-mycorrhized wild-type roots are given. FDR-corrected p-value < 0.05 for all fold changes shown. 'N.s.' depicts a statistically non-significant fold change.

			Fold change in the wild type		
Mtv4.0 ID	**Annotation**	**ID and description of best BLAST hit in *A. thaliana* (TAIR)**	**8 dpi**	**13 dpi**	**27 dpi**
Isoprenoid biosynthesis					
Medtr8g068300	1-deoxy-D-xylulose-5-phosphate synthase	AT4G15560 (1-deoxyxylulose 5-phosphate synthase)	2.7	2.3	1.7
Medtr2g094160	4-hydroxy-3-methylbut-2-enyl diphosphate synthase	AT5G60600 (4-hydroxy-3-methylbut-2-enyl diphosphate synthase)	1.6	1.7	1.8
Carotenoid and strigolactone biosynthesis					
Medtr8g097190	15-cis-zeta-carotene isomerase	AT1G10830 (15-cis-zeta-carotene isomerase)	1.5	1.6	1.6
Medtr1g081290	zeta-carotene desaturase	AT3G04870 (zeta-carotene desaturase)	n.s.	1.5	1.5
Medtr2g086700	capsanthin/capsorubin synthase	AT3G10230 (lycopene β-cyclase)	n.s.	1.6	1.5
Medtr3g109610	carotenoid cleavage dioxygenase CCD8	AT4G32810 (carotenoid cleavage dioxygenase CCD8)	2.0	2.1	2.0
Medtr7g063800	carotenoid cleavage dioxygenase	AT4G32810 (carotenoid cleavage dioxygenase CCD8)	1.9	2.0	n.s.
Medtr4g035650	chaperone dnaJ-like protein	AT5G61670 (encodes a close homolog of the Cauliflower Orange protein)	1.6	1.7	n.s.
Gibberellic acid biosynthesis					
Medtr2g105360	cytochrome P450 family ent-kaurenoic acid oxidase	AT5G25900 (ent-kaurene oxidase, cytochrome p450)	1.9	2.0	1.6
Medtr0045s0060	cytochrome P450 family 90 protein	AT2G32440 (ent-kaurenoic acid hydroxylase KAO2)	1.9	1.8	n.s.
Medtr1g102070	gibberellin 20-oxidase	AT5G51810 (gibberellin 20-oxidase)	1.9	2.3	2.1

To confirm the results obtained by RNA-seq, the expression levels of nine of the *NSP1*-dependent genes were quantified in wild-type, *nsp1-1*, *nsp2-2*, and *ram1-1* roots using qRT-PCR (Figures 4.3, 4.4, and 4.5). In general, a very good overlap was found between the results obtained by RNA-seq and qRT-PCR, with only very few discrepancies in the statistical power of the observed differences between treatments and genotypes.

These analyses further revealed that the majority of the genes that were dependent on *NSP1* before or during mycorrhization, in particular the genes involved in strigolactone and gibberellin biosynthesis, were not differentially expressed in *ram1-1* and *nsp2-2* roots (Figures 4.3, 4.4, and 4.5). Surprisingly, *D27* also belonged to this group of genes, with expression levels that were unaltered in *nsp2-2* roots compared to the wild type under non-symbiotic and symbiotic conditions (Figure 4.4 A). One exception to this was the closest homolog of *CCD8* (Medtr7g063800), whose expression was drastically reduced not only in *nsp1-1*, but also in *nsp2-2* roots under both non-symbiotic and symbiotic conditions (Figure 4.4 C), indicating that *NSP2* is involved in the transcriptional regulation of this gene in the absence of mycorrhizal fungi and during AM development.

4.2.3 *NSP2* might be involved in the regulation of defence and stress responses under non-symbiotic conditions

Although no mycorrhizal phenotype was observed for *nsp2-2* under the conditions tested here, global gene expression profiling identified a large number of genes whose expression was dependent on *NSP2* under non-symbiotic conditions and during the late stages of AM development. Specifically, 193 genes were identified that were differentially expressed in *nsp2-2* roots at all three time points in the absence of mycorrhizal fungi (Chapter 3, Figure 3.9). To investigate the biological processes that might be regulated by *NSP2* under non-symbiotic conditions, a singular GO term enrichment analysis of these genes was performed, revealing several enriched GO terms associated with defence responses, signal transduction, and the response to stress (Figure 4.6 A). Conducting a BLAST search with the corresponding protein sequences against the *A. thaliana* proteome confirmed the presence of a number of genes involved in defence and stress responses in the group of up- and downregulated genes in *nsp2-2* roots.

In addition, the functions of the genes that were consistently dependent on *NSP2* for their induction during mycorrhization were investigated to gain insights into the mycorrhizal processes that might be regulated by *NSP2*. A GO term enrichment analysis with these *NSP2*-dependent genes revealed several enriched GO terms associated with protein modification and metabolism (Figure 4.6 B). As *NSP2* appeared to have the biggest impact on gene expression at late time points during mycorrhization, the *NSP2*-dependent genes that were upregulated in wild-type roots at all three time points (four genes), at 13 dpi and 27 dpi (69 genes), and at 27 dpi (328 genes; Chapter 3, Figure 3.8) were further analysed by conducting a BLAST search with the corresponding protein sequences against the *A. thaliana* proteome. However, the analysis of the best hits did not reveal any obvious mycorrhizal processes that might be regulated by *NSP2* during AM development and could explain the slight, but not statistically significant reduction in fungal infection structures observed in *nsp2-2* roots at 27 dpi (Chapter 2).

4.2.4 A complex of NSP1 and NSP2 induces the expression of *D27* in a transient assay in *N. benthamiana*

Global gene expression profiling has revealed a number of genes that might be directly or indirectly regulated by the GRAS-domain proteins in the absence of mycorrhizal fungi and during AM development. Using a transient expression system in *N. benthamiana*, it had previously been demonstrated that *NSP1*, when co-expressed with *NSP2*, is able to activate gene expression from the promoters of Nod factor-inducible genes such as *ERN1* and *ENOD11* (Cerri et al., 2012). Thus, a similar transactivation system was developed to test the ability of the GRAS-domain proteins to directly regulate the expression of genes identified by transcriptional profiling described above. To this end, the GRAS-domain proteins were constitutively expressed in *N. benthamiana* leaves together with the firefly *LUCIFERASE* (*LUC*) gene fused to promoter sequences of known and potential direct target genes. The ability of transcription factors to activate reporter gene expression from a specific promoter sequence was determined by enzymatic quantification of the LUC activity in transformed leaf tissues. To account for variability in the efficiency of transformation and protein extraction, the LUC activity was normalized against the activity of β-glucuronidase (GUS), which was constitutively expressed in the same transformation vector (Figure 4.7 A).

The conditions for transient transformation, protein extraction, and enzyme activity assays were optimised using an expression vector containing *NSP1* or *NSP2* alone or in combination and the *LUC* gene under the control of the *ENOD11* promoter, which had previously been shown to be bound and activated by a complex of NSP1 and NSP2 (Hirsch et al., 2009; Cerri et al., 2012). The same expression vector containing all the components but lacking the genes encoding the transcription factors served as a negative control. No induction of LUC activity was observed when expressing *NSP1* alone, while a small, but statistically significant induction was seen when expressing *NSP2* (Figure 4.7 B). The expression of both *NSP1* and *NSP2* together resulted in a very strong induction of LUC activity, suggesting that the complex of NSP1 and NSP2 is able to activate gene expression from the *ENOD11* promoter more efficiently than the individual transcription factors alone. These results are consistent with the findings of Cerri and colleagues (Cerri et al., 2012) and confirm that the transactivation assay developed here is suited to measure the ability of individual transcription factors or transcription factor complexes to activate gene expression.

Next, I investigated whether NSP1 is able to activate the expression of the strigolactone biosynthesis gene *D27*, which showed a strongly reduced expression in *nsp1-1* roots compared to the wild type under low phosphate conditions and in the absence of mycorrhizal fungi (Liu et al., 2011, results presented here). The expression of *NSP1* together with *LUC* under the control of the 3 kb long *D27* promoter did not result in the induction of LUC activity, suggesting that NSP1 alone is not able to activate *D27* expression (Figure 4.7 D). By contrast, the expression of *NSP1* together with *NSP2* led to a strong induction of LUC activity. When expressing *NSP2* alone, a small induction of LUC activity was observed, however, this induction was much weaker than the one caused by the complex of NSP1 and NSP2 (Figure 4.7 D). Similar findings were obtained when testing the activation of *LUC* under the control of the 1 kb long *D27* promoter, suggesting that the first 1 kb upstream of the start codon of *D27* is sufficient for the activation by a complex of NSP1 and NSP2 (Figure 4.7 E). This is consistent with *in vitro* binding studies showing that NSP1 is able to associate with the same region of the *D27* promoter (Liu et al., 2011). Together, these findings suggest that *NSP1*, when co-expressed with *NSP2*, is able to activate gene expression from the *D27* promoter in a transient assay in *N. benthamiana* leaves. By contrast, no induction of LUC activity was seen when expressing *NSP1* and *NSP2* with the *LUC* gene under the control of the promoter of Medtr3g080840, a close homolog of *MtD27* (Figure 4.7 C; Liu et al., 2011). These results demonstrate that

the activation of the *D27* promoter by NSP1 and NSP2 observed in the transactivation assay is specific.

4.2.5 Generation of *M. truncatula* lines stably expressing GFP-tagged NSP1 and NSP2 for the identification of genome-wide DNA-binding sites

While the transactivation assay in *N. benthamiana* provides a useful tool to measure the ability of the GRAS-domain proteins to induce gene expression via individual promoter sequences, it is less well suited to test very large numbers of different promoters and combinations of transcription factors. Furthermore, as a heterologous system, the conditions for the regulation of gene expression are likely to be different in *N. benthamiana* leaves from the conditions in *M. truncatula* roots during symbiosis. Thus, *M. truncatula* lines stably expressing GFP-tagged NSP1 (generated by Jian Feng) and NSP2 were generated to identify the genome-wide binding sites of these transcription factors by performing chromatin-immunoprecipitation assays followed by Illumina deep sequencing (ChIP-seq). To ensure the functionality of the GFP-fusion proteins, the stably transformed *M. truncatula* plants expressing *GFP-NSP1* or *NSP2-GFP* in the corresponding mutant backgrounds were tested for their ability to form a functional symbiosis with rhizobial bacteria. Plants carrying a mutation in *NSP1* or *NSP2* have previously been shown to be unable to form pink nodules (Kaló et al., 2005; Smit et al., 2005). The expression of *GFP-NSP1* under the control of the endogenous *NSP1* promoter in the *nsp1-1* mutant background restored the ability of the roots to form pink nodules, confirming that the GFP-fusion protein is functional (Figure 4.8, courtesy of Jian Feng). By contrast, the expression of *NSP2-GFP* under the control of the endogenous *NSP2* promoter did not result in the formation of pink nodules in the corresponding mutant background (data not shown). Therefore, the constitutively active *Ubiquitin* promoter was used to overexpress *NSP2-GFP* in the *nsp2-2* mutant. This construct complemented the *nsp2* nodulation phenotype, suggesting that the NSP2-GFP fusion protein is functional (Figure 4.9).

To test experimental procedures for ChIP and identify DNA binding sites that can serve as positive controls for future ChIP-seq experiments, ChIP-qPCR assays were performed with *GFP-NSP1* expressing lines grown under low phosphate conditions and in the absence of mycorrhizal fungi. As several lines of evidence suggest that *D27* is directly bound by NSP1 under these conditions (Liu et al., 2011; work presented here), the

promoter sequence of this gene was used as a positive control for ChIP-qPCR assays. To test whether the promoter sequence of *D27* was enriched after immunoprecipitation of GFP-NSP1-DNA complexes using α-GFP antibodies, qPCR analysis was performed with primer pairs that amplify regions within or outside of the 1 kb promoter sequence that had previously been found to be bound by NSP1 *in vitro* (Liu et al., 2011; Figure 4.10 A). Preliminary results showed no enrichment of *D27* promoter sequences when using lines stably expressing *GFP-NSP1* compared to untransformed wild-type plants (Figure 4.10 B). These results might suggest that the promoter sequence of *D27* is not directly bound by NSP1. However, due to time limitations, the entire ChIP-qPCR assay could only be performed once, and it is likely that the experimental conditions need to be optimised to be able to detect binding of NSP1 to the *D27* promoter.

4.3 Discussion

Here, the biological processes that are controlled by *NSP1* and *NSP2* during mycorrhizal colonization and under non-symbiotic conditions were investigated by analysing the functions of the potential target genes of these two transcription factors identified by transcriptomic profiling. These analyses have revealed an important role for *NSP1* in the regulation of strigolactone and gibberellin biosynthesis in the absence of mycorrhizal fungi and partly during fungal colonization of the roots.

The function of strigolactones at the pre-symbiotic stage of AM symbiosis is relatively well understood. Under low nutrient conditions, the production of strigolactones is induced by the transcriptional upregulation of genes encoding key biosynthetic enzymes such as *D27* (Liu et al., 2012). After release into the rhizosphere, these hormones act as signalling molecules to mycorrhizal fungi, inducing spore germination and hyphal branching and thereby directing fungal growth towards the roots. *NSP1* has previously been shown to be required for the upregulation of *D27* under phosphate starvation (Liu et al., 2011). Consistent with these findings, the expression levels of *D27* and the two carotenoid cleavage dioxygenases *CCD7* and *CCD8*, which have been proposed to act downstream of *D27* to produce the immediate strigolactone precursor carlactone, were strongly reduced in *nsp1-1.* These results confirm that *NSP1* plays an important role in the regulation of strigolactone biosynthesis at the pre-contact stage of AM symbiosis. Surprisingly, the transcriptional downregulation was not just limited to genes involved in the late steps of strigolactone biosynthesis, but included many genes involved in the

biosynthesis of isoprenoids and carotenoids, from which strigolactones are derived. The key steps in isoprenoid biosynthesis are mediated by the enzymes DXS, DXR, and HDR (Cazzonelli and Pogson, 2010; Figure 4.2), all of which were transcriptionally dependent on *NSP1*. Moreover, the putative homolog of PSY, the most important regulatory enzyme in carotenoid biosynthesis (Cazzonelli and Pogson, 2010), belonged to the most strongly downregulated genes in *nsp1-1*. These findings suggest that NSP1 might not only regulate genes involved in the late steps of strigolactone biosynthesis, but might also directly control several other key genes in isoprenoid and carotenoid biosynthesis under pre-symbiotic conditions. Alternatively, the lack of *D27* expression in *nsp1-1* roots during phosphate starvation and the resulting block in strigolactone production might indirectly reduce the transcript levels of genes acting upstream and downstream of *D27* through feedback regulation mediated by other transcriptional regulators. The transactivation assay in *N. benthamiana* leaves and ChIP-seq assays with lines stably expressing GFP-tagged NSP1 provide useful tools for future research investigating which of these genes are bound and thus directly regulated by NSP1.

The observation that *NSP1*, when co-expressed with *NSP2*, is able to induce the expression of the *LUC* reporter gene from the *D27* promoter in the transactivation assay suggests that *D27* is indeed a direct target of NSP1, consistent with *in vitro* DNA binding studies reporting that NSP1 is able to directly bind to the *D27* promoter sequence (Liu et al., 2011). The observed lack of *pD27-LUC* induction when expressing *NSP1* alone further indicates that similar to the activation of the rhizobial-induced promoters *pENOD11* and *pERN1*, NSP1 requires NSP2 to be able to activate gene expression from the *D27* promoter. This is in line with findings of a previous study showing that the expression levels of *D27* are significantly reduced, although not completely abolished, under phosphate-limiting conditions in *nsp2* roots (Liu et al., 2011). Thus, it is surprising that no such reduction in *D27* transcript levels was observed in the *nsp2-2* mutant under the conditions tested here. One reason for this discrepancy could be the high nitrogen conditions under which plants were grown for global gene expression profiling (Chapter 3.2.1). Liu and colleagues have previously shown that the expression of *D27* in *M. truncatula* not only depends on phosphate, but also on nitrogen levels, with *D27* expression being induced under nitrogen starvation (Liu et al., 2011). The lack of a reduction in *D27* expression in *nsp2-2* roots observed here implies that there is some level of redundancy regarding the function of *NSP2* in the regulation of *D27* expression, at least under some conditions. Other transcription factors might be able to interact with NSP1 to activate *D27* expression. A recent study has identified the novel GRAS-domain

protein MIG1 as an interaction partner of NSP1 and DELLA1 (Heck et al., 2016). Furthermore, the *M. truncatula* genome encodes a large number of additional GRAS-domain proteins, including a close homolog of NSP2 (Lauressergues et al., 2012). It is possible that one or several of these GRAS-domain proteins are able to form an active transcription factor complex with NSP1 under non-symbiotic conditions to control the expression of *D27*, a hypothesis that could be tested using the transactivation assay in *N. benthamiana* leaves.

Interestingly, although the expression levels of most genes involved in strigolactone biosynthesis were not affected in *nsp2-2*, the transcript levels of the closest homolog of *CCD8* were drastically reduced. The *M. truncatula* genome encodes two copies of *CCD8* (Medtr3g109610, which has previously been described as *CCD8*, and Medtr7g063800, the closest homolog), both of which were shown to be transcriptionally induced during phosphate starvation (van Zeijl et al., 2015). Although the relative expression levels of Medtr7g063800 are generally lower than the ones of Medtr3g109610 (van Zeijl et al., 2015), this does not exclude the possibility that both genes have a function in strigolactone biosynthesis. Strigolactone levels in *nsp2* root exudates differ significantly from the wild type. While the strigolactone variant orobanchol accumulates to very high levels in the *nsp2* mutant, the orobanchol derivative didehydro-orobanchol is completely absent in *nsp2* root exudates (Liu et al., 2011). Based on these findings, it has been proposed that *NSP2* is required for the expression of an enzyme involved in the production of didehydro-orobanchol (Liu et al., 2011), and it would be interesting to test whether the homolog of *CCD8* could fulfil such a function.

Overall, the results of previous studies and global gene expression profiling described here indicate that *NSP1* and *NSP2* have different roles in regulating strigolactone production at the pre-symbiotic stage of AM symbiosis. Importantly, the amounts of different strigolactone variants were found to differ significantly between the two mutants, with orobanchol being completely absent in *nsp1* root exudates, but accumulating in *nsp2* roots (Liu et al., 2011). Interestingly, orobanchol has been shown to be able to induce hyphal branching of germinating fungal spores (Akiyama et al., 2010). It is therefore perhaps not surprising that *nsp2-2* appears to have a weaker mycorrhizal phenotype than *nsp1-1*, especially when assuming that the *nsp1* mutant phenotype is at least partly caused by the complete lack of strigolactones in *nsp1* root exudates at pre-symbiotic stages. The results obtained here suggest that *NSP2* is involved in regulating only a subset of genes that function in the biosynthesis of

strigolactones under low phosphate conditions, and the regulation of these genes by *NSP2* might depend on the exact growth conditions, including the availability of different nutrients in the rhizosphere.

Global gene expression profiling of non-mycorrhized and mycorrhized roots has further revealed that many genes involved in isoprenoid, carotenoid and strigolactone biosynthesis were transcriptionally induced during mycorrhization in wild-type roots. The genes encoding the two isoprenoid enzymes DXS and DXR and the carotenoid enzymes ZDS and PDS have previously been found to be upregulated upon fungal colonization in *M. truncatula* and *Nicotiana tabacum* (Fester et al., 2002; Walter et al., 2002; Lohse et al., 2005). In line with this, a recent study has shown that the levels of strigolactones increase in mycorrhized tomato roots (López-Ráez et al., 2015). These findings suggest that strigolactones are not only important at the pre-symbiotic stage of AM development, but might also play a role at later stages during the colonization of roots by AM fungi. While the role of strigolactones at the pre-contact stage of AM symbiosis is well characterised, the potential role of strigolactones during fungal colonization is less clear. It is possible that strigolactones guide fungal colonization within roots by acting as signalling molecules to the fungus, similar to their role in the rhizosphere. It is also conceivable that strigolactones act as endogenous plant hormones on the root to regulate host processes during AM development. However, a mutation in the strigolactone-receptor *D14* in rice does not result in a decrease in mycorrhization (Yoshida et al., 2012; Gutjahr et al., 2015), suggesting that during fungal colonization of the roots, strigolactones primarily act on the fungus. At late stages of the symbiosis, strigolactone production has been found to decrease in several plant species, and it has been hypothesised that this reduction in strigolactone levels serves to prevent over-colonization of the roots by AM fungi (Fernández-Aparicio et al., 2010; López-Ráez et al., 2011; Aroca et al., 2013; López-Ráez et al., 2015). In addition to strigolactones, other carotenoid cleavage products, including C13 α-ionol and C14 mycorradicin derivatives, were found to accumulate in mycorrhized roots of many plant species at late stages of the symbiosis, although the functions of these compounds in AM development are currently unknown (Walter et al., 2007). Thus, the upregulation of isoprenoid and carotenoid biosynthesis genes in mycorrhized roots observed here might promote strigolactone biosynthesis at early and intermediate time points, while at late time points, the products of these pathways might serve as precursors for mycorradicin and α-ionol derivatives.

Only a few of the genes involved in strigolactone biosynthesis showed an abolished induction in *nsp1-1* during mycorrhization, suggesting that *NSP1* is involved in the regulation of only a subset of these biosynthesis genes during fungal colonization of the roots. By contrast, the majority of the genes induced in the wild type, including *PSY* and *D27*, did not require *NSP1* for their upregulation during mycorrhizal colonization. Promoter-GUS studies indicate that *D27* is expressed in arbuscule-harbouring cells of mycorrhized roots, and this expression is not abolished in an *nsp1* mutant background (Bruno Guillotin and Guillaume Bécard, personal communication). In *L. japonicus*, a similar *NSP1*-independent induction of *D27* in mycorrhized roots has been reported (Nagae et al., 2014). Together, these results suggest that other transcription factors must be involved in the transcriptional regulation of these strigolactone biosynthesis genes during AM development. In addition, these findings imply that strigolactone biosynthesis is differentially regulated before and during mycorrhization.

Research in recent years has uncovered an important role for strigolactones not only in the establishment of AM symbiosis, but also in many other aspects of plant development, including shoot branching and root development (Al-Babili and Bouwmeester, 2015). Considering that strigolactones are not detectable in *nsp1* root exudates, one would expect that the *nsp1* mutant also shows other signs of strigolactone deficiency. Surprisingly, however, the *M. truncatula nsp1* mutant does not display changes in shoot architecture (Liu et al., 2011). Furthermore, the quantification of lateral root number and root length in *nsp1* plants only revealed a very mild effect of the loss of *NSP1* on root architecture (Bruno Guillotin and Guillaume Bécard, personal communication). The observation that many strigolactone biosynthesis genes appear to be induced during mycorrhization even in the absence of *NSP1* suggests that strigolactone production in *nsp1-1* plants does take place under some conditions. Alternative pathways must contribute to the control of strigolactone biosynthesis, which might explain the lack of a broader strigolactone phenotype in the *nsp1* mutant. It would be interesting to quantify strigolactone levels not only in *nsp1-1* root exudates, but also in other plant tissues such as shoots to investigate whether strigolactones are produced elsewhere in the mutant.

In addition to the function of *NSP1* in the control of strigolactone production, transcriptomic profiling has also revealed a role for *NSP1* in the regulation of gibberellin biosynthesis under non-symbiotic conditions. Gibberellins, just like carotenoids and strigolactones, are derived from the isoprenoid intermediate GGDP. The reduced expression levels of isoprenoid and gibberellin biosynthesis genes are likely to result in

low levels of gibberellins in *nsp1-1* roots. This hypothesis is supported by the observation that transcript levels of late gibberellin biosynthesis genes such as gibberellin-20 oxidase and gibberellin-3 oxidase were upregulated in *nsp1-1*. In *A. thaliana*, these genes have previously been shown to be regulated by a feedback mechanism, with low levels of gibberellins causing the upregulation of two gibberellin-20 oxidases and one gibberellin-3 oxidase (Mitchum et al., 2006; Rieu et al., 2008; Hedden and Thomas, 2012). The quantification of gibberellin levels in *nsp1-1* plants would clarify whether the decreased expression of early gibberellin biosynthesis genes indeed results in reduced levels of this plant hormone. If this is the case, one would also expect the *nsp1-1* mutant to show other signs of gibberellin deficiency, such as a decrease in the efficiency of seed germination.

Similar to the genes involved in strigolactone biosynthesis, several genes that are required for gibberellin biosynthesis were induced in wild-type roots during fungal colonization. This is consistent with previous studies showing that gibberellin levels and the expression of gibberellin biosynthesis genes increase in mycorrhized roots in *M. truncatula* and *L. japonicus* (Gomez et al., 2009; Guether et al., 2009; Ortu et al., 2012; Takeda et al., 2015). In *nsp1-1* roots, the induction of genes encoding KO, KAO2, and gibberellin-20 oxidase was abolished, suggesting that *NSP1* is also required for the regulation of a subset of gibberellin biosynthesis genes during AM development.

Several studies have investigated the role of gibberellins in arbuscular mycorrhization, revealing that gibberellins have both positive and negative effects on the establishment of the symbiosis. Exogenously applied gibberellic acid suppresses mycorrhization, and mutants deficient in gibberellic acid show increased numbers of arbuscules, indicating that high levels of gibberellins play a negative role in fungal infection and arbuscule development (Floss et al., 2013; Foo et al., 2013; Yu et al., 2014). In accordance with this, DELLA proteins, which are targeted for degradation upon perception of gibberellic acid, are required for normal arbuscule development (Floss et al., 2013; Foo et al., 2013; Yu et al., 2014). Meanwhile, gibberellin levels and the expression of gibberellin biosynthesis genes increase upon fungal colonization, suggesting that a certain level of gibberellins is required for AM development (Gomez et al., 2009; Guether et al., 2009; Ortu et al., 2012; Takeda et al., 2015, results presented here). Thus, the right balance of gibberellin levels appears to be crucial for the proper establishment of a functional AM symbiosis and likely requires the precise regulation of the expression of genes involved in the biosynthetic pathway. The observation that the expression of many of the genes involved

in gibberellin biosynthesis depends on *NSP1* suggests that *NSP1* contributes to maintaining the right levels of gibberellins in roots. It is conceivable that the reduction in mycorrhizal colonization observed in *nsp1-1* is not only caused by a lack of strigolactone production, but also by decreased gibberellin levels, particularly at the pre-symbiotic stages. Interestingly, the external application of strigolactones does not fully rescue the decreased levels of mycorrhization in the *L. japonicus nsp1* mutant, indicating that *NSP1* must regulate other processes that play a role in the establishment of AM symbiosis (Takeda et al., 2011). If a lack of both strigolactone and gibberellin production causes the reduced levels of mycorrhization in *nsp1-1* roots, the combined application of both plant hormones should result in a full complementation of the phenotype.

To summarise, global gene expression profiling has revealed important roles of *NSP1* in the regulation of hormone biosynthesis at pre-symbiotic stages and partially during mycorrhizal colonization of roots. The results obtained here suggest that *NSP1* is not only required for strigolactone production, but also plays a role in the regulation of gibberellin biosynthesis. Meanwhile, the role of *NSP2* in mycorrhization remains unclear. *NSP2* appears to have a different role than *NSP1* in the regulation of strigolactone production, and the unaltered expression levels of gibberellin biosynthesis genes further suggest that unlike *NSP1*, *NSP2* is not required for the regulation of gibberellin levels in roots. GO term analysis indicates that *NSP2* might be involved in regulating defence and stress responses under non-symbiotic conditions. Moreover, the expression of a considerable number of genes appears to be dependent on *NSP2* during the later stages of the AM symbiosis. However, as no consistent reduction in mycorrhizal colonization was observed in *nsp2-2 roots*, it is currently unclear whether the differential expression of these genes plays a role in AM development. Different conditions, such as using a weaker fungal inoculum or growing plants with low nitrogen levels, might be required for transcriptional profiling and the assessment of a mycorrhizal phenotype in order to uncover the role of *NSP2* in AM symbiosis.

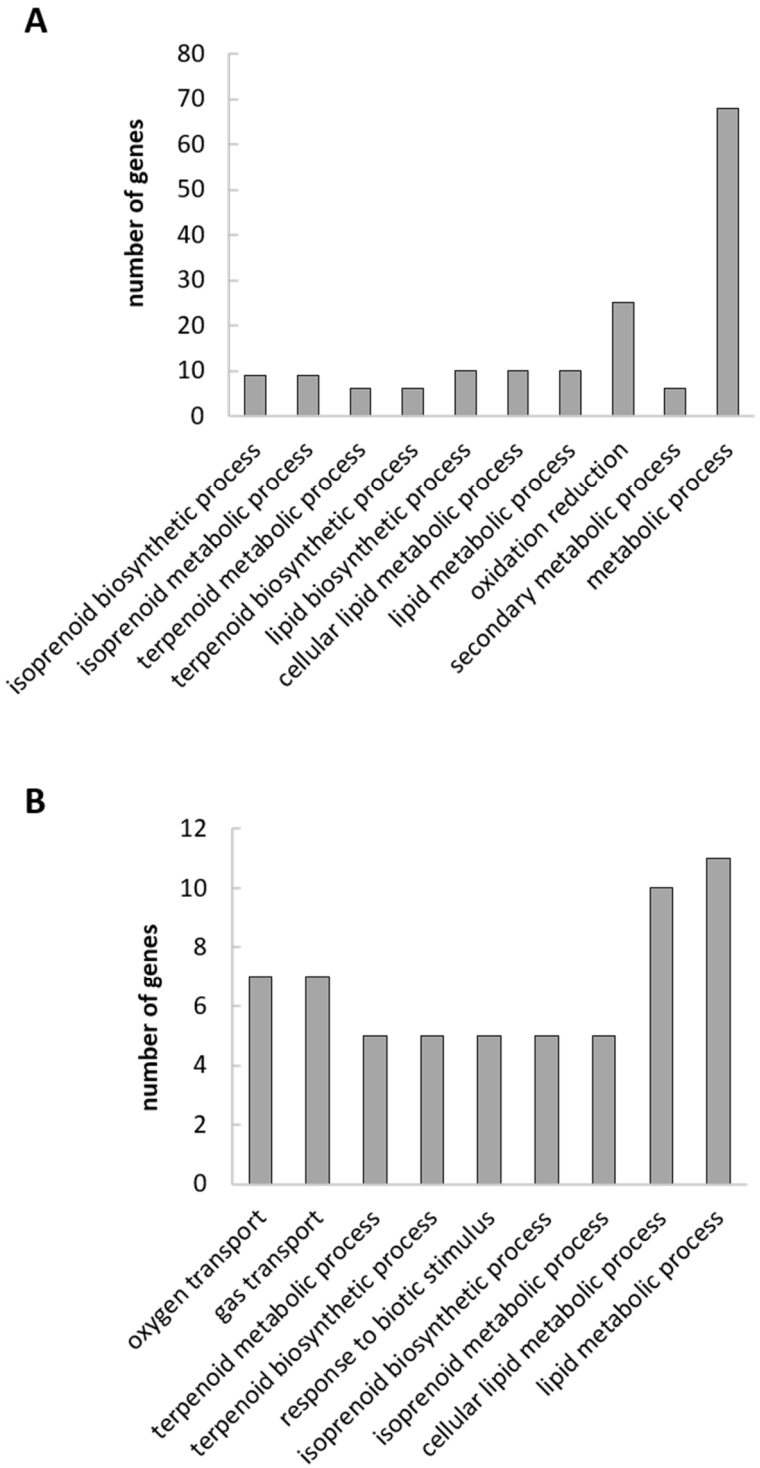

Figure 4.1: Gene ontology (GO) analysis of *NSP1*-dependent genes. Significantly enriched GO terms of genes differentially expressed in non-mycorrhized *nsp1-1* roots compared to non-mycorrhized wild-type roots **(A)** and genes that were found to be consistently dependent on *NSP1* for their induction during mycorrhization **(B)** are shown. Singular enrichment analysis was performed using Agrigo (http://bioinfo.cau.edu.cn/agriGO/index.php) and the whole *M. truncatula* genome as background. Significantly enriched terms of biological processes with an FDR-corrected p-value <0.05 are shown.

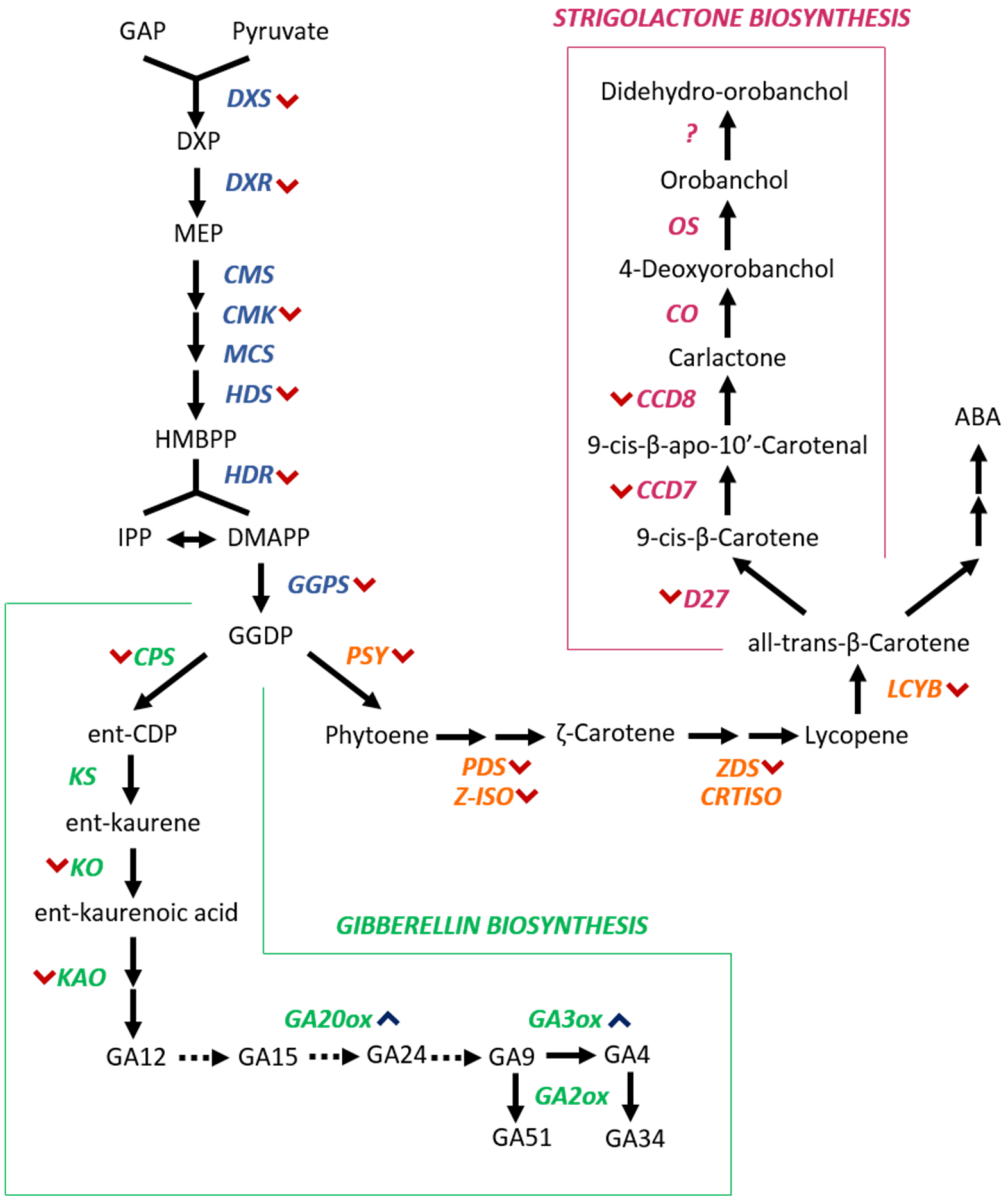

Figure 4.2: Overview of gibberellin and strigolactone biosynthesis pathways. Enzymes involved in isoprenoid, carotenoid, strigolactone, and gibberellin biosynthesis are shown in blue, orange, purple, and green, respectively. Arrowheads next to the enzymes indicate significant up- or down-regulation in *nsp1-1* roots by > 1.5 fold under non-symbiotic conditions. GAP, glyceraldehyde 3-phosphate, DXS, 1-deoxyxylulose 5-phosphate synthase, DXP, 1-deoxy-xylulose-5-phosphate, DXR, 1-deoxy-xylulose-5-phosphate reducto-isomerase, MEP, 2-methyl-erythritol-4-phosphate, CMS, 4-diphosphocytidyl-2-methyl-erythritol synthase, CMK, 4-diphosphocytidyl-2-methyl-erythritol kinase, MCS, 2-methyl-erythritol 2,4-cyclodiphosphate synthase, HDS, 4-hydroxy-3-methylbut-2-enyl diphosphate synthase, HMBPP, 1-hydroxy-2-methyl-2-butenyl 4-diphosphate, HDR, 4-hydroxy-3-methylbut-2-enyl diphosphate reductase, IPP, isopentenyl diphosphate, DMAPP, dimethylallyl diphosphate, GGPS, geranylgeranyl pyrophosphate synthase, GGDP, geranylgeranyl pyrophosphate, CPS, copalyl pyrophosphate synthase, ent-CDP, ent-copalyl diphosphate, KS, ent-kaurene synthase KO, ent-kaurene oxidase, KAO, ent-kaurenoic acid oxidase, GA, gibberellin, GA20ox, gibberellin 20-oxidase, GA3ox, gibberellin 3-oxidase, GA2ox, gibberellin 2-oxidase, PSY, phytoene synthase, PDS, phytoene desaturase, Z-ISO, zeta-carotene isomerase, ZDS, zeta-carotene desaturase, CRTISO, carotene cis-trans isomerase, LCYB, lycopene β-cyclase, D27, DWARF27, CCD7, carotenoid cleavage dioxygenase 7, CCD8, carotenoid cleavage dioxygenase 8, CO, carlactone oxidase, OS, orobanchol synthase, ABA, abscisic acid (modified after Cazzonelli and Pogson, 2010; Hedden and Thomas, 2012; Al-Babili and Bouwmeester, 2015).

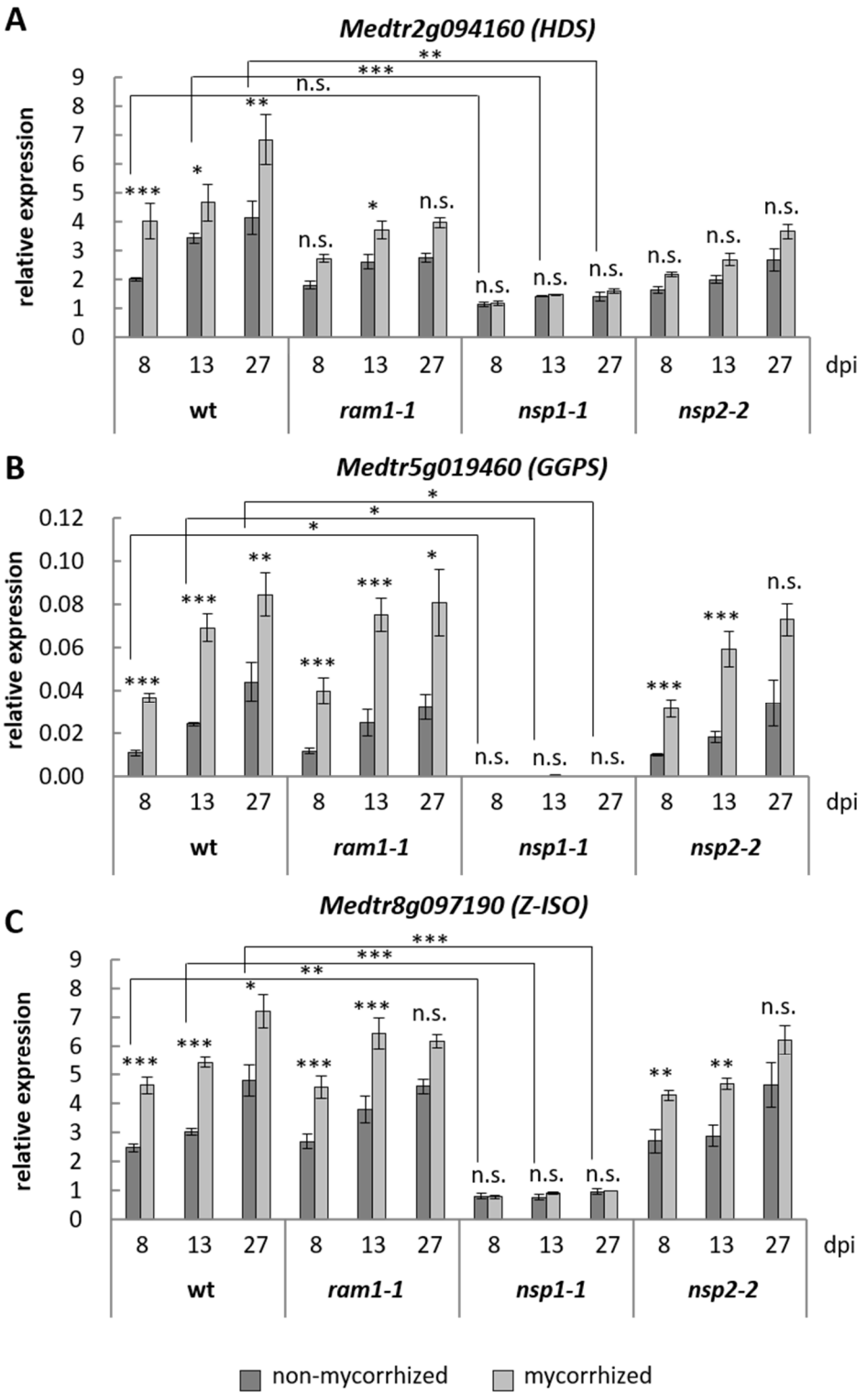

Figure 4.3: Quantification of transcript levels of genes involved in isoprenoid and carotenoid biosynthesis in non-mycorrhized and mycorrhized wild-type (wt), *ram1-1*, *nsp1-1*, and *nsp2-2* roots at 8 dpi, 13 dpi, and 27 dpi. Expression levels of the *M. truncatula* homologs of *HDS* **(A)**, *GGPS* **(B)**, and *Z-ISO* **(C)** are shown. Expression levels were measured by qRT-PCR and normalized to *Ubiquitin* expression. Bars represent means of 4 biological replicates ± SEM. Asterisks indicate significant differences in expression levels (ANOVA, post hoc Tukey, *, $P < 0.05$; **, $P < 0.01$; ***, $P < 0.001$, n.s., $P > 0.05$).

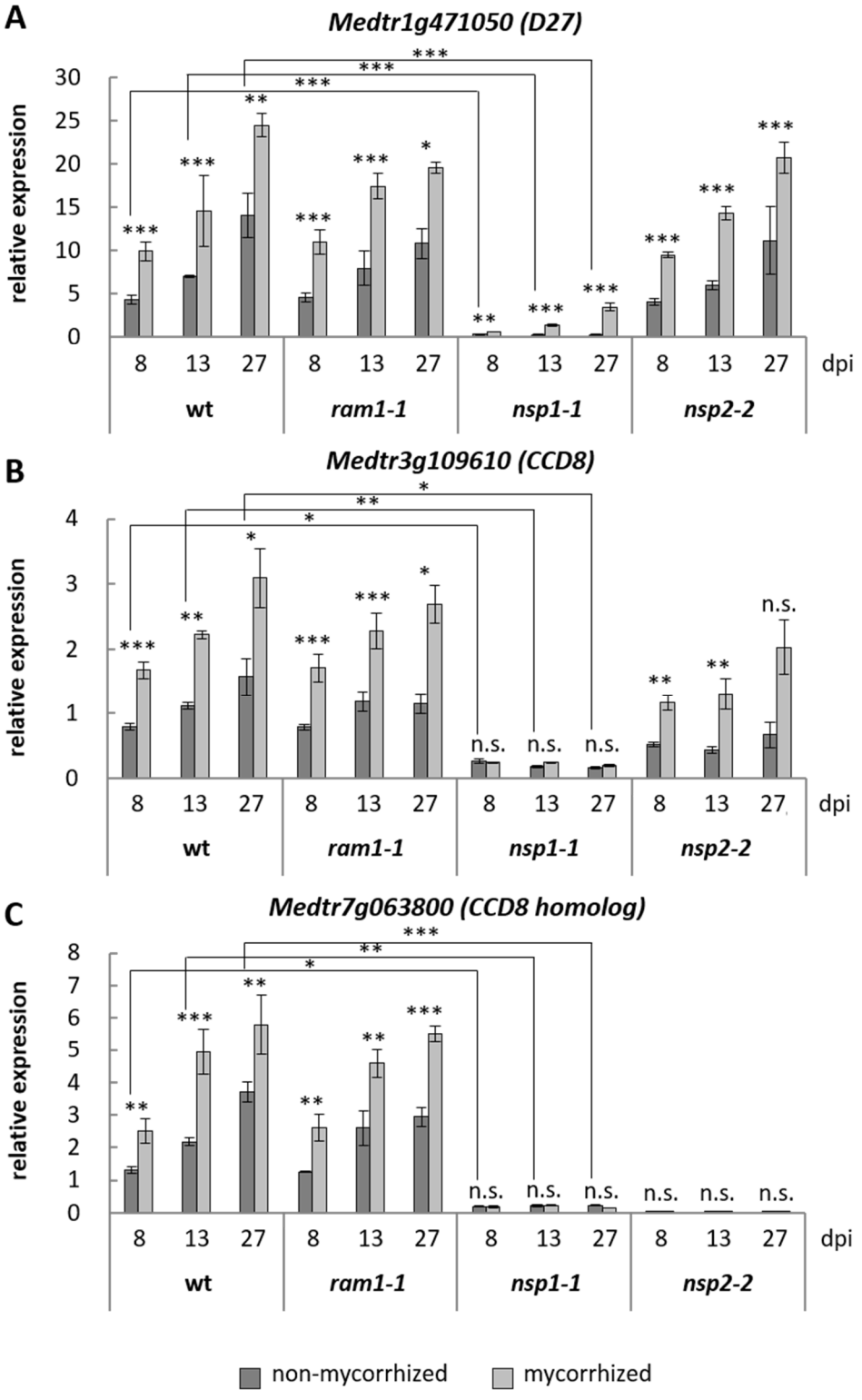

Figure 4.4: Quantification of transcript levels of genes involved in strigolactone biosynthesis in non-mycorrhized and mycorrhized wild-type (wt), *ram1-1*, *nsp1-1*, and *nsp2-2* roots at 8 dpi, 13 dpi, and 27 dpi. Expression levels of the *M. truncatula* genes *D27* **(A)**, *CCD8* **(B)**, and the closest homolog of *CCD8* **(C)** are shown. Expression levels were measured by qRT-PCR and normalized to *Ubiquitin* expression. Bars represent means of 4 biological replicates ± SEM. Asterisks indicate significant differences in expression levels (ANOVA, post hoc Tukey, *, $P < 0.05$; **, $P < 0.01$; ***, $P < 0.001$, n.s., $P > 0.05$).

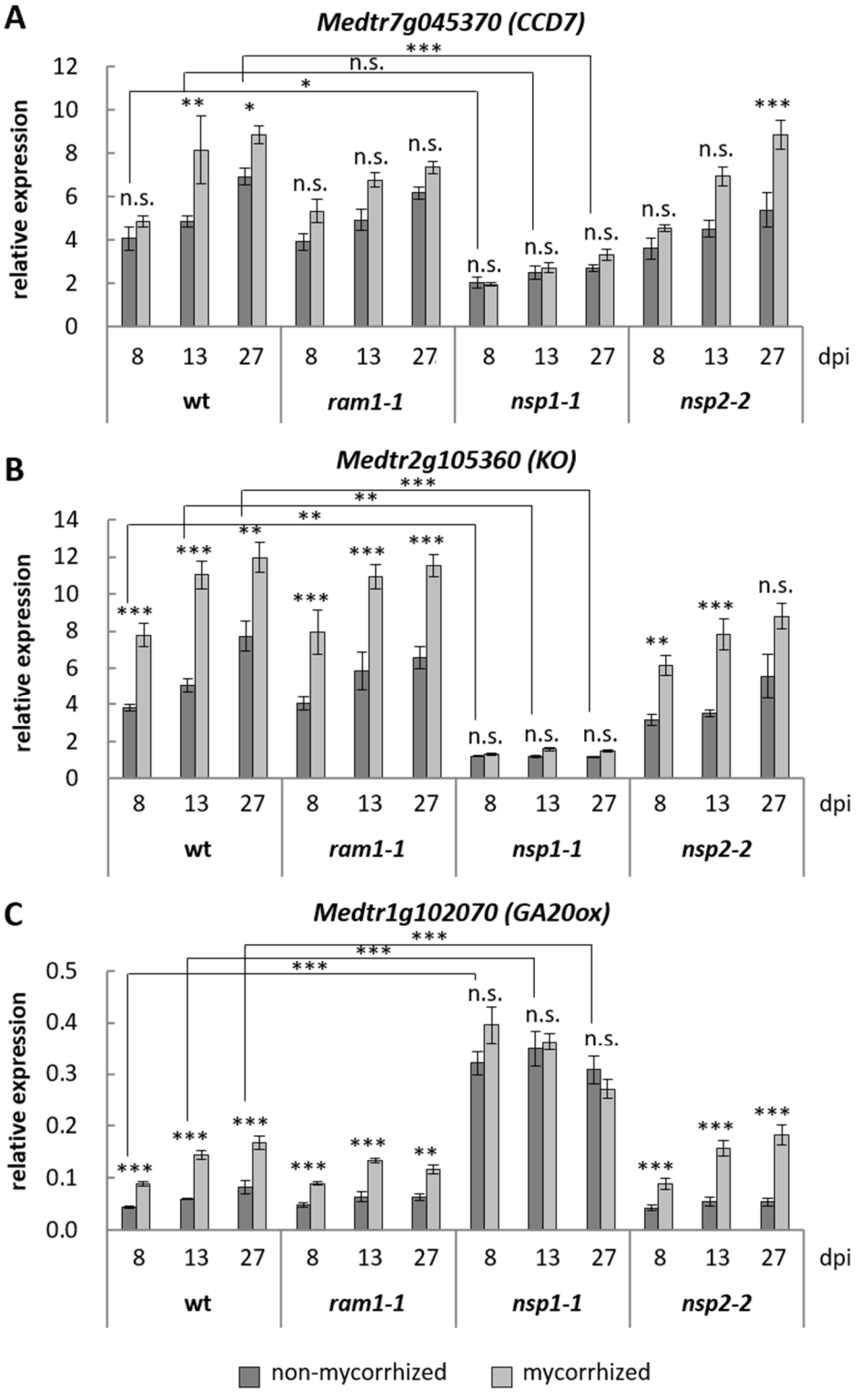

Figure 4.5: Quantification of transcript levels of genes involved in strigolactone and gibberellin biosynthesis in non-mycorrhized and mycorrhized wild-type (wt), *ram1-1*, *nsp1-1*, and *nsp2-2* roots at 8 dpi, 13 dpi, and 27 dpi. Expression levels of the *M. truncatula* homologs of *CCD7* **(A)**, *KO* **(B)**, and *GA20ox* **(C)** are shown. Expression levels were measured by qRT-PCR and normalized to *Ubiquitin* expression. Bars represent means of 4 biological replicates ± SEM. Asterisks indicate significant differences in expression levels (ANOVA; *, P < 0.05; **, P < 0.01; ***, P < 0.001, n.s., P > 0.05).

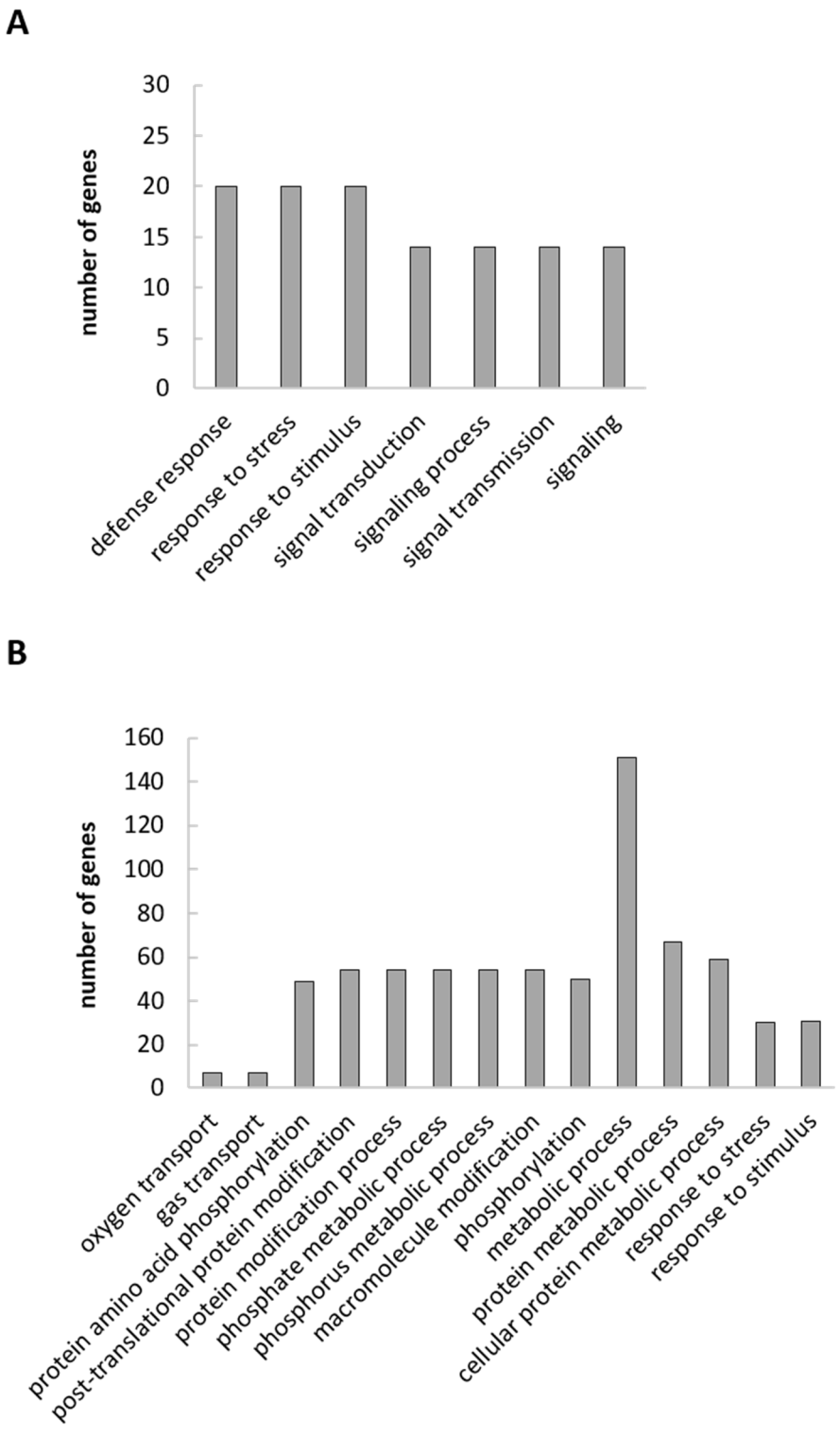

Figure 4.6: Gene ontology (GO) analysis of *NSP2*-dependent genes. Significantly enriched GO terms of genes differentially expressed in non-mycorrhized *nsp2-2* roots compared to non-mycorrhized wild-type roots **(A)** and genes that were found to be consistently dependent on *NSP2* for their induction during mycorrhization **(B)** are shown. Singular enrichment analysis was performed using Agrigo (http://bioinfo.cau.edu.cn/agriGO/index.php) and the whole *M. truncatula* genome as background. Significantly enriched terms of biological processes with an FDR-corrected p-value <0.05 are shown.

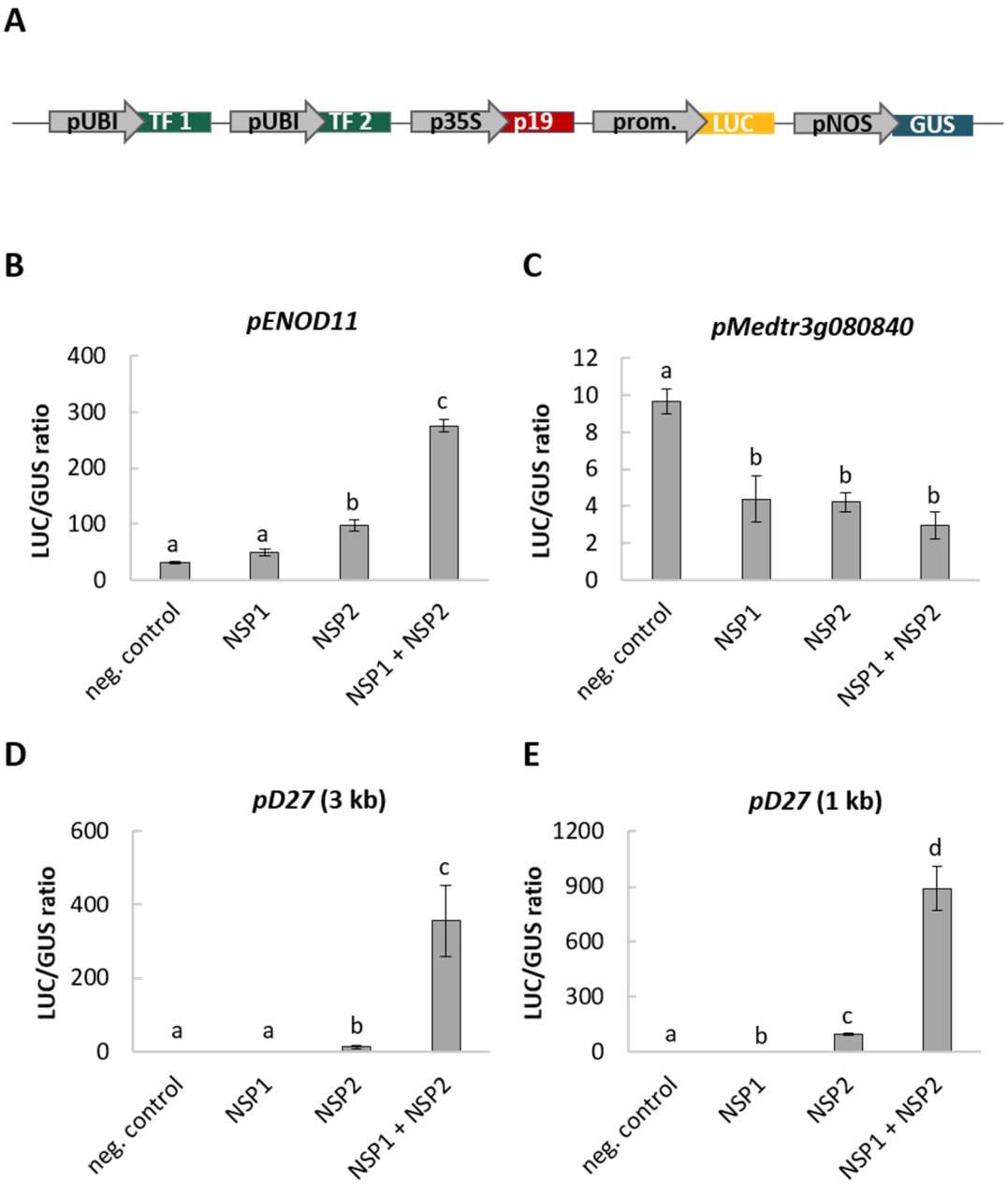

Figure 4.7: Transactivation assay with *NSP1* and *NSP2* in *N. benthamiana* leaves. **(A)** Design of expression vectors used to measure the transactivation of *LUCIFERASE* (*LUC*) under the control of different promoters by individual transcription factors (TFs) or a combination of different transcription factors. The transactivation of *pENOD11::LUC* **(B)**, *pMedtr3g080840::LUC* **(C)**, and *LUC* under the control of the 3 kilobase (kb) long *D27* promoter **(D)** or under the control of the 1 kb long *D27* promoter **(E)** by NSP1, NSP2 or a combination of the two transcription factors is shown. LUC activities were normalised against the β-glucuronidase (GUS) activities in the same leaf discs. The same expression vectors containing all the components except for the genes encoding the transcription factors served as negative controls. Bars represent means of 3 biological replicates ± SEM. Different letters indicate different statistical groups (ANOVA, post hoc Tukey, $P < 0.05$). pUBI, *LjUbiquitin* promoter, p35S, Cauliflower mosaic virus 35S promoter, pNOS, *Nopaline synthase* promoter.

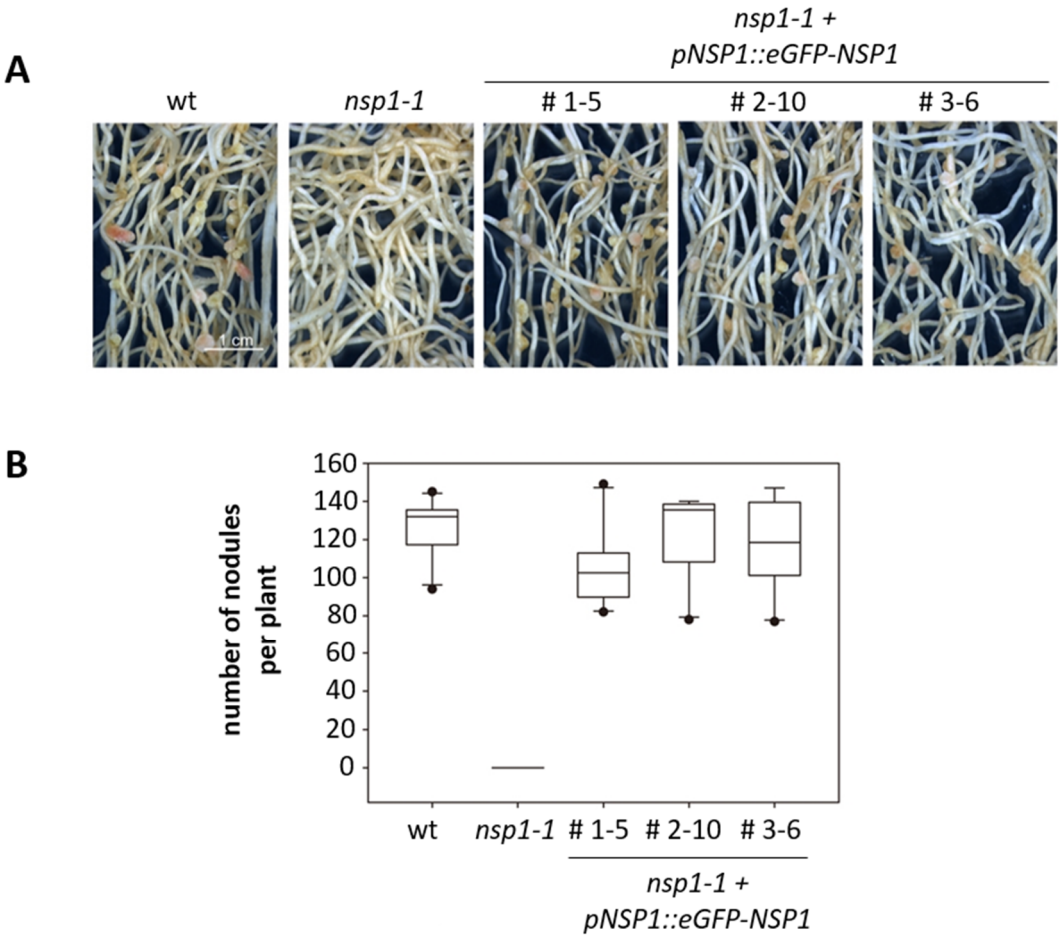

Figure 4.8: Complementation of the *nsp1-1* mutant phenotype by stable expression of *pNSP1::eGFP-NSP1*. **(A)** Pink nodules were present in wild type (wt) and *nsp1-1* plants stably expressing the eGFP-NSP1 fusion protein (#1-5, #2-10, #3-6), but absent in the untransformed *nsp1-1* mutant. **(B)** Quantification of nodule numbers in the wild type, the untransformed *nsp1-1* mutant, and *nsp1-1* plants stably expressing the eGFP-NSP1 fusion protein (#1-5, #2-10, #3-6). Figure courtesy of Jian Feng.

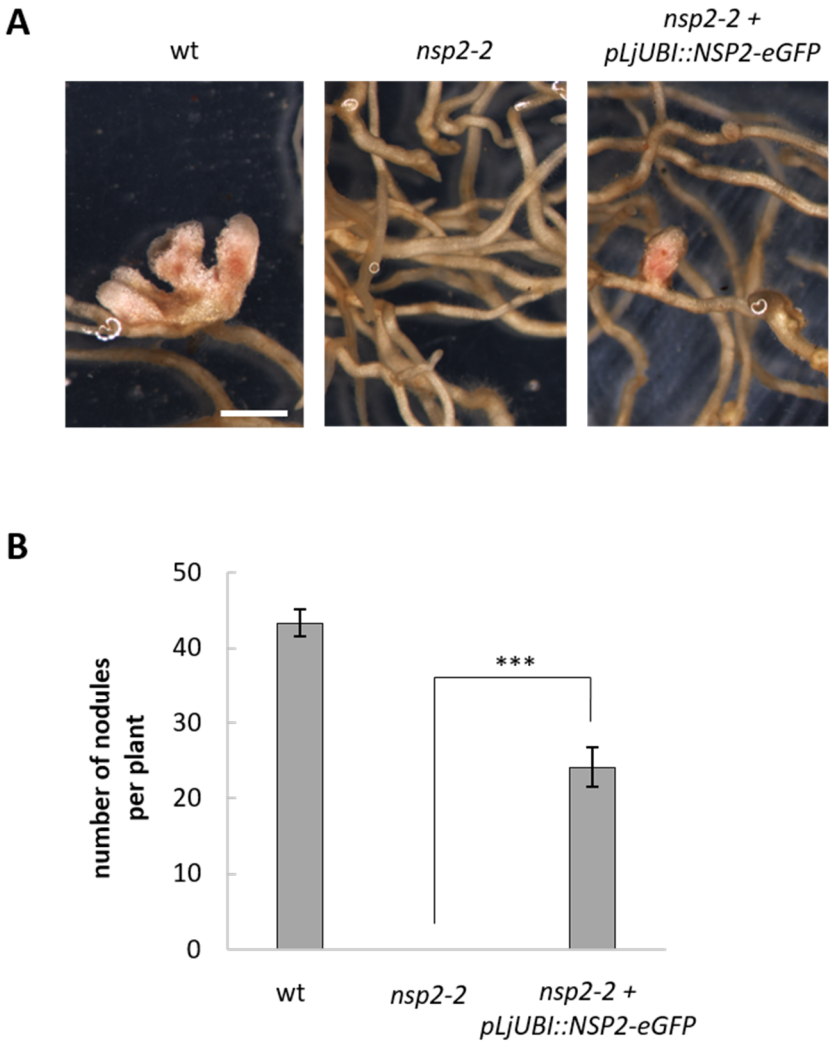

Figure 4.9: Complementation of the *nsp2-2* mutant phenotype by stable expression of *pUBI::NSP2-eGFP*. **(A)** Pink nodules were present in wild type (wt) and *nsp2-2* plants stably expressing the NSP2-eGFP fusion protein, but absent in the untransformed *nsp2-2* mutant. **(B)** Quantification of nodule numbers in the wild type, the untransformed *nsp2-2* mutant, and *nsp2-2* plants stably expressing the NSP2-eGFP fusion protein. Bars represent means of 10 biological replicates ± SEM. Asterisks indicate significant differences in nodule numbers (Student's t-test; *, $P < 0.05$; **, $P < 0.01$; ***, $P < 0.001$). Scale bar = 2 mm.

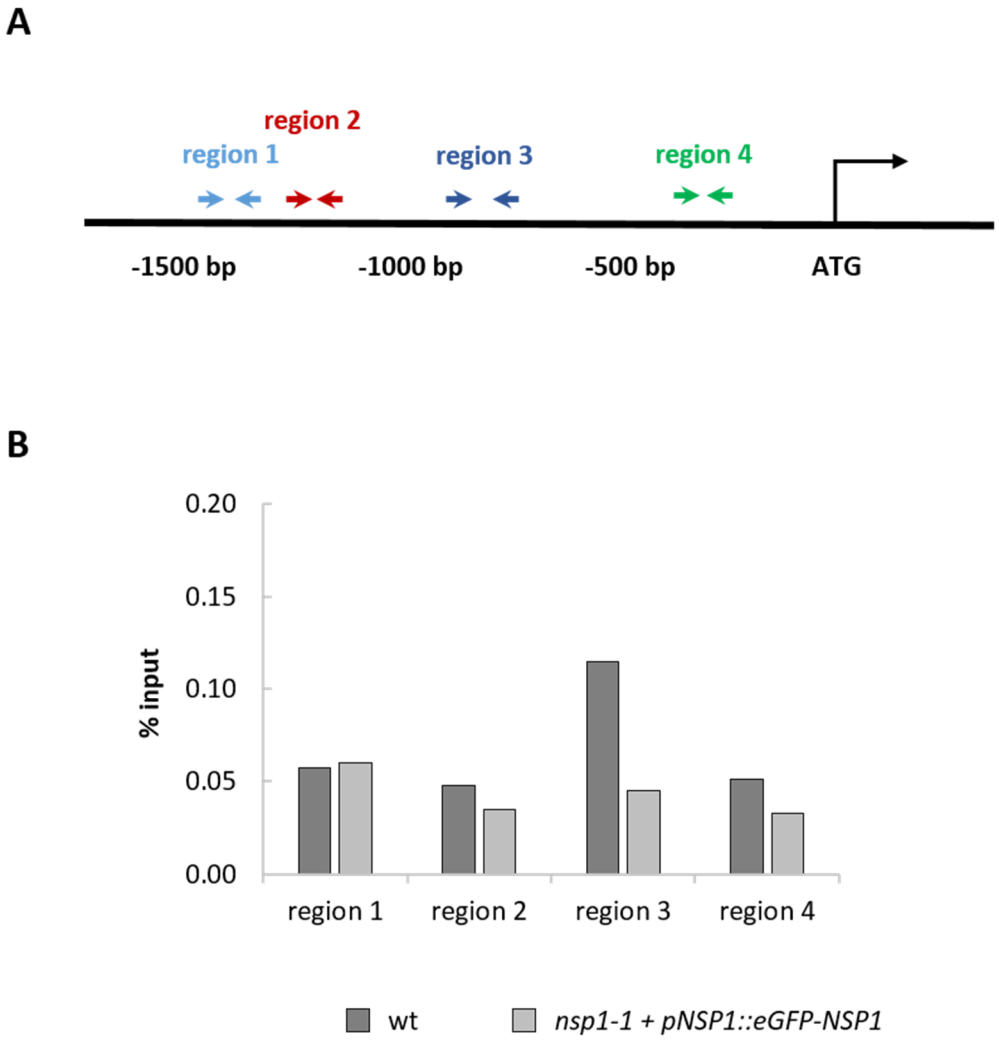

Figure 4.10: Chromatin-immunoprecipitation (ChIP) assay followed by quantitative PCR (qPCR) in *M. truncatula* lines stably expressing *pNSP1::GFP-NSP1*. **(A)** Binding sites of primers used for qPCR following ChIP in the promoter region of the strigolactone biosynthesis gene *D27* are shown. NSP1 is expected to bind within the first 1000 bp upstream of the start codon (ATG). **(B)** ChIP-qPCR using α-GFP antibodies and the primer pairs indicated in (A). ChIP was performed with stable lines expressing GFP-NSP1 (light grey) and untransformed wild type (wt) plants (dark grey) that served as negative control. No enrichment compared to the negative control was observed in any of the promoter regions tested when using the *M. truncatula* line stably expressing GFP-NSP1. One biological replicate is shown. Bars represent the means of three technical replicates of the qPCR.

CHAPTER 5

Mycorrhizal processes regulated by *RAM1*

5.1 Introduction

Plants carrying a mutation in *RAM1* show a severe defect in AM development (Gobbato et al., 2012; Park et al., 2015; Rich et al., 2015; Pimprikar et al., 2016; Chapter 2). Analysing the mycorrhizal phenotype at different time points during mycorrhization revealed that while *ram1-1* roots were transiently colonized by AM fungi at early time points, mycorrhizal infection structures were almost entirely absent at late time points. Strikingly, no fully developed arbuscules were formed in *ram1-1* roots at any of the time points tested. Global gene expression profiling has provided further insights into the transcriptional changes that take place in *ram1-1* roots and has revealed a large number of genes that are dependent on *RAM1* for their induction during mycorrhization (Chapter 3), consistent with the drastic reduction in mycorrhizal colonization observed in the mutant.

To date, the only gene that is known to be directly regulated by RAM1 during AM development is *RAM2*, a glycerol-3-phosphate acyl transferase (GPAT; Gobbato et al., 2012; Wang et al., 2012). Plants with a loss of *RAM2* function are unable to establish a

functional symbiosis with AM fungi. The number of hyphopodia at the epidermis is strongly reduced, and in cases where fungal hyphae are able to reach the inner cortex, small, defective arbuscules are formed, suggesting that *RAM2* plays a role both at early stages of the symbiosis and in arbuscule formation. Interestingly, *A. thaliana GPAT6*, an enzyme required for cutin biosynthesis, is able to restore mycorrhization in the *M. truncatula ram2* mutant when expressed under the *RAM2* promoter. Based on these findings, it has been concluded that *RAM2* similarly is involved in the production of cutin. In accordance with this, the external addition of cutin monomers is sufficient to allow hyphopodia formation in *ram2* roots, and it has been proposed that cutin monomers act as signalling molecules to the fungus to promote AM development (Wang et al., 2012). In a recent study, *RAM1* has also been shown to be required for the transcriptional induction of several other genes involved in AM development, including the GRAS-domain protein *RAD1*, the ABCG transporter *STR*, and the exocyst subunit *EXO70I* (Zhang et al., 2010; Park et al., 2015; Zhang et al., 2015; Xie et al., 2015). As these genes play a role in arbuscule development, it has been proposed that *RAM1* controls at least part of the gene expression programme that governs arbuscule formation (Park et al., 2015). However, evidence for the direct regulation of these genes by RAM1, for example through binding studies, is currently lacking.

Previous attempts to identify genes that are regulated by RAM1 have been limited to examining the expression of known mycorrhizal-induced genes in the wild type and mutant background. This targeted approach has resulted in the identification of only a few potential RAM1 targets. Global gene expression profiling of non-mycorrhized and mycorrhized roots performed here has provided a large number of novel candidates for genes that might be directly regulated by RAM1. The aim of the research presented in this chapter was to investigate the mycorrhizal processes that are regulated by *RAM1* by performing an in-depth functional analysis of the genes that were found to be dependent on *RAM1* for their induction during mycorrhization. From these analyses, several new candidates for mycorrhization emerged, including three AP2-domain proteins with homology to *A. thaliana WRINKLED* transcription factors and two ABCG transporters with a putative role in lipid secretion. The role of these genes during mycorrhizal colonization was investigated by examining their spatial expression patterns in mycorrhized roots. Furthermore, plants carrying TNT1 insertions in one of the putative lipid transporters were characterised for fungal colonization in a mycorrhizal time course. In addition, this chapter also describes several approaches used to validate whether the identified potential target genes are directly regulated by RAM1.

5.2 Results

5.2.1 *RAM1* is required for the transcriptional upregulation of genes involved in the nutrient exchange during AM symbiosis

Unlike in *nsp1-1* and *nsp2-2*, global gene expression profiling of non-mycorrhized *ram1-1* roots identified only a very small number of genes that were consistently up- or downregulated in the absence of mycorrhizal fungi at all three time points tested (Chapter 3, Figure 3.10, Table A5). Investigating the potential functions of these genes did not reveal any obvious biological processes they might be involved in. Thus, *RAM1* appears to have only a minor role in the regulation of gene expression under non-symbiotic conditions. Therefore, further investigations into the biological processes that might be regulated by *RAM1* focused on analysing the functions of the genes that were found to be dependent on *RAM1* during AM development.

Comparing the mycorrhizal-induced genes in wild-type roots to the genes induced in *ram1-1* roots led to the identification of 768 genes whose upregulation was consistently dependent on *RAM1* over the whole time course of fungal colonization (Chapter 3, Figure 3.6). These genes likely include direct transcriptional targets of RAM1 and were therefore further investigated regarding their potential functions in AM development. First, a singular GO term enrichment analysis of the *RAM1*-dependent genes was performed with the whole *M. truncatula* genome as background using the analysis tool Agrigo (http://bioinfo.cau.edu.cn/agriGO/). Several significantly enriched GO terms were identified, including terms associated with lipid and carbohydrate metabolism as well as transport across membranes (Figure 5.1). To further investigate the functions of the individual potential target genes, a BLAST search with the corresponding protein sequences was conducted against the proteome of *A. thaliana* and the functions of the best hits were analysed in more detail.

In accordance with the results of the GO term analysis, several genes that are known or are likely to be required for the nutrient transport across the periarbuscular membrane were found to be among the genes whose upregulation upon mycorrhization was dependent on *RAM1* (Table 5.1). The phosphate transporter *PT4*, which was shown to mediate the uptake of phosphate across the periarbuscular membrane (Harrison et al., 2002), belonged to the most strongly induced genes in mycorrhized wild-type roots, but was not significantly upregulated in *ram1-1*, consistent with the qPCR results described in Chapter 3 (Figure 3.1). Similarly, the two AMT2 family ammonium transporters *AMT2-*

3 and *AMT2-5* lacked induction in mycorrhized *ram1-1* roots. Both genes have previously been shown to be induced during AM symbiosis (Breuillin-Sessoms et al., 2015). *AMT2-3* was found to be required for the suppression of premature arbuscule degeneration in nitrogen-deprived *pt4* mutant roots and has been speculated to have a signalling function to inform the plant about the nutrient status (Breuillin-Sessoms et al., 2015). *AMT2-5* is less well characterised, and it is currently unknown whether the encoded protein localises to the periarbuscular membrane and is required for the transport of ammonium from the fungus to the plant (Breuillin-Sessoms et al., 2015). Interestingly, the induction of *AMT2-4*, the third member of the *M. truncatula* AMT2 family that has been shown to be transcriptionally induced during mycorrhization (Breuillin-Sessoms et al., 2015), did not appear to be directly dependent on *RAM1*, as the fold changes in gene expression were comparable in wild-type and *ram1-1* roots at 8 dpi and 13 dpi, and were only reduced in the mutant at 27 dpi (Table A1). Together, these results suggest that *RAM1* is involved in the transcriptional regulation of the phosphate transporter *PT4* and a subset of the mycorrhizal-induced AMT2 family ammonium transporters during AM development.

Several genes involved in sugar metabolism and transport were also found to be dependent on *RAM1* for their transcriptional induction during mycorrhization (Table 5.1). Among these genes were a number of genes encoding enzymes that catalyse the late steps of glycolysis, including a glyceraldehyde-3-phosphate-dehydrogenase, three subunits of pyruvate kinase, and a subunit of the pyruvate dehydrogenase complex. Furthermore, four putative sugar transporters lacked transcriptional induction in *ram1-1*. The bidirectional transporter *SWEET1b* showed a relatively strong transcriptional upregulation in wild-type roots at 13 dpi and 27 dpi, but was not significantly induced at any time point in *ram1-1*. Analysing the expression of this gene in the *M. truncatula* gene expression atlas (http://mtgea.noble.org/v3/) revealed that *SWEET1b* is most strongly induced in arbuscule-containing cells. A recent study into the family of *SWEET* sugar transporters in potato has proposed that these transporters might be involved in providing sugars to the fungus, consistent with the expression of some of the transporters in arbuscule-containing cells (Manck-Götzenberger and Requena, 2016). Together, these findings suggest that *RAM1* is involved in the regulation of several genes required for the late steps of glycolysis and the transport of sugars across membranes.

Table 5.1: List of mycorrhizal genes whose induction was consistently dependent on *RAM1* across the whole time course during fungal colonization. Fold changes of genes in mycorrhized versus non-mycorrhized wild-type roots are given. FDR-corrected p-value < 0.05 for all fold changes shown. 'N.s.' depicts a statistically non-significant fold change.

			Fold change in the wild type		
Mtv4.0 ID	**Annotation**	**ID and description of best BLAST hit in *A. thaliana* (TAIR)**	**8 dpi**	**13 dpi**	**27 dpi**
Phosphate and ammonium transport					
Medtr1g028600	high affinity inorganic phosphate transporter PT4	AT5G43370, encodes a phosphate transporter Pht1-2	1298	22666	12472
Medtr8g074750	ammonium transporter 1 protein AMT2-3	AT2G38290, encodes a high-affinity ammonium transporter	n.s.	72	55
Medtr1g036410	ammonium transporter 1 protein AMT2-5	AT2G38290, encodes a high-affinity ammonium transporter	242	7735	3979
Sugar metabolism and transport					
Medtr3g089125	bidirectional sugar transporter SWEET1b	AT1G21460, nodulin MtN3 family protein	n.s.	91.7	47.2
Medtr4g131800	glucose 6-phosphate/phosphate translocator 1	AT1G61810, beta-glucosidase 45	n.s.	2.4	4.3
Medtr4g090600	polyol/monosaccharide transporter 1	AT1G11260, encodes a H+/hexose cotransporter	n.s.	2.4	11.1
Medtr8g077890	polyol/monosaccharide transporter 1	AT2G18480, major facilitator superfamily protein with sugar-hydrogen symporter activity	n.s.	35.5	87.5
Medtr6g022630	glyceraldehyde-3-phosphate dehydrogenase	AT1G13440, glyceraldehyde-3-phosphate dehydrogenase C2	n.s.	n.s.	26.9
Medtr6g034195	pyruvate kinase family protein	AT5G52920, chloroplast pyruvate kinase beta subunit	n.s.	n.s.	1.8
Medtr1g105965	pyruvate kinase family protein	AT3G22960, chloroplast pyruvate kinase alpha subunit	n.s.	1.7	3.0
Medtr1g076540	pyruvate kinase family protein	AT3G22960, chloroplast pyruvate kinase alpha subunit	n.s.	n.s.	1.5
Medtr8g024310	pyruvate dehydrogenase E1 component	AT1G01090, pyruvate dehydrogenase E1 alpha subunit	n.s.	n.s.	2.2

continued overleaf

Table 5.1: continued.

			Fold change in the wild type		
Mtv4.0 ID	**Annotation**	**ID and description of best BLAST hit in *A. thaliana* (TAIR)**	**8 dpi**	**13 dpi**	**27 dpi**
Lipid biosynthesis and secretion					
Medtr7g009410	AP2 domain transcription factor	AT3G54320, WRINKLED1	37.2	513	732
Medtr6g011490	AP2 domain transcription factor	AT3G54320, WRINKLED1	5.9	72.1	127
Medtr8g468920	AP2-like ethylene-responsive transcription factor	AT3G54320, WRINKLED1	85.5	1053	1152
Medtr1g040500	glycerol-3-phosphate acyltransferase RAM2	AT2G38110, glycerol-3-phosphate acyltransferase	4.0	39.3	71.9
Medtr1g109110	palmitoyl-acyl carrier thioesterase FatM	AT1G08510, acyl-acyl carrier protein thioesterase	13.1	171	166
Medtr4g093845	white-brown-complex ABC transporter	AT1G17840, ABC transporter required for cutin transport	39.7	209	2495
Medtr4g094090	white-brown-complex ABC transporter	AT1G17840, ABC transporter required for cutin transport	n.s.	2.1	n.s.
Medtr6g021915	glycerol-3-phosphate dehydrogenase, NAD	AT5G40610, NAD-dependent glycerol-3-phosphate dehydrogenase family protein	n.s.	1.7	3.7
Medtr4g043650	glycerol-3-phosphate dehydrogenase	AT2G41540, NAD-dependent glycerol-3-phosphate dehydrogenase family protein	n.s.	n.s.	1.7
Medtr6g015020	biotin carboxyl carrier acetyl-CoA carboxylase	AT5G16390, biotin carboxyl-carrier subunit of the multi-enzyme plastidial acetyl-coenzyme A carboxylase complex	n.s.	1.7	2.9
Medtr3g073820	acetyl-CoA carboxylase	AT1G36160, encodes an acetyl-CoA carboxylase	n.s.	26.7	84.3
Medtr5g084950	triacylglycerol lipase-like protein	AT5G14180, Myzus persicae-induced lipase 1	n.s.	2.3	3.3
Medtr7g081050	triacylglycerol lipase-like protein	AT5G14180, Myzus persicae-induced lipase 1	n.s.	299	2612

continued overleaf

Table 5.1: continued.

			Fold change in the wild type		
Mtv4.0 ID	**Annotation**	**ID and description of best BLAST hit in *A. thaliana* (TAIR)**	**8 dpi**	**13 dpi**	**27 dpi**
Medtr7g117280	triacylglycerol lipase	AT3G61680, alpha/beta-hydrolase with triglyceride lipase activity	n.s.	3.0	5.4
Medtr8g074560	GDSL-like lipase/acylhydrolase	AT5G55050, GDSL-like lipase/acylhydrolase superfamily protein	49.1	511	1981
Medtr1g030220	GDSL-like lipase/acylhydrolase	AT3G26430, GDSL-like Lipase/Acylhydrolase	n.s.	n.s.	3.2
Medtr4g077180	lipid transfer protein	AT4G33550, lipid-transfer protein	288	7122	2412
Medtr4g076150	lipid transfer protein	AT4G33550, lipid-transfer protein	n.s.	426	973
Medtr5g081780	polyketide cyclase/dehydrase and lipid transporter	AT2G25770, polyketide cyclase/dehydrase and lipid transporter	49.0	328	1239
Medtr3g079190	neutral/alkaline non-lysosomal ceramidase	AT2G38010, neutral/alkaline non-lysosomal ceramidase	319	4894	6947
Medtr8g094740	fatty acid amide hydrolase-like protein	AT5G64440, fatty acid amide hydrolase	n.s.	1.7	2.0
Medtr2g010180	fatty acid amide hydrolase-like protein	AT5G64440, fatty acid amide hydrolase	n.s.	n.s.	1.6
Medtr1g103110	acetyltransferase (GNAT) domain protein	AT2G32020, acyl-CoA N-acyltransferase	n.s.	n.s.	2.8
Medtr1g077930	alpha/beta-hydrolase superfamily protein	AT1G64670, alpha-beta hydrolase BODYGUARD, required for normal cuticle formation	n.s.	1.7	1.9

In line with the GO term analysis, the largest group of genes that were consistently dependent on *RAM1* during mycorrhization were associated with lipid biosynthesis and putative lipid secretion (Table 5.1). Consistent with previous findings, the transcriptional induction of the glycerol-3-phosphate acyltransferase *RAM2* was completely abolished in *ram1-1* roots at all three time points tested (Gobbato et al., 2012; Park et al., 2015; Rich et al, 2015). Furthermore, the expression of the palmitoyl-acyl carrier thioesterase *FatM,* a gene that has recently been found to be evolutionarily conserved in AM-forming species, was dependent on *RAM1* (Bravo et al., 2016). In addition, a number of other genes involved in lipid metabolism, including several putative triacylglycerol lipases, GDSL-like lipases, and a non-lysosomal ceramidase were found to be among the potential RAM1 targets. In addition to the genes involved in lipid metabolism, three AP2-domain transcription factors showed a strong transcriptional upregulation during fungal colonization in the wild type, while their induction was completely abolished in *ram1-1*. Conducting a BLAST search with the corresponding protein sequences against the *A. thaliana* proteome revealed that these proteins are homologs of the *A. thaliana WRINKLED* (*WRI*) transcription factors, which have been shown to be required for the transcriptional regulation of late glycolytic and early fatty acid biosynthesis genes involved in the production of triacylglycerols in seeds and cutin in floral tissues (Baud et al., 2007; Baud et al., 2009; To et al., 2012). The target genes of the *A. thaliana* WRI transcription factors include several subunits of pyruvate kinase (AT3g22960 and AT5g52920) and pyruvate dehydrogenase (AT1g01090), as well as the genes encoding a glycerol-3-phosphate dehydrogenase (AT2G41540) and a subunit of the acetyl-coenzyme A carboxylase complex (AT5g15530; Baud et al., 2007; Baud et al., 2009; To et al., 2012). The *M. truncatula* homologs of these genes were among the genes that lacked induction in *ram1-1* (Table 5.1), suggesting that the WRI homologs in *M. truncatula* might regulate the equivalent target genes in glycolysis and fatty acid biosynthesis during AM symbiosis. A phylogenetic analysis with the closest homologs of the WRI proteins in *M. truncatula*, *A. thaliana*, *Oryza sativa*, and *Marchantia paleacea* further revealed that the genome of *M. truncatula* encodes eight *WRI*-like genes, which subsequently are referred to as *MtWRI1*-*MtWRI8* (Figure 5.2). The analysis of the transcript levels of all the *MtWRI* homologs showed that in addition to the *RAM1*-dependent genes *MtWRI1*, *MtWRI2*, and *MtWRI3*, two homologs (*MtWRI4* and *MtWRI5*) were transcriptionally induced in mycorrhized wild-type roots in a *RAM1*-independent manner. These findings suggest that *RAM1* regulates only a subset of the *MtWRI* genes during the colonization by mycorrhizal fungi. Finally, several putative lipid transporters

were found to be among the *RAM1*-dependent genes, including two half-size ABCG transporters that cluster with the *A. thaliana* ABCG transporters required for wax, cutin, and suberin export (Figure 5.3; Pighin et al., 2004; Bird et al., 2007; Panikashvili et al., 2010; Panikashvili et al., 2011). As two other half-size ABCG transporters involved in mycorrhization (*STR* and *STR2*) have been named *MtABCG1* and *MtABCG2*, respectively (Zhang et al., 2010), the two ABCG transporters identified here are subsequently referred to as *MtABCG3* (Medtr4g093845) and *MtABCG4* (Medtr4g094090). While *MtABCG3* showed a very strong induction in mycorrhized wild-type roots at all three time points, *MtABCG4* was weakly upregulated in wild-type roots only at 13 dpi. Finally, two genes encoding lipid transfer proteins, which have been proposed to function in the secretion of lipids (Samuels et al., 2008), were strongly upregulated in mycorrhized wild-type, but not *ram1-1* roots (Table 5.1).

To confirm the results obtained by RNA-seq, the expression levels of *RAM2*, *FatM*, *MtABCG3*, and *MtWRI1* were examined using qRT-PCR (Figure 5.4). No significant upregulation of these genes was observed in mycorrhized *ram1-1* roots, while all the tested genes showed a strong induction in mycorrhized wild-type, *nsp1-1*, and *nsp2-2* roots. These results confirm that *RAM1* is essential for the upregulation of several genes involved in lipid metabolism and putative lipid secretion during fungal colonization, while *NSP1* and *NSP2* do not appear to be involved in the transcriptional regulation of these genes.

5.2.2 Genes involved in lipid biosynthesis and putative lipid secretion are co-expressed in arbuscule-harbouring cells

Several studies have previously demonstrated that the expression of lipid biosynthesis genes and root lipid content increases upon mycorrhization (Schliemann et al., 2008; Gomez et al., 2009; Gaude et al., 2012). It has been suggested that this observed increase in lipid production is required to meet the higher demand for membrane lipids for the formation of the periarbuscular membrane (Gaude et al., 2012). A recent study into the genome of *R. irregularis* has further proposed that lipids produced by the plant might be transported to the fungus, as mycorrhizal fungi do not appear to encode genes for type I fatty acid synthase, and are therefore unlikely to be capable of *de novo* fatty acid synthesis (Tisserant et al., 2013; Wewer et al., 2014). Labelling studies suggest that lipid transfer from the plant to the fungus does indeed take place and is essential for a

functional AM symbiosis (Peter Eastmond and Ertao Wang, personal communication). Moreover, lipid transport is abolished in *ram2* mutants, indicating that *RAM2* is not only involved in cutin biosynthesis during the early stages of AM development (Wang et al., 2012), but is also a critical component of the lipid export pathway potentially feeding the fungus (Peter Eastmond and Ertao Wang, personal communication). Other components of this pathway are currently unknown, however, several of the genes described above are good candidates to be involved in the transfer of lipids to mycorrhizal fungi. To further investigate whether the lipid-related genes identified by global gene expression profiling could be involved in the same lipid export pathway as *RAM2*, the spatial expression patterns of *RAM2*, *FatM*, *MtABCG3*, and the three *RAM1*-dependent *WRI* transcription factors (*MtWRI1, MtWRI2, and MtWRI3*) were examined in mycorrhized and non-mycorrhized roots. In addition, *MtWRI4*, which was upregulated during mycorrhization in a *RAM1*-independent manner, and *MtWRI6*, which did not display an increased expression upon fungal colonization, were included in the analysis. To this end, the promoter sequences were fused to the *GUS* reporter gene and expressed in *M. truncatula* roots by transformation with *Agrobacterium rhizogenes*. Composite plants were grown in the presence or absence of mycorrhizal fungi and stained for GUS activity and mycorrhizal structures at 4 weeks post inoculation (wpi).

As reported previously, *RAM2* promoter activity was strongly associated with cortical cells hosting arbuscules, while no *GUS* expression was observed in epidermal cells that were in direct contact with fungal hyphae (Figure 5.5; Gobbato et al., 2013). In the absence of mycorrhizal fungi, *RAM2* expression was localized to the tip regions of the roots. Very similar expression patterns were observed for *FatM, MtABCG3*, and the four mycorrhizal-induced *WRI* genes, which all showed a strong induction of promoter activity in arbuscule-containing cells, but did not appear to be expressed in cells surrounding hyphopodia (Figures 5.6 – 5.11). In non-mycorrhized roots, a weak expression of *FatM* and several *WRI* genes was visible in the cortex and in root tips, suggesting that the expression of these genes is not entirely specific to colonized root tissues. In accordance with the findings of the global gene expression profiling, no GUS staining associated with mycorrhizal structures was observed in colonized roots expressing the *pMtWRI6*-GUS fusion (Figure 5.12). Occasionally, promoter activity of *MtWRI6* was detected in the root endodermis in non-colonized roots, indicating that this gene might have a function under non-symbiotic conditions.

Together, these results show that *RAM2, FatM*, *MtABCG3*, and several *WRI* transcription factors are co-expressed in arbuscule-containing cells of colonized *M. truncatula* roots and suggest that these genes could be part of the same lipid biosynthesis and export pathway.

5.2.3 Mycorrhizal colonization is only weakly affected in plants carrying a mutation in the half-size ABCG transporter *MtABCG3*

The strong transcriptional upregulation in arbuscule-containing cells and the close phylogenetic relationship with *A. thaliana* lipid transporters make the mycorrhizal ABCG transporter *MtABCG3* a good candidate for mediating lipid transfer to the fungus. To further investigate whether this transporter has a function in AM symbiosis, seeds from three *M. truncatula* lines (NF20376, NF11484, and NF1558) carrying a TNT1 insertion in the coding sequence of *MtABCG3* were obtained from the Samuel Roberts Noble foundation (Tadege et al., 2008). The insertion line NF20376 carries a TNT1 insertion in the third exon of Mt*ABCG3*, which corresponds to the predicted AAA$^+$-ATPase domain in the protein sequence (Figure 5.13). The line NF11484 contains a TNT1 insertion in the fourth exon, which is predicted to encode the linker region between the AAA$^+$-ATPase domain and the six transmembrane domains at the C-terminal end of the protein. The third insertion line, NF1558, carries a TNT1 insertion in the last exon, which corresponds to the protein sequence between the last two transmembrane domains at the C-terminus. The presence of the TNT1 insertions was confirmed by genotyping, and homozygous plants were bulked to produce seeds for further experiments.

The TNT1 transposon is approximately 5000 bp long and is therefore anticipated to create null mutants when located in an exon. To confirm that no full-length transcript was expressed in the three mutant lines, RT-PCR was performed with RNA from mycorrhized roots. Using gene-specific primers that flank all three TNT1-insertion sites, a cDNA fragment of 1760 bp was amplified in the wild type line (Figure 5.13). As expected, no full-length transcript was expressed in the two lines NF20376 and NF1558. However, the RT-PCR with RNA from line NF11484 did amplify a product with a size slightly smaller than 1760 bp. Sequencing of the PCR product revealed that the TNT1 insertion, including the whole sequence of exon four (81 bp), was spliced out of the transcript in line NF11484. Although it is likely that the excision of a whole exon results

in a non-functional protein, it cannot be excluded that a shorter version of the protein is still expressed in this line and might retain some functionality.

To assess the mycorrhizal phenotype of plants carrying a mutation in *MtABCG3*, fungal infection structures were quantified in the wild type and the three TNT1-insertion lines in a mycorrhizal time course experiment at 2 wpi, 3 wpi, and 7.5 wpi. At 2 wpi, no difference in the quantity of fungal infection structures was observed between the wild type and the mutant lines, suggesting that mycorrhization at early stages is not impaired in the *abcg3* mutants (Figure 5.14 A). By contrast, all three mutant lines showed a weak, but statistically significant reduction in the number of hyphopodia and arbuscules at 3 wpi. In addition, the two TNT1-insertion lines NF20376 and NF11484 also had fewer vesicles than the wild type at 3 wpi (Figure 5.14 B). At 7.5 wpi, the reduction in mycorrhizal colonization disappeared, and the levels of mycorrhization in the TNT1-insertion lines were again comparable to the wild type (Figure 5.14 C). The mycorrhizal time course was repeated with the two insertion lines NF20376 and NF11484 with similar results. Ink staining of the fungal infection structures further revealed that fully developed arbuscules were present in the three mutant lines at all three time points tested (Figure 5.15). Together, these results indicate that mutations in *MtABCG3* only have minor effects on the levels of mycorrhization and do not impair the development of fungal infection structures inside the roots.

5.2.4 *RAM1* is essential for the transcriptional induction of *EXO70I*, but not the previously proposed targets *STR* and *RAD1*

It has previously been reported that genes involved in arbuscule development, including the exocyst subunit *EXO70I*, the ABCG transporter *STR*, and the GRAS-domain transcription factor *RAD1*, are dependent on *RAM1* for their induction during mycorrhization (Park et al., 2015). Thus, I investigated whether the upregulation of these genes was also abolished in *ram1-1* roots in the mycorrhizal time course performed here.

Consistent with previous findings, the expression of *EXO70I* was significantly induced in colonized wild-type roots at all three time points tested, while no induction was observed in mycorrhized *ram1-1* roots, showing that *RAM1* is essential for the transcriptional induction of *EXO70I* (Table 5.2). In addition to *EXO70I*, two other genes encoding putative subunits of the exocyst complex showed a weak upregulation in the

wild type during mycorrhization, but were not induced in *ram1-1*, indicating that RAM1 might be involved in the transcriptional regulation of several exocyst components.

The transcript levels of the two genes *STR* and *STR2* were significantly induced in wild-type roots at all three time points during mycorrhization (Table 5.2). However, although no significant transcriptional upregulation of *STR* and *STR2* was observed in mycorrhized *ram1-1* roots at 27 dpi, their expression levels were significantly induced in the mutant at 8 dpi and 13 dpi, with fold changes that were comparable to the ones observed in the wild type. Similarly, *RAD1* was still significantly induced in *ram1-1* during mycorrhization, even though fold changes were slightly lower than in the wild type (Table 5.2). These results suggest that, at least at early time points, *RAM1* is not essential for the transcriptional upregulation of *STR*, *STR2*, and *RAD1* during AM development.

Table 5.2: Fold changes of genes involved in arbuscule development during the mycorrhizal time course in wild-type and *ram1-1* roots. FDR-corrected p-value < 0.05 for all fold changes shown. 'N.s.' depicts a statistically non-significant fold change.

		Fold change in the wild type			**Fold change in *ram1-1***		
Mtv4.0 ID	**Annotation**	**8 dpi**	**13 dpi**	**27 dpi**	**8 dpi**	**13 dpi**	**27 dpi**
Medtr1g017910	exocyst subunit exo70 family protein, EXO70I	2.0	13	18	n.s.	n.s.	n.s.
Medtr2g096230	exocyst subunit exo70 family protein	n.s.	2.6	n.s.	n.s.	n.s.	n.s.
Medtr4g062330	exocyst subunit exo70 family protein	n.s.	n.s.	1.7	n.s.	n.s.	n.s.
Medtr8g107450	white-brown-complex ABC transporter family protein STR	3.2	33.3	70.3	3.2	4.7	n.s.
Medtr5g030910	white-brown-complex ABC transporter family protein STR2	7.2	204	364	5.6	14.9	n.s.
Medtr4g104020	GRAS family transcription factor RAD1	39.9	237	696	12	168	45.3

5.2.5 *RAM1* activates gene expression in an unspecific manner when overexpressed in *N. benthamiana* leaves

Global gene expression profiling has identified a large number of genes whose upregulation during mycorrhization was dependent on *RAM1* at all three time points tested, and it is likely that this group of genes contains direct targets of RAM1. However, the lack of gene induction during mycorrhization in *ram1-1* could also be caused by the absence of fully developed arbuscules in the mutant. To identify direct targets of RAM1, the ability of RAM1 to induce the expression of the reporter gene *LUC* under the control of different mycorrhizal-induced promoters was tested in a transactivation assay in *N. benthamiana* leaves (described in Chapter 4.2.4).

First, I investigated whether RAM1 is able to activate gene expression from the promoter sequence of *RAM2*, the only confirmed direct target of RAM1 to date (Gobbato et al., 2012). As expected, the expression of *RAM1* together with *LUC* under the control of the *RAM2* promoter resulted in a strong induction of LUC activity in transformed leaf tissues (Figure 5.16). Similarly, RAM1 was able to activate the expression of *LUC* from the promoter sequences of the mycorrhizal-induced genes *MNR* (*MYCORRHIZAL NITRATE REDUCTASE*) and *ENOD11* (Weidmann et al.,2004; Journet et al., 2001). As a negative control, I next tested whether RAM1 induces the expression of *NIN*, a gene that is specifically upregulated during nodulation (Schauser et al., 1999), but has not been reported to be differentially expressed during mycorrhization and is therefore not predicted to be directly targeted by RAM1. Surprisingly, however, a strong induction of LUC activity was also observed when overexpressing *RAM1* together with the *LUC* gene under the control of the *NIN* promoter (Figure 5.16). Furthermore, RAM1 appeared to be able to activate the promoters of the nodulation-specific gene *NPL* (Xie et al., 2012), the meristem marker *WUS* (*WUSCHEL*; Osipova et al., 2012) and the *A. thaliana* gene *PLT1* (*PLETHORA1*; Aida et al., 2004). Finally, the alcohol-inducible promoter *alcA* (Kinkema et al., 2014) and six copies of the lac operon (Samalova et al., 2005) were fused to the *LUC* gene and activation of these promoter sequences by RAM1 was tested. Although the relative LUC/GUS ratios were considerably lower than when testing the *M. truncatula* and *A. thaliana* promoters, a significant induction of LUC activity by RAM1 was also observed for these two plant-unrelated promoters (Figure 5.16). Considering that the majority of the tested promoters are not expected to be transcriptionally regulated by RAM1, these results suggest that *RAM1* activates gene expression

unspecifically when overexpressed in *N. benthamiana* leaves. Thus, the transactivation assay in *N. benthamiana* leaves does not appear to be a suitable method to test the ability of RAM1 to activate gene expression in a specific manner.

The conditions for the regulation of gene expression in *N. benthamiana* leaves are likely to be different from the conditions in *M. truncatula* roots during AM development. It is possible that the activity of RAM1 is tightly regulated under symbiotic conditions, and that this regulation is absent when overexpressing *RAM1* in *N. benthamiana* leaves. To test whether a similar unspecific activation of gene expression is observed when overexpressing *RAM1* in *M. truncatula* roots, the same expression vectors that were used for the transactivation assay in *N. benthamiana* leaves were expressed in *M. truncatula* roots by transformation with *A. rhizogenes*.

Unlike in the transient assay in *N. benthamiana* leaves, no induction of LUC activity was observed when expressing *RAM1* together with the *LUC* gene fused to the promoter of *MNR* in *M. truncatula* roots (Figure 5.17 A). To test whether the hemagglutinin (HA)-tagged RAM1 protein used for the transactivation assay is functional in *M. truncatula* roots during AM symbiosis, *ram1-1* roots transformed with the same expression vectors as used for the transactivation assay were inoculated with AM fungi and mycorrhizal infection structures were quantified at 4 wpi. While *ram1-1* roots transformed with the vector control only displayed very low levels of mycorrhization and were unable to form fully developed arbuscules, the expression of the HA-tagged RAM1 protein resulted in significantly higher levels of fungal colonization (Figure 5.17 B). Furthermore, WGA staining of mycorrhized roots confirmed the presence of fully developed arbuscules in roots expressing HA-RAM1, demonstrating that the fusion protein is functional during AM development. Overall, these results suggest that unlike in *N. benthamiana* leaves, the overexpression of a functional RAM1 protein in *M. truncatula* roots does not result in the unspecific activation of gene expression.

5.2.6 Ectopic overexpression of *RAM1* in *M. truncatula* roots is sufficient to activate the expression of genes involved in nutrient exchange in the absence of mycorrhizal fungi

As performing the transactivation assay in *M. truncatula* roots is considerably more time-consuming than in *N. benthamiana* leaves and therefore lacks the advantage of rapid testing of many different promoter sequences, an alternative approach was sought

to identify genes that might be directly regulated by RAM1. To this end, *RAM1* was overexpressed to high levels in *M. truncatula* roots and the expression of potential direct target genes in the absence of mycorrhizal fungi was measured by qRT-PCR. The transcript levels of the mycorrhizal-induced genes *RAM2*, *FatM*, *MtABCG3*, *MtWRI2*, and *PT4* were significantly induced in roots overexpressing *RAM1* compared to control roots overexpressing *GFP* (Figure 5.18). By contrast, the expression levels of *MtWRI1* were slightly lower in *RAM1*-overexpressing roots compared to control roots. These results suggest that the overexpression of *RAM1* is sufficient to induce the transcription of several genes involved in phosphate transport, lipid metabolism and potential lipid secretion in the absence of mycorrhizal fungi.

5.2.7 Generation of *M. truncatula* lines stably expressing GFP-tagged RAM1 for the identification of genome-wide DNA binding sites

To confirm that RAM1 directly binds to the promoter sequences of the target genes identified above, *M. truncatula* lines stably expressing GFP-tagged RAM1 were generated to identify genome-wide DNA binding sites of RAM1 by performing ChIP-seq assays. To ensure that the GFP-tag does not impair the functionality of RAM1 in AM development, *GFP-RAM1* was expressed under the native *RAM1* promoter in *ram1-1* roots by transformation with *A. rhizogenes* and composite plants were inoculated with mycorrhizal fungi. As a negative control, *ram1-1* roots expressing *GFP* alone were inoculated. Fungal infection structures were quantified at 4 wpi, revealing that a significantly higher number of hyphopodia, intraradical hyphae, and arbuscules were present in *ram1-1* roots expressing *GFP-RAM1* when compared to the negative control. Furthermore, WGA staining of mycorrhized roots confirmed that *ram1-1* roots expressing *GFP-RAM1* were able to form fully developed arbuscules. These results demonstrate that the GFP-fusion protein is functional during AM symbiosis. Thus, the expression vector encoding *pRAM1::GFP-RAM1* was used for stable transformation of *ram1-1* plants. The ability of T1 plants to form fully developed arbuscules was confirmed by ink-staining, and stable lines that were able to enter a fully functional symbiosis with AM fungi were bulked to produce T2 seeds. However, the time limitations of this project did not allow the production of enough T1 or T2 seeds to perform a ChIP assay with this stable line.

5.3 Discussion

Here, the mycorrhizal processes regulated by *RAM1* were investigated by performing an in-depth functional analysis of the genes that were found to be induced during AM development in a *RAM1*-dependent manner. These analyses have uncovered an important role for *RAM1* in the regulation of genes involved in arbuscule development, the transfer of mineral nutrients from the fungus to the plant, and lipid biosynthesis and putative export to fungal hyphae.

Based on gene expression analyses of *ram1* mutants at late time points during mycorrhization and ectopic overexpression of *RAM1* in *M. truncatula* roots, *RAM1* has previously been proposed to control several genes involved in arbuscule development, including *EXO70I*, *STR*, and *RAD1* (Park et al., 2015; Rich et al., 2015). The gene expression profiling performed here has revealed that while the transcriptional induction of all these genes was abolished or strongly reduced at 27 dpi in *ram1-1*, the upregulation of *STR*, *STR2*, and *RAD1* at 8 dpi and 13 dpi was comparable to the wild type or only slightly impaired. These findings suggest that *RAM1* is not essential for the transcriptional induction of *STR*/*STR2* and *RAD1* at early time points during fungal colonization, indicating that other transcriptional regulators must be involved in the upregulation of these genes during mycorrhizal colonization. Furthermore, considering the severely reduced levels of fungal colonization in *ram1* mutants at late time points, it is possible that the reduced induction of *RAD1* and *STR*/*STR2* observed in *ram1* is due the loss of AM symbiosis rather than the direct control of the expression of these genes by RAM1. By contrast, the expression of the exocyst subunit *EXO70I* was completely abolished in *ram1-1* not only at late, but also at early time points, making this gene a good candidate to be a direct target of RAM1. *EXO70I* is involved in the formation of the branch domain of the periarbuscular membrane and was shown to be required for the efficient incorporation of the two ABCG transporters STR and STR2 (Zhang et al., 2015). In line with this, plants carrying a mutation in *EXO70I* are unable to form fully developed arbuscules (Zhang et al., 2015). This lack of induction of *EXO70I* in *ram1-1* is in accordance with the arrest in arbuscule development observed in colonized *ram1-1* roots. In addition to *EXO70I*, two other putative subunits of the exocyst complex were upregulated during mycorrhizal colonization in a *RAM1*-dependent manner, although the transcriptional induction of these two genes in the wild type was relatively weak and was only observed at some, but not all time points. One of these two subunits, encoded by Medtr2g096320, has previously been found to be expressed in arbuscule-containing

cells, and it has been proposed that a number of exocyst subunits are involved in arbuscule development (Zhang et al., 2015). Together, these findings suggest that *RAM1* is involved in the transcriptional regulation of several components of the exocyst complex, which provides a secretory function during the formation of the periarbuscular membrane.

One of the main benefits of the AM symbiosis for plants is the drastically improved acquisition of water and mineral nutrients from the soil. In particular, the fungus provides the plant with substantial amounts of phosphate and ammonium. In *M. truncatula*, the phosphate transporter *PT4* has been shown to be essential for phosphate uptake across the periarbuscular membrane (Harrison et al., 2002; Javot et al., 2007). PT4 localizes specifically to the membrane surrounding the fine branches of arbuscules (Pumplin and Harrison, 2009). It is therefore maybe not surprising that *PT4* expression was completely abolished in *ram1-1*, as only underdeveloped arbuscules were formed in the mutant roots at all three time points tested (Chapter 2), and the lack of *PT4* induction could simply be caused by the absence of fully developed arbuscules in *ram1-1* rather than the lack of transcriptional activity of RAM1. However, the ectopic overexpression of *RAM1* in *M. truncatula* roots was sufficient to significantly induce the expression of *PT4* even in the absence of mycorrhizal fungi, suggesting that RAM1 has a more direct role in the regulation of *PT4* expression. It is possible that RAM1 controls *PT4* transcript levels by directly associating with its promoter sequence. Alternatively, RAM1 might activate other transcriptional regulators that can induce *PT4* expression. Binding studies such as ChIP assays or electrophoretic mobility shift assays (EMSAs) would help to answer these questions. Interestingly, *RAM1* was also required for the upregulation of two ammonium transporter family proteins, *AMT2-3* and *AMT2-5*, while it did not appear to be essential for the induction of the third mycorrhizal-induced family member *AMT2-4* (Breuillin-Sessoms et al., 2015). Of these three genes, only AMT2-3 has been characterised in more detail. It has been shown that the protein encoded by *AMT2-3* localises to the periarbuscular membrane and is required for the suppression of premature arbuscule degeneration in *pt4* under nitrogen-starved conditions (Breuillin-Sessoms et al., 2015). As AMT2-3 does not seem to be able to transport ammonium in yeast, it has been hypothesised that this member of the AMT family has a signalling function rather than mediating the uptake of ammonium into plant cells. It is currently unclear whether AMT2-4 and AMT2-5 are involved in the symbiotic import of ammonium across the periarbuscular membrane. *AMT2-4* is able to complement a yeast ammonium transport mutant, suggesting that this protein has ammonium transport

activities, however, nothing is known about the subcellular localisation of the encoded protein (Breuillin-Sessoms et al., 2015). The observation that *AMT2-3* and *AMT2-5*, but not *AMT2-4*, are dependent on *RAM1* for their transcriptional upregulation during fungal colonization suggests that the mycorrhizal-induced AMT2 family members are differentially regulated during symbiosis and might hint at distinct functions of these transporters during mycorrhization.

In exchange for receiving water and mineral nutrients, plants provide the obligate biotrophic fungus with considerable amounts of fixed carbon (Ho and Trappe, 1973; Shachar-Hill et al., 2005; Parniske, 2008). Up to 20% of the plant photosynthesis products are delivered to the fungus (Bago et al., 2002), resulting in a significant increase of the carbon sink strength of mycorrhized roots and the large accumulation of sugars and lipids (Wright et al., 1998). Until recently, plant-derived sugars have been thought to be the only carbon source for the fungus. Based on labelling studies, it has been proposed that intraradical fungal hyphae convert the plant-derived sugars into triacylglycerols for the export to extraradical hyphae (Trepanier et al., 2005), as lipids are the main energy storage form of AM fungi (Beilby and Kidby, 1980). However, a recent study investigating lipid biosynthesis and metabolism in *R. irregularis* has been unable to find genes encoding subunits of type I fatty acid synthase (FAS) in the genome of the fungus, suggesting that the fungus is not capable of *de novo* fatty acid synthesis and therefore relies entirely on the plant for the supply with lipids (Wewer et al., 2014). Consistent with this, radioisotopic labelling experiments show that lipids are exported from the plant to the fungus (Peter Eastmond and Ertao Wang, personal communication). *RAM2* has previously been proposed to be involved in cutin biosynthesis and is required for hyphopodia formation and arbuscule development (Wang et al., 2012). Interestingly, growing *ram2* plants in the presence of a nurse plant that shares a common fungal mycelium restores fungal colonization levels and arbuscule formation in *ram2* roots, suggesting that RAM2 has a nutritional role in AM symbiosis (Peter Eastmond and Ertao Wang, personal communication). Labelling studies provide further evidence that the lipid transfer between the plant and the fungus is abolished in *ram2* roots, indicating that RAM2 is a critical component of the lipid export pathway (Peter Eastmond and Ertao Wang, personal communication). Based on promoter binding studies and expression analyses, it has previously been demonstrated that the expression of *RAM2* is directly regulated by RAM1 (Gobbato et al., 2012). In accordance with these findings, the transcriptional profiling performed here showed that the transcript levels of *RAM2* were strongly upregulated during mycorrhizal colonization in

a *RAM1*-dependent manner. In addition to *RAM2*, a large number of genes involved in lipid biosynthesis and putative lipid secretion were found to be among the genes whose mycorrhizal induction was entirely dependent on *RAM1*, including several homologs of the *A. thaliana WRI* transcription factors, the acyl-ACP (acyl carrier protein) thioesterase *FatM*, and two half-size ABCG transporters with a putative function in lipid secretion. The spatial gene expression patterns of these genes in mycorrhized roots indicate that they are co-expressed with *RAM2* in arbuscule-containing cells, suggesting that they might be involved in the same lipid export pathway as *RAM2*.

The role of the *WRI* transcription factors in *A. thaliana* has been well characterised (Marchive et al., 2014). In seeds and floral tissues, these transcription factors regulate the expression of late glycolysis and early fatty acid biosynthesis genes to support the production of triacylglycerols and cutin (Baud et al., 2009; To et al., 2012). Although *AtWRI1*, *AtWRI3*, and *AtWRI4* are differentially expressed in the plant, the three transcription factors were found to be functionally redundant, as both *AtWRI3* and *AtWRI4* are able to complement the *Atwri1* mutant seed phenotype (To et al., 2012). The close phylogenetic relationship of these transcription factors with the mycorrhizal-induced AP2-domain proteins in *M. truncatula* suggests that the *M. truncatula* homologs might have a similar function in regulating the *de novo* production of acyl-chains, which could serve as precursors for lipids that are exported to mycorrhizal fungi. This hypothesis is further supported by the observation that similar to *MtWRI1*, *MtWRI2*, and *MtWRI3*, many homologs of the known *AtWRI* target genes, including genes encoding pyruvate kinase and acetyl-CoA carboxylase subunits, were found in the group of *RAM1*-dependent genes. However, further evidence is required to confirm that the *WRI* transcription factors in *M. truncatula* are involved in the upregulation of *de novo* fatty acid biosynthesis as part of the lipid export pathway. Complementation assays of *A. thaliana wri* mutants with the *M. truncatula* homologs would clarify whether the *M. truncatula WRI* transcription factors have the same function in lipid production as their homologs in *A. thaliana*. Interestingly, RNA silencing of *MtWRI2* (also called *MtERF1*) has previously been reported to decrease fungal colonization and impair arbuscule formation in *M. truncatula* roots (Devers et al., 2013). These results suggest that similar to *RAM1* and *RAM2*, *MtWRI2* is required for proper arbuscule development. However, it cannot be excluded that the expression of additional *WRI* homologs other than *MtWRI2* were silenced in these roots. Several TNT1 insertion lines are available that carry mutations in the mycorrhizal-induced *WRI* genes, and a detailed analysis of the mycorrhizal colonization in these mutants might provide more insights into the

functions of these genes during AM symbiosis. *RAM1* was required for the upregulation of only three of the five *WRI* genes that were induced during fungal colonization. Promoter-GUS studies showed that the *RAM1*-independent *MtWRI4* is expressed in arbuscule-containing cells, similar to the three *RAM1*-dependent *WRI* homologs. It is possible that all five WRI homologs are involved in providing precursors for the production of lipids delivered to the fungus. Alternatively, some of these homologs might be required for the production of other complex fatty acids with a function in AM development.

The acyl ACP-thioesterase *FatM* has previously been shown to be upregulated in mycorrhized *M. truncatula* roots and is evolutionarily conserved in mycorrhizal plant species (Gomez et al., 2009; Bravo et al., 2016). *FatM* is a homolog of *A. thaliana FatB*, which is involved in the release of palmitic acid from the plastid into the cytosol (Salas and Ohlrogge, 2002; Bonaventure et al., 2003). The biochemical characterisation of *RAM2* has shown that the encoded enzyme preferentially uses palmitoyl-CoenzymeA to produce 2-monopalmitin (Peter Eastmond, personal communication), a lipid that has been found to accumulate in mycorrhized roots (Schliemann et al., 2008). Thus, FatM is an ideal candidate to provide the substrate for RAM2 in the lipid export pathway. In line with this hypothesis, *M. truncatula* plants carrying a mutation in *FatM* show reduced levels of fungal colonization and are unable to form fully developed arbuscules (Bravo et al., 2016). It would be interesting to test whether the inoculation of *fatm* with a nurse plant inoculum can restore arbuscule development in colonized mutant roots and would further clarify whether *FatM*, like *RAM2*, has a nutritional role during AM symbiosis.

In *A. thaliana*, several ABCG transporters have been found to mediate the active export of lipids across the plasma membrane (Li et al., 2015). Based on loss-of-function phenotypes, the three half-size ABCG transporters *AtABCG11*, *AtABCG12*, and *AtABCG13* have been proposed to be required for the export of waxes, cutin and suberin to the cell wall (Pighin et al., 2004; Bird et al., 2007; Panikashvili et al., 2010; Panikashvili et al., 2011). Plants carrying mutations in these transporters show a reduced deposition of surface lipids, however, the exact identity of the substrates that are transported across the membrane remains unknown (Li et al., 2015). In *M. truncatula*, two homologs of these lipid transporters, *MtABCG3* and *MtABCG4*, were significantly upregulated during mycorrhization in a *RAM1*-dependent manner. Promoter-GUS analyses in mycorrhized roots further indicate that *MtABCG3* is strongly expressed in arbuscule containing cells. Together, these findings suggest that MtABCG3, and possibly MtABCG4, might have a

role in mediating the export of plant-derived lipids across the periarbuscular membrane to the fungus. To test this hypothesis, the mycorrhizal phenotypes of three *M. truncatula* lines carrying a TNT1 insertion in *MtABCG3* were examined, however, only a weak reduction in fungal colonization was observed in these three lines at intermediate time points. Furthermore, arbuscule development did not appear to be affected in *abcg3* roots at any of the time points tested. If lipid export to the fungus was disrupted in these *abcg3* mutant lines, one would expect the roots to display a similar mycorrhizal phenotype as *ram2* and *fatm*, which show low levels of colonization and are not able to form fully developed arbuscules (Wang et al., 2012; Gobbato et al., 2013). It is possible that *MtABCG3* has a different function during mycorrhization and is not involved in the lipid export pathway. Alternatively, lipid export might be retained in *abcg3* mutants due to the presence of the close homolog *MtABCG4,* which might act redundantly during AM symbiosis. Although gene expression profiling only revealed a weak upregulation of *MtABCG4* in mycorrhized roots, the basal expression levels of this transporter might be sufficient to compensate for the loss of *MtABCG3*. Half-size ABCG transporters must form homo- or heterodimers to be able to transport substrates across membranes, as they only possess one transmembrane and one ATPase domain, while full-size ABC transporters have two of each domain. In *A. thaliana*, AtABCG11 has been shown to interact with several other half-size ABCG transporters, but can also form homodimers (McFarlane et al., 2010). During mycorrhization, MtABCG3 and MtABCG4 might form a heterodimer to export lipids across the periarbuscular membrane, and the loss of one of the two subunits might be compensated for by forming a homodimer. Thus, it might be necessary to disrupt the expression of both genes simultaneously to be able to see a reduction in fungal colonization and a potential defect in arbuscule formation. As the two genes encoding these transporters are located in tandem on the *M. truncatula* genome, a simultaneous knockdown using RNA silencing or CRISPR would be required to test this hypothesis. Moreover, examining the subcellular localisation of MtABCG3 and MtABCG4 to test whether these two proteins localize to the periarbuscular membrane would further clarify whether they could be involved in transporting a substrate to the fungus. Two other half-size ABCG transporters, *STR* and *STR2*, have previously been shown to be required for arbuscule formation and localise to the periarbuscular membrane (Zhang et al., 2010; Gutjahr et al., 2012). The substrate transported by *STR* and *STR2* is currently unknown, however, the inoculation of the rice *str* mutant with a nurse plant inoculum does not restore the arbuscular defect, suggesting that these two transporters do not have a nutritional role in AM symbiosis (Gutjahr et al., 2012).

Global gene expression profiling revealed that *RAM1* is essential for the upregulation of genes involved in lipid metabolism and putative lipid secretion at all three time points during mycorrhization. The ectopic overexpression of *RAM1* in *M. truncatula* roots and the analysis of transcript levels of putative direct targets by qRT-PCR further showed that *RAM1* is sufficient to induce several of the lipid-related genes, including *RAM2*, *FatM*, *MtABCG3,* and *MtWRI2,* even in the absence of mycorrhizal fungi. These findings suggest that RAM1 regulates a number of genes with a putative function in the lipid export pathway. Interestingly, the expression of *MtWRI1* was not induced in *RAM1*-overexpression lines. It is possible that other transcription factors are required for the upregulation of *MtWRI1*. RAM1 has been shown to physically interact with several GRAS-domain proteins, including RAD1, DIP1, NSP2, and the DELLA proteins (Gobbato et al., 2012; Yu et al., 2014; Xue et al., 2015; Fonouni-Farde et al., 2016; Jin et al., 2016), and it might be necessary to overexpress a transcription factor complex rather than individual transcriptional regulators to be able to detect the induction of some of the putative target genes of RAM1. *In vitro* and *in vivo* binding studies such as EMSAs and ChIP-assays would help to further investigate whether RAM1 directly binds to the promoters of these putative target genes.

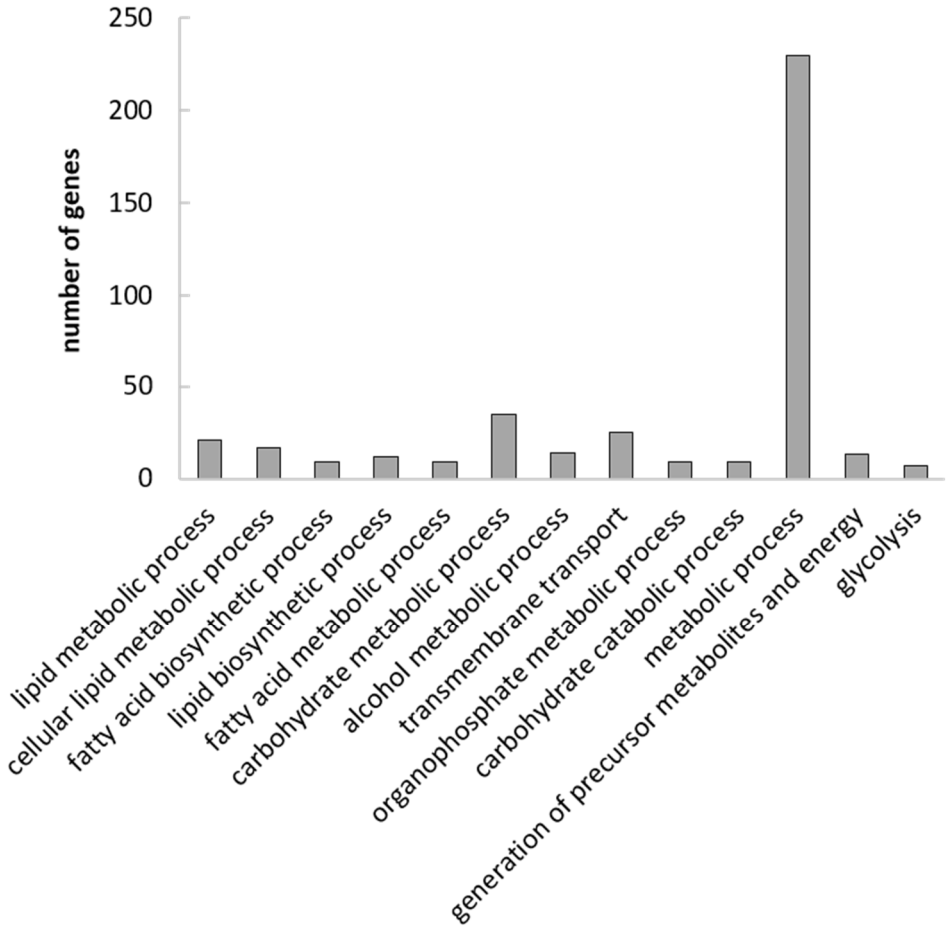

Figure 5.1: Gene ontology (GO) analysis of genes that were found to be consistently dependent on *RAM1* for their induction during mycorrhization. Singular enrichment analysis was performed using Agrigo (http://bioinfo.cau.edu.cn/agriGO/index.php) and the whole *M. truncatula* genome as background. Significantly enriched terms of biological processes with an FDR-corrected p-value <0.05 are shown.

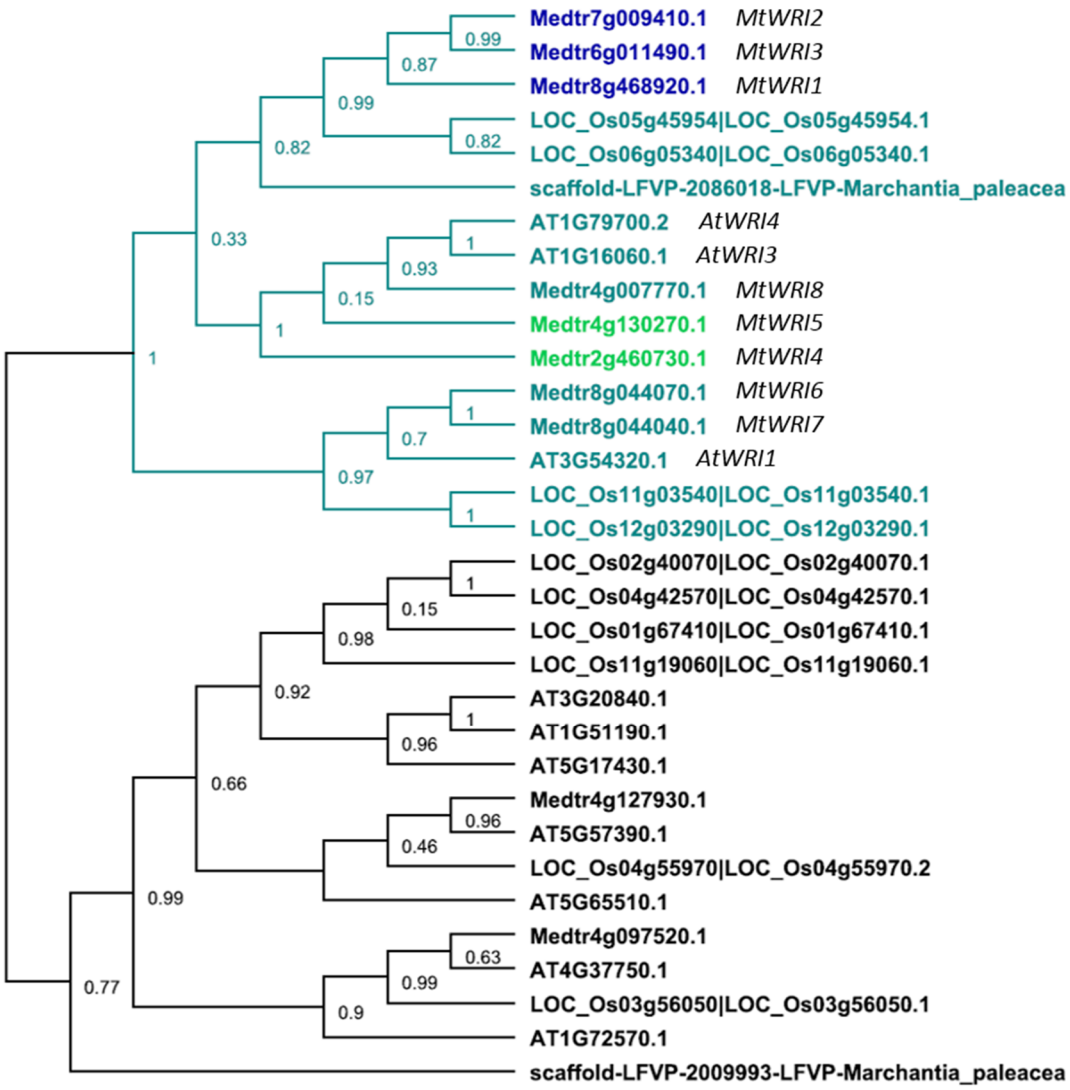

Figure 5.2: Phylogenetic relationship of *WRI* (*WRINKLED*) transcription factors. A maximum likelihood phylogenetic tree of the closest homologs of the *WRI* genes in *A. thaliana*, *M. truncatula, O. sativa*, and *M. paleacea* with bootstrap values for each branch is shown. The alignment and the tree were made using Geneious 6.06. The WRI-like clade is indicated in dark green. Genes in blue indicate the homologs that are significantly upregulated during mycorrhization in a *RAM1*-dependent manner. Genes in light green indicate the homologs that are significantly upregulated during mycorrhization in a *RAM1*-independent manner. The three *A. thaliana* genes *AtWRI1*, *AtWRI3*, and *AtWRI4* are indicated. The *M. truncatula WRI* homologs are named as indicated. Figure produced in collaboration with Guru Radhakrishnan.

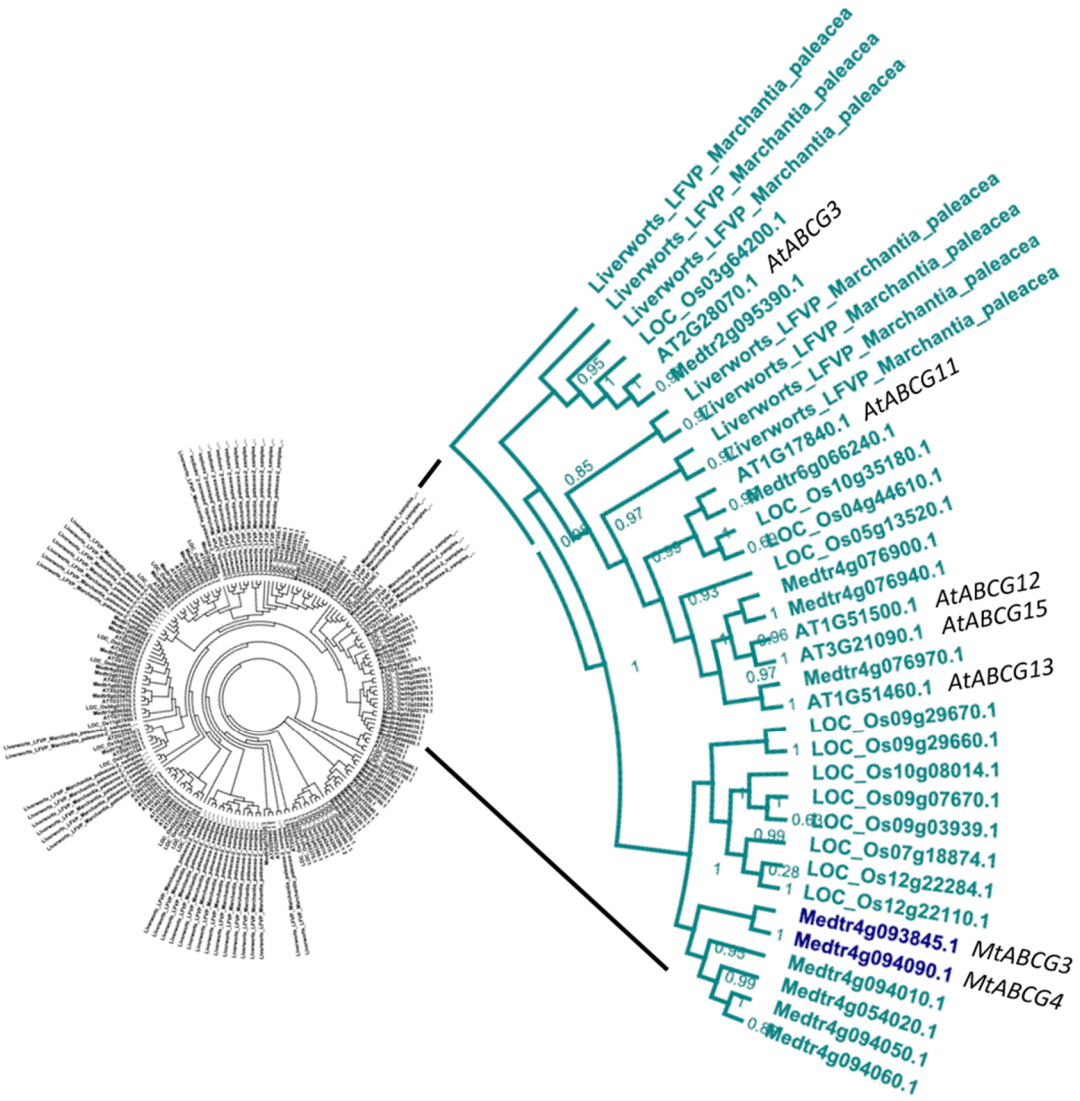

Figure 5.3: Phylogenetic relationship of ABCG half-size transporters with a putative role in lipid transport. A maximum likelihood phylogenetic tree of the closest homologs of the *ABCG* genes in *A. thaliana*, *M. truncatula, O. sativa*, and *M. paleacea* with bootstrap values for each branch is shown. The alignment and the tree were made using Geneious 6.06. Genes in blue indicate the *M. truncatula* homologs that are significantly upregulated during mycorrhization in a *RAM1*-dependent manner. The five *A. thaliana* genes *AtABCG3*, *AtABCG11*, *AtABCG12, AtABCG13,* and *AtABCG15* are indicated. Figure produced in collaboration with Guru Radhakrishnan.

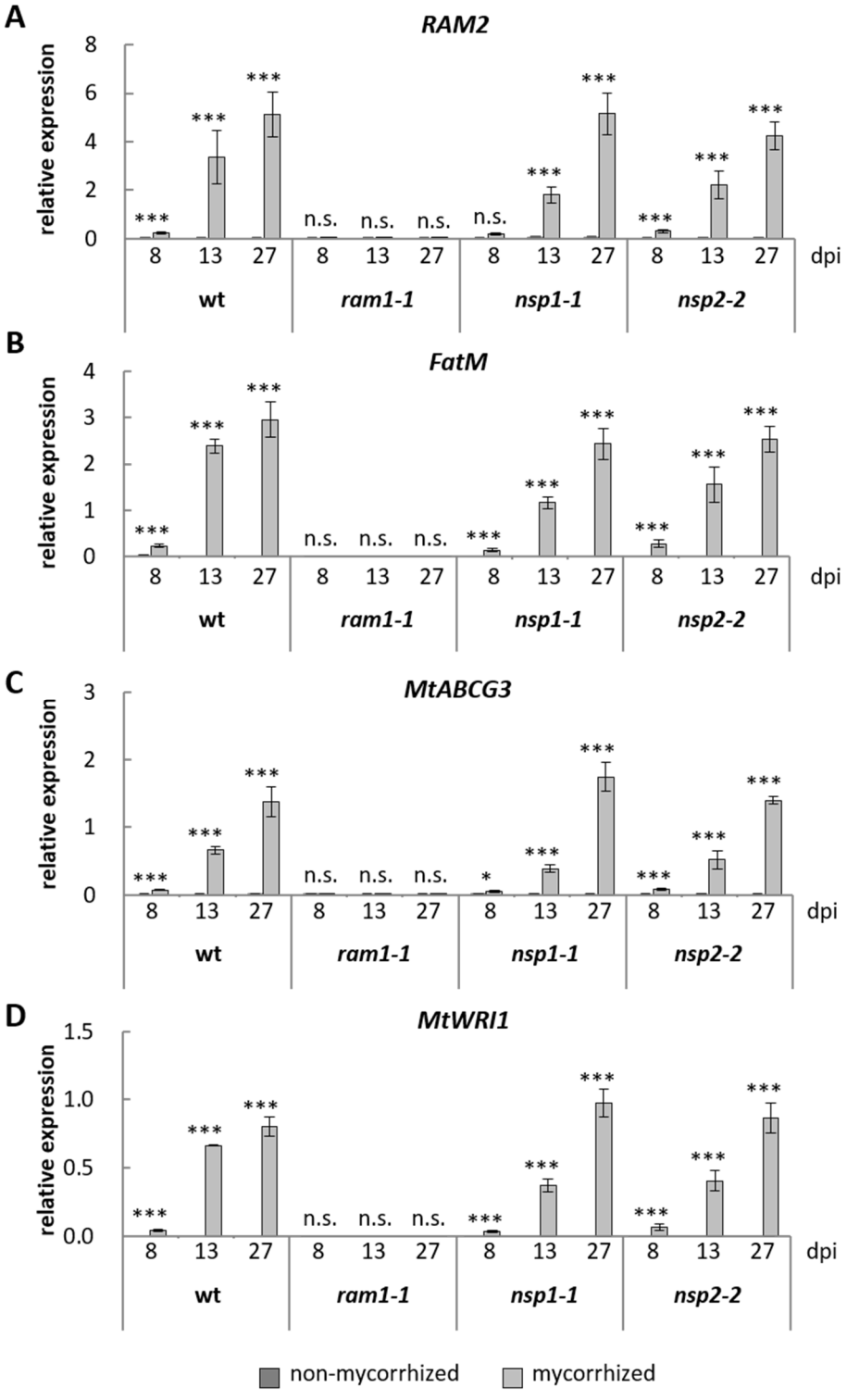

Figure 5.4: Quantification of transcript levels of genes involved in lipid metabolism and putative lipid transport in non-mycorrhized and mycorrhized wild-type (wt), *ram1-1*, *nsp1-1*, and *nsp2-2* roots at 8 dpi, 13 dpi, and 27 dpi. Expression levels of *RAM2* **(A)**, *FatM* **(B)**, *MtABCG3* **(C),** and *MtWRI1* **(D)** are shown. Expression levels were measured by qRT-PCR and normalized to *Ubiquitin* expression. Bars represent means of 4 biological replicates ± SEM. Asterisks indicate significant differences between expression levels in mycorrhized and non-mycorrhized roots of the same genotype at the corresponding time point (ANOVA, post hoc Tukey, *, $P < 0.05$; **, $P < 0.01$; ***, $P < 0.001$, n.s., $P > 0.05$).

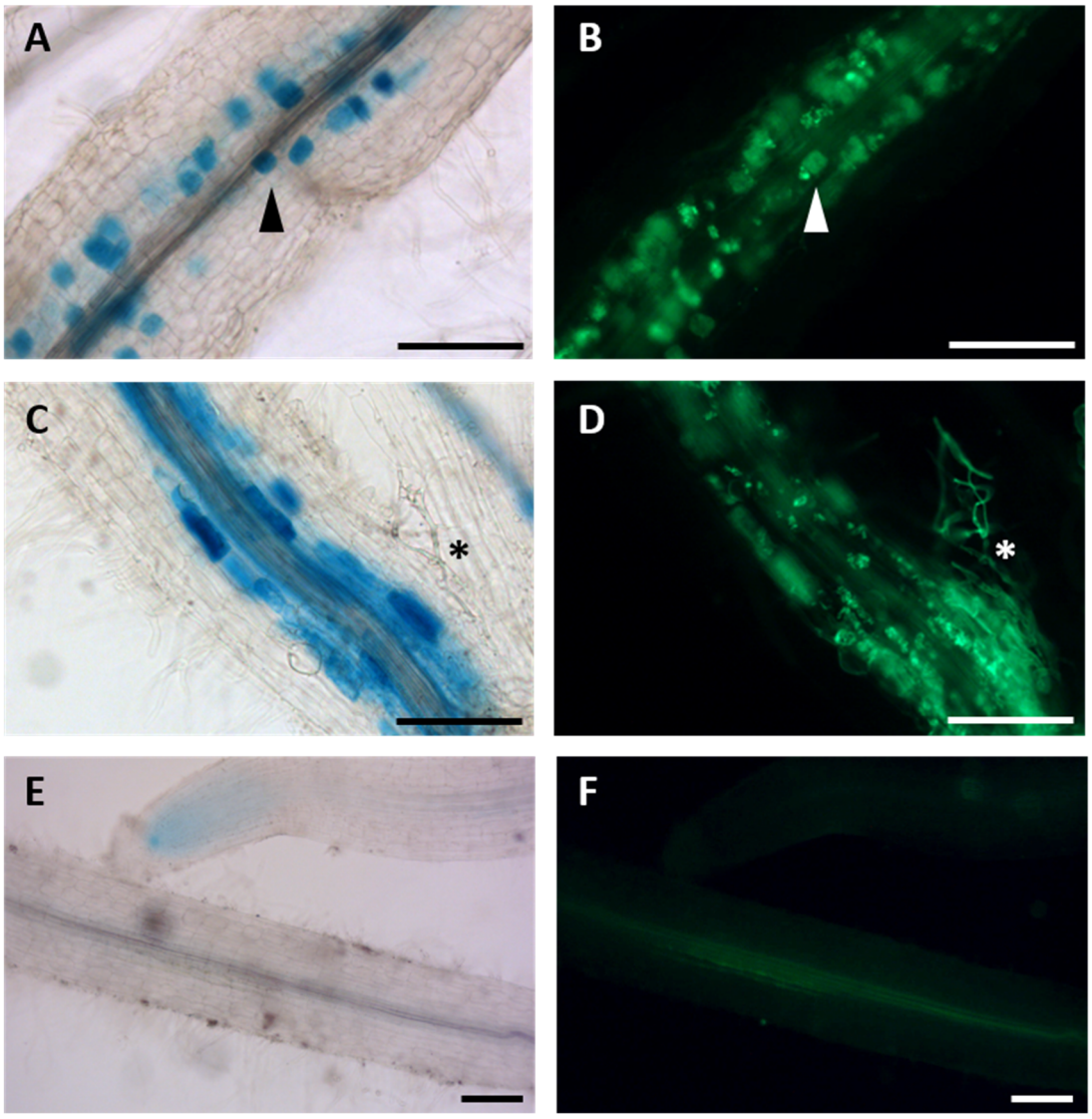

Figure 5.5: Activity of the *RAM2* promoter in mycorrhized and non-mycorrhized *M. truncatula* roots. Bright field (**A, C, E**) and the corresponding green fluorescence (**B, D, F**) images of *M. truncatula* hairy roots expressing the *β-glucuronidase (GUS)* gene under the control of the *RAM2* promoter are shown. Roots were grown in the presence (**A, B, C, D**) and absence (**E, F**) of mycorrhizal fungi. *RAM2* promoter activity was visualised by GUS staining. Fungal structures were visualised by staining roots with Alexa Fluor 488 WGA. Arrowheads indicate cells containing fully developed arbuscules. Stars indicate hyphopodia. Scale bars = 150 µm.

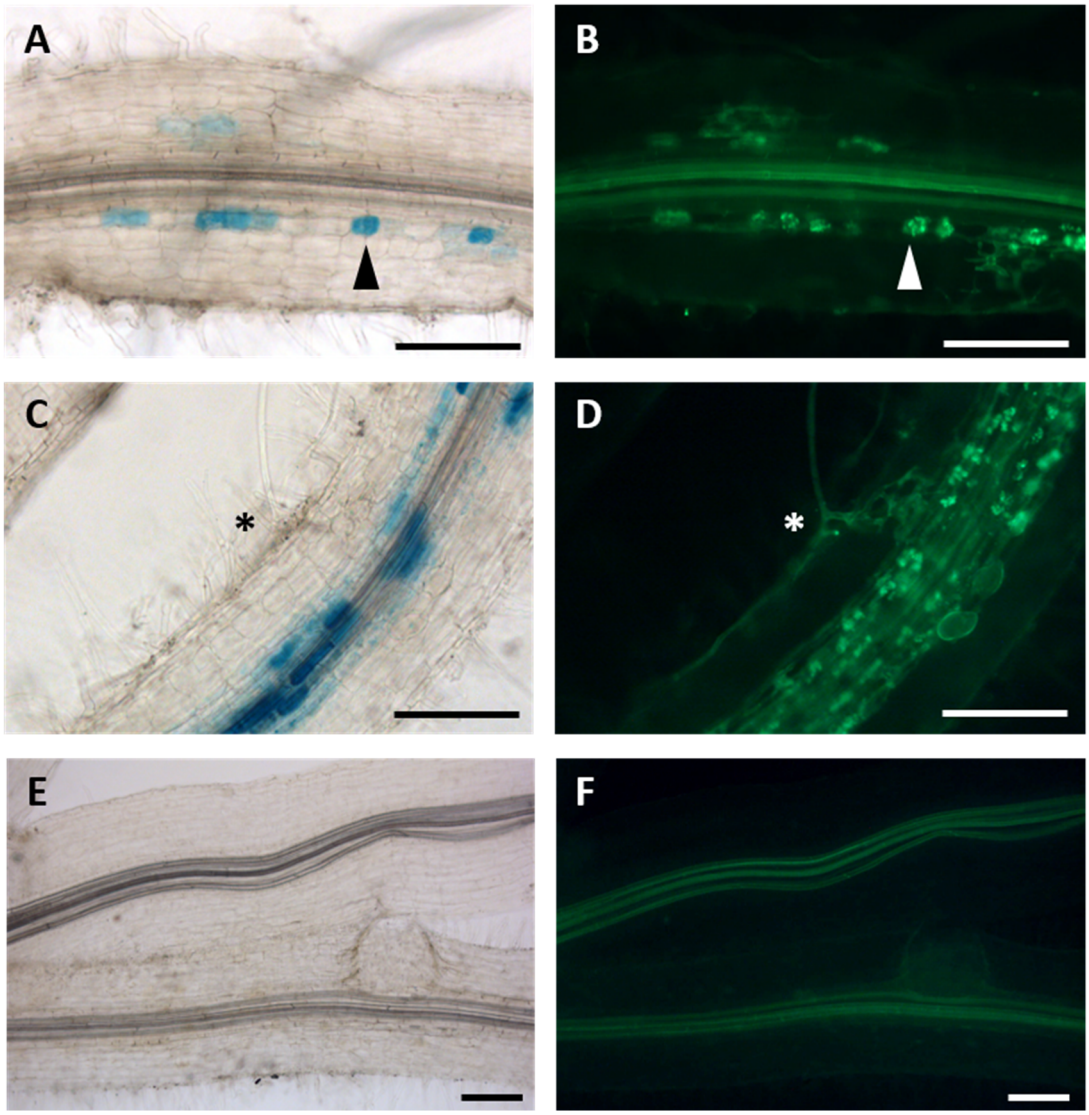

Figure 5.6: Activity of the *MtABCG3* promoter in mycorrhized and non-mycorrhized *M. truncatula* roots. Bright field (**A, C, E**) and the corresponding green fluorescence (**B, D, F**) images of *M. truncatula* hairy roots expressing the *β-glucuronidase (GUS)* gene under the control of the *MtABCG3* promoter are shown. Roots were grown in the presence (**A, B, C, D**) and absence (**E, F**) of mycorrhizal fungi. *MtABCG3* promoter activity was visualised by GUS staining. Fungal structures were visualised by staining roots with Alexa Fluor 488 WGA. Arrowheads indicate cells containing fully developed arbuscules. Stars indicate hyphopodia. Scale bars = 150 µm.

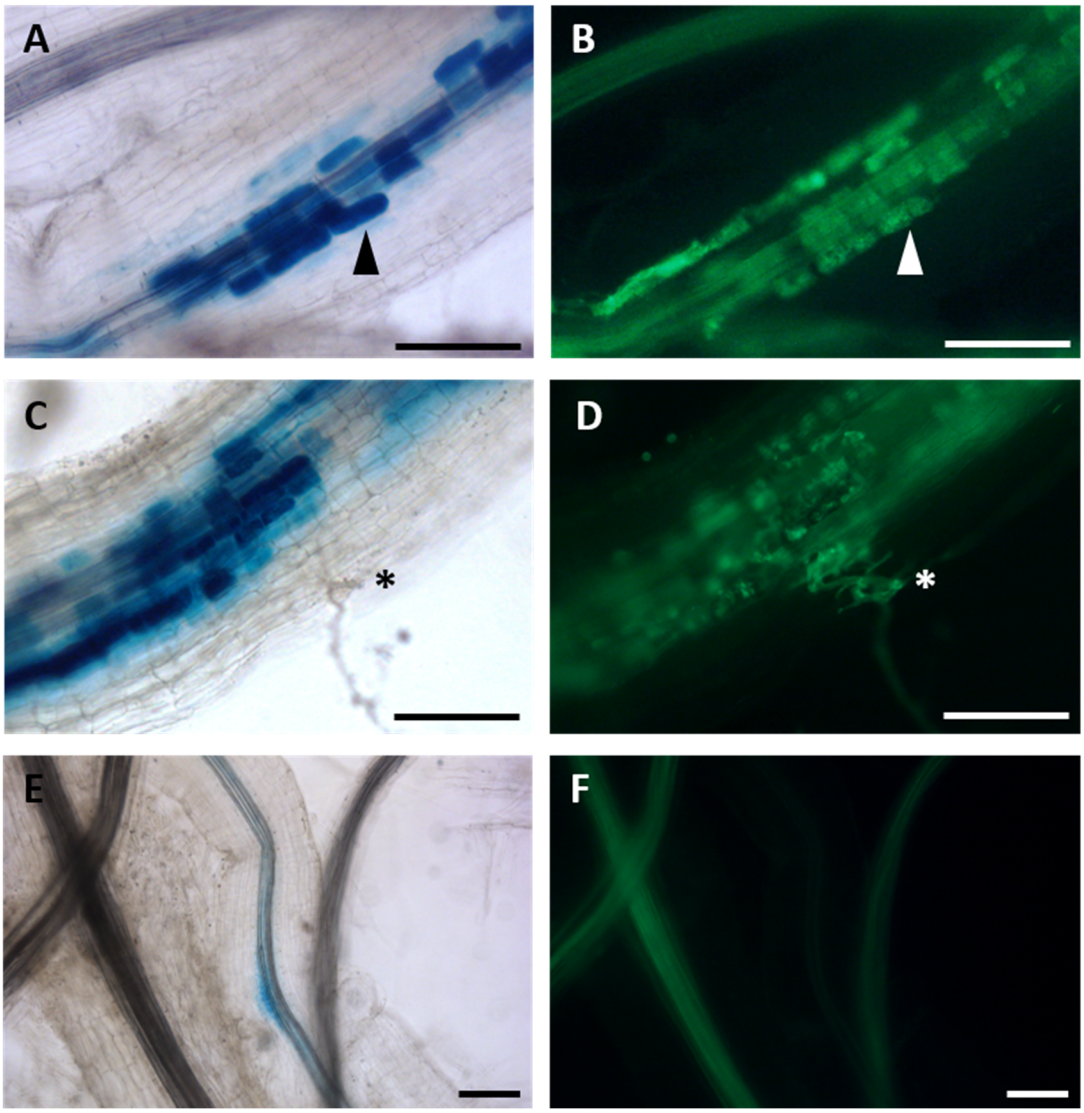

Figure 5.7: Activity of the *FatM* promoter in mycorrhized and non-mycorrhized *M. truncatula* roots. Bright field (**A, C, E**) and the corresponding green fluorescence (**B, D, F**) images of *M. truncatula* hairy roots expressing the *β-glucuronidase (GUS)* gene under the control of the *FatM* promoter are shown. Roots were grown in the presence (**A, B, C, D**) and absence (**E, F**) of mycorrhizal fungi. *FatM* promoter activity was visualised by GUS staining. Fungal structures were visualised by staining roots with Alexa Fluor 488 WGA. Arrowheads indicate cells containing fully developed arbuscules. Stars indicate hyphopodia. Scale bars = 150 µm.

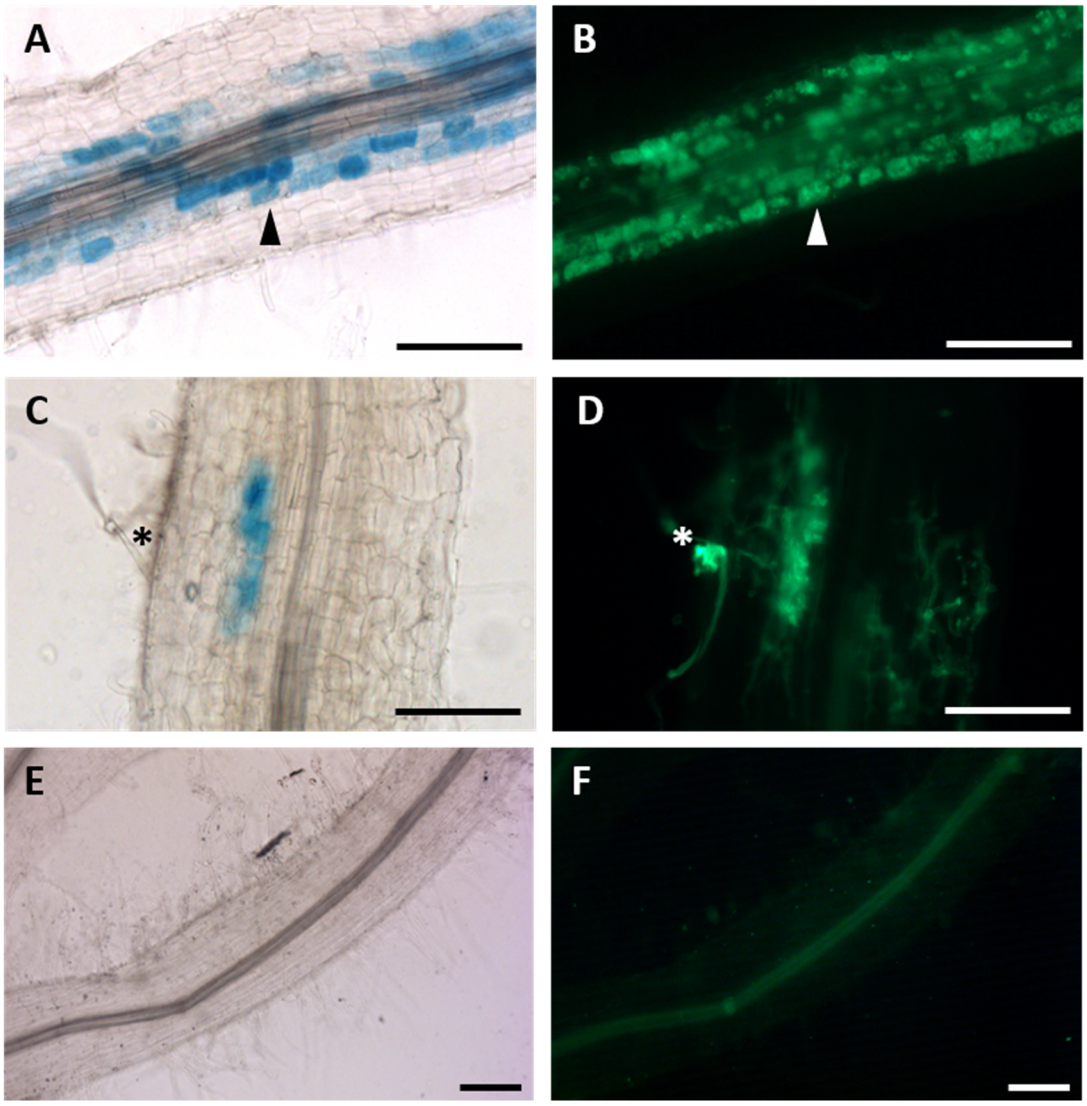

Figure 5.8: Activity of the *MtWRI1* promoter in mycorrhized and non-mycorrhized *M. truncatula* roots. Bright field (**A, C, E**) and the corresponding green fluorescence (**B, D, F**) images of *M. truncatula* hairy roots expressing the *β-glucuronidase (GUS)* gene under the control of the *MtWRI1* promoter are shown. Roots were grown in the presence (**A, B, C, D**) and absence (**E, F**) of mycorrhizal fungi. *MtWRI1* promoter activity was visualised by GUS staining. Fungal structures were visualised by staining roots with Alexa Fluor 488 WGA. Arrowheads indicate cells containing fully developed arbuscules. Stars indicate hyphopodia. Scale bars = 150 µm.

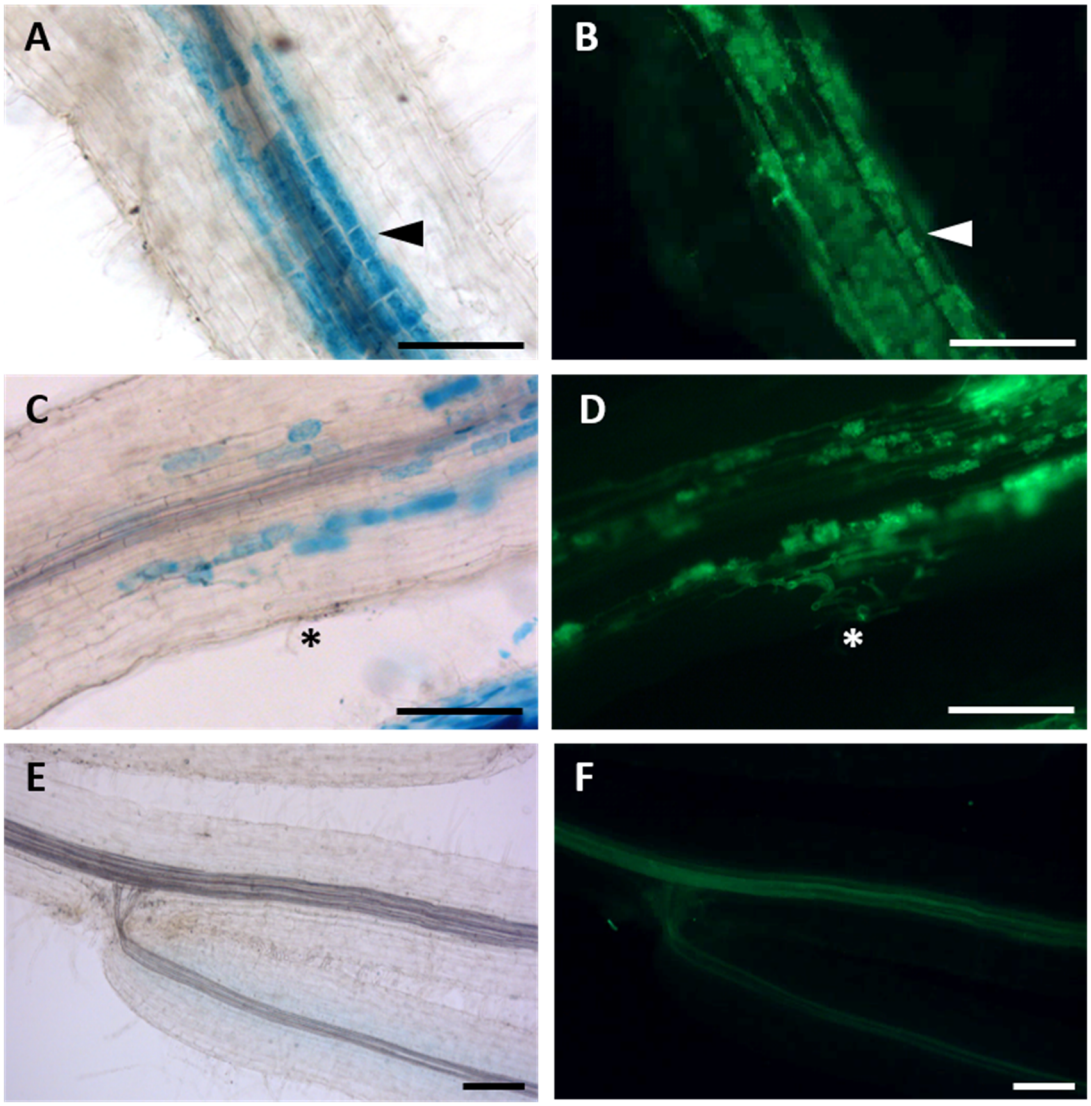

Figure 5.9: Activity of the *MtWRI2* promoter in mycorrhized and non-mycorrhized *M. truncatula* roots. Bright field (**A, C, E**) and the corresponding green fluorescence (**B, D, F**) images of *M. truncatula* hairy roots expressing the *β-glucuronidase (GUS)* gene under the control of the *MtWRI2* promoter are shown. Roots were grown in the presence (**A, B, C, D**) and absence (**E, F**) of mycorrhizal fungi. *MtWRI2* promoter activity was visualised by GUS staining. Fungal structures were visualised by staining roots with Alexa Fluor 488 WGA. Arrowheads indicate cells containing fully developed arbuscules. Stars indicate hyphopodia. Scale bars = 150 µm.

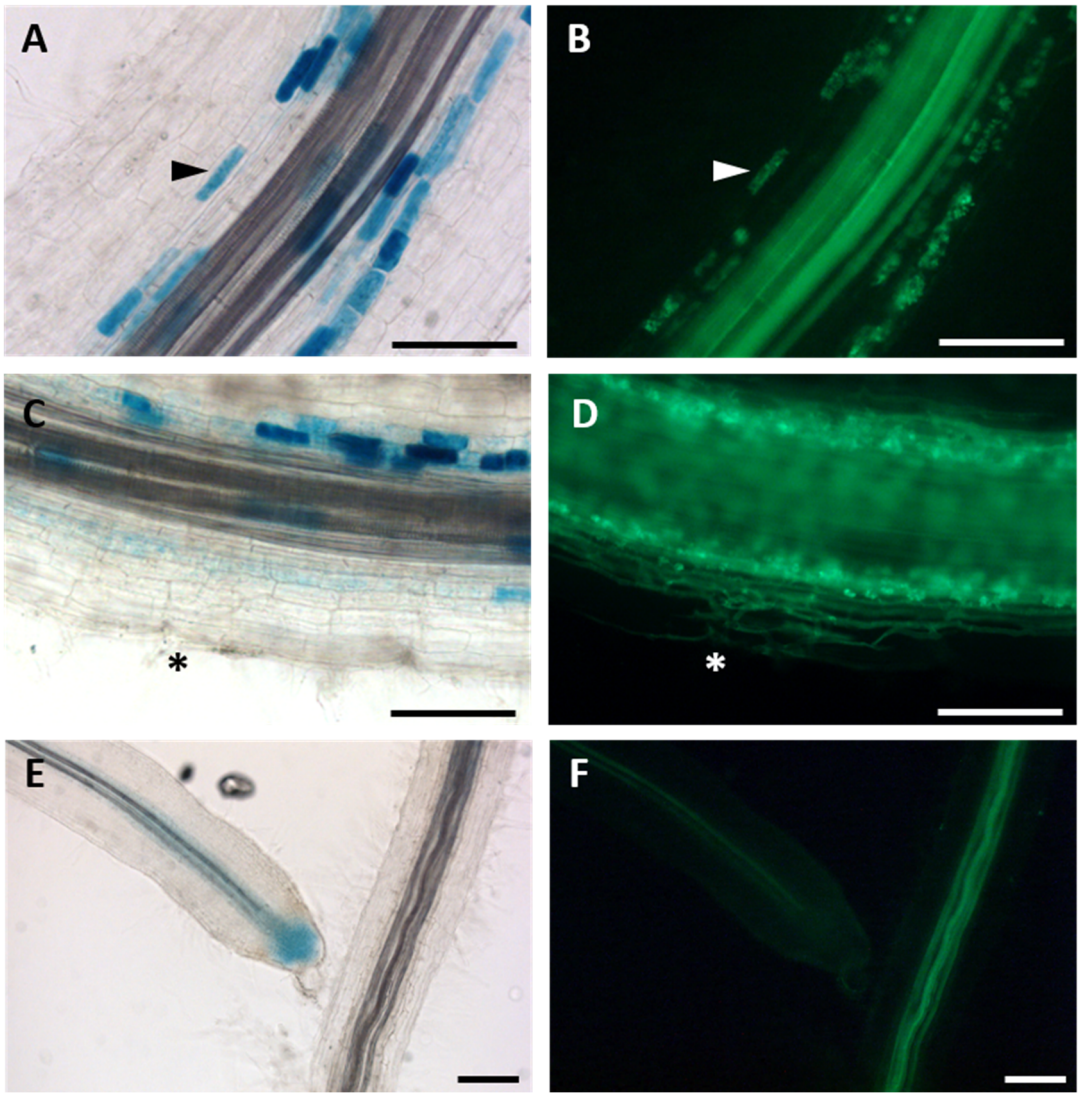

Figure 5.10: Activity of the *MtWRI3* promoter in mycorrhized and non-mycorrhized *M. truncatula* roots. Bright field (**A, C, E**) and the corresponding green fluorescence (**B, D, F**) images of *M. truncatula* hairy roots expressing the *β-glucuronidase (GUS)* gene under the control of the *MtWRI3* promoter are shown. Roots were grown in the presence (**A, B, C, D**) and absence (**E, F**) of mycorrhizal fungi. *MtWRI3* promoter activity was visualised by GUS staining. Fungal structures were visualised by staining roots with Alexa Fluor 488 WGA. Arrowheads indicate cells containing fully developed arbuscules. Stars indicate hyphopodia. Scale bars = 150 µm.

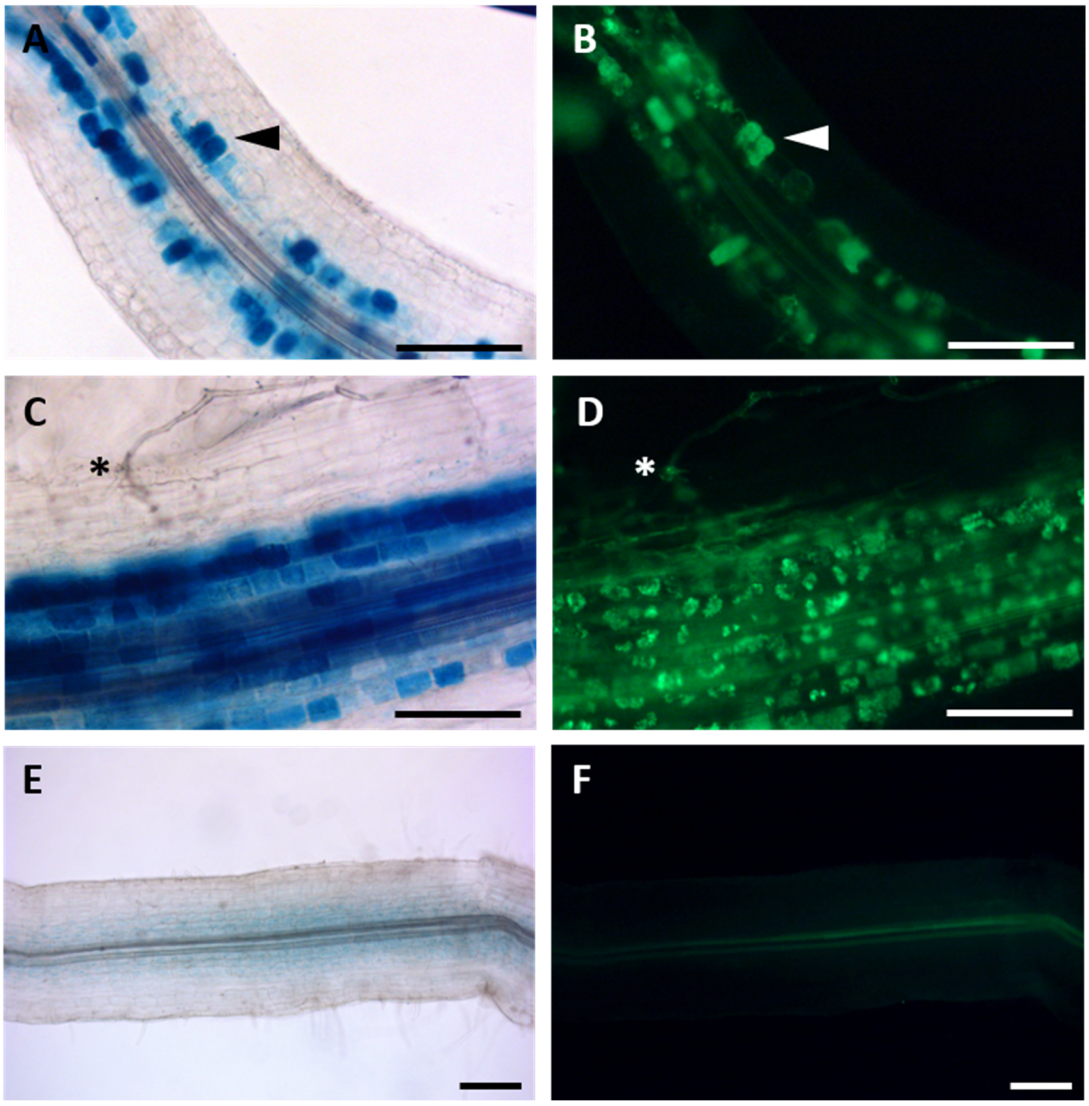

Figure 5.11: Activity of the *MtWRI4* promoter in mycorrhized and non-mycorrhized *M. truncatula* roots. Bright field (**A, C, E**) and the corresponding green fluorescence (**B, D, F**) images of *M. truncatula* hairy roots expressing the *β-glucuronidase (GUS)* gene under the control of the *MtWRI4* promoter are shown. Roots were grown in the presence (**A, B, C, D**) and absence (**E, F**) of mycorrhizal fungi. *MtWRI4* promoter activity was visualised by GUS staining. Fungal structures were visualised by staining roots with Alexa Fluor 488 WGA. Arrowheads indicate cells containing fully developed arbuscules. Stars indicate hyphopodia. Scale bars = 150 µm.

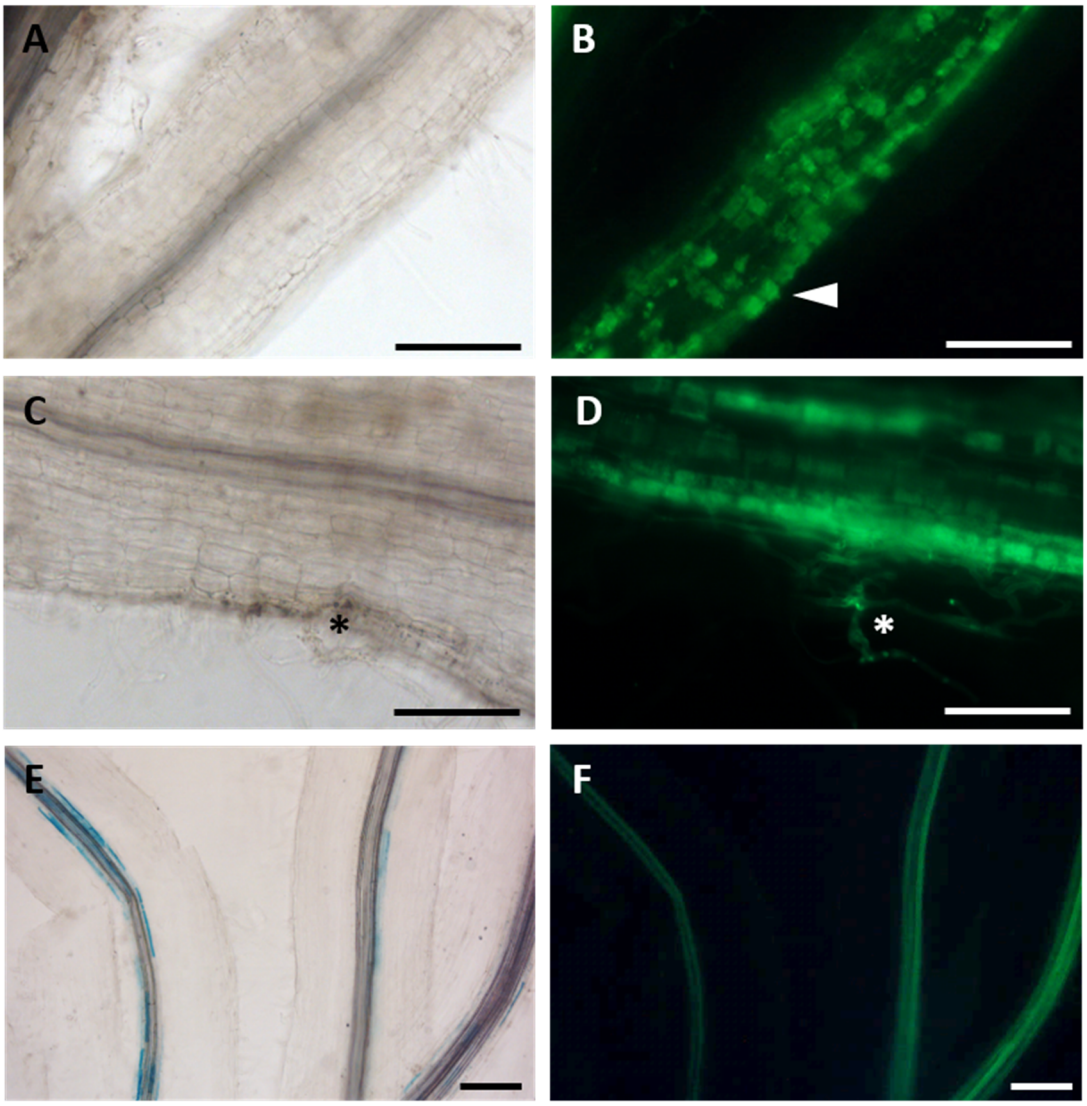

Figure 5.12: Activity of the *MtWRI6* promoter in mycorrhized and non-mycorrhized *M. truncatula* roots. Bright field (**A, C, E**) and the corresponding green fluorescence (**B, D, F**) images of *M. truncatula* hairy roots expressing the *β-glucuronidase (GUS)* gene under the control of the *MtWRI6* promoter are shown. Roots were grown in the presence (**A, B, C, D**) and absence (**E, F**) of mycorrhizal fungi. *MtWRI6* promoter activity was visualised by GUS staining. Fungal structures were visualised by staining roots with Alexa Fluor 488 WGA. Arrowheads indicate cells containing fully developed arbuscules. Stars indicate hyphopodia. Scale bars = 150 µm.

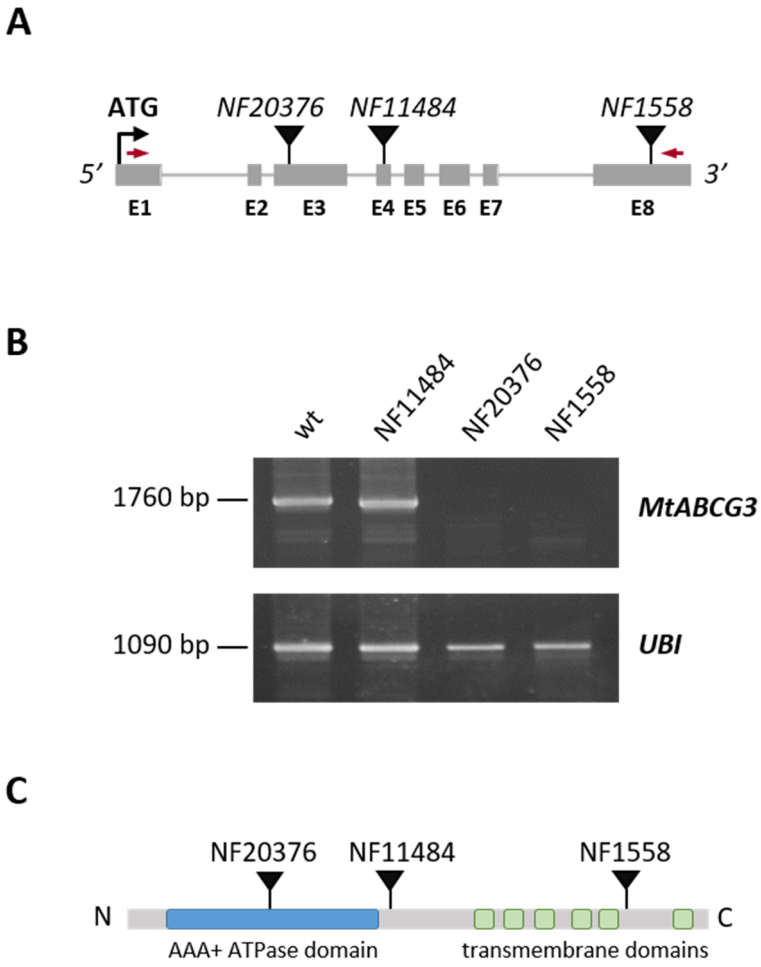

Figure 5.13: Overview of TNT1-insertion lines carrying an insertion in *MtABCG3*. **(A)** Positions of the TNT1 insertions in the *MtABCG3* gene in the lines NF20376, NF11484, and NF1558 are marked with triangles. Exons (E1-E8) are indicated in grey. **(B)** RT-PCR of the full length *MtABCG3* cDNA and the *Ubiquitin* (UBI) cDNA from mycorrhized roots of wild-type (R108) plants and the TNT1-insertion lines. Binding sites of the primers used for the amplification of the *MtABCG3* cDNA are indicated by red arrows in (A). Expected size of the amplified full length *MtABCG3* cDNA = 1760 bp. Expected size of the amplified *UBI* cDNA = 1090 bp. **(C)** Predicted protein structure of the MtABCG3 transporter. Expected positions of the TNT1 insertions are marked with triangles.

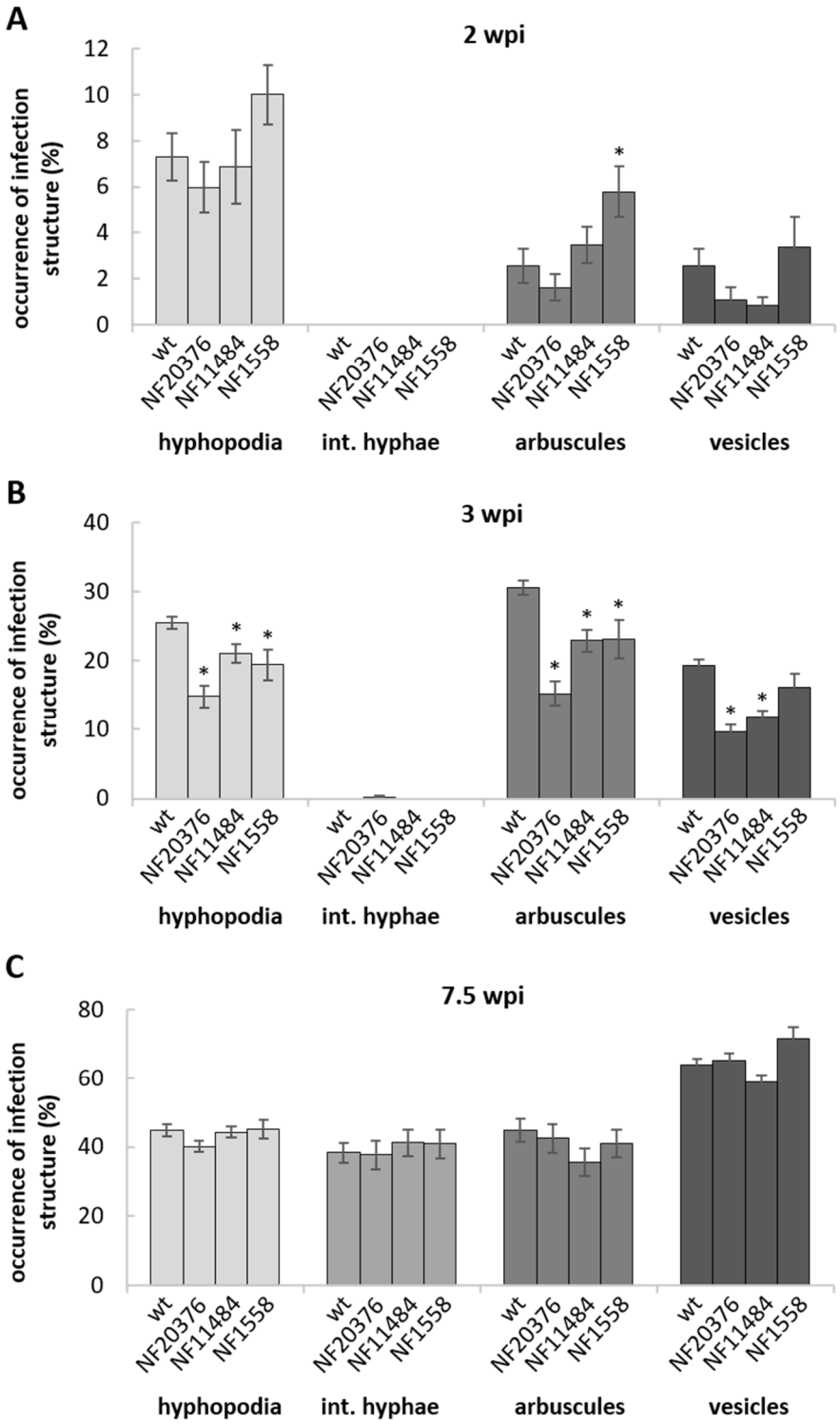

Figure 5.14: Quantification of mycorrhizal infection structures in wild-type (wt) roots and *Mtabcg3* mutant roots**.** The occurrence of hyphopodia, intraradical hyphae (int. hyphae), arbuscules, and vesicles in ink-stained root pieces of the wild type and the TNT1-insertion lines NF20376, NF11484, NF1558 is shown as percentage of the total number of root pieces examined. Fungal infection structures were quantified at 2 wpi **(A)**, 3 wpi **(B)**, and 7.5 wpi **(C)**. Bars represent the average of at least 12 biological replicates ± SEM. Asterisks indicate significant differences between the wild type and the mutant lines in each group of infection type (Student's t-test; *, $P < 0.05$; **, $P < 0.01$; ***, $P < 0.001$).

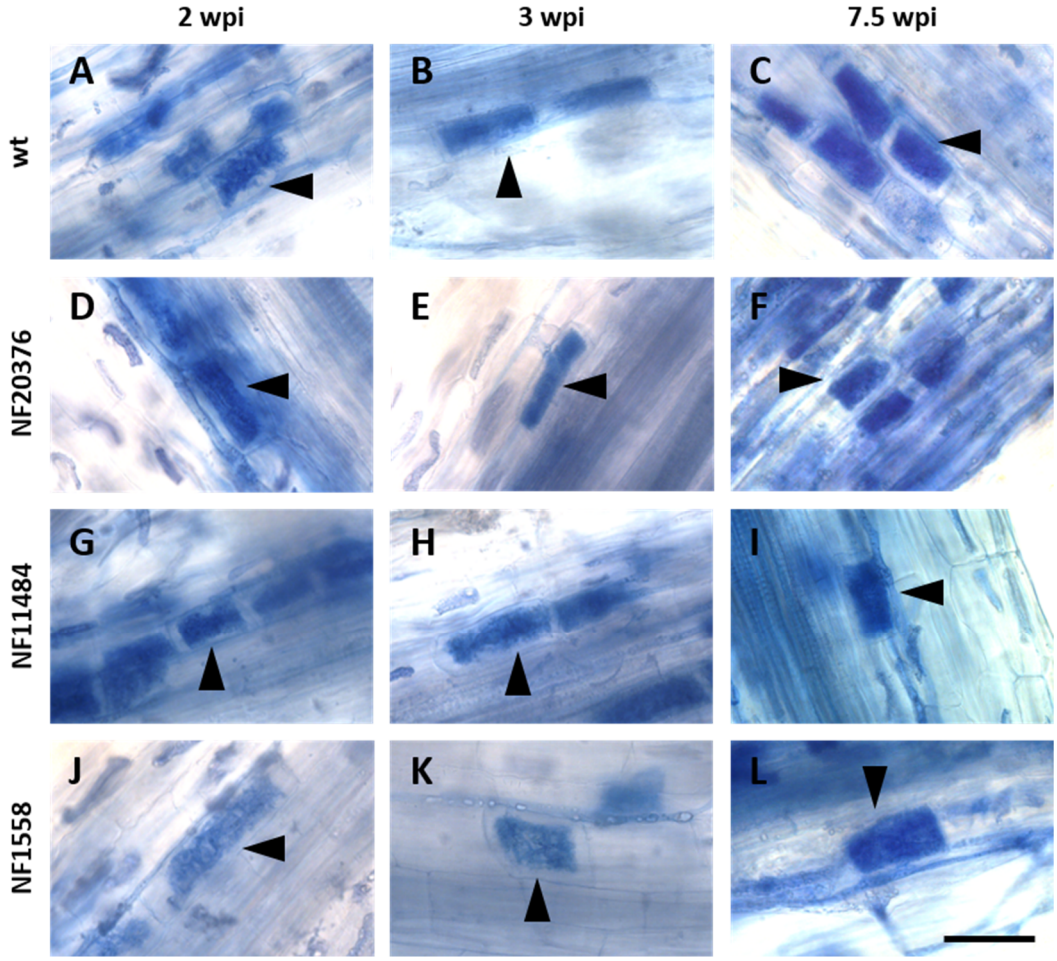

Figure 5.15: Appearance of arbuscules in wild-type (R108) roots and *Mtabcg3* mutant roots at different time points during fungal colonization**.** Bright field images of ink-stained R108 roots (**A, B, C**), NF20376 roots (**D, E, F**), NF11484 roots (**G, H, I**) and NF1558 roots (**J, K, L**) at 2 wpi, 3 wpi, and 7.5 wpi (as indicated) are shown. Arrowheads indicate fully developed arbuscules. Scale bar = 50 µm.

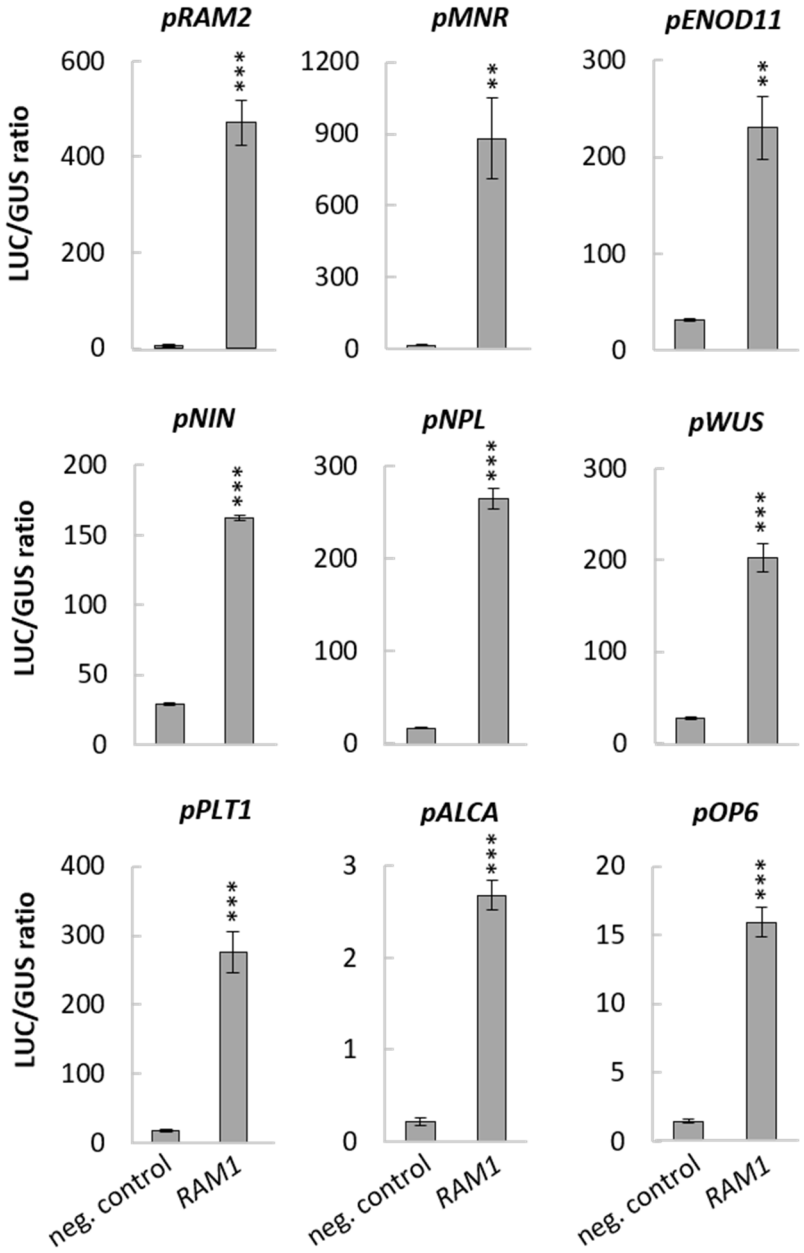

Figure 5.16: Unspecific activation of gene expression by *RAM1* in *N. benthamiana* leaves. The activation of the *LUCIFERASE* (*LUC*) gene under the control of a number of different promoters (as indicated) by *RAM1* is shown. LUC activities were normalised against the β-glucuronidase (GUS) activities quantified in the same leaf discs. The same expression vectors containing all the components except for the gene encoding RAM1 served as negative controls. Bars represent means of 3 biological replicates ± SEM. Asterisks indicate significant differences between the negative control and leaves overexpressing *RAM1* (Student's t-test; *, P < 0.05; **, P < 0.01; ***, P < 0.001).

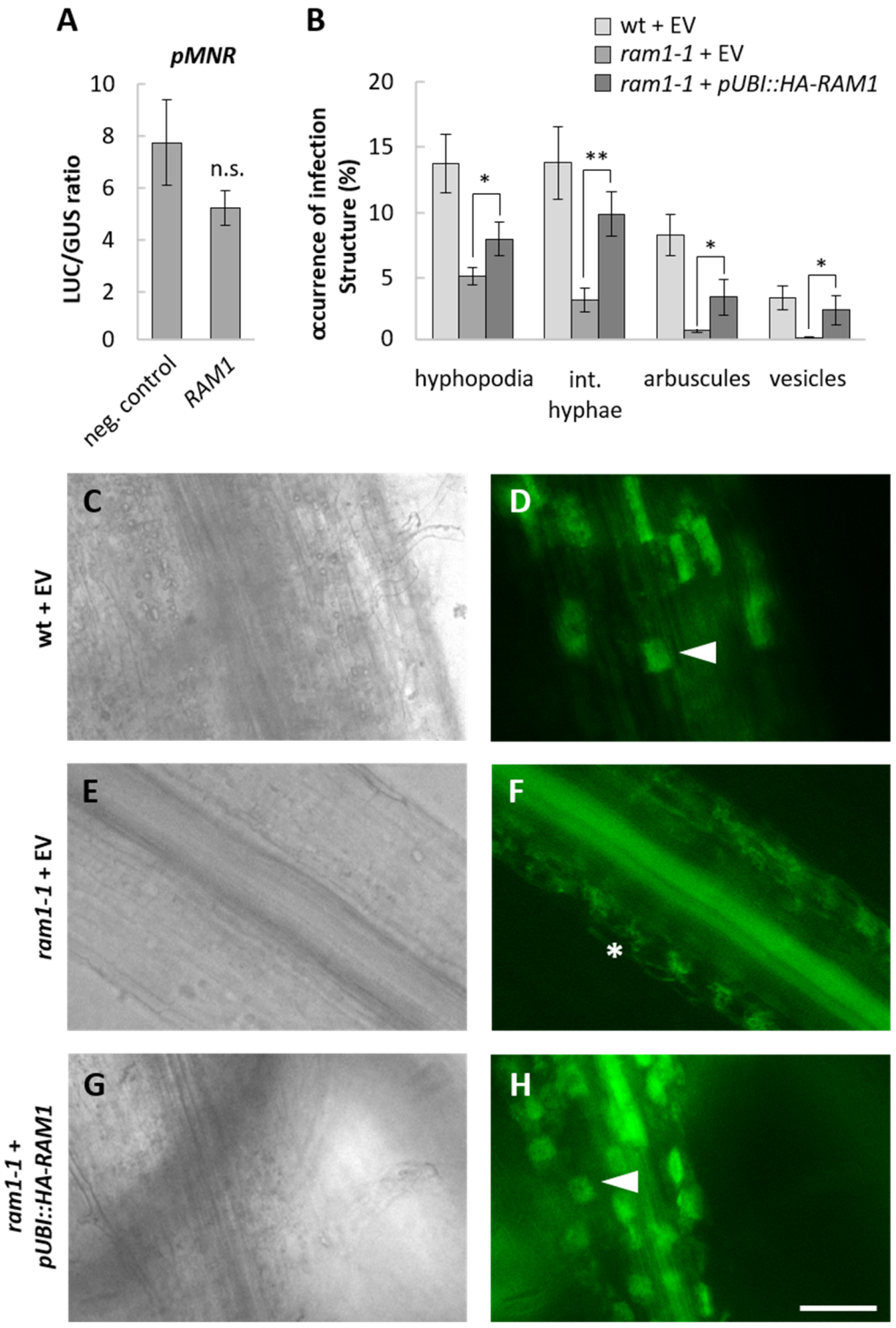

Figure 5.17: Complementation of the *ram1-1* mutant phenotype by expressing the vector used for the transactivation assay with *RAM1* and the *pMNR-LUC* reporter (description continued overleaf).

(A) The ability of *RAM1* to induce the expression of the *LUC* gene under the control of the *MNR* promoter was measured in a transactivation assay in *M. truncatula* hairy roots. LUC activities were normalised against the β-glucuronidase (GUS) activities quantified in the same root samples. The same expression vector containing all the components except for the gene encoding RAM1 served as negative control. Bars represent means of 3 biological replicates ± SEM. N.s. depicts a non-significant difference, Student's t-test. **(B)** Quantification of mycorrhizal structures in wild-type (wt) roots and *ram1-1* roots transformed with the same vectors as used for the transactivation assay described in (A). The occurrence of hyphopodia, intraradical hyphae (int. hyphae), arbuscules, and vesicles in ink-stained root pieces is shown as percentage of the total number of root pieces examined. Fungal infection structures were quantified at 4 wpi. Bars represent the average of 12 biological replicates ± SEM. Asterisks indicate significant differences between *ram1-1* roots expressing the vector control and *ram1-1* roots overexpressing *HA-RAM1* (Student's t-test; *, $P < 0.05$; **, $P < 0.01$; ***, $P < 0.001$). **(C) – (H)** Appearance of mycorrhizal structures in wild-type (wt) roots and *ram1-1* roots transformed with the vectors used in the transactivation assay described in (A). Colonized roots were stained with Alexa Fluor 488 WGA. Bright field (**C**, **E**, **G**) and respective green fluorescence (**D**, **F**, **H**) images are shown. Arrowheads indicate fully developed arbuscules. Stars indicate underdeveloped arbuscules. Scale bar = 100 µm. EV, empty vector.

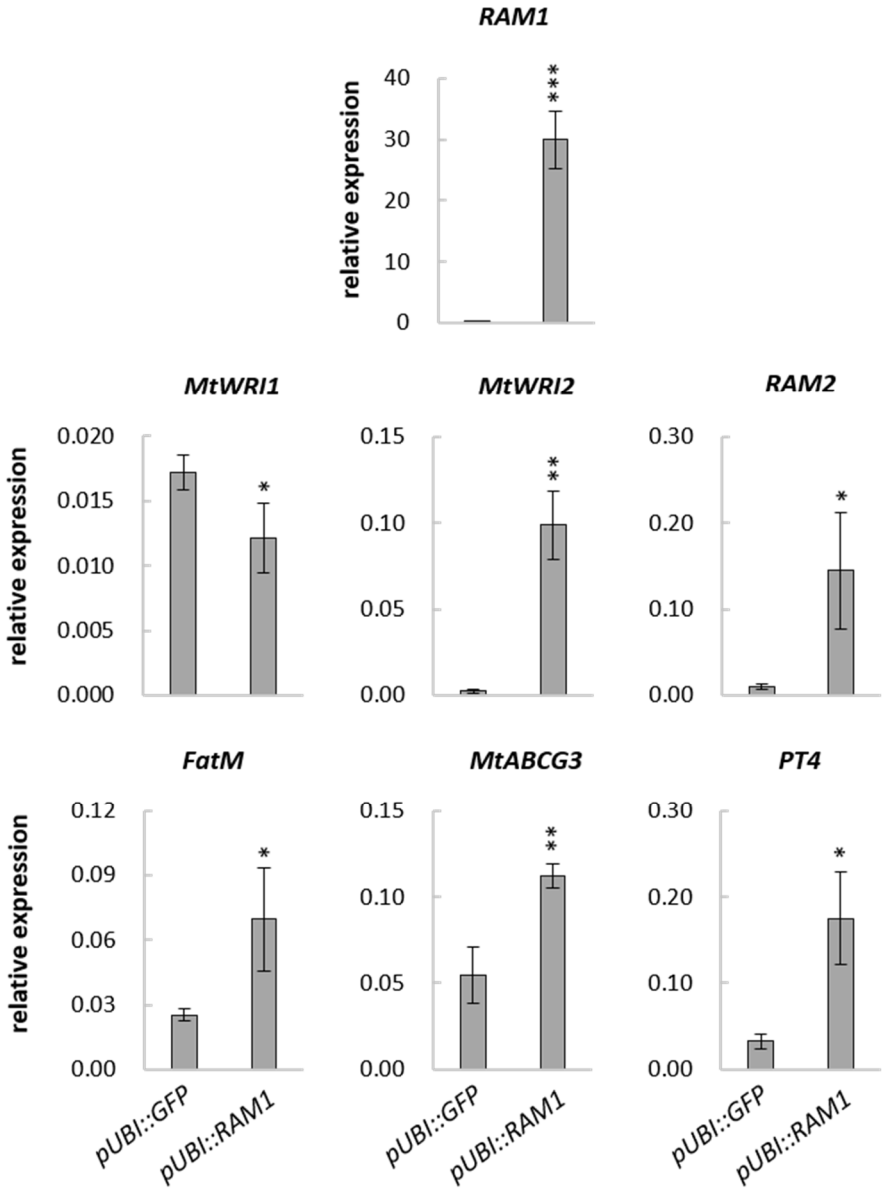

Figure 5.18: Quantification of transcript levels of putative RAM1 target genes in *M. truncatula* roots overexpressing *RAM1*. Gene expression was measured by qRT-PCR in *M. truncatula* roots overexpressing GFP (*pUBI::GFP*) or RAM1 (*pUBI::RAM1*) in the absence of mycorrhizal fungi. Expression levels of *RAM1*, *MtWRI1*, *MtWRI2*, *RAM2*, *FatM*, *MtABCG3*, and the phosphate transporter *PT4* are shown. Expression levels were normalized to *Ubiquitin* expression. Bars represent means of 3 biological replicates (each containing 5-7 root systems from individually transformed plants) ± SEM. Asterisks indicate significant differences between *GFP*-overexpressing roots and *RAM1*-overexpressing roots (Student's t-test; *, $P < 0.05$; **, $P < 0.01$; ***, $P < 0.001$).

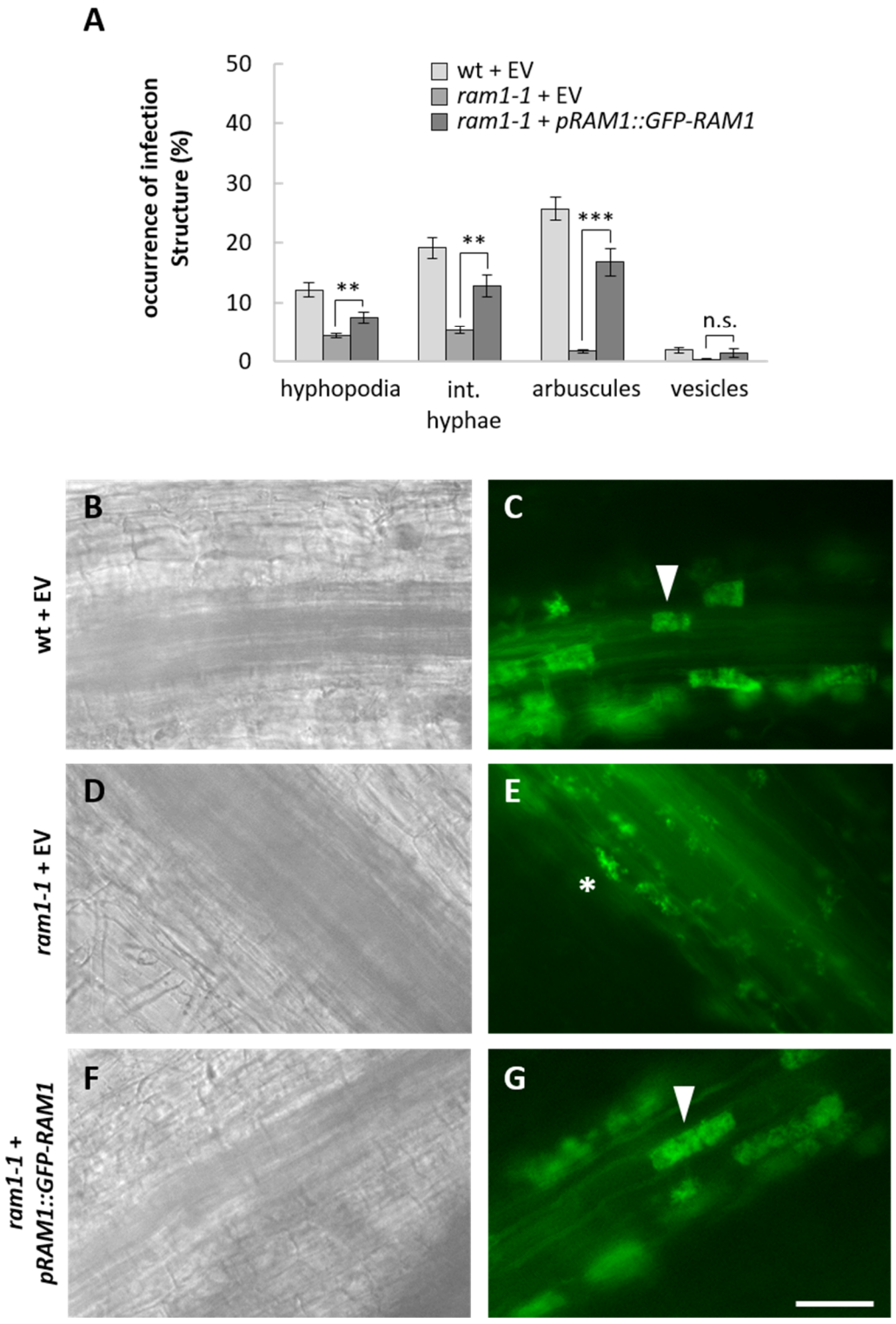

Figure 5.19: Complementation of the *ram1-1* mutant phenotype by the expression of *pRAM1::GFP-RAM1* (description continued overleaf).

(A) Quantification of mycorrhizal infection structures in wild-type (wt) roots and *ram1-1* roots transformed with an empty vector control (EV) or *pRAM1::GFP-RAM1*. The occurrence of hyphopodia, intraradical hyphae (int. hyphae), arbuscules, and vesicles in ink-stained root pieces is shown as percentage of the total number of root pieces examined. Fungal infection structures were quantified at 4 wpi. Bars represent the average of at least 10 biological replicates ± SEM. Asterisks indicate significant differences between *ram1-1* roots expressing the empty vector control and *ram1-1* roots expressing *pRAM1::GFP-RAM1* (Student's t-test; *, $P < 0.05$; **, $P < 0.01$; ***, $P < 0.001$). **(B) – (G)** Appearance of mycorrhizal structures in wild-type (wt) roots and *ram1-1* roots transformed with the empty vector control or *pRAM1::GFP-RAM1*. Colonized roots were stained with Alexa Fluor 488 WGA. Bright field (**B, D, F**) and corresponding green fluorescence (**C, E, G**) images are shown. Arrowheads indicate fully developed arbuscules. Stars indicate underdeveloped arbuscules. Scale bar = 100 µm.

CHAPTER 6

General discussion

The colonization of plant roots by arbuscular mycorrhizal fungi requires the extensive transcriptional reprogramming of host cells to ensure the proper accommodation of the fungal symbiont. Several members of the GRAS-domain protein family have emerged as important regulators of gene expression during AM development. Amongst these proteins are NSP1 and NSP2, which were originally discovered due to their critical role as transcription factors in the root-nodule symbiosis with rhizobia (Catoira et al., 2000; Wais et al., 2000; Oldroyd and Long 2003; Kaló et al., 2005; Smit et al., 2005). NSP1 and NSP2 physically interact with each other to form a transcriptionally active complex, and this interaction appears to be crucial for gene regulation and the successful establishment of the symbiosis with rhizobia (Hirsch et al., 2009; Cerri et al., 2012). Plants carrying a mutation in either *NSP1* or *NSP2* are unable to form infection threads or nodules, suggesting that both proteins are essential to regulate gene expression and act in a non-redundant way (Catoira et al., 2000; Wais et al., 2000; Oldroyd and Long 2003). Based on these observations, it has been proposed that NSP1 and NSP2 act together to regulate the same genes during the root-nodule symbiosis (Hirsch et al., 2009). The corresponding loss-of function mutants were also found to have reduced

levels of mycorrhization, suggesting that these two proteins are involved in regulating the expression of genes that are relevant for the symbiosis with AM fungi (Liu et al., 2011; Maillet et al., 2011; Delaux et al., 2013). In addition to NSP1 and NSP2, RAM1 was shown to act as a transcriptional regulator during mycorrhization (Gobbato et al., 2012; Park et al., 2015, Rich et al., 2015; Pimprikar et al., 2016). RAM1 is able to interact with NSP2, and it has been hypothesised that these two proteins form a transcription factor complex to regulate the expression of mycorrhizal genes (Gobbato et al., 2012). These findings raise the question whether NSP1, NSP2 and RAM1 have similar or different functions in the regulation of gene expression during the establishment of AM symbiosis. The phenotypic and transcriptional analyses of the corresponding loss-of-function mutants performed here indicate that these three GRAS-domain proteins play largely different roles in regulating the transcriptional reprogramming of roots during fungal colonization.

6.1 *NSP1* and *NSP2* have different roles in the regulation of gene expression during AM symbiosis

Plants carrying a mutation in *NSP1* displayed a relatively subtle mycorrhizal phenotype, with fungal colonization levels being slightly reduced in *nsp1-1* roots compared to the wild type at both early and late time points during AM symbiosis (Chapter 2). Meanwhile, no qualitative differences in the infection structures were observed, and fungal colonization inside the roots progressed normally. These results suggest that the onset of mycorrhization is delayed in *nsp1-1* roots compared to the wild type, and in line with this hypothesis, global gene expression profiling revealed a delay in the transcriptional induction of the majority of the mycorrhizal genes in *nsp1-1* (Chapter 3). At the same time, only a few genes were found to be consistently dependent on *NSP1* for their induction during mycorrhization, indicating that *NSP1* plays only a minor role in the regulation of gene expression during fungal colonization. By contrast, transcriptional profiling of *nsp1-1* roots grown in the absence of mycorrhizal fungi revealed that *NSP1* has an important role in the regulation of gene expression under non- or pre-symbiotic conditions (Chapter 3). Notably, a large number of genes involved in the biosynthesis of strigolactones were significantly downregulated, indicating that NSP1 might regulate several steps in the production of strigolactones. These findings are in line with a study demonstrating that the levels of orobanchol and didehydro-orobanchol, the two major

strigolactones present in *M. truncatula*, are almost entirely absent in *nsp1* root exudates (Liu et al., 2011). As strigolactones are known to induce spore germination and hyphal branching of mycorrhizal fungi (Akiyama et al., 2005; Besserer et al., 2006), a lack of strigolactone production in *nsp1-1* roots is a likely reason for the delay in fungal colonization and induction of mycorrhizal gene expression observed here. The finding that several genes involved in the biosynthesis of gibberellins were also differentially expressed in non-mycorrhized *nsp1-1* roots indicates that NSP1 might not only regulate strigolactone, but also gibberellin production under non-symbiotic conditions. The gene expression pattern of gibberellin biosynthesis genes in *nsp1-1* suggests that gibberellin levels are reduced in the mutant. Gibberellins appear to have both positive and negative effects on fungal colonization (Floss et al., 2013; Foo et al., 2013; Yu et al., 2014; Takeda et al., 2015), however, the role of these plant hormones at the pre-symbiotic stage of mycorrhization is currently unclear. It would be interesting to test whether the combined application of both gibberellins and strigolactones is sufficient to complement the mycorrhizal phenotype of *nsp1-1*, and would further shed light on the potential role of gibberellins at the pre-contact stage of the symbiosis. Together, the phenotypic and transcriptional analyses of *nsp1-1* suggest that *NSP1* plays a major role in the transcriptional regulation of roots under non-symbiotic conditions or at the pre-symbiotic stage of the AM symbiosis, while it appears to be less important for the control of gene expression once the fungus has entered the root.

Unlike *nsp1-1*, *nsp2-2* roots did not show any significant quantitative or qualitative differences in fungal colonization under the conditions tested here (Chapter 2). These findings are somewhat surprising, as it had previously been shown that fungal colonization is reduced in *nsp2* mutants (Maillet et al., 2011; Lauressergues et al., 2012). It is likely that the mycorrhizal phenotype of *nsp2* depends on the nutrient conditions or the strength of the fungal inoculum, as has previously been described for the *nsp1* mutant phenotype (Delaux et al., 2013). The differences in the severity of the mycorrhizal phenotypes of *nsp1-1* and *nsp2-2* observed here show that *NSP1* and *NSP2* are unlikely to fulfil identical roles in the transcriptional reprogramming of roots during AM symbiosis. Interestingly, although no significant reduction in mycorrhizal colonization was observed in *nsp2-2* roots, global gene expression profiling identified a number of genes whose induction was dependent on *NSP2* at late time points during mycorrhization, suggesting that *NSP2* might have a role at later stages of the symbiosis. However, no obvious functions of these potential target genes in AM development were identified (Chapter 3 and 4). Importantly, most of the strigolactone and gibberellin

biosynthesis genes that were found to be differentially expressed in *nsp1-1* were not affected in *nsp2-2*, suggesting that unlike *NSP1*, *NSP2* is not essential for the expression of these genes. This does not exclude the possibility that NSP2 acts together with NSP1 to regulate some of these genes. In fact, a complex of NSP1 and NSP2 did activate the expression of *D27* in a transactivation assay in *N. benthamiana* leaves, while the individual transcription factors were significantly less active (Chapter 4). However, the results of the phenotypic analyses and the global gene expression profiling strongly indicate that there is some level of redundancy for the function of *NSP2* in AM development, at least under the conditions tested here, and that other transcription factors might be able to interact with NSP1 to regulate gene expression during mycorrhization. This situation is different from the regulation of gene expression by the NSP1-NSP2 complex in the root-nodule symbiosis, where both proteins appear to be equally important for successfully entering a symbiosis with rhizobia.

6.2 Non-mycorrhizal roles of *NSP1* and *NSP2*

Despite the fact that *NSP1* and *NSP2* were discovered to have a critical function in nodulation a long time ago, little is known about the genes that are controlled by NSP1 and NSP2 during the establishment of the root-nodule symbiosis. Targeted DNA binding studies and transactivation assays have shown that the NSP1-NSP2 complex associates with and activates the promoters of the rhizobial-induced genes *NIN*, *ERN1*, and *ENOD11* (Hirsch et al., 2009; Cerri et al., 2012). However, additional target genes of NSP1 and NSP2 during nodulation are largely unknown, as no global gene expression or genome-wide DNA-binding studies have been performed so far.

The process leading to rhizobial infection and nodule formation shares many similarities with AM development, and many of the same developmental and signalling processes are required for both symbioses. It has therefore been suggested that the root-nodule symbiosis has evolved by recruiting the symbiotic programme that is required for AM development (Parniske, 2008; Oldroyd, 2013). Thus, it is conceivable that NSP1 and NSP2 regulate similar processes during both the root-nodule and the AM symbiosis. In accordance with this, research in recent years has uncovered an important role of strigolactones not only during mycorrhization, but also during nodulation. In *M. truncatula*, the external application of strigolactones was found to promote nodule formation at low concentrations, while higher concentrations appear to inhibit

nodulation (Soto et al., 2010; De Cuyper et al., 2014). Furthermore, *L. japonicus* and pea mutants deficient in strigolactones display a reduced number of nodules (Foo et al., 2011; Liu et al., 2013). Consistent with these observations, the expression levels of several genes involved in carotenoid and strigolactone biosynthesis, including *ZDS*, *Z-ISO*, *D27* and *CCD8*, were shown to increase in root hairs after inoculation with rhizobia (Breakspear et al., 2014). A recent study has demonstrated that *D27*, *CCD7* and *CCD8* are co-expressed in nodule primordia and mature nodules (van Zeijl et al., 2015). Interestingly, *D27* was further found to be induced in response to Nod factors, and this induction appears to be at least partly under the control of NSP1 and NSP2. These findings provide further insights into the role of NSP1 and NSP2 during nodulation and suggest that the regulation of *D27* by NSP1 and NSP2 has been co-opted in the root-nodule symbiosis (van Zeijl et al., 2015).

In addition to strigolactones, gibberellins are known to play an important role during the establishment of the root-nodule symbiosis. Similar to the AM symbiosis, the right level of gibberellins appears to be crucial for the proper establishment of the root-nodule symbiosis, as both insufficient and excessive gibberellin levels inhibit nodulation (Ferguson et al., 2005; Maekawa et al., 2009; Hayashi et al., 2014). In addition, several gibberellin biosynthesis genes were found to be upregulated in root hairs in response to rhizobia and Nod factors, suggesting that gibberellins might have a function in the rhizobial infection process (Breakspear et al., 2014). The global gene expression profiling performed here revealed a possible role for *NSP1* in regulating gibberellin levels through the control of gibberellin biosynthesis genes under non- or pre-symbiotic conditions (Chapter 4). It would be interesting to test whether *NSP1* has a similar function in the regulation of gibberellin biosynthesis during rhizobial infection or nodule formation. Promoter-GUS studies in the wild type and *nsp1* mutant might provide further insights into the expression pattern of gibberellin biosynthesis genes during the establishment of the root-nodule symbiosis, and would help clarify whether the expression of these genes requires *NSP1*.

The severity of the *nsp1* and *nsp2* phenotype in nodulation suggests that these two transcription factors have an essential role in the regulation of gene expression during the root-nodule symbiosis, while they appear to have less critical functions during AM symbiosis, as the mycorrhizal phenotypes of the mutants are much weaker. It is therefore likely that *NSP1* and *NSP2* have acquired additional functions in legumes to regulate gene expression during the root-nodule symbiosis. For example, NSP1 and

NSP2 are known to target *NIN*, a gene that has a specific role in nodulation, but is not involved in mycorrhization (Schauser et al., 1999; Hirsch et al., 2009). Global gene expression profiling of *nsp1* and *nsp2* roots upon rhizobial infection might identify further genes that are regulated by NSP1 and NSP2 during the root-nodule symbiosis. Intriguingly, the rice homologs of *NSP1* and *NSP2* are able to fully restore the defect in root-nodule symbiosis of the respective *L. japonicus* mutants (Yokota et al., 2010). These findings indicate that NSP1 and NSP2 are functionally conserved even in plant species that do not nodulate. It remains to be elucidated how the activity of NSP1 and NSP2 is regulated during the establishment of the root-nodule symbiosis to achieve the rhizobial-specific transcriptional reprogramming required for nodule formation.

Transcriptional profiling revealed that a large number of genes were differentially regulated in *M. truncatula nsp1-1* and *nsp2-2* under non-symbiotic conditions (Chapter 3). While some of these genes are likely to be involved in the pre-contact stage of AM symbiosis, others might function in processes unrelated to symbiosis. Interestingly, homologs of *NSP1* and *NSP2* were found in plant species that do not enter a symbiosis with mycorrhizal fungi or rhizobia, including *A. thaliana* (Delaux et al., 2013). The function of these two transcription factors in non-host species is currently unknown. It is possible that NSP1 and NSP2 have a more general role in controlling the biosynthesis of strigolactones, which are not only involved in the establishment of different symbioses, but also act as important plant hormones to regulate plant developmental processes such as shoot architecture and root development (Al-Babili and Bouwmeester, 2015). In addition, NSP1 and NSP2 might control genes involved in as yet unidentified non-symbiotic processes. The characterisation of *A. thaliana nsp1* and *nsp2* mutants would provide further insights into the non-symbiotic functions of these transcription factors.

6.3 *RAM1* regulates symbiotic processes specific to AM symbiosis

Unlike *NSP1* and *NSP2*, *RAM1* is specifically involved in mycorrhization, but does not have a role in nodulation, as it is not required for Nod factor induced gene expression and lateral root growth (Gobbato et al., 2012). Furthermore, gene expression profiling of *ram1-1* roots grown in the absence of mycorrhizal fungi only identified very few genes that were consistently differentially expressed in *ram1-1* at all three time points tested, suggesting that *RAM1* has no or only a minor role in regulating gene expression under

non-symbiotic conditions (Chapter 2). Interestingly, *RAM1* was shown to be evolutionarily conserved only in species that are able to enter a symbiosis with mycorrhizal fungi. In non-host species, such as *A. thaliana* and lupines (which do not mycorrhize, but are still able to form nodules), no *RAM1* homolog was identified, further supporting the hypothesis that *RAM1* acts specifically during AM development (Delaux et al., 2013).

Out of the three GRAS transcription factor mutants investigated here, *ram1-1* displayed the most severe defect in AM symbiosis (Chapter 2). A slightly reduced, transient fungal colonization was observed in *ram1-1* at early time points, while mycorrhizal infection structures were almost entirely absent in the mutant at late time points. Importantly, *ram1-1* appeared to be unable to form fully developed arbuscules at any of the time points tested, indicating that *RAM1* is required for normal arbuscule development. Consistent with the severe mycorrhizal phenotype, global gene expression profiling revealed that the transcriptional upregulation of a large number of mycorrhizal genes was abolished in *ram1-1* roots (Chapter 5). Among these *RAM1*-dependent genes were the phosphate transporter *PT4* and the two ammonium transporter family proteins *AMT2-3* and *AMT2-5*, suggesting that RAM1 might regulate the expression of genes involved in the nutrient uptake across the PAM. In addition, many genes involved in lipid biosynthesis and putative lipid secretion were dependent on *RAM1* for their induction during mycorrhization, including *RAM2*, *FatM*, several homologs of the *A. thaliana WRI* transcription factors, and two ABCG transporters with homology to lipid transporters in *A. thaliana*. *RAM2* has recently been found to be essential for the export of lipids to the fungus *R. irregularis*, which does not encode genes for type I fatty acid synthase and has therefore been proposed to rely on the plant as a source for lipids (Wewer et al., 2014; Peter Eastmond and Ertao Wang, personal communication). Promoter-GUS analyses showed that many of these *RAM1*-dependent lipid-related genes are co-expressed with *RAM2* in arbuscule-containing cells, suggesting that they might act in the same lipid-export pathway. The ectopic overexpression of *RAM1* in *M. truncatula* roots was sufficient to induce the expression of several of the lipid-related genes even in the absence of mycorrhizal fungi, providing further evidence that RAM1 directly or indirectly controls this putative lipid-export pathway.

Genome sequencing has so far only been completed for the mycorrhizal fungus *R. irregularis* (Tisserant et al., 2013), for which no genes encoding subunits of the type I fatty acid synthase were found (Wewer et al., 2014). This raises the question how

widespread the inability to synthesise fatty acids is among AM fungal species. In a recent study investigating the transcriptome of the mycorrhizal fungus *Gigaspora rosea,* no fungal transcripts for fatty acid synthase were found, indicating that the genes encoding this enzyme might not only be missing in *R. irregularis*, but also in *G. rosea* (Tang et al., 2016). These findings suggest that the dependence of mycorrhizal fungi on their host plant to provide lipids might be a shared characteristic of AM fungi. Studying the gene repertoire of additional AM fungal species and investigating whether lipid transfer takes place between different plants and fungal symbionts would provide further insights into the prevalence of lipid auxotrophy in mycorrhizal fungi. Notably, *RAM2, FatM,* and the *M. truncatula* homologs of the *AtWRI* transcription factors belong to a set of genes that are evolutionarily conserved in species entering a symbiosis with AM fungi (Delaux et al., 2013; Bravo et al., 2016). If all of these genes play a role in the production of lipids exported to the fungus, this would suggest that lipid transfer to the fungus could be a common feature of the AM symbiosis between many different plant and AM fungal species.

Growing *ram2* mutants together with nurse plants restores the arbuscular defect in *ram2* roots, confirming that *RAM2* has a nutritional role in AM symbiosis, rather than being directly involved in arbuscule formation (Peter Eastmond and Ertao Wang, personal communication). A similar experiment with *ram1-1* roots showed that although the extent of fungal colonization in the mutant was comparable to the wild type, arbuscule development was not rescued by the presence of nurse plants (Chapter 2). These results suggest that *RAM1* must have additional roles during AM symbiosis. Consistent with this, the expression of the exocyst subunit *EXO70I*, a gene known to be required for the development of the PAM surrounding the fine branches of arbuscules (Zhang et al., 2015), was abolished in *ram1-1* roots at all three time points during mycorrhization. Together, these findings indicate that RAM1 directly or indirectly controls key genes required for arbuscule development in addition to regulating the exchange of lipids and mineral nutrients between the plant and the fungus.

RAM1 has previously also been proposed to regulate the formation of hyphopodia at the root surface through the direct control of *RAM2*. The number of hyphopodia was shown to be strongly reduced in both the *ram1* and the *ram2* mutant, however, infection structures were only quantified at late time points during mycorrhization (Gobbato et al., 2012; Wang et al., 2012). Here, the quantification of infection structures showed that the number of hyphopodia was slightly reduced in *ram1-1* roots also at early time points

during mycorrhization, although the statistical significance varied between experiments (Chapter 2). By contrast, a recent study investigating fungal colonization in two mutant alleles of *RAM1* reported that hyphopodia formation was not impaired in these mutants (Park et al., 2015). It is therefore currently unclear whether *RAM1* has a role in the regulation of hyphopodia formation at the epidermis of the root. Transcriptional profiling did not reveal any *RAM1*-dependent genes that play an obvious role in hyphopodia formation other than *RAM2* (Chapter 5). It is possible that the expression of many early mycorrhizal genes was too diluted in whole roots to be detected by gene expression profiling performed here. A study investigating the transcriptional response to Myc-LCOs found that *RAM1* is required for the expression of the majority of the genes that are induced upon recognition of these early signalling molecules (Hohnjec et al., 2015). These results suggest that *RAM1* is involved in regulating gene expression during the early stages of the AM symbiosis, and it is possible that some of these *RAM1*-dependent genes have a function in hyphopodia formation. A role of *RAM1* in regulating the early stages of AM development would also be consistent with promoter-GUS studies showing that *RAM1* is expressed in all tissues of colonized *M. truncatula* roots, including the epidermal cell layer (Gobbato et al., 2013).

The expression of the majority of the *RAM1*-dependent genes identified here, including the genes involved in arbuscule development and the nutrient exchange between the plant and the fungus, did not appear to depend on *NSP1* or *NSP2* under non-symbiotic conditions or during mycorrhization (Chapter 4 and 5). Similarly, *RAM1* was not required for the regulation of strigolactone and gibberellin biosynthesis genes in the absence of mycorrhizal fungi. Considering that RAM1 is unable to form a complex with NSP1, at least in a heterologous system (Gobbato et al., 2012), it is not surprising that NSP1 and RAM1 have mostly specific functions during AM symbiosis. By contrast, RAM1 was found to form a complex with NSP2 (Gobbato et al., 2012). As *NSP2* was not required for the regulation of the putative RAM1 target genes identified here, the relevance of the RAM1-NSP2 transcription factor complex during AM symbiosis remains to be elucidated.

6.4 How is GRAS-domain protein activity regulated under symbiotic and non-symbiotic conditions?

The activity of GRAS-domain proteins is under the control of several regulatory mechanisms, including transcriptional and post-transcriptional regulation. Gene

expression profiling showed that *NSP1*, *NSP2* and *RAM1* are transcriptionally induced in mycorrhized roots (Chapter 3). *RAM1* in particular is strongly upregulated during AM development, and this transcriptional induction has recently been found to be mediated by a CCaMK-CYCLOPS-DELLA complex in *L. japonicus* (Pimprikar et al., 2016). The same study also found that overexpressing *RAM1* in roots treated with gibberellins restores arbuscule formation, suggesting that the main output of gibberellin signalling through the DELLAs during mycorrhization is the transcriptional regulation of *RAM1*. Similarly, the overexpression of *RAM1* in *cyclops* restores the arbuscular defect in these mutants (Pimprikar et al., 2016). It would be interesting to test whether the expression of the putative target genes of RAM1 identified here are also abolished in *cyclops* and *della* mutants and would further clarify whether the signalling through CYCLOPS and the DELLA proteins activating *RAM1* is the only pathway inducing these genes during mycorrhization.

Unlike *RAM1*, *NSP1* and *NSP2* were only weakly induced during mycorrhization (Chapter 3). Delaux and colleagues found that *NSP1* is also slightly upregulated in response to Myc factors, and this induction appears to be dependent on the common Sym pathway, as it is abolished in *ipd3* roots (Delaux et al., 2013). It is possible that IPD3 and the DELLA proteins are able to directly induce the expression of *NSP1* and *NSP2*, similar to what has been described for *RAM1*. *NSP1* and *NSP2* were further shown to be transcriptionally induced during the root-nodule symbiosis (Kaló et al., 2005; Smit et al., 2005). Interestingly, the binding of the NSP1-NSP2 complex to the promoter of *ENOD11* was found to be enhanced after treatment with Nod factors, and it has been proposed that in addition to their transcriptional regulation, NSP1 and NSP2 might also be modified at the protein level to regulate their activity in response to rhizobial signals (Hirsch et al., 2009). The nuclear-localized CCaMK is an obvious candidate for regulating the activity of NSP1 and NSP2 by post-transcriptional modifications, but until now no evidence has been reported for an interaction between CCaMK and these potential targets.

In the absence of symbiotic partners, the activity of NSP1 and NSP2 appears to be regulated differently. Unlike during mycorrhization and nodulation, the transcript levels of *NSP1* and *NSP2* do not change significantly under nutrient-limiting conditions (Liu et al., 2011). Yet, when phosphate levels are low, the expression of the strigolactone biosynthesis gene *D27* is induced in an *NSP1*- and partially *NSP2*-dependent manner. Moreover, the induction of *D27* does not require components of the common Sym pathway (Liu et al., 2011; van Zeijl et al., 2015). These observations indicate that the

activity of NSP1 and NSP2 must be regulated at the protein level through a signalling pathway other than the common Sym pathway, and the change in nutrient availability appears to play a role in this putative regulatory mechanism. Intriguingly, the overexpression of *NSP1* together with *NSP2* in tobacco leaves induces gene expression from promoters such as *ENOD11* and *D27* (Cerri et al., 2012; Chapter 4). These findings suggest that in a heterologous system, the presence of both these transcription factors is sufficient for the activation of gene expression. It has been hypothesised that in the absence of an appropriate signal, a repressor system might act in *M. truncatula* roots to inhibit the transcriptional activity or NSP1 and NSP2, possibly through the inhibition of complex formation, and this repressor system is likely to be absent in tobacco leaves (Cerri et al., 2012). Upon the perception of symbiotic signals or a change in the nutrient conditions of the plant, this putative repressor might be removed, thus allowing the induction of gene expression mediated by NSP1 and/or NSP2.

In addition to NSP1 and NSP2, many of the other GRAS-domain proteins with a role in mycorrhization were shown to physically interact with each other (described in Chapter 1.4). However, it is still an open question how important the formation of transcription factor complexes is for the transcriptional reprogramming of roots during the establishment of AM symbiosis. Interestingly, only some of the GRAS-domain proteins appear to have DNA-binding domains, including NSP1 and RAM1 (Hirsch et al., 2009; Xue et al., 2015). Others, such as RAD1 and NSP2, do not have a predicted DNA-binding domain and have therefore been proposed to rely on the interaction with other DNA-binding proteins to regulate gene expression (Hirsch et al., 2009; Xue et al., 2015). In the case of NSP1 and NSP2, the transactivation assay in *N. benthamiana* has proven to be a useful tool to investigate the activity of individual transcription factors or transcription factor complexes towards different promoters. However, unspecific activation of gene expression was observed when overexpressing *RAM1* in tobacco leaves, indicating that this assay is not suitable to test the transcriptional activity of all GRAS-domain proteins (Chapter 5). Unlike in tobacco, the ectopic overexpression of *RAM1* in *M. truncatula* roots resulted in the induction of only some, but not all tested putative target genes (Chapter 5). RAM1 was shown to interact with several other GRAS-domain proteins, including NSP2, RAD1, and DIP1 (Gobbato et al., 2012; Xue et al., 2015; Yu et al., 2015), however, it is not known whether RAM1 requires the interaction with these proteins to be able to induce gene expression. Considering that the overexpression of *RAM1* in *M. truncatula* roots appears to be sufficient to induce the expression of several of its putative targets, it seems possible that RAM1 is able to regulate gene expression without the interaction

with other GRAS-domain proteins. Alternatively, if complex formation is required, the endogenous levels of the interaction partners of RAM1 in *M. truncatula* roots might be sufficient for the formation of transcriptionally active protein complexes. Comparing the ability of RAM1 to induce gene expression in wild type and *nsp2*, *rad1*, and *dip1* mutant backgrounds might clarify whether RAM1 acts alone or as part of a transcription factor complex. It is also possible that the combined expression of several of these interaction partners results in the induction of additional genes that would not be observed by expressing just one GRAS-domain protein.

All the interactions between the GRAS-domain proteins described in previous studies were tested in heterologous systems such as *N. benthamiana* leaves or yeast. It is therefore important to validate these findings in *M. truncatula* roots, ideally under both symbiotic and non-symbiotic conditions. *M. truncatula* lines stably expressing GFP-tagged NSP1, NSP2, and RAM1 provide a valuable resource to investigate complex formation of these proteins in relevant conditions by performing co-immunoprecipitation assays. These experiments might also clarify whether different transcription factor complexes are formed during nodulation or mycorrhization and under non-symbiotic conditions.

6.5 Conclusions

The work presented here has begun to address the question how GRAS-domain proteins regulate the extensive transcriptional reprogramming of roots during the colonization by AM fungi. The functions of *NSP1*, *NSP2* and *RAM1* in this process were investigated by performing detailed phenotypic and transcriptional analyses of the corresponding loss-of-function mutants. The results of these analyses suggest that all three transcription factors have largely different roles in the regulation of gene expression during mycorrhization. While *NSP1* is required for the expression of strigolactone and gibberellin biosynthesis genes at the pre-symbiotic stages of the symbiosis, *RAM1* plays an important role in regulating genes involved in arbuscule development and the nutrient exchange between the plant and the fungus. Meanwhile, the exact function of *NSP2* remains unclear, and different growth conditions might be required to unravel the role of this transcription factor in AM symbiosis. NSP1, NSP2 and RAM1 represent only a subset of transcription factors that are involved in the transcriptional reprogramming of roots during mycorrhization. Research in recent years has identified a large number

of additional GRAS-domain proteins that appear to be required for AM development. The direct target genes of these transcription factors are largely unknown. The approach taken here has proven useful to disentangle the functions of different transcriptional regulators and could similarly be used to investigate the roles of these additional GRAS-domain proteins during mycorrhization. Global DNA-binding studies would complement transcriptional approaches by providing insights into the genes that are directly bound by these transcription factors. Interaction studies further suggest that many GRAS-domain proteins act as multicomponent complexes. Future investigations will shed light on the importance of this complex formation during AM symbiosis and will provide insights into how various mycorrhizal processes are regulated by this gene regulatory network.

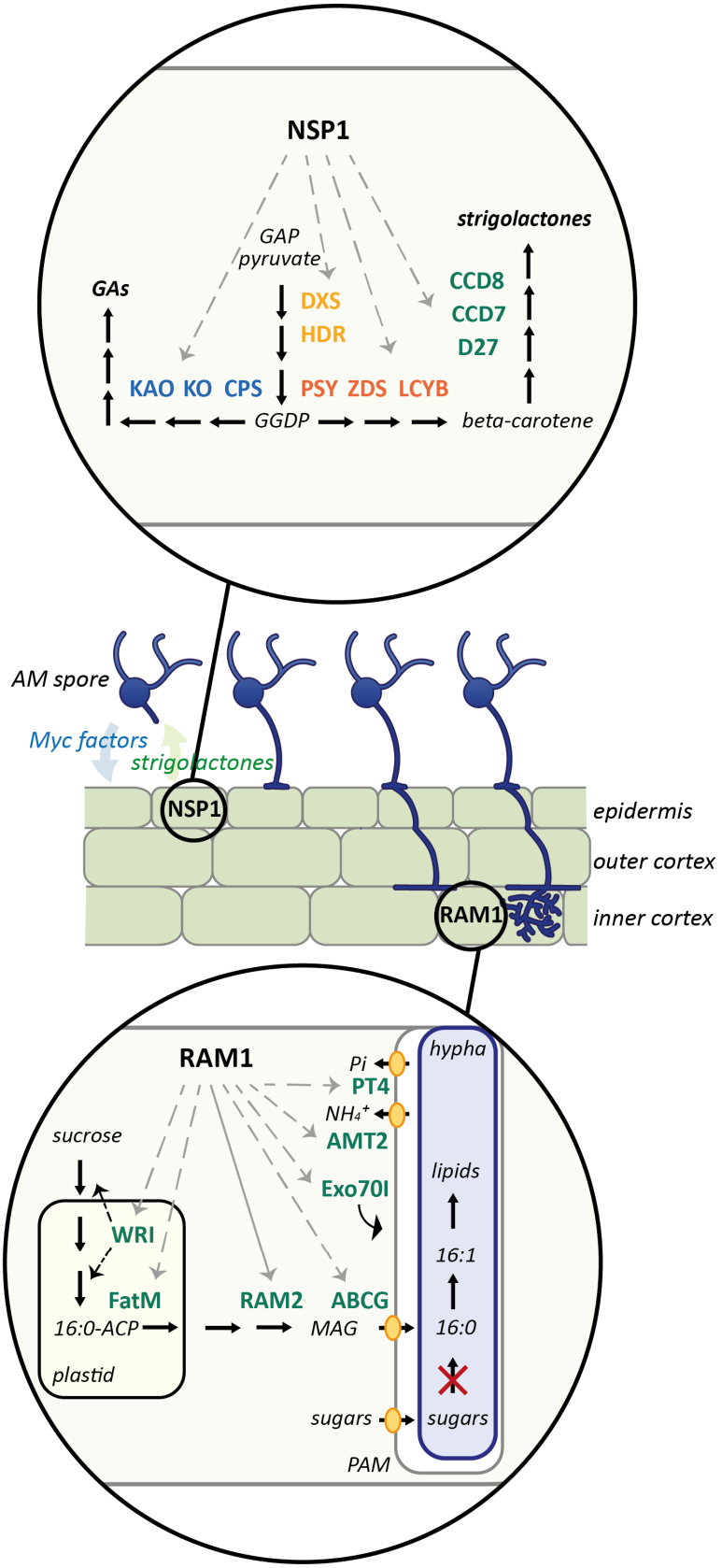

Figure 6.1: Proposed target genes of NSP1 and RAM1 at pre-symbiotic stages and during the colonization of plant roots by mycorrhizal fungi (description continued overleaf).

NSP1 is required for the expression of a large number of genes involved in isoprenoid (indicated in yellow), carotenoid (indicated in orange), strigolactone (indicated in green), and gibberellin biosynthesis (GAs; indicated in blue) at the pre-symbiotic stage of AM symbiosis. During mycorrhization, *RAM1* is required for the induction of genes involved in lipid biosynthesis and putative lipid secretion (including homologs of the *AtWRI* transcription factors, *FatM*, *RAM2*, and the two ABCG transporters *MtABCG3* and *MtABCG4*), mineral nutrient transport across the PAM (including *PT4* and the two AMT2 family genes *AMT2-3* and *AMT2-5*), and arbuscule development (including *EXO70I*). GAP, glyceraldehyde-3-phosphate, GGDP, geranylgeranyl pyrophosphate, ACP, acyl carrier protein, MAG, monoacylglycerol.

CHAPTER 7

Material and methods

7.1 Plant material and growth conditions

M. truncatula cultivar Jemalong A17 and R108 were used as wild type. All mutant lines used in this study are derived from one of these two genetic backgrounds (Table 7.1). *M. truncatula* seeds were scarified with sandpaper and surface-sterilised in 10% sodium hypochlorite solution for 3 min. Seeds were washed 5 times with sterile water and imbibed in water for at least 2 hours before plating on water agar (DWA; Table 7.2). After stratification at 4°C for 5 days in the dark, seeds were germinated overnight at room temperature.

For seed bulking, germinated seedlings were transferred to pods containing John Innes cereal mix (Table 7.2) and grown to maturity in glasshouses, where additional light and heat was provided during winter. For hairy root transformations, plants were grown on plates containing modified Fahraeus plant agar medium (modFP agar; Table 7.2) in a controlled environment room (23°C, 16-hour photoperiod, with 32% relative humidity and 300 µmol m^{-2} s^{-1} light intensity). For mycorrhization and nodulation assays, germinated seedlings were first grown on modFP agar plates as described above. After

10 days, plants were transferred to pods containing a 1:1 mix of terragreen and sand, inoculated with fungal or rhizobial inoculum (Section 7.6), and grown in a controlled environment room (23°C, 16-hour photoperiod, 300 µmol m^{-2} s^{-1}). Transparent plastic lids were used to cover the plants for 3 days after transferring them to soil or terragreen and sand.

Table 7.1: *M. truncatula* mutant lines.

Mutant	Background	Description	Reference
nsp1-1 (B85)	A17	Ethyl methane sulphonate induced point mutation (C718T) leads to a premature stop codon and truncated protein (NSP1 1-239)	Smit et al., 2005
nsp2-2 (0-4)	A17	Fast neutron induced 435 bp deletion at position 480 leads to the removal of 145 amino acids (NSP2 Δ161-305)	Kaló et al., 2005
ram1-1 (C1)	A17	Fast neutron induced 71 kb deletion leads to the removal of 9 predicted genes including *RAM1*	Gobbato et al., 2012
NF20376	R108	TNT1-insertion line with an insertion in the third exon of *MtABCG3*	Samuel Roberts Noble Foundation
NF11484	R108	TNT1-insertion line with an insertion in the fourth exon of *MtABCG3*	Samuel Roberts Noble Foundation
NF1558	R108	TNT1-insertion line with an insertion in the eighth exon of *MtABCG3*	Samuel Roberts Noble Foundation

7.2 Media and antibiotics

The composition of media and soils used for bacterial and plant growth are described in Table 7.2. Where required, antibiotics were added to the media for growth selection of bacteria (Table 7.3).

Table 7.2: List of media and soil for bacterial and plant growth.

Medium	Composition
Lysogeny broth-Lennox (L)	Tryptone 10 g, yeast extract 5 g, NaCl 5 g, D-Glucose 1 g. For solid medium 10 g Lab M No.1 agar were added.
Luria-Bertani (LB)	L medium lacking D-Glucose.
Super orbital broth (SOC)	Tryptone 20 g, yeast extract 5 g, NaCl 0.58 g, KCl 0.19 g, $MgCl_2$ 2.03 g, $MgSO_4(7H_2O)$ 2.46 g, Glucose 3.6 g.
Rhizobium complete medium (TY)	Tryptone 5 g, yeast extract 3 g, $CaCl_2(6H_2O)$ 1.32 g. For solid medium 10 g Lab M No.1 agar was added.
Water agar (DWA)	Bacto agar 15 g.
Modified FP (modFP)	$CaCl_2(2H_2O)$ 0.1 g, $MgSO_4$ 0.12 g, $KHPO_4$ 0.01 g, $Na_2HPO_4(12H_2O)$ 0.150 g, ferric citrate 5 mg, H3BO3 2.86 g, $MnSO_4$ 2.03 g, $ZnSO_4$(7H2O) 0.22 g, $CuSO_4(5H_2O)$ 0.08 g, $H_2MoO_4(4H_2O)$ 0.08 g, NH_4NO_3 0.5 mM, Formedium agar 8 g, pH 6.0.
Buffered nodulation medium (BNM)	MES (2-(N-morpholino) ethanesulfonic acid) buffer 390 mg, $CaSO_4(2H_2O)$ 344 mg, KH_2PO_4 0.125 g, $MgSO_4(7H_2O)$ 122 mg, Na_2EDTA 18.65 mg, $FeSO_4(7H_2O)$ 13.9 mg, $ZnSO_4(7H_2O)$ 4.6 mg, H_3BO_3 3.1 mg, $MnSO_4(H_2O)$ 8.45 mg, $Na_2MoO_4(2H_2O)$ 0.25 mg, $CuSO_4(5H_2O)$ 0.016 mg, $CoCl_2(6H_2O)$ 0.025 mg, pH 6.0. For solid medium 11.5 g Formedium agar was added.
Terragreen and sand mix	1:1 mix of terragreen (Oil-dry UK ltd) and sharp sand (BB Minerals).
John Innes Cereal mix	Medium grade peat 40 %, sterilised soil 40 %, horticultural grit 20%, PG mix 14-16-18 + Te base fertiliser 1.3 kg m^{-3}, Osmocote, Mini 16-8-11 2 mg + Te 0.02 % B 1 kg m^{-3}, wetting agent, Maglime 3 kg m^{-3}, Exemptor 300 g m^{-3}.

Table 7.3: List of antibiotics for growth selection of bacteria.

Antibiotic	Solvent	Final concentration (µg/ml)
Carbenicillin	dH_2O	100
Gentamycin	dH_2O	40
Kanamycin	dH_2O	25
Rifampicin	methanol	50
Spectinomycin	dH_2O	100

7.3 Genotyping of *M. truncatula* TNT1-insertion lines

For genomic DNA extractions, *M. truncatula* trifoliate leaves were harvested and frozen at -20°C. DNA extractions were performed by Richard Goram (John Innes Centre) using the DNeasy Plant kit (Qiagen) according to the manufacturer's instructions. For genotyping, two PCRs were set up with primers spanning the wild type gene or one end of the TNT1 insertion and one end of the mutated gene. Primers used for genotyping are listed in Table 7.4. A 50 µl PCR mix was set up containing 0.5 µl Taq polymerase (Invitrogen), 5 µl 10 x buffer, 1 µl dNTP mix, 1.5 µl $MgCl_2$, 1 µl forward primer (10 µM,) 1 µl reverse primer (10 µM), 2 µl genomic DNA, and 38 µl water. Cycling conditions for DNA amplification were as follows: 94 °C for 3 min followed by 30 cycles at 94°C for 30 s, 56 °C for 30 s and 72 °C for 1 min, with a final extension step of 10 min at 72 °C. The PCR product was run by TRIS/acetic acid/EDTA gel electrophoresis on a 1 % (w/v) agarose gel and stained for 20 min in a 1 µg/ml ethidium bromide solution.

Table 7.4: Primer sequences used for genotyping of *M. truncatula* TNT1-insertion lines.

Name	Primer sequence
TNT1 fwd	TCCTTGTTGGATTGGTAGCC
TNT1 rev	CAGTGAACGAGCAGAACCTGTG
NF20376 fwd	GGGCTATGTAACACAAGACG
NF20376 rev	CTGAATAGATGCCGAACCAC
NF11484 fwd	TCCTAGGAACTCGAAGGT
NF11484 rev	CTTCTTCTGTGGTTACTCCC
NF1558 fwd	GTGGTTCGGCATCTATTCAG
NF1558 rev	CAACTTCTCCTTGCTCTTGG

7.4 Molecular cloning

7.4.1 Golden Gate cloning

All vectors used in this study were cloned using the Golden Gate cloning technique (Engler et al., 2009; Weber et al., 2011). To design level 0 modules, DNA sequences for the promoter, coding, and terminator regions were retrieved from the Phytozome database (Mtv4.0). DNA components were synthesised by GeneArt (Life Technologies). To generate level 1 vectors, a 15 µl reaction mix was set up containing 100 ng of each

level 0 plasmid, 100 ng backbone plasmid, 0.15 µl 100 x BSA, 1.5 µl 10 x T4 buffer, 1 µl BsaI (New England Biolabs), 1 µl T4 DNA ligase (New England Biolabs) and water. Cycling conditions for digestion and ligation of the DNA components were as follows: 25 cycles of 3 min at 37°C and 4 min at 16°C, followed by 5 min at 50°C and 5 min at 80°C. To generate level 2 vectors, a 15 µl reaction mix was set up containing 100 ng of each level 1 plasmid, 100 ng of the backbone plasmid pICH50505 (Icon-Genetics), 0.15 µl 100 x BSA, 1 µl BpiI (Thermo Fisher Scientific), 1.5 µl 10 x T4 buffer, 1 µl T4 DNA ligase (New England Biolabs) and water. The same cycling conditions as for level 1 reactions were used for digestion and ligation of the DNA components. Level 2 vectors used in this study are listed in Table 7.5.

7.4.2 Transformation of *Escherichia coli* for plasmid amplification

Chemically competent *E. coli* strains DH5α and DH10β (Invitrogen) were used for the cloning of Golden Gate level 1 and level 2 vectors, respectively. To transform bacterial cells, 1 µl of the Golden Gate reaction mix was added to 20 µl of chemically competent cells and incubated on ice for 10 min. Cells were heat-shocked at 42°C for 30 s and incubated on ice for 2 min prior to adding 500 µl SOC medium (Table 7.2). Bacteria were incubated at 37°C for 1 h with agitation at 220 rpm. Cells were streaked out on L plates (Table 7.2) containing the appropriate antibiotics and grown at 37°C overnight. Positive clones were checked for the presence of the target construct using colony PCR. A PCR mix was set up containing 5 µl GoTaq G2 Green polymerase (Promega), 1 µl forward primer (20 µM,) 1 µl reverse primer (20 µM), and 3 µl water. Bacterial cells from a single colony were transferred to the PCR mix using a pipette tip. The following cycling conditions were used for DNA amplification: 98 °C for 10 min followed by 30 cycles at 98°C for 10 s, 52 °C for 20 s and 72 °C for 2 min, with a final extension step of 5 min at 72 °C. The PCR product was run by TRIS/acetic acid/EDTA gel electrophoresis on a 1 % (w/v) agarose gel and stained for 20 min in a 1 µg/ml ethidium bromide solution. To obtain plasmid from transformed *E. coli*, bacterial cells from a single positive colony were grown in 10 ml of liquid L medium (Table 7.2) at 37°C overnight with agitation at 220 rpm. Plasmids were extracted using the QIAprep Spin Miniprep Kit (Qiagen) according to the manufacturer's instructions. To ensure that the cloning reactions resulted in the correct assembly of level 0 and level 1 sequences, plasmids were sent for sequencing to Eurofins Genomics (Germany).

Table 7.5: Design of Golden Gate level 2 binary expression vectors.

Number	Position 1	Position 2	Position 3	Position 4	Position 5	Position 6
Constructs for transactivation assays						
EC10101	EC10156 pL1M-R1-pNOS-GUS-tNOS	EC10132 pL1M-R2-pMNR-LUC-tAct	EC15034 pL1M-R3-pAtUBI10-dsRed-tNOS	EC10155 pL1M-R4-p35S-P19-t35S	-	-
EC10102	EC10156 pL1M-R1-pNOS-GUS-tNOS	EC10096 pL1M-R2-pNIN-LUC-tAct	EC15034 pL1M-R3-pAtUBI10-dsRed-tNOS	EC10155 pL1M-R4-p35S-P19-t35S	-	-
EC10107	EC10156 pL1M-R1-pNOS-GUS-tNOS	EC10148 pL1M-R2-pENOD11-LUC-tAct	EC15034 pL1M-R3-pAtUBI10-dsRed-tNOS	EC10155 pL1M-R4-p35S-P19-t35S	-	-
EC10502	EC10156 pL1M-R1-pNOS-GUS-tNOS	EC10493 pL1M-R2-pMtWUS-LUC-tAct	EC15034 pL1M-R3-pAtUBI10-dsRed-tNOS	EC10155 pL1M-R4-p35S-P19-t35S	-	-
EC10503	EC10156 pL1M-R1-pNOS-GUS-tNOS	EC10494 pL1M-R2-pAtPLT1-LUC-tAct	EC15034 pL1M-R3-pAtUBI10-dsRed-tNOS	EC10155 pL1M-R4-p35S-P19-t35S	-	-
EC10505	EC10156 pL1M-R1-pNOS-GUS-tNOS	EC10496 pL1M-R2-palcA-LUC-tAct	EC15034 pL1M-R3-pAtUBI10-dsRed-tNOS	EC10155 pL1M-R4-p35S-P19-t35S	-	-
EC10506	EC10156 pL1M-R1-pNOS-GUS-tNOS	EC10497 pL1M-R2-pOP6-LUC-tAct	EC15034 pL1M-R3-pAtUBI10-dsRed-tNOS	EC10155 pL1M-R4-p35S-P19-t35S	-	-
EC10508	EC10156 pL1M-R1-pNOS-GUS-tNOS	EC10499 pL1M-R2-pNPL-LUC-tAct	EC15034 pL1M-R3-pAtUBI10-dsRed-tNOS	EC10155 pL1M-R4-p35S-P19-t35S	-	-
EC20706	EC10156 pL1M-R1-pNOS-GUS-tNOS	EC20677 pL1M-R2-pD27short-LUC-tAct	EC15034 pL1M-R3-pAtUBI10-dsRed-tNOS	EC10155 pL1M-R4-p35S-P19-t35S	-	-
EC20969	EC10156 pL1M-R1-pNOS-GUS-tNOS	EC20968 pL1M-R2-pD27long-LUC-tAct	EC15034 pL1M-R3-pAtUBI10-dsRed-tNOS	EC10155 pL1M-R4-p35S-P19-t35S	-	-
EC20970	EC10156 pL1M-R1-pNOS-GUS-tNOS	EC20967 pL1M-R2-pRAM2-LUC-tAct	EC15034 pL1M-R3-pAtUBI10-dsRed-tNOS	EC10155 pL1M-R4-p35S-P19-t35S	-	-
EC20971	EC10156 pL1M-R1-pNOS-GUS-tNOS	EC20677 pL1M-R2-pD27short-LUC-tAct	EC15034 pL1M-R3-pAtUBI10-dsRed-tNOS	EC10155 pL1M-R4-p35S-P19-t35S	EC10150 pL1M-R5-pUBI-3xHA-NSP1-tOcs	-
EC20972	EC10156 pL1M-R1-pNOS-GUS-tNOS	EC20677 pL1M-R2-pD27short-LUC-tAct	EC15034 pL1M-R3-pAtUBI10-dsRed-tNOS	EC10155 pL1M-R4-p35S-P19-t35S	EC10141 pL1M-R5-pUBI-3xHA-NSP2-tOcs	-
EC20973	EC10156 pL1M-R1-pNOS-GUS-tNOS	EC20677 pL1M-R2-pD27short-LUC-tAct	EC15034 pL1M-R3-pAtUBI10-dsRed-tNOS	EC10155 pL1M-R4-p35S-P19-t35S	EC10150 pL1M-R5-pUBI-3xHA-NSP1-tOcs	EC10151 pL1M-R6-pUBI-3xHA-NSP2-tOcs

continued overleaf

Table 7.5: continued.

Number	Position 1	Position 2	Position 3	Position 4	Position 5	Position 6
EC20978	EC10156 pL1M-R1-pNOS-GUS-tNOS	EC20968 pL1M-R2 -pD27long-LUC-tAct	EC15034 pL1M-R3-pAtUBI10-dsRed-tNOS	EC10155 pL1M-R4-p35S-P19-t35S	EC10150 pL1M-R5-pUBI-3xHA-NSP1-tOcs	-
EC20979	EC10156 pL1M-R1-pNOS-GUS-tNOS	EC20968 pL1M-R2-pD27long-LUC-tAct	EC15034 pL1M-R3-pAtUBI10-dsRed-tNOS	EC10155 pL1M-R4-p35S-P19-t35S	EC10141 pL1M-R5-pUBI-3xHA-NSP2-tOcs	-
EC20980	EC10156 pL1M-R1-pNOS-GUS-tNOS	EC20968 pL1M-R2-pD27long-LUC-tAct	EC15034 pL1M-R3-pAtUBI10-dsRed-tNOS	EC10155 pL1M-R4-p35S-P19-t35S	EC10150 pL1M-R5-pUBI-3xHA-NSP1-tOcs	EC10151 pL1M-R6-pUBI-3xHA-NSP2-tOcs
EC10121	EC10156 pL1M-R1-pNOS-GUS-tNOS	EC10148 pL1M-R2-pENOD11-LUC-tAct	EC15034 pL1M-R3-pAtUBI10-dsRed-tNOS	EC10155 pL1M-R4-p35S-P19-t35S	EC10150 pL1M-R5-pUBI-3xHA-NSP1-tOcs	-
EC10122	EC10156 pL1M-R1-pNOS-GUS-tNOS	EC10148 pL1M-R2-pENOD11-LUC-tAct	EC15034 pL1M-R3-pAtUBI10-dsRed-tNOS	EC10155 pL1M-R4-p35S-P19-t35S	EC10141pL1M-R5 -pUBI-3xHA-NSP2-tOcs	-
EC10123	EC10156 pL1M-R1-pNOS-GUS-tNOS	EC10148 pL1M-R2-pENOD11-LUC-tAct	EC15034 pL1M-R3-pAtUBI10-dsRed-tNOS	EC10155 pL1M-R4-p35S-P19-t35S	EC10150 pL1M-R5-pUBI-3xHA-NSP1-tOcs	EC10151 pL1M-R6-pUBI-3xHA-NSP2-tOcs
EC20981	EC10156 pL1M-R1-pNOS-GUS-tNOS	EC20967 pL1M-R2-pRAM2-LUC-tAct	EC15034 pL1M-R3-pAtUBI10-dsRed-tNOS	EC10155 pL1M-R4-p35S-P19-t35S	EC10466 pL1M-R5 -pUBI-3xHA-RAM1-tOcs	-
EC10469	EC10156 pL1M-R1-pNOS-GUS-tNOS	EC10132 pL1M-R2-pMNR-LUC-tAct	EC15034 pL1M-R3-pAtUBI10-dsRed-tNOS	EC10155 pL1M-R4-p35S-P19-t35S	EC10466 pL1M-R5-pUBI-3xHA-RAM1-tOcs	-
EC10448	EC10156 pL1M-R1-pNOS-GUS-tNOS	EC10096 pL1M-R2-pNIN-LUC-tAct	EC15034 pL1M-R3 -pAtUBI10-dsRed-tNOS	EC10155 pL1M-R4-p35S-P19-t35S	EC10466 pL1M-R5-pUBI-3xHA-RAM1-tOcs	-
EC10511	EC10156 pL1M-R1-pNOS-GUS-tNOS	EC10493 pL1M-R2-pMtWUS-LUC-tAct	EC15034 pL1M-R3-pAtUBI10-dsRed-tNOS	EC10155 pL1M-R4-p35S-P19-t35S	EC10466 pL1M-R5-pUBI-3xHA-RAM1-tOcs	-
EC10512	EC10156 pL1M-R1-pNOS-GUS-tNOS	EC10494 pL1M-R2-pAtPLT1-LUC-tAct	EC15034 pL1M-R3-pAtUBI10-dsRed-tNOS	EC10155 pL1M-R4-p35S-P19-t35S	EC10466 pL1M-R5-pUBI-3xHA-RAM1-tOcs	-
EC10514	EC10156 pL1M-R1-pNOS-GUS-tNOS	EC10496 pL1M-R2-palcA-LUC-tAct	EC15034 pL1M-R3-pAtUBI10-dsRed-tNOS	EC10155 pL1M-R4-p35S-P19-t35S	EC10466 pL1M-R5-pUBI-3xHA-RAM1-tOcs	-
EC10515	EC10156 pL1M-R1-pNOS-GUS-tNOS	EC10497 pL1M-R2-pOP6-LUC-tAct	EC15034 pL1M-R3-pAtUBI10-dsRed-tNOS	EC10155 pL1M-R4-p35S-P19-t35S	EC10466 pL1M-R5-pUBI-3xHA-RAM1-tOcs	-
EC10517	EC10156 pL1M-R1-pNOS-GUS-tNOS	EC10499 pL1M-R2-pNPL-LUC-tAct	EC15034 pL1M-R3-pAtUBI10-dsRed-tNOS	EC10155 pL1M-R4-p35S-P19-t35S	EC10466 pL1M-R5-pUBI-3xHA-RAM1-tOcs	-

continued overleaf

Table 7.5: continued.

Number	Position 1	Position 2	Position 3	Position 4	Position 5	Position 6
Constructs for transcription factor overexpression in M. truncatula						
EC20678	pL1M-R1-pAtUBI10-dsRed-tNOS	EC20631 pL1M-R2-pLjUBI-RAM1-tOcs1	-	-	-	-
EC20681	pL1M-R1-pAtUBI10-dsRed-tNOS	EC15489 pL1M-R2-pLjUBI-GFP-tOcs1	-	-	-	-
Constructs for promoter-GUS in M. truncatula						
EC20945	EC21950 pL1M-R1-pAtUBI10-dsRed-tNOS	EC20649 pL1M-R2-pMtWRI1-GUS-tMtWRI1	-	-	-	-
EC20946	EC21950 pL1M-R1-pAtUBI10-dsRed-tNOS	EC20650 pL1M-R2-pMtWRI2-GUS-tMtWRI2	-	-	-	-
EC20947	EC21950 pL1M-R1-pAtUBI10-dsRed-tNOS	EC20651 pL1M-R2-pMtWRI3-GUS-tMtWRI3	-	-	-	-
EC20948	EC21950 pL1M-R1-pAtUBI10-dsRed-tNOS	EC20652 pL1M-R2-pMtWRI4-GUS-tMtWRI4	-	-	-	-
EC20952	EC21950 pL1M-R1-pAtUBI10-dsRed-tNOS	EC20656 pL1M-R2-pMtABCG3-GUS-tMtABCG3	-	-	-	-
EC20953	EC21950 pL1M-R1-pAtUBI10-dsRed-tNOS	EC20657 pL1M-R2-pMtFatM-GUS-tMtFatM	-	-	-	-
EC20954	EC21950 pL1M-R1-pAtUBI10-dsRed-tNOS	EC20658 pL1M-R2-pMtRAM2-GUS-tMtRAM2	-	-	-	-
Constructs for stable transformation of M. truncatula						
EC15474	EC15324 pL1M-R1-pNOS-BAR-tNOS-15324	EC15483 pL1M-R2-pMtRAM1::3xHA-GFP-MtRAM1-t35S	-	-	-	-
EC10538	EC15324 pL1M-R1-pNOS-BAR-tNOS-15324	EC10540 pL1M-R2-pLjUBI::NSP2-GFP-3xFLAG-t35S	-	-	-	-
EC10686	EC15324 pL1M-R1-pNOS-BAR-tNOS-15324	pMtNSP1-GFP-MtNSP1(cDNA)-t35s	-	-	-	-

7.4.3 Transformation of *A. tumefaciens* and *A. rhizogenes* for plant transformation

Electro-competent *A. tumefaciens* strains GV3101 and AGL1 (for transformation of *N. benthamiana* and stable transformation of *M. truncatula*, respectively) and *A. rhizogenes* strain AR1193 (for hairy root transformation of *M. truncatula*) were transformed with Golden Gate level 2 vectors by mixing 100 ng of the plasmid with 20 µl of electro-competent cells and incubating on ice for 10 min. Bacteria were transferred to an electroporation cuvette (Geneflow) and subjected to an electroshock (125 volts, 25 µ farad, 200 ohms; Gene-Pulser (BioRad)) prior to adding 500 µl SOC medium (Table 7.2). Bacteria were incubated at 28°C for 2 h with agitation at 220 rpm. Cells were streaked out on LB plates (Table 7.2) containing the appropriate antibiotics and grown at 28°C for 2-3 days. Positive clones were checked for the presence of the target construct using colony PCR and gel electrophoresis as described in Section 7.4.2.

7.5 Hairy root transformation of *M. truncatula*

M. truncatula seeds were sterilised and germinated overnight as described in Section 7.1. Roots were transformed by cutting off the tip of the radicles and dipping the ends of each cut radicle into a large drop of a cell suspension of *A. rhizogenes* AR1193 carrying the appropriate Golden Gate level 2 vector. To prepare *A. rhizogenes* cell suspension for dipping, bacterial cells were grown in liquid LB medium (Table 7.2) with antibiotics for 2 days, spun down by centrifugation for 10 min at 4000 rpm and resuspended in fresh LB medium without antibiotics. After dipping the radicles into *A. rhizogenes*, seedlings were placed onto modFP plates (Table 7.2), sealed with 3M Micropore tape (Miller Medical Supplies) and placed upright in a controlled environment room as described in Section 7.1. Four weeks after transformation, plants were screened for transformed roots using a DMR/MZFLIII microscope (Leica) to visualise the transformation marker dsRed. Plants with transformed roots were used for mycorrhization or nodulation assays, gene expression analyses, or for transactivation assays.

7.6 Stable transformation of *M. truncatula*

Stable transformation of *M. truncatula* was performed by Matthew Smoker (The Sainsbury Laboratory, Norwich). *A. tumefaciens* strain AGL1 transformed with the appropriate Golden Gate level 2 binary expression vectors (Table 7.5) were used to transform *nsp1-1*, *nsp2-2*, or *ram1-1* leaf tissue. For selection of transformed tissue, the herbicide BASTA was used. Regenerated transformed plants were transferred to soil for the production of T1 seeds. T1 plants were tested for their ability to form nodules (for GFP-NSP1 and NSP2-GFP expressing plants) or fully developed arbuscules (for GFP-RAM1 expressing plants). Plants that were able to enter a fully functional symbiosis were bulked to produce T2 seeds.

7.7 Mycorrhization assays

7.7.1 Inoculation of *M. truncatula* with mycorrhizal fungi

To assess the mycorrhizal phenotype of *M. truncatula* mutant lines, seeds were sterilised and germinated as described in Section 7.1. Germinated seedlings were placed on filter paper on modFP plates (Table 7.2) and grown for 10 days in a controlled environment room (described in Section 7.1). Plants were transferred to a 1:1 terragreen and sand mix (Table 7.2) containing 7% (v/v) of commercial mycorrhizal inoculum and grown in a controlled environment room as described in Section 7.1. For RNA-sequencing and phenotyping of A17, *nsp1-1*, *nsp2-2* and *ram1-1*, the mycorrhizal inoculum Solrize Pro (Agrauxine, France) was used, which contains a mixture of *R. irregularis* and *Glomus mosseae* spores and hyphae. For mycorrhizal phenotyping of R108 and TNT1-insertion lines, the mycorrhizal inoculum P-3201 (Premier Tech, Canada) was used, which contains spores from *R. irregularis*. For complementation assays and growth of *M. truncatula* with nurse plants, plants were transferred to a 1:1 terragreen and sand mix containing 20% (v/v) of chive inoculum (mycorrhized chive roots mixed with terragreen and sand).

7.7.2 Ink staining and quantification of fungal infection structures

To quantify mycorrhization, fungal infection structures were visualised by ink staining. Roots were washed in water and pre-cleared by incubation in 10% (w/v) KOH at 95°C

for 18 min. Roots were rinsed 3 times with distilled water and stained with a solution containing 5% ink and 5% acetic acid at 95°C for 6 min. Roots were de-stained in water for 1 day. Mycorrhizal infection structures (hyphopodia, intraradical hyphae, arbuscules and vesicles) were quantified using the gridline intersect method (Giovannetti and Mosse, 1980). Fungal colonization was visualised using a DM 6000 microscope (Leica) and a DFC420 colour camera (Leica).

7.7.3 Wheat Germ Agglutinin (WGA) staining

To assess the appearance of fungal infection structures, roots were stained with Alexa Fluor 488 WGA. Roots were incubated in 20% (w/v) KOH at room temperature for 2 days before rinsing with distilled water and incubating in 0.1M HCl for 2 h. Subsequently, roots were rinsed once with distilled water and once with 1x phosphate buffered saline (PBS; 137 mM NaCl, 2.7 mM KCl, 10 mM Na_2HPO_4, 1.8 mM KH_2PO_4). Pre-cleared roots were stained with WGA by incubation in a 1x PBS solution containing 0.2 µg/ml Alexa Fluor 488 WGA (Sigma) in the dark at 4°C for 1-2 days. Green fluorescence was visualised using a DM 6000 microscope (Leica) and a DFC420 colour camera (Leica).

7.8 Nodulation assays

For nodulation complementation assays, *M. truncatula* seeds were sterilised and germinated as described in Section 7.1. Germinated seedlings were transferred to a 1:1 mix of terragreen and sand and grown in a controlled environment room (Section 7.1) for 1 week, before inoculating roots with *Sinorhizobium meliloti* strain 1021. To prepare *S. meliloti*, bacterial cells were grown in liquid TY medium (Table 7.2) for 2 days, spun down by centrifugation for 10 min at 4000 rpm and resuspended in fresh BNM medium to a final OD600 of 0.03. Nodules were quantified 4 weeks after inoculation.

7.9 Histochemical GUS staining of *M. truncatula* roots

To visualise GUS activity in *M. truncatula* hairy roots, roots were washed with distilled water and incubated in GUS staining solution (50 mM phosphate buffer pH 7.2, 0.5 mM $K_3Fe(CN)_6$, 0.5 mM $K_4Fe(CN)_6$, 50 mM EDTA, 1% (v/v) Triton-X and 2 mM X-Gluc (5-bromo-4-chloro-3-indolyl-beta-D-glucuronide)) in the dark at 37°C for 6 h or overnight.

To test whether GUS activity correlates with mycorrhizal infection structures, GUS-stained roots were additionally stained with Alexa Fluor 488 WGA as described in Section 7.7.3. Images were obtained using a DM 6000 microscope (Leica) and a DFC420 colour camera (Leica).

7.10 Quantification of gene expression

7.10.1 RNA isolation

For RNA extraction, root tissue was frozen at -80°C and ground to a fine powder in liquid nitrogen using a mortar and pestle. For RNA sequencing and qRT-PCR analysis of mycorrhized and non-mycorrhized roots, 4-5 root systems were pooled to obtain 1 biological replicate, and 4 biological replicates per treatment and genotype were analysed. For qRT-PCR analysis of *GFP*- and *RAM1*-overexpression lines, 6 root systems were pooled for 1 biological replicate, and 3 biological replicates per line were analysed. RNA was extracted from 100 mg of root tissue using the RNeasy plant mini kit (Qiagen) according to the manufacturer's instructions. To remove genomic DNA, the on column RNase free DNase kit (Qiagen) was used according to the manufacturer's instructions. RNA was eluted in 30 µl RNase-free water. RNA concentration and quality were determined using a NanoDrop ND-1000 Spectrophotometer (NanoDrop Technologies). To assess the integrity of the extracted RNA, 1 µg of RNA was run by TRIS/acetic acid/EDTA gel electrophoresis on a 1.2% (w/v) agarose gel and stained for 20 min in a 1 µg/ml ethidium bromide solution.

7.10.2 Quantitative reverse transcription PCR (qRT-PCR)

Reverse transcription was carried out with 1 µg of RNA using the iScript cDNA synthesis kit (Bio-Rad) according to the manufacturer's instructions. Primers for qPCR were designed using the primer design tool Quantprime (http://quantprime.mpimp-golm.mpg.de/) or the NCBI design tool Primer-BLAST (primer sequences are listed in Table 7.6). The amplification efficiency of primer pairs was tested using a cDNA dilution series. Generally, primers with an amplification efficiency of 90-110% were considered acceptable. The specificity of primer pairs was confirmed by analysing the dissociation curves (65°C to 95°C). For the quantification of transcript levels, qPCRs were performed

using a C1000 touch thermal cycler (Bio-Rad). Reactions were set up in 96-well plates using 10 µl SYBR Green mix (Bio-Rad), 0.7 µl primer mix (containing 10 µM forward primer and 10 µM reverse primer), 2 µl 1:10 diluted cDNA, and 7.3 µl water. The following cycling conditions were used for DNA amplification: 95 °C for 2 min followed by 40 cycles at 95°C for 15 s, 58 °C for 15 s and 72 °C for 30 s. Data were analysed using the $2^{-\Delta\Delta Ct}$ method (Livak and Schmittgen, 2001) with *Ubiquitin* as a reference gene. For comparison of two samples, Student's t-test was used to test for significant differences in expression levels. For comparison of more than two samples, ANOVA and Tukey's HSD mean-separation test was used to test for significant differences in expression levels. Where required, data were log10 transformed to ensure equal variance.

Table 7.6: Primer sequences used for qRT-PCRs.

Name	Primer sequence
MtRAM2_F	CCTTCATGGCTTTGTGCAAGGAG
MtRAM2_R	CACTGTTGTTACCTTTGGCTTTGC
MtRAM1_F	AAGCCATTTTCGAGGCGTTT
MtRAM1_R	CGTTAAGCATCGTCCGGTTT
MtWRI1_F2	AGAGGAGTAGCAAGGCACCATC
MtWRI1_R2	TGCCGAACACTCTTCCAATCCTTG
MtWRI2_F3	TGTACCAAAAATAGGTGATGATGCT
MtWRI2_R3	TCCATCTATGCCTGCTAACACC
MtFATM_F2	ATGGGTTGGAGCATCGGGAAAG
MtFATM_R2	TGTTCATCATCACCCATGTGCTTG
MtABCG3_F2	CATTGGCTCAAGTAGTGGTTCG
MtABCG3_R2	GAATCCACCAACAAGGGTCATG
MtUbiquitin_F	GCAGATAGACACGCTGGGA
MtUbiquitin_R	AACTCTTGGGCAGGCAATAA
MtCCD7_F	GATGTGGGGGAAGAAGCTATTG
MtCCD7_R	TCCCAATCGTATCCAACGTG
MtCCD8_F	GAAGATGGGAGGGTAACTGCTG
MtCCD8_R	AGAACATCTTCGCCGTTAAATG
Medtr2g094160_F3	CGGAGCAGCTAACAAAGCCATTAC
Medtr2g094160_R3	ACAACCAAGCGTGTGCCTTG
Medtr5g019460_F2	TGTCCGTCCGGTACTCTGTATTGC
Medtr5g019460_R2	CGCATGCCGATGGAATTGATGC
Medtr8g068300_F	TGCCTCCTTAAACCAAACCACTC

continued overleaf

Table 7.6: continued.

Name	Primer sequence
Medtr8g068300_R	ATGAAGCCATCACACAGAACTGG
Medtr8g097190_F2	GTTGCAGCAGTTGACAAGCCTAAG
Medtr8g097190_R2	CCACATGACCTGTCCAACCATCTG
Medtr7g063800_F2	CAGAGGAAGATGATGGTGTGGTA
Medtr7g063800_R2	AAGGGAACTTAGCTGTAGCG
Medtr2g105360_F1	CAACCAGCCATGGACACTCT
Medtr2g105360_R1	TGGAACCGCTGGTACATGAG
Medtr1g102070.1_F	TCACTGGCAGATTCTCTTCCAAGC
Medtr1g102070.1_R	ACTCATTGCCCATTGTGTTGCAC
MtPT4_ F	GACACGAGGCGCTTTCATAGCAGC
MtPT4_R	GTCATCGCAGCTGGAACAGCACCG

7.10.3 RNA-sequencing

To quantify global gene expression, RNA sequencing was performed by IMGM Laboratories (Martinsried, Germany). In brief, RNA sequencing libraries were prepared with the Illumina TruSeq® Stranded mRNA HT technology, an approach that uses fragmentation of the RNA, a poly-T oligo pulldown and sequencing adapter ligation. RNA sequencing was performed on the Illumina NextSeq500 next generation sequencing system and the high output mode with 1 x 75 bp single-end read chemistry. The resulting reads were quality controlled and mapped against the most recent version of the *M. truncatula* reference genome (Mtv4.0). Differentially expressed genes (DEGs) were identified by pair-wise comparisons of expression levels (total exon reads) using the CLC Genomics Workbench tool 'Empirical analysis of DGE' (EDGE). For further analyses, only DEGs with a fold change larger than 1.5 and a false discovery rate (FDR)-corrected p-value smaller than 0.05 were considered.

7.11 Chromatin-immunoprecipitation (ChIP)

To identify DNA-binding sites of NSP1, ChIP was performed according to the method described by Kaufmann et al., (2010) with some modifications. For each biological replicate, roots from *M. truncatula* lines stably expressing *pNSP1:GFP-NSP1* grown on plates with media containing 15 mM KNO_3 and a 1/100 dilution of BNM (Table 7.2) were

pooled to obtain 3.5 g of fresh root tissue. As a negative control, roots from untransformed *M. truncatula* A17 grown under the same conditions were used.

7.11.1 Crosslinking

To crosslink DNA and proteins, fresh plant tissue was vacuum-infiltrated with fixation buffer (0.4 M sucrose, 10 mM TRIS pH 8, 1 mM EDTA pH 8.5, 1% formaldehyde, 100 µM PMSF) for 20 min on ice. Formaldehyde was quenched by adding 0.1 M glycine and incubating for 10 min on ice. Tissue was washed twice with sterile water and dry-blotted before being frozen in liquid nitrogen.

7.11.2 Nuclei extraction

To extract nuclei from crosslinked roots, the frozen tissue was ground to a fine powder in liquid nitrogen using a mortar and pestle. The ground tissue was resuspended in 25 ml lysis buffer M1 (10 mM sodium phosphate pH 7, 0.1 M NaCl, 1 M 2-methyl 2,4-pentanediol, 10 mM ß-mercaptoethanol, EDTA-free protease inhibitor cocktail (Roche)) by rotating the tubes at 4°C for 15 min. The lysate was filtered through 2 layers of miracloth (Merck Chemicals) and spun down by centrifugation at 1000 g for 20 min at 4°C with decreased acceleration and deceleration. The supernatant was discarded and the pellet was resuspended in 15 ml wash buffer M2 (10 mM sodium phosphate buffer pH 7, 0.1 M NaCl, 1 M 2-methyl 2,4-pentanediol, 10 mM ß-mercaptoethanol, EDTA-free protease inhibitor cocktail (Roche), 10 mM $MgCl_2$ and 0.5% Triton X-100). After centrifugation at 1000 g for 10 min at 4°C with decreased acceleration and deceleration, the supernatant was discarded and the pellet was resuspended in 7.5 ml wash buffer M3 (10 mM sodium phosphate buffer pH 7, 0.1 M NaCl, 10 mM ß-mercaptoethanol, EDTA-free protease inhibitor cocktail (Roche)). The resuspended samples were spun down by centrifugation at 1000 g for 10 min at 4°C with decreased acceleration and deceleration. The supernatant was discarded and the pellet was resuspended in 1 ml sonication buffer (0.5 M Hepes, 150 mM NaCl, 5 mM $MgCl_2$ and 10% Triton X-100 and EDTA-free protease inhibitor cocktail (Roche)).

7.11.3 Chromatin fragmentation

For DNA fragmentation, nuclei were sonicated in a Bioruptor water bath sonicator (Diagenode) at 4°C (2 x 5 min at a high power level with 30 s on/30 s off cycles) to obtain an average fragment size of ~ 500 bp. After sonication, samples were cleared from debris by centrifugation at 16000 g for 15 min. The supernatant was transferred to a new tube and the centrifugation step repeated. 50 µl of the cleared supernatant were taken as DNA input sample and kept on ice.

7.11.4 Immunoprecipitation

Lysed nuclei were diluted by adding 500 µl immunoprecipitation buffer (0.5 M Hepes, 150 mM NaCl, 5 mM $MgCl_2$ 10% Triton X-100, 1 mg/ml bovine serum albumin (BSA, added fresh)). To each tube, 25 µl of anti-GFP µMACS Microbeads (Miltenyi Biotec) were added and mixed by inverting. The samples were incubated on ice for 30 min to allow binding of the beads to GFP-tagged NSP1. Subsequently, samples were loaded on µColumns (Miltenyi Biotec) equilibrated with 200 µl immunoprecipitation buffer and placed on a magnetic µMACS separator (Miltenyi Biotec). Once the entire sample volume had passed the columns, the beads were washed twice with 400 µl immunoprecipitation buffer and twice with 200 µl immunoprecipitation buffer. In addition, beads were washed twice with 200 µl TE buffer (100 mM Tris pH 8, 10 mM EDTA pH 8). To elute the protein-DNA complexes, 20 µl pre-heated elution buffer (95°C; 50 mM Tris pH 8, 10 mM EDTA, 50 mM DTT, 1% SDS) were added to the column. After incubating for 5 min, 2 x 50 µl hot elution buffer were added to the column for final elution and the eluate was collected in low binding Eppendorf tubes.

7.11.5 DNA clean-up

The eluted samples and DNA input samples were diluted by adding 100 µl TE buffer. For reverse crosslinking, 9 µl of 25 mg/ml Proteinase K (Sigma) were added and incubated at 37°C overnight. The next day, 9 µl of fresh 25 mg/ml Proteinase K (Sigma) were added and incubated at 65°C for 8 h. DNA was cleaned up using the NucleoSpin Gel and PCR Clean-up kit (Macherey-Nagel) according to the manufacturer's instructions. As the DNA samples contain SDS, buffer NTB (Macherey-Nagel) was used for DNA clean-up. DNA was eluted in 30 µl elution buffer (Macherey-Nagel).

7.11.6 qPCR

For the quantification of DNA enrichment, 1 µl of the purified immuno-precipitated DNA and 1 µl of the 1/10 diluted input sample was used for qPCR as described in Section 7.10.2. Primers used for ChIP-qPCR are listed in Table 7.7. Primers were designed using the NCBI design tool Primer-BLAST and specificity and efficiency tested as described in Section 7.10.2. Three technical replicates were performed for each sample and primer pair. The enrichment of DNA in the immuno-precipitated samples relative to the input samples were calculated based on the difference in the Ct values with the following equation: %input = 2^(average Ct(input) – x – average Ct(IP)) x 100, where x = dilution factor of the input versus IP sample.

Table 7.7: Primer sequences used for ChIP-qPCR.

Name	Primer sequence
D27_1_F	TCATTGGCGTTTCCTCCCTG
D27_1_R	TGCCCAAGTTTTGTATGCAGT
D27_2_F	ACATGTGTCTGCAGCTATATCAG
D27_2_R	CTGCATCTACTTCATAACCGACC
D27_3_F	TAACAACTGTTCCCAGCGCA
D27_3_R	TGACATACTCTAACAACCGATTCT
D27_4_F	AGAATCGGTTGTTAGAGTATGTCA
D27_4_R	AATTGCGTCCCTCGGTCAAT

7.12 Transactivation assays

7.12.1 Transformation of *N. benthamiana* leaves

Leaves of three-week old *N. benthamiana* plants were transformed using *A. tumefaciens* strain GV3101 carrying the appropriate Golden Gate level 2 vector (Table 7.5). To this end, bacterial cultures were set up 48 h prior to the transformation and grown in LB media (Table 7.2) containing the appropriate antibiotics at 28°C with agitation at 220 rpm. Bacteria were spun down at 4000 g for 15 min at RT and resuspended in infiltration buffer (10 mM $MgCl_2$, 10 mM MES pH 5.6, 100 µM acetosyringone) to a final OD600 of 0.3. After incubating for 3 h at room temperature in the dark, resuspended bacteria were

infiltrated into plant leaves using a 1-ml needleless syringe. Leaf discs with a diameter of 1.5 cm were collected at 72 h post infiltration and frozen in liquid nitrogen before extracting proteins for enzymatic GUS and LUC activity assays as described below.

7.12.2 Protein extraction

To extract proteins from transformed leaf tissues, frozen leaf discs were ground to a fine powder in liquid nitrogen using a blue polypropylene pestle (Sigma Aldrich). To extract proteins from transformed *M. truncatula* roots, frozen tissue was ground in liquid nitrogen using a mortar and pestle. Immediately after grinding, 150 µl of 1x Luciferase cell culture lysis reagent (Promega) supplemented with EDTA-free protease inhibitor cocktail (Roche) was added to the plant tissue (one *N. benthamiana* leaf disc or 100 mg *M. truncatula* root tissue) and incubated on ice for 10 min. Cell extracts were cleared from debris by centrifugation at 16000 g for 10 min at 4°C.

7.12.3 GUS activity assays

For enzymatic fluorometric GUS assays, 40 µl protein extracts were mixed with 100 µl MUG assay buffer (50 mM phosphate buffer pH 7, 1 mM EDTA, 0.1% TritonX-100, 0.1% sodium lauroyl sarcosinate and 10 mM β-mercaptoethanol, 2 mM MUG) and incubated at 37°C. The reactions were stopped at T0 (to use as a blank) and after 30 min by adding 20 µl of the reaction mix to 180 µl 200 mM Na_2CO_3. The fluorescence of 4-methylumbelliferone released from MUG was measured in black 96-well microtitre plates (Greiner Bio-One) on a Varioskan microplate reader (Thermo Fisher Scientific) with an excitation wavelength of 365 nm and an emission wavelength of 455 nm.

7.12.4 LUC activity assays

To detect LUC activity in protein extracts, 10 µl protein extract were mixed with 100 µl luciferase assay reagent (Promega) in a white 96-well microtitre plate (Greiner Bio-One). Luminescence was measured on a Varioskan microplate reader (Thermo Fisher Scientific) with 5 s integration time. The LUC activity assessed in a sample was normalized to the transformation efficiency measured as GUS activity in the same sample. ANOVA and Tukey's HSD mean-separation test was used to test for significant

differences in transactivation levels (measured as LUC/GUS ratios). Where required, data were log10 transformed to ensure equal variance.

7.13 Phylogenetic analyses

Phylogenetic analyses were performed using protein sequences from *M. truncatula*, *A. thaliana*, *O. sativa*, and *M. paleacea*. With the exception of *M. paleacea*, the putative homologs of *MtABCG3* and *MtWRI1* were extracted from the Phytozome database using BLASTP with the corresponding full-length protein sequence as query. Sequences from *M. paleacea* were obtained from Guru Radhakrishnan (unpublished data). All the identified potential homologs were aligned using MAFFT and maximum likelihood trees were constructed with Geneious 6.06.

7.14 Bioinformatics

To produce heat maps showing fold changes of differentially expressed genes, the web-based tool GENE-E (now called Morpheus, https://software.broadinstitute.org/GENE-E/index.html) was used. Hierarchical clustering of genes was performed using a Euclidean distance metric.

To identify significantly enriched gene ontology (GO) terms of *NSP1-*, *NSP2-*, and *RAM1*-dependent genes identified by clustering, a singular enrichment analysis was performed using the web-based tool AgriGO (http://bioinfo.cau.edu.cn/agriGO/index.php). *M. truncatula* gene identifiers (Mtv4.0) were used for the input sample list, and the analysis was performed using the whole *M. truncatula* genome (Mtv4.0) as background. To test for significance, Fisher's exact test was used, and only GO terms with an FDR-corrected p-value smaller than 0.05 were considered (calculated using the multi-test method Yekutieli).

REFERENCES

Agren GI, Wetterstedt JÅM, Billberger MFK (2012) Nutrient limitation on terrestrial plant growth - modeling the interaction between nitrogen and phosphorus. New Phytol **194**: 953–960

Aida M, Beis D, Heidstra R, Willemsen V, Blilou I, Galinha C, Nussaume L, Noh YS, Amasino R, Scheres B (2004) The PLETHORA genes mediate patterning of the Arabidopsis root stem cell niche. Cell **119**: 119–120

Akiyama K, Hayashi H (2006) Strigolactones: Chemical signals for fungal symbionts and parasitic weeds in plant roots. Handb Environ Chem **97**: 925–931

Akiyama K, Matsuzaki K, Hayashi H (2005) Plant sesquiterpenes induce hyphal branching in arbuscular mycorrhizal fungi. Nature **435**: 824–7

Akiyama K, Ogasawara S, Ito S, Hayashi H (2010) Structural requirements of strigolactones for hyphal branching in AM fungi. Plant Cell Physiol **51**: 1104–1117

Al-Babili S, Bouwmeester HJ (2015) Strigolactones, a novel carotenoid-derived plant hormone. Annu Rev Plant Biol **66**: 161–86

Alder A, Jamil M, Marzorati M, Bruno M, Vermathen M, Bigler P, Ghisla S, Bouwmeester H, Beyer P, Al-babili S (2012) The Path from b-Carotene to Carlactone, a Strigolactone-Like Plant Hormone. Science **335**: 1348–1351

Alexander T, Toth R, Meier R, Weber HC (1989) Dynamics of arbuscule development and degeneration in onion, bean, and tomato with reference to vesicular–arbuscular mycorrhizae in grasses. Can J Bot **67**: 2505–2513

Allen JW, Shachar-Hill Y (2009) Sulfur transfer through an arbuscular mycorrhiza. Plant Physiol **149**: 549–560

Ames RN, Reid CPP, Porter LK, Cambardella C (1983) Hyphal Uptake and Transport of Nitrogen from Two 15N-Labelled Sources by Glomus mosseae, a Vesicular-Arbuscular Mycorrhizal Fungus. New Phytol **95**: 381–396

Amor B Ben, Shaw SL, Oldroyd GED, Maillet F, Penmetsa RV, Cook D, Long SR, Dénarié J, Gough C (2003) The NFP locus of Medicago truncatula controls an early step of Nod factor signal transduction upstream of a rapid calcium flux and root hair deformation. Plant J **34**: 495–506

Ané J-M, Kiss GB, Riely BK, Penmetsa RV, Oldroyd GED, Ayax C, Lévy J, Debellé F, Baek J, Kaló P, et al (2004) Medicago truncatula DMI1 required for bacterial and fungal symbioses in legumes. Science **303**: 1364–1367

Aroca R, Ruiz-Lozano JM, Zamarreño AM, Paz JA, García-Mina JM, Pozo MJ, López-Ráez JA (2013) Arbuscular mycorrhizal symbiosis influences strigolactone production under salinity and alleviates salt stress in lettuce plants. J Plant Physiol **170**: 47–55

Arrighi J-F, Barre A, Amor B Ben, Bersoult A, Soriano LC, Mirabella R, de Carvalho-Niebel F, Journet E-P, Ghérardi M, Huguet T, et al (2006) The Medicago truncatula Lysine Motif-Receptor-like Kinase Gene Family Includes NFP and New Nodule-Expressed Genes. Plant Physiol **142**: 265

Bago B, Pfeffer PE, Shachar-hill Y (2000) Update on Symbiosis Arbuscular Mycorrhizas. Plant Physiol **124**: 949–957

Bago B, Zipfel W, Williams RM, Jun J, Arreola R, Lammers PJ, Pfeffer PE, Shachar-Hill Y (2002) Translocation and utilization of fungal storage lipid in the arbuscular mycorrhizal symbiosis. Plant Physiol **128**: 108–124

Baier MC, Keck M, Gödde V, Niehaus K, Küster H, Hohnjec N (2010) Knockdown of the symbiotic sucrose synthase MtSucS1 affects arbuscule maturation and maintenance in mycorrhizal roots of Medicago truncatula. Plant Physiol **152**: 1000–1014

Balestrini R, Bonfante P (2014) Cell wall remodeling in mycorrhizal symbiosis: a way towards biotrophism. Front Plant Sci **5**: 1–10

Balzergue C, Puech-Pags V, Bécard G, Rochange SF (2011) The regulation of arbuscular mycorrhizal symbiosis by phosphate in pea involves early and systemic signalling events. J Exp Bot **62**: 1049–1060

Baud S, Mendoza MS, To A, Harscoët E, Lepiniec L, Dubreucq B (2007) WRINKLED1 specifies the regulatory action of LEAFY COTYLEDON2 towards fatty acid metabolism during seed maturation in Arabidopsis. Plant J **50**: 825–838

Baud S, Wuillème S, To A, Rochat C, Lepiniec L (2009) Role of WRINKLED1 in the transcriptional regulation of glycolytic and fatty acid biosynthetic genes in Arabidopsis. Plant J **60**: 933–947

Bécard G, Douds DD, Pfeffer PE (1992) Extensive in vitro hyphal growth of vesicular-arbuscular mycorrhizal fungi in the presence of CO2 and flavonols. Appl Environ Microbiol **58**: 821–825

Bécard G, Taylor LP, Douds DD, Pfeffer PE, Doner LW (1995) Flavonoids Are Not Necessary Plant Signal Compounds in Arbuscular Mycorrhizal Symbioses. Mol Plant-Microbe Interact **8**: 252

Beilby JP, Kidby DK (1980) Biochemistry of ungerminated and germinated spores of the vesicular-arbuscular mycorrhizal fungus, Glomus caledonius: changes in neutral and polar lipids. J Lipid Res **21**: 739–750

Benedetto A, Magurno F, Bonfante P, Lanfranco L (2005) Expression profiles of a phosphate transporter gene (GmosPT) from the endomycorrhizal fungus Glomus mosseae. Mycorrhiza **15**: 620–627

Benedito VA, Torres-Jerez I, Murray JD, Andriankaja A, Allen S, Kakar K, Wandrey M, Verdier J, Zuber H, Ott T, et al (2008) A gene expression atlas of the model legume Medicago truncatula. Plant J **55**: 504–513

Besserer A, Bécard G, Jauneau A, Roux C, Séjalon-Delmas N (2008) GR24, a synthetic analog of strigolactones, stimulates the mitosis and growth of the arbuscular mycorrhizal fungus Gigaspora rosea by boosting its energy metabolism. Plant Physiol **148**: 402–413

Besserer A, Puech-Pagès V, Kiefer P, Gomez-Roldan V, Jauneau A, Roy S, Portais JC, Roux C, Bécard G, Séjalon-Delmas N (2006) Strigolactones stimulate arbuscular mycorrhizal fungi by activating mitochondria. PLoS Biol **4**: 1239–1247

Bird D, Beisson F, Brigham A, Shin J, Greer S, Jetter R, Kunst L, Wu X, Yephremov A, Samuels L (2007) Characterization of Arabidopsis ABCG11/WBC11, an ATP binding cassette (ABC) transporter that is required for cuticular lipid secretion. Plant J **52**: 485–498

Blee KA, Anderson AJ (1998) Regulation of arbuscle formation by carbon in the plant. Plant J **16**: 523–530

Bolle C (2004) The role of GRAS proteins in plant signal transduction and development. Planta **218**: 683–92

Bonaventure G, Salas JJ, Pollard MR, Ohlrogge JB (2003) Disruption of the FATB gene in Arabidopsis demonstrates an essential role of saturated fatty acids in plant growth. Plant Cell **15**: 1020–33

Bonfante P, Genre A (2015) Arbuscular mycorrhizal dialogues: do you speak “plantish” or “fungish”? Trends Plant Sci **20**: 150–154

Bravo A, York T, Pumplin N, Mueller LA, Harrison MJ (2016) Genes conserved for arbuscular mycorrhizal symbiosis identified through phylogenomics. Nat Plants **2**: 1–6

Breakspear A, Liu C, Roy S, Stacey N, Rogers C, Trick M, Morieri G, Mysore KS, Wen J, Oldroyd GED, et al (2014) The root hair “infectome” of Medicago truncatula uncovers changes in cell cycle genes and reveals a requirement for Auxin signaling in rhizobial infection. Plant Cell **26**: 4680–701

Brechenmacher L, Weidmann S, van Tuinen D, Chatagnier O, Gianinazzi S, Franken P, Gianinazzi-Pearson V (2004) Expression profiling of up-regulated plant and fungal genes in early and late stages of Medicago truncatula-Glomus mosseae interactions. Mycorrhiza **14**: 253–62

Breuillin F, Schramm J, Hajirezaei M, Ahkami A, Favre P, Druege U, Hause B, Bucher M, Kretzschmar T, Bossolini E, et al (2010) Phosphate systemically inhibits development of arbuscular mycorrhiza in Petunia hybrida and represses genes involved in mycorrhizal functioning. Plant J **64**: 1002–1017

Breuillin-Sessoms F, Floss DS, Gomez SK, Pumplin N, Ding Y, Levesque-Tremblay V, Noar RD, Daniels D a., Bravo A, Eaglesham JB, et al (2015) Suppression of Arbuscule Degeneration in Medicago truncatula phosphate transporter4 Mutants Is Dependent on the Ammonium Transporter 2 Family Protein AMT2;3. Plant Cell **27**: 1352-1366

Broghammer a., Krusell L, Blaise M, Sauer J, Sullivan JT, Maolanon N, Vinther M, Lorentzen A, Madsen EB, Jensen KJ, et al (2012) Legume receptors perceive the rhizobial lipochitin oligosaccharide signal molecules by direct binding. Proc Natl Acad Sci **109**: 13859–13864

Buendia L, Wang T, Girardin A, Lefebvre B (2016) The LysM receptor-like kinase SlLYK10 regulates the arbuscular mycorrhizal symbiosis in tomato. New Phytol **210**: 184–195

Campos-Soriano L, García-Martínez J, Segundo BS (2012) The arbuscular mycorrhizal symbiosis promotes the systemic induction of regulatory defence-related genes in rice leaves and confers resistance to pathogen infection. Mol Plant Pathol **13**: 579–592

Camps C, Jardinaud M-F, Rengel D, Carrère S, Hervé C, Debellé F, Gamas P, Bensmihen S, Gough C (2015) Combined genetic and transcriptomic analysis reveals three major signalling pathways activated by Myc-LCOs in Medicago truncatula. New Phytol **208**: 224-240

Capoen W, Sun J, Wysham D, Otegui MS, Venkateshwaran M, Hirsch S, Miwa H, Downie JA, Morris RJ, Ané J-M, et al (2011) Nuclear membranes control symbiotic calcium signaling of legumes. Proc Natl Acad Sci **108**: 14348–53

Carbonnel S, Gutjahr C (2014) Control of arbuscular mycorrhiza development by nutrient signals. Front Plant Sci **5**: 462

Casieri L, Gallardo K, Wipf D (2012) Transcriptional response of Medicago truncatula sulphate transporters to arbuscular mycorrhizal symbiosis with and without sulphur stress. Planta **235**: 1431–1447

Catoira R, Galera C, de Billy F, Penmetsa R V, Journet EP, Maillet F, Rosenberg C, Cook D, Gough C, Dénarié J (2000) Four genes of Medicago truncatula controlling components of a nod factor transduction pathway. Plant Cell **12**: 1647–66

Cazzonelli CI, Pogson BJ (2010) Source to sink: regulation of carotenoid biosynthesis in plants. Trends Plant Sci **15**: 266–274

Cerri MR, Frances L, Laloum T, Auriac M-C, Niebel A, Oldroyd GED, Barker DG, Fournier J, de Carvalho-Niebel F (2012) Medicago truncatula ERN transcription factors: regulatory interplay with NSP1/NSP2 GRAS factors and expression dynamics throughout rhizobial infection. Plant Physiol **160**: 2155–72

Chabaud M, Genre A, Sieberer BJ, Faccio A, Fournier J, Novero M, Barker DG, Bonfante P (2011) Arbuscular mycorrhizal hyphopodia and germinated spore exudates trigger Ca2+ spiking in the legume and nonlegume root epidermis. New Phytol **189**: 347–355

Charpentier M, Bredemeier R, Wanner G, Takeda N, Schleiff E, Parniske M (2008) Lotus japonicus CASTOR and POLLUX are ion channels essential for perinuclear calcium spiking in legume root endosymbiosis. Plant Cell **20**: 3467–79

Charpentier M, Sun J, Martins TV, Radhakrishnan G V, Findlay K, Soumpourou E, Thouin J, Véry A, Sanders D, Morris RJ, et al (2016) Symbiotic Calcium Oscillations. Science **352**: 1102–5

Chen C, Ané J-M, Zhu H (2008) OsIPD3, an ortholog of the Medicago truncatula DMI3 interacting protein IPD3, is required for mycorrhizal symbiosis in rice. New Phytol **180**: 311–315

Chen T, Zhu H, Ke D, Cai K, Wang C, Gou H, Hong Z, Zhang Z (2012) A MAP kinase kinase interacts with SymRK and regulates nodule organogenesis in Lotus japonicus. Plant Cell **24**: 823–38

Cook CE, Whichard LP, Turner B, Wall ME, Egley GH (1966) Germination of Witchweed (Striga lutea Lour.): Isolation and Properties of a Potent Stimulant. Science **154**: 1189–90

Cordier C, Pozo MJ, Barea JM, Gianinazzi S (1998) Cell Defense Responses Associated with Localized and Systemic Resistance to Phytophthora parasitica Induced in Tomato by an Arbuscular Mycorrhizal Fungus. Mol Plant-Microbe Interact **11**: 1017–1028

Cruz C, Egsgaard H, Trujillo C, Ambus P, Requena N, Martins-Loução MA, Jakobsen I (2007) Enzymatic evidence for the key role of arginine in nitrogen translocation by arbuscular mycorrhizal fungi. Plant Physiol **144**: 782–792

Czaja LF, Hogekamp C, Lamm P, Maillet F, Martinez EA, Samain E, Dénarié J, Küster H, Hohnjec N (2012) Transcriptional responses toward diffusible signals from symbiotic microbes reveal MtNFP- and MtDMI3-dependent reprogramming of host gene expression by arbuscular mycorrhizal fungal lipochitooligosaccharides. Plant Physiol **159**: 1671–85

De Cuyper C, Fromentin J, Yocgo RE, De Keyser A, Guillotin B, Kunert K, Boyer FD, Goormachtig S (2014) From lateral root density to nodule number, the strigolactone analogue GR24 shapes the root architecture of Medicago truncatula. J Exp Bot **66**: 137–146

Delaux PM, Varala K, Edger PP, Coruzzi GM, Pires JC, Ane JM (2014) Comparative Phylogenomics Uncovers the Impact of Symbiotic Associations on Host Genome Evolution. PLoS Genet **10**: 7

Delaux P-M, Bécard G, Combier J-P (2013) NSP1 is a component of the Myc signaling pathway. New Phytol **199**: 59–65

Delaux P-M, Radhakrishnan G V., Jayaraman D, Cheema J, Malbreil M, Volkening JD, Sekimoto H, Nishiyama T, Melkonian M, Pokorny L, et al (2015) Algal ancestor of land plants was preadapted for symbiosis. Proc Natl Acad Sci **112**: 201515426

Devers EA, Teply J, Reinert A, Gaude N, Krajinski F (2013) An endogenous artificial microRNA system for unraveling the function of root endosymbioses related genes in Medicago truncatula. BMC Plant Biol **13**: 82

Dickson S (2004) The Arum-Paris continuum of mycorrhizal symbioses. New Phytol **163**: 187–200

Douds DD, Pfeffer PE, Shachar-hill Y (2000) Application of in vitro methods to study carbon uptake and transport by AM fungi. Plant Soil **226**: 255–261

Endre G, Kereszt A, Kevei Z, Mihacea S, Kaló P, Kiss GB (2002) A receptor kinase gene regulating symbiotic nodule development. Nature **417**: 962–966

Engler C, Gruetzner R, Kandzia R, Marillonnet S (2009) Golden gate shuffling: a one-pot DNA shuffling method based on type IIs restriction enzymes. PLoS One **4**: e5553

Ezawa T, Smith SE, Smith FA (2002) P metabolism and transport in AM fungi. Plant Soil **244**: 221–230

Feddermann N, Muni RRD, Zeier T, Stuurman J, Ercolin F, Schorderet M, Reinhardt D (2010) The PAM1 gene of petunia, required for intracellular accommodation and morphogenesis of arbuscular mycorrhizal fungi, encodes a homologue of VAPYRIN. Plant J **64**: 470–81

Ferguson BJ, Ross JJ, Reid JB (2005) Nodulation phenotypes of gibberellin and brassinosteroid mutants of pea. Plant Physiol **138**: 2396–2405

Fernández-Aparicio M, García-Garrido JM, Ocampo JA, Rubiales D (2010) Colonisation of field pea roots by arbuscular mycorrhizal fungi reduces Orobanche and Phelipanche species seed germination. Weed Res **50**: 262–268

Fester T, Schmidt D, Lohse S, Walter MH, Giuliano G, Bramley PM, Fraser PD, Hause B, Strack D (2002) Stimulation of carotenoid metabolism in arbuscular mycorrhizal roots. Planta **216**: 148–154

Fiorilli V, Catoni M, Miozzi L, Novero M, Accotto GP, Lanfranco L (2009) Global and cell-type gene expression profiles in tomato plants colonized by an arbuscular mycorrhizal fungus. New Phytol **184**: 975–987

Fiorilli V, Lanfranco L, Bonfante P (2013) The expression of GintPT, the phosphate transporter of Rhizophagus irregularis, depends on the symbiotic status and phosphate availability. Planta **237**: 1267–1277

Floss DS, Levy JG, Lévesque-Tremblay V, Pumplin N, Harrison MJ (2013) DELLA proteins regulate arbuscule formation in arbuscular mycorrhizal symbiosis. Proc Natl Acad Sci **110**: E5025–34

Fonouni-Farde C, Tan S, Baudin M, Brault M, Wen J, Mysore KS, Niebel A, Frugier F, Diet A (2016) DELLA-mediated gibberellin signalling regulates Nod factor signalling and rhizobial infection. Nat Commun **7**: 12636

Foo E, Davies NW (2011) Strigolactones promote nodulation in pea. Planta **234**: 1073–1081

Foo E, Ross JJ, Jones WT, Reid JB (2013) Plant hormones in arbuscular mycorrhizal symbioses: an emerging role for gibberellins. Ann Bot **111**: 769–779

Gao XH, Xiao SL, Yao QF, Wang YJ, Fu XD (2011) An updated GA signaling "relief of repression" regulatory model. Mol Plant **4**: 601–606

Gaude N, Schulze WX, Franken P, Krajinski F (2012) Cell type-specific protein and transcription profiles implicate periarbuscular membrane synthesis as an important carbon sink in the mycorrhizal symbiosis. Plant Signal Behav **7**: 461–464

Genre A, Chabaud M, Faccio A, Barker DG, Bonfante P (2008) Prepenetration Apparatus Assembly Precedes and Predicts the Colonization Patterns of Arbuscular Mycorrhizal Fungi within the Root Cortex of Both Medicago truncatula and Daucus carota. Plant Cell **20**: 1407–1420

Genre A, Ivanov S, Fendrych M, Faccio A, Zarsky V, Bisseling T, Bonfante P (2012) Multiple Exocytotic Markers Accumulate at the Sites of Perifungal Membrane Biogenesis in Arbuscular Mycorrhizas. Plant Cell Physiol **53**: 244–255

Genre A, Bonfante P (1998) Actin versus tubulin configuration in arbuscule-containing cells from mycorrhizal tobacco roots. New Phytol **140**: 745–752

Genre A, Chabaud M, Balzergue C, Puech-Pagès V, Novero M, Rey T, Fournier J, Rochange S, Bécard G, Bonfante P, et al (2013) Short-chain chitin oligomers from arbuscular mycorrhizal fungi trigger nuclear Ca2+ spiking in Medicago truncatula roots and their production is enhanced by strigolactone. New Phytol **198**: 179–189

Genre A, Chabaud M, Timmers T, Bonfante P, Barker DG (2005) Arbuscular Mycorrhizal Fungi Elicit a Novel Intracellular Apparatus in Medicago truncatula Root Epidermal Cells before Infection. Plant Cell **17**: 3489–3499

Gianinazzi-Pearson V (1996) Plant Cell Responses to Arbuscular Mycorrhizal Fungi: Getting to the Roots of the Symbiosis. Plant Cell **8**: 1871–1883

Gianinazzi-Pearson V, Arnould C, Oufattole M, Arango M, Gianinazzi S (2000) Differential activation of H+-ATPase genes by an arbuscular mycorrhizal fungus in root cells of transgenic tobacco. Planta **211**: 609–13

Giovannetti M, Mosse B (1980) An evaluation of techniques for measuring vesicular arbuscular mycorrhizal infection in roots. New Phytol **84**: 489–500

Gleason C, Chaudhuri S, Yang T, Muñoz A, Poovaiah BW, Oldroyd GED (2006) Nodulation independent of rhizobia induced by a calcium-activated kinase lacking autoinhibition. Nature **441**: 1149–52

Gobbato E, Marsh JF, Vernié T, Wang E, Maillet F, Kim J, Miller JB, Sun J, Bano SA, Ratet P, et al (2012) A GRAS-type transcription factor with a specific function in mycorrhizal signaling. Curr Biol **22**: 2236–41

Gobbato E, Wang E, Higgins G, Bano SA, Henry C, Schultze M, Oldroyd GED (2013) RAM1 and RAM2 function and expression during arbuscular mycorrhizal symbiosis and Aphanomyces euteiches colonization. Plant Signal Behav **8**: 1–5

Gomez SK, Harrison MJ (2009) Laser microdissection and its application to analyze gene expression in arbuscular mycorrhizal symbiosis. Pest Manag Sci **65**: 504–11

Gomez-Roldan V, Fermas S, Brewer PB, Puech-Pagès V, Dun E a, Pillot J-P, Letisse F, Matusova R, Danoun S, Portais J-C, et al (2008) Strigolactone inhibition of shoot branching. Nature **455**: 189–94

Govindarajulu M, Pfeffer PE, Jin H, Abubaker J, Douds DD, Allen JW, Bücking H, Lammers PJ, Shachar-Hill Y (2005) Nitrogen transfer in the arbuscular mycorrhizal symbiosis. Nature **435**: 819–823

Granqvist E, Wysham D, Hazledine S, Kozlowski W, Sun J, Charpentier M, Martins TV, Haleux P, Tsaneva-Atanasova K, Downie JA, et al (2012) Buffering capacity explains signal variation in symbiotic calcium oscillations. Plant Physiol **160**: 2300–10

Groth M, Takeda N, Perry J, Uchida H, Dräxl S, Brachmann A, Sato S, Tabata S, Kawaguchi M, Wang TL, et al (2010) NENA, a Lotus japonicus homolog of Sec13, is required for rhizodermal infection by arbuscular mycorrhiza fungi and rhizobia but dispensable for cortical endosymbiotic development. Plant Cell **22**: 2509–26

Guether M, Neuhauser B, Balestrini R, Dynowski M, Ludewig U, Bonfante P (2009) A Mycorrhizal-Specific Ammonium Transporter from Lotus japonicus Acquires Nitrogen Released by Arbuscular Mycorrhizal Fungi. Plant Physiol **150**: 73–83

Güimil S, Chang H, Zhu T, Sesma A, Osbourn A, Roux C, Ioannidis V, Oakeley EJ, Docquier M, Descombes P, et al (2005) Comparative transcriptomics of rice reveals an ancient pattern of response to microbial colonization. Proc Natl Acad Sci **102**: 8066–8070

Gutjahr C, Parniske M (2013) Cell and developmental biology of arbuscular mycorrhiza symbiosis. Annu Rev Cell Dev Biol **29**: 593–617

Gutjahr C, Banba M, Croset V, An K, Miyao A, An G, Hirochika H, Imaizumi-Anraku H, Paszkowski U (2008) Arbuscular mycorrhiza-specific signaling in rice transcends the common symbiosis signaling pathway. Plant Cell **20**: 2989–3005

Gutjahr C, Gobbato E, Choi J, Riemann M, Johnston MG, Summers W, Carbonnel S, Mansfield C, Yang S-Y, Nadal M, et al (2015) Rice perception of symbiotic arbuscular mycorrhizal fungi requires the karrikin receptor complex. Science **350**: 1521–1524

Gutjahr C, Radovanovic D, Geoffroy J, Zhang Q, Siegler H, Chiapello M, Casieri L, An K, An G, Guiderdoni E, et al (2012) The half-size ABC transporters STR1 and STR2 are indispensable for mycorrhizal arbuscule formation in rice. Plant J **69**: 906–920

Handa Y, Nishide H, Takeda N, Suzuki Y, Kawaguchi M, Saito K (2015) RNA-seq Transcriptional Profiling of an Arbuscular Mycorrhiza Provides Insights into Regulated and Coordinated Gene Expression in Lotus japonicus and Rhizophagus irregularis. Plant Cell Physiol **56**: 1490–1511

Harrison MJ (1996) A sugar transporter from Medicago truncatula: altered expression pattern in roots during vesicular-arbuscular (VA) mycorrhizal associations. Plant J **9**: 491–503

Harrison MJ (1998) Development of the arbuscular mycorrhizal symbiosis. Curr Opin Plant Biol **1**: 360–365

Harrison MJ (2005) Signaling in the arbuscular mycorrhizal symbiosis. Annu Rev Microbiol **59**: 19–42

Harrison MJ (2012) Cellular programs for arbuscular mycorrhizal symbiosis. Curr Opin Plant Biol **15**: 691–698

Harrison MJ, van Buuren ML (1995) A phosphate transporter from the mycorrhizal fungus Glomus versiforme. Nature **378**: 626–629

Harrison M, Dewbre G, Liu J (2002) A phosphate transporter from Medicago truncatula involved in the acquisition of phosphate released by arbuscular mycorrhizal fungi. Plant Cell **14**: 2413–2429

Hayashi S, Gresshoff PM, Ferguson BJ (2014) Mechanistic action of gibberellins in legume nodulation. J Integr Plant Biol **56**: 971–978

Hayashi T, Banba M, Shimoda Y, Kouchi H, Hayashi M, Imaizumi-Anraku H (2010) A dominant function of CCaMK in intracellular accommodation of bacterial and fungal endosymbionts. Plant J **63**: 141–54

Heck C, Kuhn H, Heidt S, Walter S, Rieger N, Requena N (2016) Symbiotic Fungi Control Plant Root Cortex Development through the Novel GRAS Transcription Factor MIG1. Curr Biol **26**: 2770–2778

Heckmann AB, Lombardo F, Miwa H, Perry JA, Bunnewell S, Parniske M, Wang TL, Downie JA (2006) Lotus japonicus nodulation requires two GRAS domain regulators, one of which is functionally conserved in a non-legume. Plant Physiol **142**: 1739–50

Hedden P, Thomas SG (2012) Gibberellin biosynthesis and its regulation. Biochem J **444**: 11–25

Helber N, Wippel K, Sauer N, Schaarschmidt S, Hause B, Requena N (2011) A Versatile Monosaccharide Transporter That Operates in the Arbuscular Mycorrhizal Fungus Glomus sp Is Crucial for the Symbiotic Relationship with Plants. Plant Cell **23**: 3812–3823

Hijikata N, Masatake M, Tani C, Ohtomo R, Osaki M, Ezawa T (2010) Polyphosphate has a central role in the rapid and massive accumulation of phosphorus in extraradical mycelium of an arbuscular mycorrhizal fungus. New Phytol **186**: 263–264

Hirsch S, Kim J, Muñoz A, Heckmann AB, Downie JA, Oldroyd GED (2009) GRAS proteins form a DNA binding complex to induce gene expression during nodulation signaling in Medicago truncatula. Plant Cell **21**: 545–57

Ho I, Trappe JM (1973) Translocation of 14C from Festuca Plants to their Endomycorrhizal Fungi. Nature **244**: 30–31

Hogekamp C, Arndt D, Pereira P a, Becker JD, Hohnjec N, Küster H (2011) Laser microdissection unravels cell-type-specific transcription in arbuscular mycorrhizal roots, including CAAT-box transcription factor gene expression correlating with fungal contact and spread. Plant Physiol **157**: 2023–43

Hogekamp C, Küster H (2013) A roadmap of cell-type specific gene expression during sequential stages of the arbuscular mycorrhiza symbiosis. BMC Genomics **14**: 306

Hohnjec N, Czaja-Hasse LF, Hogekamp C, Küster H (2015) Pre-announcement of symbiotic guests: transcriptional reprogramming by mycorrhizal lipochitooligosaccharides shows a strict co-dependency on the GRAS transcription factors NSP1 and RAM1. BMC Genomics **16**: 994

Hohnjec N, Perlick AM, Pühler A, Küster H (2003) The Medicago truncatula sucrose synthase gene MtSucS1 is activated both in the infected region of root nodules and in the cortex of roots colonized by arbuscular mycorrhizal fungi. Mol Plant-Microbe Interact **16**: 903–15

Hohnjec N, Vieweg M, Pühler A (2005) Overlaps in the transcriptional profiles of Medicago truncatula roots inoculated with two different Glomus fungi provide insights into the genetic program activated during arbuscular mycorrhiza. Plant Physiol **137**: 1283–1301

Horváth B, Yeun LH, Domonkos A, Halász G, Gobbato E, Ayaydin F, Miró K, Hirsch S, Sun J, Tadege M, et al (2011) Medicago truncatula IPD3 is a member of the common symbiotic signaling pathway required for rhizobial and mycorrhizal symbioses. Mol Plant-Microbe Interact **24**: 1345–58

Humphreys CP, Franks PJ, Rees M, Bidartondo MI, Leake JR, Beerling DJ (2010) Mutualistic mycorrhiza-like symbiosis in the most ancient group of land plants. Nat Commun **1**: 103

Indrasumunar A, Kereszt A, Searle I, Miyagi M, Li D, Nguyen CDT, Men A, Carroll BJ, Gresshoff PM (2010) Inactivation of duplicated nod factor receptor 5 (NFR5) genes in recessive loss-of-function non-nodulation mutants of allotetraploid soybean (Glycine max L. Merr.). Plant Cell Physiol **51**: 201–214

Ivanov S, Fedorova EE, Limpens E, De Mita S, Genre a., Bonfante P, Bisseling T (2012) Rhizobium-legume symbiosis shares an exocytotic pathway required for arbuscule formation. Proc Natl Acad Sci **109**: 8316–8321

Javot H, Penmetsa RV, Terzaghi N, Cook DR, Harrison MJ (2007) A Medicago truncatula phosphate transporter indispensable for the arbuscular mycorrhizal symbiosis. Proc Natl Acad Sci **104**: 1720–1725

Javot H, Penmetsa RV, Breuillin F, Bhattarai KK, Noar RD, Gomez SK, Zhang Q, Cook DR, Harrison MJ (2011) Medicago truncatula mtpt4 mutants reveal a role for nitrogen in the regulation of arbuscule degeneration in arbuscular mycorrhizal symbiosis. Plant J **68**: 954–965

Javot H, Pumplin N, Harrison MJ (2007) Phosphate in the arbuscular mycorrhizal symbiosis: transport properties and regulatory roles. Plant, Cell Environ **30**: 310–322

Jin Y, Liu H, Luo D, Yu N, Dong W, Wang C, Zhang X, Dai H, Yang J, Wang E (2016) DELLA proteins are common components of symbiotic rhizobial and mycorrhizal signalling pathways. Nat Commun **7**: 12433

Journet EP, El-Gachtouli N, Vernoud V, de Billy F, Pichon M, Dedieu A, Arnould C, Morandi D, Barker DG, Gianinazzi-Pearson V (2001) Medicago truncatula ENOD11: a novel RPRP-encoding early nodulin gene expressed during mycorrhization in arbuscule-containing cells. Mol Plant-Microbe Interact **14**: 737–48

Kaló P, Gleason C, Edwards A, Marsh J, Mitra RM, Hirsch S, Jakab J, Sims S, Long SR, Rogers J, et al (2005) Nodulation signaling in legumes requires NSP2, a member of the GRAS family of transcriptional regulators. Science **308**: 1786–9

Kanamori N, Madsen LH, Radutoiu S, Frantescu M, Quistgaard EMH, Miwa H, Downie JA, James EK, Felle HH, Haaning LL, et al (2006) A nucleoporin is required for induction of Ca2+ spiking in legume nodule development and essential for rhizobial and fungal symbiosis. Proc Natl Acad Sci **103**: 359–364

Kaufmann K, Muiño JM, Østerås M, Farinelli L, Krajewski P, Angenent GC (2010) Chromatin immunoprecipitation (ChIP) of plant transcription factors followed by sequencing (ChIP-SEQ) or hybridization to whole genome arrays (ChIP-CHIP). Nat Protoc **5**: 457–72

Kevei Z, Lougnon G, Mergaert P, Horváth G V, Kereszt A, Jayaraman D, Zaman N, Marcel F, Regulski K, Kiss GB, et al (2007) 3-hydroxy-3-methylglutaryl coenzyme a reductase 1 interacts with NORK and is crucial for nodulation in Medicago truncatula. Plant Cell **19**: 3974–89

Kinkema M, Geijskes RJ, Shand K, Coleman HD, De Lucca PC, Palupe A, Harrison MD, Jepson I, Dale JL, Sainz MB (2014) An improved chemically inducible gene switch that functions in the monocotyledonous plant sugar cane. Plant Mol Biol **84**: 443–454

Kistner C, Winzer T, Pitzschke A (2005) Seven Lotus japonicus genes required for transcriptional reprogramming of the root during fungal and bacterial symbiosis. Plant Cell **17**: 2217–2229

Kistner C, Parniske M (2002) Evolution of signal transduction in intracellular symbiosis. Trends Plant Sci **7**: 511–518

Kobae Y, Hata S (2010) Dynamics of periarbuscular membranes visualized with a fluorescent phosphate transporter in arbuscular mycorrhizal roots of rice. Plant Cell Physiol **51**: 341–353

Kobae Y, Tamura Y, Takai S, Banba M, Hata S (2010) Localized expression of arbuscular mycorrhiza-inducible ammonium transporters in soybean. Plant Cell Physiol **51**: 1411–5

Koegel S, Ait Lahmidi N, Arnould C, Chatagnier O, Walder F, Ineichen K, Boller T, Wipf D, Wiemken A, Courty PE (2013) The family of ammonium transporters (AMT) in Sorghum bicolor: Two AMT members are induced locally, but not systemically in roots colonized by arbuscular mycorrhizal fungi. New Phytol **198**: 853–865

Koltai H, LekKala SP, Bhattacharya C, Mayzlish-Gati E, Resnick N, Wininger S, Dor E, Yoneyama K, Yoneyama K, Hershenhorn J, et al (2010) A tomato strigolactone-impaired mutant displays aberrant shoot morphology and plant interactions. J Exp Bot **61**: 1739–49

Kosuta S, Chabaud M, Lougnon G (2003) A diffusible factor from arbuscular mycorrhizal fungi induces symbiosis-specific MtENOD11 expression in roots ofMedicago truncatula. Plant Physiol. doi: 10.1104/pp.011882.1

Kosuta S, Hazledine S, Sun J, Miwa H, Morris RJ, Downie JA, Oldroyd GED (2008) Differential and chaotic calcium signatures in the symbiosis signaling pathway of legumes. Proc Natl Acad Sci **105**: 9823–8

Krajinski F, Courty P-E, Sieh D, Franken P, Zhang H, Bucher M, Gerlach N, Kryvoruchko I, Zoeller D, Udvardi M, et al (2014) The H+-ATPase HA1 of Medicago truncatula Is Essential for Phosphate Transport and Plant Growth during Arbuscular Mycorrhizal Symbiosis. Plant Cell **26**: 1808–1817

Krajinski F, Frenzel A (2007) Towards the elucidation of AM-specific transcription in Medicago truncatula. Phytochemistry **68**: 75–81

Krajinski F, Hause B, Gianinazzi-Pearson V, Franken P (2002) Mtha1, a Plasma Membrane H+-ATPase Gene from Medicago truncatula, Shows Arbuscule-Specific Induced Expression in Mycorrhizal Tissue. Plant Biol **4**: 754–761

Kretzschmar T, Kohlen W, Sasse J, Borghi L, Schlegel M, Bachelier JB, Reinhardt D, Bours R, Bouwmeester HJ, Martinoia E (2012) A petunia ABC protein controls strigolactone-dependent symbiotic signalling and branching. Nature **483**: 341–344

Kuhn H, Küster H, Requena N (2010) Membrane steroid-binding protein 1 induced by a diffusible fungal signal is critical for mycorrhization in Medicago truncatula. New Phytol **185**: 716–33

Küster H, Vieweg MF, Manthey K, Baier MC, Hohnjec N, Perlick AM (2007) Identification and expression regulation of symbiotically activated legume genes. Phytochemistry **68**: 8–18

Lauressergues D, Delaux P-M, Formey D, Lelandais-Brière C, Fort S, Cottaz S, Bécard G, Niebel A, Roux C, Combier J-P (2012) The microRNA miR171h modulates arbuscular mycorrhizal colonization of Medicago truncatula by targeting NSP2. Plant J **72**: 512–22

Leigh J, Hodge A, Fitter AH (2009) Arbuscular mycorrhizal fungi can transfer substantial amounts of nitrogen to their host plant from organic material. New Phytol **181**: 199–207

Lévy J, Bres C, Geurts R, Chalhoub B, Kulikova O, Duc G, Journet E-P, Ané J-M, Lauber E, Bisseling T, et al (2004) A putative Ca2+ and calmodulin-dependent protein kinase required for bacterial and fungal symbioses. Science **303**: 1361–4

Li N, Xu C, Li-Beisson Y, Philippar K (2015) Fatty Acid and Lipid Transport in Plant Cells. Trends Plant Sci **21**: 145–158

Liao J, Singh S, Hossain MS, Andersen SU, Ross L, Bonetta D, Zhou Y, Sato S, Tabata S, Stougaard J, et al (2012) Negative regulation of CCaMK is essential for symbiotic infection. Plant J **72**: 572–84

Liu J, Blaylock L, Endre G, Cho J (2003) Transcript profiling coupled with spatial expression analyses reveals genes involved in distinct developmental stages of an arbuscular mycorrhizal symbiosis. Plant Cell **15**: 2106–2123

Liu J, Maldonado-Mendoza I, Lopez-Meyer M, Cheung F, Town CD, Harrison MJ (2007) Arbuscular mycorrhizal symbiosis is accompanied by local and systemic alterations in gene expression and an increase in disease resistance in the shoots. Plant J **50**: 529–544

Liu J, Novero M, Charnikhova T, Ferrandino A, Schubert A, Ruyter-Spira C, Bonfante P, Lovisolo C, Bouwmeester HJ, Cardinale F (2013) Carotenoid cleavage dioxygenase 7 modulates plant growth, reproduction, senescence, and determinate nodulation in the model legume Lotus japonicus. J Exp Bot **64**: 1967–1981

Liu W, Kohlen W, Lillo A, Op den Camp R, Ivanov S, Hartog M, Limpens E, Jamil M, Smaczniak C, Kaufmann K, et al (2011) Strigolactone biosynthesis in Medicago truncatula and rice requires the symbiotic GRAS-type transcription factors NSP1 and NSP2. Plant Cell **23**: 3853–65

Livak KJ, Schmittgen TD (2001) Analysis of relative gene expression data using real-time quantitative PCR and. Methods **25**: 402–408

Lohse S, Schliemann W, Ammer C, Kopka J, Strack D, Fester T (2005) Organization and metabolism of plastids and mitochondria in arbuscular mycorrhizal roots of Medicago truncatula. Plant Physiol **139**: 329–40

López-Pedrosa A, González-Guerrero M, Valderas A, Azcón-Aguilar C, Ferrol N (2006) GintAMT1 encodes a functional high-affinity ammonium transporter that is expressed in the extraradical mycelium of Glomus intraradices. Fungal Genet Biol **43**: 102–110

López-Ráez J a., Charnikhova T, Fernández I, Bouwmeester H, Pozo MJ (2011) Arbuscular mycorrhizal symbiosis decreases strigolactone production in tomato. J Plant Physiol **168**: 294–297

López-Ráez JA, Fernandez I, Garcia JM, Berrio E, Bonfante P, Walter MH, Pozo MJ (2015) Differential spatio-temporal expression of carotenoid cleavage dioxygenases regulates apocarotenoid fluxes during AM symbiosis. Plant Sci **230**: 59–69

López-Ráez JA, Bouwmeester H (2008) Fine-tuning regulation of strigolactone biosynthesis under phosphate starvation. Plant Signal Behav **3**: 963–5

Lu S, Eck J van, Zhou XJ, Lopez AB, O'Halloran DM, Cosman KM, Conlin BJ, Paolillo DJ, Garvin DF, Vrebalov J, et al (2006) The cauliflower Or gene encodes a DnaJ cysteine-rich domain-containing protein that mediates high levels of b-carotene accumulation. Plant Cell **18**: 3594–3605

Luginbuehl L, Oldroyd GED (2016) Calcium signaling and transcriptional regulation in arbuscular mycorrhizal symbiosis. Mol. Mycorrhizal Symbiosis Chapter 8

Maeda D, Ashida K, Iguchi K, Chechetka SA, Hijikata A, Okusako Y, Deguchi Y, Izui K, Hata S (2006) Knockdown of an Arbuscular Mycorrhiza-inducible Phosphate Transporter Gene of Lotus japonicus Suppresses Mutualistic Symbiosis. Plant Cell Physiol **47:** 807–817

Maekawa T, Maekawa-Yoshikawa M, Takeda N, Imaizumi-Anraku H, Murooka Y, Hayashi M (2009) Gibberellin controls the nodulation signaling pathway in Lotus japonicus. Plant J **58**: 183–94

Maillet F, Poinsot V, André O, Puech-Pagès V, Haouy A, Gueunier M, Cromer L, Giraudet D, Formey D, Niebel A, et al (2011) Fungal lipochitooligosaccharide symbiotic signals in arbuscular mycorrhiza. Nature **469**: 58–63

Maldonado-Mendoza I, Dewbre G, Harrison M (2001) A phosphate transporter gene from the extraradical mycelilum of an arbuscular my- corrhizal fungus Glomus intraradices is regulated in response to phosphate in the environment. Mol Plant-Microbe Interact **14**: 1140–1148

Manck-Götzenberger J, Requena N (2016) Arbuscular mycorrhiza Symbiosis Induces a Major Transcriptional Reprogramming of the Potato SWEET Sugar Transporter Family. Front Plant Sci **7**: 1–14

Manthey K, Krajinski F (2004) Transcriptome profiling in root nodules and arbuscular mycorrhiza identifies a collection of novel genes induced during Medicago truncatula root endosymbioses. Mol Plant-Microbe Interact **17**: 1063–1077

Marchive C, Nikovics K, To A, Lepiniec L, Baud S (2014) Transcriptional regulation of fatty acid production in higher plants: Molecular bases and biotechnological outcomes. Eur J Lipid Sci Technol **116**: 1332–1343

McFarlane HE, Shin JJH, Bird DA, Samuels AL (2010) Arabidopsis ABCG transporters, which are required for export of diverse cuticular lipids, dimerize in different combinations. Plant Cell **22**: 3066–75

Messinese E, Mun J-H, Yeun LH, Jayaraman D, Rougé P, Barre A, Lougnon G, Schornack S, Bono J-J, Cook DR, et al (2007) A novel nuclear protein interacts with the symbiotic DMI3 calcium- and calmodulin-dependent protein kinase of Medicago truncatula. Mol Plant-Microbe Interact **20**: 912–21

Mitchum MG, Yamaguchi S, Hanada A, Kuwahara A, Yoshioka Y, Kato T, Tabata S, Kamiya Y, Sun TP (2006) Distinct and overlapping roles of two gibberellin 3-oxidases in Arabidopsis development. Plant J **45**: 804–818

Mitra RM, Gleason C a, Edwards A, Hadfield J, Downie JA, Oldroyd GED, Long SR (2004) A Ca2+/calmodulin-dependent protein kinase required for symbiotic nodule development: Gene identification by transcript-based cloning. Proc Natl Acad Sci **101**: 4701–5

Mitra RM, Shaw SL, Long SR (2004) Six nonnodulating plant mutants defective for Nod factor-induced transcriptional changes associated with the legume-rhizobia symbiosis. Proc Natl Acad Sci **101**: 10217–22

Miwa H, Sun J, Oldroyd GED, Downie JA (2006) Analysis of calcium spiking using a cameleon calcium sensor reveals that nodulation gene expression is regulated by calcium spike number and the developmental status of the cell. Plant J **48**: 883–94

Miyata K, Kozaki T, Kouzai Y, Ozawa K, Ishii K, Asamizu E, Okabe Y, Umehara Y, Miyamoto A, Kobae Y, et al (2014) The bifunctional plant receptor, OsCERK1, regulates both chitin-triggered immunity and arbuscular mycorrhizal symbiosis in rice. Plant Cell Physiol **55**: 1864-1872

Moscatiello R, Sello S, Novero M, Negro A, Bonfante P, Navazio L (2014) The intracellular delivery of TAT-aequorin reveals calcium-mediated sensing of environmental and symbiotic signals by the arbuscular mycorrhizal fungus Gigaspora margarita. New Phytol **203**: 1012–1020

Murakami Y, Miwa H, Imaizumi-Anraku H, Kouchi H, Downie JA, Kawaguchi M, Kawasaki S (2006) Positional cloning identifies Lotus japonicus NSP2, a putative transcription factor of the GRAS family, required for NIN and ENOD40 gene expression in nodule initiation. DNA Res **13**: 255–65

Murray JD, Muni RRD, Torres-Jerez I, Tang Y, Allen S, Andriankaja M, Li G, Laxmi A, Cheng X, Wen J, et al (2011) Vapyrin, a gene essential for intracellular progression of arbuscular mycorrhizal symbiosis, is also essential for infection by rhizobia in the nodule symbiosis of Medicago truncatula. Plant J **65**: 244–252

Nadal M, Paszkowski U (2013) Polyphony in the rhizosphere: Presymbiotic communication in arbuscular mycorrhizal symbiosis. Curr Opin Plant Biol **16**: 473–479

Nagae M, Takeda N, Kawaguchi M (2014) Common symbiosis genes CERBERUS and NSP1 provide additional insight into the establishment of arbuscular mycorrhizal and root nodule symbioses in Lotus japonicus. Plant Signal Behav **9**: 37–41

Nagahashi G, Douds DD (2011) The effects of hydroxy fatty acids on the hyphal branching of germinated spores of AM fungi. Fungal Biol **115**: 351–8

Nagy R, Karandashov V, Chague V, Kalinkevich K, Tamasloukht M, Xu G, Jakobsen I, Levy AA, Amrhein N, Bucher M (2005) The characterization of novel mycorrhiza-specific phosphate transporters from Lycopersicon esculentum and Solanum tuberosum uncovers functional redundancy in symbiotic phosphate transport in solanaceous species. Plant J **42**: 236–250

Navazio L, Moscatiello R, Genre A, Novero M, Baldan B, Bonfante P, Mariani P (2007) A diffusible signal from arbuscular mycorrhizal fungi elicits a transient cytosolic calcium elevation in host plant cells. Plant Physiol **144**: 673–81

Nelson DC, Scaf A, Dun EA, Waters MT, Flematti GR, Dixon KW, Beveridge CA, Ghisalberti EL, Smith SM (2011) F-box protein MAX2 has dual roles in karrikin and strigolactone signaling in *Arabidopsis thaliana*. Proc Natl Acad Sci **108**: 8897–8902

Oláh B, Brière C, Bécard G, Dénarié J, Gough C (2005) Nod factors and a diffusible factor from arbuscular mycorrhizal fungi stimulate lateral root formation in Medicago truncatula via the DMI1/DMI2 signalling pathway. Plant J **44**: 195–207

Oldroyd GED (2013) Speak, friend, and enter: signalling systems that promote beneficial symbiotic associations in plants. Nat Rev Microbiol **11**: 252–63

Oldroyd GED, Downie JA (2004) Calcium, kinases and nodulation signalling in legumes. Nat Rev Mol Cell Biol **5**: 566–576

Oldroyd GED, Harrison MJ, Paszkowski U (2009) Reprogramming plant cells for endosymbiosis. Science **324**: 753–4

Op den Camp R, Streng A, De Mita S, Cao Q, Polone E, Liu W, Ammiraju JSS, Kudrna D, Wing R, Untergasser A, et al (2011) LysM-Type Mycorrhizal Receptor. Science 331: 909–912

Ortu G, Balestrini R, Pereira PA, Becker JD, Küster H, Bonfante P (2012) Plant genes related to gibberellin biosynthesis and signaling are differentially regulated during the early Stages of AM fungal interactions. Mol Plant **5**: 951–954

Osipova M a., Mortier V, Demchenko KN, Tsyganov VE, Tikhonovich I a., Lutova L a., Dolgikh E a., Goormachtig S (2012) WUSCHEL-RELATED HOMEOBOX5 Gene Expression and Interaction of CLE Peptides with Components of the Systemic Control Add Two Pieces to the Puzzle of Autoregulation of Nodulation. Plant Physiol **158**: 1329–1341

Ovchinnikova E, Journet E, Chabaud M, Cosson V, Ratet P, Duc G, Fedorova E, Liu W, den Camp RO, Zhukov V, et al (2011) IPD3 controls the formation of nitrogen-fixing symbiosomes in pea and Medicago Spp. Mol Plant-Microbe Interact **24**: 1333–44

Pan H, Oztas O, Zhang X, Wu X, Stonoha C, Wang E, Wang B, Wang D (2016) A symbiotic SNARE protein generated by alternative termination of transcription. Nat Plants **2**: 15197

Panikashvili D, Shi JX, Bocobza S, Franke RB, Schreiber L, Aharoni A (2010) The arabidopsis DSO/ABCG11 transporter affects cutin metabolism in reproductive organs and suberin in roots. Mol Plant **3**: 563–575

Panikashvili D, Shi JX, Schreiber L, Aharoni A (2011) The Arabidopsis ABCG13 transporter is required for flower cuticle secretion and patterning of the petal epidermis. New Phytol **190**: 113–124

Pao SS, Paulsen IT, Saier MH (1998) Major facilitator superfamily. Microbiol Mol Biol Rev **62**: 1–34

Park H-J, Floss DS, Levesque-Tremblay V, Bravo A, Harrison MJ (2015) Hyphal Branching during Arbuscule Development Requires Reduced Arbuscular Mycorrhiza1. Plant Physiol **169**: 2774–88

Parniske M (2008) Arbuscular mycorrhiza: the mother of plant root endosymbioses. Nat Rev Microbiol **6**: 763–775

Parniske M (2004) Molecular genetics of the arbuscular mycorrhizal symbiosis. Curr Opin Plant Biol **7**: 414–421

Paszkowski U, Kroken S, Roux C, Briggs SP (2002) Rice phosphate transporters include an evolutionarily divergent gene specifically activated in arbuscular mycorrhizal symbiosis. Proc Natl Acad Sci **99**: 13324–13329

Peiter E, Sun J, Heckmann AB, Venkateshwaran M, Riely BK, Otegui MS, Edwards A, Freshour G, Hahn MG, Cook DR, et al (2007) The Medicago truncatula DMI1 protein modulates cytosolic calcium signaling. Plant Physiol **145**: 192–203

Pfeffer PE, Douds DD, Bécard G, Shachar-Hill Y (1999) Carbon Uptake and the Metabolism and Transport of Lipids in an Arbuscular Mycorrhiza1. Plant Physiol **120**: 587–598

Pighin J a, Zheng H, Balakshin LJ, Goodman IP, Western TL, Jetter R, Kunst L, Samuels a L (2004) Plant cuticular lipid export requires an ABC transporter. Science **306**: 702–4

Pimprikar P, Carbonnel S, Paries M, Katzer K, Klingl V, Bohmer MJ, Karl L, Floss DS, Harrison MJ, Parniske M, et al (2016) A CCaMK-CYCLOPS-DELLA Complex Activates Transcription of RAM1 to Regulate Arbuscule Branching. Curr Biol **26**: 987–998

Prell J, Poole P (2006) Metabolic changes of rhizobia in legume nodules. Trends Microbiol **14**: 161–168

Pumplin N, Harrison MJ (2009) Live-cell imaging reveals periarbuscular membrane domains and organelle location in Medicago truncatula roots during arbuscular mycorrhizal symbiosis. Plant Physiol **151**: 809–19

Pumplin N, Mondo SJ, Topp S, Starker CG, Gantt JS, Harrison MJ (2010) Medicago truncatula Vapyrin is a novel protein required for arbuscular mycorrhizal symbiosis. Plant J **61**: 482–94

Pumplin N, Zhang X, Noar RD, Harrison MJ (2012) Polar localization of a symbiosis-specific phosphate transporter is mediated by a transient reorientation of secretion. Proc Natl Acad Sci **109**: E665–72

Radutoiu S, Madsen LH, Madsen EB, Felle HH, Umehara Y, Grønlund M, Sato S, Nakamura Y, Tabata S, Sandal N, et al (2003) Plant recognition of symbiotic bacteria requires two LysM receptor-like kinases. Nature **425**: 585–592

Rausch C, Daram P, Brunner S, Jansa J (2001) A phosphate transporter expressed in arbuscule-containing cells in potato. Nature **414**: 462-466

Remy W, Taylor T, Hass H, Kerp H (1994) Four hundred-million-year-old vesicular arbuscular mycorrhizae. Proc Natl Acad Sci **91**: 11841–11843

Rich MK, Schorderet M, Bapaume L, Falquet L, Morel P, Vandenbussche M, Reinhardt D (2015) The Petunia GRAS Transcription Factor ATA/RAM1 Regulates Symbiotic Gene Expression and Fungal Morphogenesis in Arbuscular Mycorrhiza. Plant Physiol **168**: 788–797

Rieu I, Ruiz-Rivero O, Fernandez-Garcia N, Griffiths J, Powers SJ, Gong F, Linhartova T, Eriksson S, Nilsson O, Thomas SG, et al (2008) The gibberellin biosynthetic genes AtGA20ox1 and AtGA20ox2 act, partially redundantly, to promote growth and development throughout the Arabidopsis life cycle. Plant J **53**: 488–504

Routray P, Miller JB, Du L, Oldroyd G, Poovaiah BW (2013) Phosphorylation of S344 in the calmodulin-binding domain negatively affects CCaMK function during bacterial and fungal symbioses. Plant J **76**: 287–96

Roux B, Rodde N, Jardinaud MF, Timmers T, Sauviac L, Cottret L, Carrère S, Sallet E, Courcelle E, Moreau S, et al (2014) An integrated analysis of plant and bacterial gene expression in symbiotic root nodules using laser-capture microdissection coupled to RNA sequencing. Plant J **77**: 817–837

Ruyter-Spira C, Al-Babili S, van der Krol S, Bouwmeester H (2013) The biology of strigolactones. Trends Plant Sci **18**: 72–83

Saito K, Yoshikawa M, Yano K, Miwa H, Uchida H, Asamizu E, Sato S, Tabata S, Imaizumi-Anraku H, Umehara Y, et al (2007) NUCLEOPORIN85 is required for calcium spiking, fungal and bacterial symbioses, and seed production in Lotus japonicus. Plant Cell **19**: 610–24

Salas JJ, Ohlrogge JB (2002) Characterization of substrate specificity of plant FatA and FatB acyl-ACP thioesterases. Arch Biochem Biophys **403**: 25–34

Samalova M, Brzobohaty B, Moore I (2005) pOp6/LhGR: A stringently regulated and highly responsive dexamethasone-inducible gene expression system for tobacco. Plant J **41**: 919–935

Samuels L, Kunst L, Jetter R (2008) Sealing plant surfaces: cuticular wax formation by epidermal cells. Annu Rev Plant Biol **59**: 683–707

Sathyanarayanan P V., Cremo CR, Poovaiah BW (2000) Plant chimeric Ca2+/calmodulin-dependent protein kinase. Role of the neural visinin-like domain in regulating autophosphorylation and calmodulin affinity. J Biol Chem **275**: 30417–30422

Sathyanarayanan P V., Siems WF, Jones JP, Poovaiah BW (2001) Calcium-stimulated Autophosphorylation Site of Plant Chimeric Calcium/Calmodulin-dependent Protein Kinase. J Biol Chem **276**: 32940–32947

Schaarschmidt S, Gresshoff PM, Hause B (2013) Analyzing the soybean transcriptome during autoregulation of mycorrhization identifies the transcription factors GmNF-YA1a/b as positive regulators of arbuscular mycorrhization. Genome Biol **14**: R62

Schaarschmidt S, Roitsch T, Hause B (2006) Arbuscular mycorrhiza induces gene expression of the apoplastic invertase LIN6 in tomato (Lycopersicon esculentum) roots. J Exp Bot **57**: 4015–4023

Schauser L, Roussis a, Stiller J, Stougaard J (1999) A plant regulator controlling development of symbiotic root nodules. Nature **402**: 191–195

Schliemann W, Ammer C, Strack D (2008) Metabolite profiling of mycorrhizal roots of Medicago truncatula. Phytochemistry **69**: 112–146

Schwartz SH, Qin X, Loewen MC (2004) The biochemical characterization of two carotenoid cleavage enzymes from Arabidopsis indicates that a carotenoid-derived compound inhibits lateral branching. J Biol Chem **279**: 46940–46945

Sekhara Reddy DMR, Schorderet M, Feller U, Reinhardt D (2007) A petunia mutant affected in intracellular accommodation and morphogenesis of arbuscular mycorrhizal fungi. Plant J **51**: 739–750

Shachar-Hill Y, Pfeffer PE, Douds D, Osman SF, Doner LW, Ratcliffe RG (1995) Partitioning of Intermediary Carbon Metabolism in Vesicular-Arbuscular Mycorrhizal Leek. Plant Physiol **108**: 7–15

Shimizu T, Nakano T, Takamizawa D, Desaki Y, Ishii-Minami N, Nishizawa Y, Minami E, Okada K, Yamane H, Kaku H, et al (2010) Two LysM receptor molecules, CEBiP and OsCERK1, cooperatively regulate chitin elicitor signaling in rice. Plant J **64**: 204–214

Shimoda Y, Han L, Yamazaki T, Suzuki R, Hayashi M, Imaizumi-Anraku H (2012) Rhizobial and fungal symbioses show different requirements for calmodulin binding to calcium calmodulin-dependent protein kinase in Lotus japonicus. Plant Cell **24**: 304–21

Siciliano V, Genre A, Balestrini R, Cappellazzo G, deWit PJGM, Bonfante P (2007) Transcriptome analysis of arbuscular mycorrhizal roots during development of the prepenetration apparatus. Plant Physiol **144**: 1455–66

Sieberer BJ, Chabaud M, Fournier J, Timmers ACJ, Barker DG (2012) A switch in Ca2+ spiking signature is concomitant with endosymbiotic microbe entry into cortical root cells of Medicago truncatula. Plant J **69**: 822–30

Singh S, Katzer K, Lambert J, Cerri M, Parniske M (2014) CYCLOPS, a DNA-binding transcriptional activator, orchestrates symbiotic root nodule development. Cell Host Microbe **15**: 139–52

Smit P, Limpens E, Geurts R, Fedorova E, Dolgikh E, Gough C, Bisseling T (2007) Medicago LYK3, an entry receptor in rhizobial nodulation factor signaling. Plant Physiol **145**: 183–91

Smit P, Raedts J, Portyanko V, Debellé F, Gough C, Bisseling T, Geurts R (2005) NSP1 of the GRAS protein family is essential for rhizobial Nod factor-induced transcription. Science **308**: 1789–91

Smith SE, Read DJ (2008) Mycorrhizal symbiosis. Acad. Press 3rd edition

Smith SE, Smith FA (2011) Roles of arbuscular mycorrhizas in plant nutrition and growth: new paradigms from cellular to ecosystem scales. Annu Rev Cell Dev Biol plant Biol **62**: 227–50

Solaiman MZ, Saito M (1997) Use of sugars by intraradical hyphae of arbuscular mycorrhizal fungi revealed by radiorespirometry. New Phytol **136**: 533–538

Soto MJ, Fernández-Aparicio M, Castellanos-Morales V, García-Garrido JM, Ocampo JA, Delgado MJ, Vierheilig H (2010) First indications for the involvement of strigolactones on nodule formation in alfalfa (Medicago sativa). Soil Biol Biochem **42**: 383–385

Stracke S, Kistner C, Yoshida S, Mulder L, Sato S, Kaneko T, Tabata S, Sandal N, Stougaard J, Szczyglowski K, et al (2002) A plant receptor-like kinase required for both bacterial and fungal symbiosis. Nature **417**: 959–962

Sun J, Miller JB, Granqvist E, Wiley-Kalil A, Gobbato E, Maillet F, Cottaz S, Samain E, Venkateshwaran M, Fort S, et al (2015) Activation of Symbiosis Signaling by Arbuscular Mycorrhizal Fungi in Legumes and Rice. Plant Cell **27**: 823-838

Swainsbury DJK, Zhou L, Oldroyd GED, Bornemann S (2012) Calcium ion binding properties of Medicago truncatula calcium/calmodulin-dependent protein kinase. Biochemistry **51**: 6895–6907

Tadege M, Wen J, He J, Tu H, Kwak Y, Eschstruth A, Cayrel A, Endre G, Zhao PX, Chabaud M, et al (2008) Large-scale insertional mutagenesis using the Tnt1 retrotransposon in the model legume Medicago truncatula. Plant J **54**: 335–347

Takeda N, Haage K, Sato S, Tabata S, Parniske M (2011) Activation of a Lotus japonicus subtilase gene during arbuscular mycorrhiza is dependent on the common symbiosis genes and two cis-active promoter regions. Mol Plant-Microbe Interact **24**: 662–670

Takeda N, Handa Y, Tsuzuki S, Kojima M (2015) Gibberellins Interfere with Symbiosis Signaling and Gene Expression and Alter Colonization by Arbuscular Mycorrhizal Fungi in Lotus japonicus. Plant Physiol **167**: 545–557

Takeda N, Maekawa T, Hayashi M (2012) Nuclear-localized and deregulated calcium- and calmodulin-dependent protein kinase activates rhizobial and mycorrhizal responses in Lotus japonicus. Plant Cell **24**: 810–22

Takeda N, Sato S, Asamizu E, Tabata S, Parniske M (2009) Apoplastic plant subtilases support arbuscular mycorrhiza development in Lotus japonicus. Plant J **58**: 766–77

Takeda N, Tsuzuki S, Suzaki T, Parniske M, Kawaguchi M (2013) CERBERUS and NSP1 of lotus japonicus are common symbiosis genes that modulate arbuscular mycorrhiza development. Plant Cell Physiol **54**: 1711–1723

Takezawa D, Ramachandiran S, Paranjape V, Poovaiah BW (1996) Dual regulation of a chimeric plant serine/threonine kinase by calcium and calcium/calmodulin. J Biol Chem **271**: 8126–8132

Tamura Y, Kobae Y, Mizuno T, Hata S (2012) Identification and Expression Analysis of Arbuscular Mycorrhiza-Inducible Phosphate Transporter Genes of Soybean. Biosci Biotechnol Biochem **76**: 309–313

Tanaka Y, Yano K (2005) Nitrogen delivery to maize via mycorrhizal hyphae depends on the form of N supplied. Plant, Cell Environ **28**: 1247–1254

Tang N, San Clemente H, Roy S, Bécard G, Zhao B, Roux C (2016) A Survey of the gene repertoire of Gigaspora rosea unravels conserved features among glomeromycota for obligate biotrophy. Front Microbiol **7**: 1–16

Tirichine L, Imaizumi-Anraku H, Yoshida S, Murakami Y, Madsen LH, Miwa H, Nakagawa T, Sandal N, Albrektsen AS, Kawaguchi M, et al (2006) Deregulation of a Ca2+/calmodulin-dependent kinase leads to spontaneous nodule development. Nature **441**: 1153–6

Tisserant E, Malbreil M, Kuo a., Kohler a., Symeonidi a., Balestrini R, Charron P, Duensing N, Frei dit Frey N, Gianinazzi-Pearson V, et al (2013) Genome of an arbuscular mycorrhizal fungus provides insight into the oldest plant symbiosis. Proc Natl Acad Sci **110**: 20117–20122

To A, Joubès J, Barthole G, Lécureuil A, Scagnelli A, Jasinski S, Lepiniec L, Baud S (2012) WRINKLED transcription factors orchestrate tissue-specific regulation of fatty acid biosynthesis in Arabidopsis. Plant Cell **24**: 5007–23

Toth R, Miller RM (1984) Dynamics of Arbuscule Development and Degeneration in a Zea Mays Mycorrhiza. Am J Bot **71**: 449–460

Trépanier M, Bécard G, Moutoglis P, Willemot C, Gagné S, Avis TJ, Rioux J, Tre M, Be G, Gagne S (2005) Dependence of Arbuscular-Mycorrhizal Fungi on Their Plant Host for Palmitic Acid Synthesis. Appl Environ Microbiol **71**: 5341–5347

Tsuzuki S, Handa Y, Takeda N, Kawaguchi M (2016) Strigolactone-induced putative secreted protein 1 is required for the establishment of symbiosis by the arbuscular mycorrhizal fungus Rhizophagus irregularis. Mol Plant-Microbe Interact **29**: 1–59

van Zeijl A, Liu W, Xiao TT, Kohlen W, Yang W-C, Bisseling T, Geurts R (2015) The strigolactone biosynthesis gene DWARF27 is co-opted in rhizobium symbiosis. BMC Plant Biol **15**: 260

Venkateshwaran M, Jayaraman D, Chabaud M, Genre A, Balloon AJ, Maeda J, Forshey K, den Os D, Kwiecien NW, Coon JJ, et al (2015) A role for the mevalonate pathway in early plant symbiotic signaling. Proc Natl Acad Sci **112**: 9781–9786

Wais RJ, Galera C, Oldroyd G, Catoira R, Penmetsa RV, Cook D, Gough C, Denarié J, Long SR (2000) Genetic analysis of calcium spiking responses in nodulation mutants of Medicago truncatula. Proc Natl Acad Sci **97**: 13407–13412

Walter MH, Floss DS, Hans J, Fester T, Strack D (2007) Apocarotenoid biosynthesis in arbuscular mycorrhizal roots: Contributions from methylerythritol phosphate pathway isogenes and tools for its manipulation. Phytochemistry **68**: 130–138

Walter MH, Hans J, Strack D (2002) Two distantly related genes encoding 1-deoxy-D-xylulose 5-phosphate synthases: Differential regulation in shoots and apocarotenoid-accumulating mycorrhizal roots. Plant J **31**: 243–254

Wang E, Schornack S, Marsh JF, Gobbato E, Schwessinger B, Eastmond P, Schultze M, Kamoun S, Oldroyd GED (2012) A common signaling process that promotes mycorrhizal and oomycete colonization of plants. Curr Biol **22**: 2242–6

Wang E, Yu N, Bano SA, Liu C, Miller AJ, Cousins D, Zhang X, Ratet P, Tadege M, Mysore KS, et al (2014) A H+-ATPase That Energizes Nutrient Uptake during Mycorrhizal Symbioses in Rice and Medicago truncatula. Plant Cell **26**: 1818–1830

Weber E, Engler C, Gruetzner R, Werner S, Marillonnet S (2011) A modular cloning system for standardized assembly of multigene constructs. PLoS One **6**: e16765

Weidmann S, Sanchez L, Descombin J, Chatagnier O, Gianinazzi S, Gianinazzi-Pearson V (2004) Fungal elicitation of signal transduction-related plant genes precedes mycorrhiza establishment and requires the dmi3 gene in Medicago truncatula. Mol Plant-Microbe Interact **17**: 1385–93

Wewer V, Brands M, Dörmann P (2014) Fatty acid synthesis and lipid metabolism in the obligate biotrophic fungus Rhizophagus irregularis during mycorrhization of Lotus japonicus. Plant J **79**: 398–412

Wright DP, Read DJ, Scholes JD (1998) Mycorrhizal sink strength influences whole plant carbon balance of Trifolium repens L. Plant, Cell Environ **21**: 881–891

Wulf A, Manthey K, Doll J (2003) Transcriptional changes in response to arbuscular mycorrhiza development in the model plant Medicago truncatula. Mol Plant-Microbe Interact **16**: 306–314

Xie F, Murray JD, Kim J, Heckmann AB, Edwards A, Oldroyd GED, Downie JA (2012) Legume pectate lyase required for root infection by rhizobia. Proc Natl Acad Sci **109**: 633–638

Xie X, Huang W, Liu F, Tang N, Liu Y, Lin H, Zhao B (2013) Functional analysis of the novel mycorrhiza-specific phosphate transporter AsPT1 and PHT1 family from Astragalus sinicus during the arbuscular mycorrhizal symbiosis. New Phytol **198**: 836–852

Xue L, Cui H, Buer B, Vijayakumar V, Delaux P-M, Junkermann S, Bucher M (2015) Network of GRAS Transcription Factors Involved in the Control of Arbuscule Development in Lotus japonicus. Plant Physiol **167**: 854–871

Yang S-Y, Gronlund M, Jakobsen I, Grotemeyer MS, Rentsch D, Miyao A, Hirochika H, Kumar CS, Sundaresan V, Salamin N, et al (2012) Nonredundant Regulation of Rice Arbuscular Mycorrhizal Symbiosis by Two Members of the PHOSPHATE TRANSPORTER1 Gene Family. Plant Cell **24**: 4236–4251

Yang S-Y, Paszkowski U (2011) Phosphate import at the arbuscule: just a nutrient? Mol Plant-Microbe Interact **24**: 1296–9

Yano K, Yoshida S, Müller J, Singh S, Banba M, Vickers K, Markmann K, White C, Schuller B, Sato S, et al (2008) CYCLOPS, a mediator of symbiotic intracellular accommodation. Proc Natl Acad Sci **105**: 20540–5

Yokota K, Soyano T, Kouchi H, Hayashi M (2010) Function of GRAS proteins in root nodule symbiosis is retained in homologs of a non-legume, rice. Plant Cell Physiol **51**: 1436–1442

Yoneyama K, Yoneyama K, Takeuchi Y, Sekimoto H (2007) Phosphorus deficiency in red clover promotes exudation of orobanchol, the signal for mycorrhizal symbionts and germination stimulant for root parasites. Planta **225**: 1031–1038

Yoshida S, Kameoka H, Tempo M, Akiyama K, Umehara M, Yamaguchi S, Hayashi H, Kyozuka J, Shirasu K (2012) The D3 F-box protein is a key component in host strigolactone responses essential for arbuscular mycorrhizal symbiosis. New Phytol **196**: 1208–1216

Yu N, Luo D, Zhang X, Liu J, Wang W, Jin Y, Dong W, Liu J, Liu H, Yang W, et al (2014) A DELLA protein complex controls the arbuscular mycorrhizal symbiosis in plants. Cell Res **24**: 130–3

Zhang Q, Blaylock L a, Harrison MJ (2010) Two Medicago truncatula half-ABC transporters are essential for arbuscule development in arbuscular mycorrhizal symbiosis. Plant Cell **22**: 1483–1497

Zhang X, Dong W, Sun J, Feng F, Deng Y, He Z, Oldroyd GED, Wang E (2015) The receptor kinase CERK1 has dual functions in symbiosis and immunity signalling. Plant J **81**: 258-267

Zhang X, Pumplin N, Ivanov S, Harrison MJ (2015) EXO70I Is Required for Development of a Sub-domain of the Periarbuscular Membrane during Arbuscular Mycorrhizal Symbiosis. Curr Biol **25**: 2189–2195

APPENDIX

The following tables can be found in the appendix of the electronic version of this thesis:

Table A1: List of genes differentially expressed in wild-type roots during mycorrhization.

Table A2: List of genes consistently dependent on *RAM1* at all three time points during mycorrhization.

Table A3: List of genes consistently dependent on *NSP1* at all three time points during mycorrhization.

Table A4: List of genes consistently dependent on *NSP2* at all three time points during mycorrhization.

Table A5: List of genes differentially expressed in *ram1-1* at all three time points under non-symbiotic conditions.

Table A6: List of genes differentially expressed in *nsp1-1* at all three time points under non-symbiotic conditions.

Table A7: List of genes differentially expressed in *nsp2-2* at all three time points under non-symbiotic conditions.